

*Heterologous Production, Characterization and
Isolation of Selected G Protein-Coupled Receptors
for Structural Studies*

Dissertation

zur Erlangung des Doktorgrades der Naturwissenschaften

vorgelegt beim Fachbereich Biochemische, Chemische und Pharmazeutische

Wissenschaften der Johann Wolfgang Goethe – Universität

in Frankfurt am Main

von

Arun Kumar Shukla

aus Kushinagar

Indien

Frankfurt am Main

2005

**Vom Fachbereich Biochemische, Chemische und Pharmazeutische Wissenschaften
der Johann Wolfgang Goethe Universität als Dissertation angenommen.**

Dekan: Prof. Harald Schwalbe

Erster Gutachter: Prof. Dieter Steinhilber

Zweiter Gutachter: Prof. Hartmut Michel

Datum der Disputation:

Table of Contents

	Page
Summary	1
<u>1. Introduction</u>	
1.1 G protein-coupled receptors (GPCRs)	5
1.2 GPCR classification	6
1.3 GPCR activation	7
1.4 GPCR desensitization and internalization	10
1.5 GPCR dimerization	10
1.6 Structural studies on GPCRs	12
1.6.1 Biophysical approach	12
1.6.2 Nuclear Magnetic Resonance (NMR) studies on GPCRs	13
1.6.2.1 Solid-state NMR	13
1.6.3 Three-dimensional crystallization trials	15
1.7 Renin-Angiotensin-Kinin system	16
1.7.1 Kinins and their receptors	16
1.7.1.1 Bradykinin receptor (B ₂ R)	18
1.7.1.2 Ligand binding region of B ₂ R	18
1.7.1.3 Post-translational modifications of B ₂ R	19
1.7.1.4 B ₂ R interactome	20
1.7.2 Angiotensin II and its receptors	21
1.7.2.1 Angiotensin II type 1a receptor (AT _{1a} R)	21
1.7.2.2 Ligand binding region of AT _{1a} R	22
1.7.2.3 Post-translational modifications of AT _{1a} R	23
1.7.2.4 AT _{1a} R interactome	23
1.8 Neuromedin U and its receptors	24
1.8.1 Neuromedin U subtype 2 receptor (NmU ₂ R)	25
1.8.2 Signalling pathways of NmU ₂ R	25
1.8.3 Post-translational modifications and interactome	26
1.9 Heterologous expression systems for GPCRs	26

1.9.1 <i>Escherchia coli</i> (<i>E. coli</i>) expression system	26
1.9.2 <i>Pichia pastoris</i> expression system	27
1.9.3 Baculovirus expression system	28
1.9.4. Semliki Forest Virus (SFV) expression system	29
1.10 Aim of the project	31
1.10.1 Production, characterization and isolation of GPCRs	31
1.10.2 Structural characterization of GPCRs	31
1.10.3 Interaction of GPCRs with their binding partners	31

2. Materials and Methods

2.1 Materials

2.1.1 General chemicals	33
2.1.2 Radioactive chemicals	34
2.1.3 Detergents	34
2.1.4 Protease inhibitors	35
2.1.5 Chromatography matrices	35
2.1.6 Enzymes	36
2.1.7 Antibodies	36
2.1.8 Kits	36
2.1.9 DNA and protein markers	36
2.1.10 Buffers and solutions	37
2.1.10.1 Buffers for purification	39
2.1.11 <i>E. coli</i> strain and culture medium	40
2.1.12 <i>Pichia pastoris</i> strain and culture medium	42
2.1.13 Insect cell lines and culture media	42
2.1.14 Mammalian cell lines and culture media	42
2.1.15 General apparatus	43
2.1.16 Centrifuges	43
2.1.17 Filters and membranes	43
2.1.18 Primers	43

2.2 Methods	
2.2.1 <i>E. coli</i> cultivation and competent cell preparation	45
2.2.2 DNA isolation and transformation	45
2.2.3 Restriction digestion and ligation of DNA	46
2.2.4 <i>Pichia</i> culture and transformation	46
2.2.5 Clone selection and expression in <i>Pichia pastoris</i>	46
2.2.6 Insect cell culture	
2.2.6.1 Transfection	47
2.2.6.2 Plaque assay	47
2.2.6.3 Virus stock and titre determination	47
2.2.6.4 Protein expression in insect cells	48
2.2.7 Mammalian cell culture	
2.2.7.1 <i>In vitro</i> transcription	48
2.2.7.2 Electroporation of mRNA into Baby Hamster Kidney (BHK) cells	48
2.2.7.3 Collection and activation of virus	49
2.2.7.4 Protein expression in mammalian cells	49
2.2.8 Membrane preparation from <i>Pichia pastoris</i>	
2.2.8.1 Analytical scale	49
2.2.8.2 Preparative scale	50
2.2.9 Membrane preparation from insect cells and mammalian cells	50
2.2.10 Determination of protein concentration	51
2.2.11 SDS-PAGE analysis	51
2.2.12 Western blot analysis	51
2.2.13 Radioligand binding analysis	
2.2.13.1 On membranes	52
2.2.13.2 On solubilized and purified receptors	52
2.2.14 G protein coupling assay	53

2.2.15	Localization of recombinant receptors	
2.2.15.1	Confocal microscopy	53
2.2.15.2	Electron microscopy	54
2.2.16	Solubilization of receptors	55
2.2.17	Purification of receptors	
2.2.17.1	Immobilized Metal Affinity Chromatography	55
2.2.17.2	Purification via monomeric avidin	55
2.2.17.3	Purification via anti-Flag antibody matrix	56
2.2.17.4	Purification via streptactin matrix	56
2.2.18	Concentration of proteins after purification	56
2.2.19	Coomassie and silver staining of proteins	56
2.2.20	Analytical gel filtration	57
2.2.21	Sample preparation for solid-state NMR analysis	57
2.2.22	Three-dimensional crystallization trials	57

3. Production, characterization and isolation of B₂R

3.1	Production and isolation of B₂R from <i>Pichia pastoris</i>	59
3.1.1	Sub-cloning of B₂R gene in <i>Pichia</i> expression vector	59
3.1.2	Expression construct	59
3.1.3	Production of recombinant receptor	
3.1.3.1	Western blot analysis	60
3.1.3.2	[³H] bradykinin binding analysis	61
3.1.4	Optimization of functional expression of B₂R	62
3.1.5	Glycosylation analysis	63
3.1.6	Solubilization of recombinant B₂R	64
3.1.7	Purification of recombinant B₂R	65
3.2	Production and isolation of B₂R from insect cells	
3.2.1	Sub-cloning of B₂R gene in the baculovirus vectors	67
3.2.2	Expression constructs	67

3.2.3 Production of recombinant receptor	
3.2.3.1 Western blot analysis	69
3.2.3.2 [³ H] bradykinin binding	69
3.2.4 Optimization of functional expression of B₂R	71
3.2.5 Glycosylation analysis	71
3.2.6 Localization of recombinant B₂R	
3.2.6.1 Immunogold labeling experiment	73
3.2.6.2 Confocal microscopy	75
3.2.7 Large-scale production of recombinant B₂R	75
3.2.8 Solubilization and purification of recombinant B₂R	77
3.2.8.1 Purification of recombinant B ₂ R via Ni-NTA and monomeric avidin columns	77
3.2.8.2 Purification of recombinant B ₂ R via Ni-NTA and anti-Flag antibody matrix	77
3.2.8.3 Identification of the 65 kDa band	79
3.3 Production and isolation of B₂R from mammalian cells	
3.3.1 Sub-cloning of B ₂ R gene in SFV expression vectors	80
3.3.2 Expression constructs	81
3.3.3 Production of recombinant receptor	82
3.3.3.1 Comparison of different construct for B ₂ R production in BHK cells	82
3.3.3.2 Western blot analysis	83
3.3.3.3 [³ H] bradykinin binding	83
3.3.4 Optimization of functional expression of B ₂ R	
3.3.4.1 Adherent vs. suspension culture	84
3.3.4.2 Time scale of B ₂ R expression in BHK cells	85
3.3.4.3 Effect of Dimethylsulphoxide (DMSO) on B ₂ R expression	85
3.3.4.4 Effect of cell type on B ₂ R expression	86
3.3.5 Glycosylation analysis	86

3.3.6 Localization of recombinant B ₂ R	
3.3.6.1 Immunogold labeling experiment	87
3.3.6.2 Confocal microscopy	89
3.3.7 G protein coupling assay for recombinant B ₂ R	89
3.3.8 Solubilization and purification of B ₂ R	90
3.3.9 Stability analysis of purified B ₂ R	92

4. Structural studies with B₂R

4.1 Solid-state NMR analysis of bradykinin bound to B ₂ R	94
4.1.1 Sample preparation (peptide and receptor)	94
4.1.2 ¹³ C Cross-polarization (CP) spectrum of lyophilized bradykinin	95
4.1.3 Two-dimensional single quantum/double quantum ¹³ C NMR spectrum	96
4.1.4 Comparison of 1-dimensional spectra of bradykinin in different states	96
4.1.5 Reducing the measurement time	98
4.1.5.1 Receptor aggregation at high concentration	98
4.1.5.2 Effect of temperature on signal/noise ratio	99
4.1.6 Two-dimensional spectrum of ¹³ C/ ¹⁵ N bradykinin bound to B ₂ R	100
4.2 Three-dimensional crystallization trials of B ₂ R	100
4.3 Interaction of B ₂ R with β-arrestin	101

5. Production, characterization and isolation of AT_{1a}R

5.1 Production and isolation of AT _{1a} R from <i>Pichia pastoris</i>	104
5.1.1 Sub-cloning of AT _{1a} R gene in <i>Pichia</i> expression vector	104
5.1.2 Expression construct	104

5.1.3 Production of recombinant receptor	105
5.1.3.1 Western blot analysis	105
5.1.3.2 [³ H] angiotensin II binding	105
5.1.4 Optimization of functional expression of AT _{1a} R	107
5.1.5 Glycosylation analysis	108
5.1.6 Solubilization of recombinant AT _{1a} R	109
5.1.7 Purification of recombinant AT _{1a} R	109
5.1.7.1 Purification via Ni-NTA and monomeric avidin columns	110
5.1.7.2 Purification via Ni-NTA and streptactin columns	111
5.1.7.3 Fluorescein labeled angiotensin II as a probe to monitor AT _{1a} R purification	112
5.1.8 Stability of purified AT _{1a} R	112
5.2 Production and isolation of AT _{1a} R from insect cells	
5.2.1 Sub-cloning of AT _{1a} R gene in baculovirus vectors	113
5.2.2 Expression constructs	114
5.2.3 Production of recombinant receptor	
5.2.3.1 Western blot analysis	114
5.2.3.2 [³ H] angiotensin II binding	115
5.2.4 Glycosylation analysis	116
5.2.5 Solubilization and purification of recombinant AT _{1a} R	117
5.3 Production and isolation of AT _{1a} R from mammalian cells	
5.3.1 Sub-cloning of AT _{1a} R gene in SFV expression vectors	118
5.3.2 Expression constructs	118
5.3.3 Production of recombinant receptor	119
5.3.3.1 Western blot analysis	119
5.3.3.2 [³ H] angiotensin II binding	120
5.3.4 Glycosylation analysis	120
5.3.5 Localization of AT _{1a} R by confocal microscopy	121
5.3.6 Solubilization and purification of AT _{1a} R	123

5.3.7 Proteolytic degradation of purified AT _{1a} R	124
5.3.8 Three-dimensional crystallization trials of AT _{1a} R	124

6. Coexpression of B₂R and AT_{1a}R and isolation of the heterodimer complex

6.1 Coexpression of B ₂ R and AT _{1a} R	127
6.1.1 Constructs for Coexpression	127
6.1.2 Coinfection of BHK cells	128
6.2 Coexpression of B ₂ R with AT _{1a} R results in surface trafficking of B ₂ R	128
6.2.1 Surface expression analysis by ligand binding assay	128
6.2.2 Surface expression analysis by confocal microscopy	129
6.3 Agonist induced cointernalization of B ₂ R and AT _{1a} R	130
6.4 Colocalization of B ₂ R and AT _{1a} R in human foreskin fibroblasts	132
6.5 Isolation of the heterodimer complex	132
6.5.1 Analysis by silver staining and Western blot	133
6.5.2 Analysis by gel filtration	133
6.5.3 Analysis by ligand binding assay	134
6.6 Stability of the heterodimer complex	134

7. Production, characterization and isolation of NmU₂R

7.1 Production and isolation of NmU ₂ R from <i>Pichia pastoris</i>	137
7.1.1 Sub-cloning of NmU ₂ R gene in <i>Pichia</i> expression vector	137
7.1.2 Expression construct	137
7.1.3 Production of recombinant receptor	138
7.1.3.1 Western blot analysis	138
7.1.3.2 [¹²⁵ I] NmU binding	138
7.1.4 Optimization of functional expression of NmU ₂ R	140
7.1.5 Glycosylation analysis	140
7.1.6 Solubilization of recombinant NmU ₂ R	141

7.1.7 Purification of recombinant NmU ₂ R	142
7.2 Production and isolation of NmU ₂ R from mammalian cells	
7.2.1 Sub-cloning of NmU ₂ R gene in SFV expression vector	143
7.2.2 Expression construct	144
7.2.3 Production of recombinant receptor	144
7.2.3.1 Western blot analysis	144
7.2.3.2 [¹²⁵ I] NmU binding	145
7.2.3.3 Effect of DMSO on NmU ₂ R expression	145
7.2.4 Glycosylation analysis	146
7.2.5 Localization analysis of NmU ₂ R	148
7.2.6 Solubilization and purification of NmU ₂ R	148

8. Discussion

8.1 Structural studies on GPCRs	151
8.2 Heterologous production of B ₂ R in different host systems	152
8.3 Characterization of recombinant B ₂ R	155
8.4 Intracellular localization of recombinant B ₂ R	157
8.5 Isolation of recombinant B ₂ R	158
8.6 Structural studies on B ₂ R	
8.6.1 Three-dimensional crystallization trials	159
8.6.2 Solid-state NMR studies	160
8.7 Coexpression of B ₂ R and AT _{1a} R	161
8.7.1 Heterodimerization with AT _{1a} R promotes surface localization of B ₂ R	161
8.7.2 Isolation of the heterodimer complex	163
8.8 Production, characterization and isolation of AT _{1a} R	163
8.9 Production, characterization and isolation of NmU ₂ R	165
8.10 Effect of DMSO on expression of recombinant receptors	165
8.11 Future perspectives	166

References	168
Zusammenfassung	191
Abbreviations	197
Appendix	199
Acknowledgements	202
Curriculum vitae	204

Summary

G protein-coupled receptors (GPCRs) play regulatory roles in many different physiological processes and they represent one of the most important class of drug targets. However, due to the lack of three-dimensional structures, structure based drug design has not been possible. The major bottleneck in getting three-dimensional crystal structure of GPCRs is to obtain milligram quantities of pure, homogenous and stable protein. Therefore, during my Ph.D. thesis, I focused on expression, characterization and isolation of three GPCRs namely human bradykinin receptor subtype 2 (B₂R), human angiotensin II receptor subtype 1 (AT_{1a}R), and human neuromedin U receptor subtype 2 (NmU₂R). These receptors were heterologously produced in three different expression systems (i.e. *Pichia pastoris*, insect cells and mammalian cells), biochemically characterized and subsequently solubilized and purified for structural studies

The human bradykinin receptor subtype 2 (B₂R) is constitutively expressed in a variety of cells, including endothelial cells, vascular smooth muscle cells and cardiomyocytes. Activation of B₂R is important in pathogenesis of inflammation, pain, tissue injury and cardioprotective mechanisms. During this study, recombinant B₂R was produced in methylotrophic yeast *Pichia pastoris* (3.5 pmol/mg), insect cells (10 pmol/mg) and mammalian cells (60 pmol/mg). The recombinant receptor was characterized in terms of [³H] bradykinin binding, G protein coupling, localization, and glycosylation. Subsequently, it was solubilized and purified using affinity chromatography. Homogeneity and stability of purified B₂R was monitored by gel filtration analysis. Milligram amounts of pure and stable receptor were obtained from BHK cells and Sf9 cells, which were used for three-dimensional crystallization attempts.

The second receptor, which I worked on, is human angiotensin II receptor subtype 1 (AT_{1a}R). AT_{1a}R is distributed in smooth muscle cells, liver, kidney, heart, lung and testis. Activation of AT_{1a}R is implicated in the regulation of blood pressure, hypertension and cardiovascular diseases. Recombinant AT_{1a}R was produced at high levels in *Pichia pastoris* (167 pmol/mg), while at moderate levels in insect cells (29 pmol/mg) and mammalian cells (32 pmol/mg). The recombinant receptor was characterized in terms of [³H] angiotensin II binding, localization, and glycosylation. Subsequently, the receptor

was solubilized and purified using affinity chromatography. Homogeneity and stability of purified AT_{1a}R was monitored by gel filtration analysis. Milligram amounts of pure and stable receptor were obtained from *Pichia pastoris*, which were used for three-dimensional crystallization attempts.

In addition to B₂R and AT_{1a}R, I also attempted to produce and isolate the human neuromedin U receptor subtype 2 (NmU₂R), which was deorphanized recently. It is found in highest abundance in the central nervous system, particularly the medulla oblongata, spinal cord and thalamus. The distribution of this receptor suggests its regulatory role in sensory transmission and modulation. During this study, recombinant NmU₂R was produced in *Pichia pastoris* (6 pmol/mg) and BHK cells (9 pmol/mg). Recombinant receptor was characterized with regard to [¹²⁵I] NmU binding, localization and glycosylation. Subsequently, the receptor was solubilized and purified using affinity chromatography. Due to its low expression level, further expression optimization is required in order to obtain milligram amounts for structural studies.

The long-term goal of this study was to obtain three-dimensional crystal structure of recombinant GPCRs. However, 3-dimensional crystallization of human recombinant membrane proteins still remains a difficult task. On the other hand, recent advances in the solid-state NMR spectroscopy offer ample opportunities to study receptor-ligand systems, provided milligram quantities of purified receptor are available. Therefore, in parallel to 3-dimensional crystallization trials, purified B₂R was also used for solid-state NMR analysis in order to investigate the receptor bound conformation of bradykinin. Preliminary results are promising and indicate significant structural changes in bradykinin upon binding to B₂R. Further experiments are ongoing and will hopefully result in the structure of receptor bound bradykinin.

One of the challenges in GPCR crystallization is the small hydrophilic surface area that is available to make crystal contacts. One possibility to overcome this problem can be the reconstitution of a GPCR complex with an interacting protein for cocrystallization. For this purpose, I coexpressed B₂R and AT_{1a}R, which form a stable heterodimer complex, in BHK cells. I could successfully isolate the heterodimer complex by using two-step affinity purification. Unfortunately, this complex was not stable over time and disassociates within three days of purification. However, during coexpression of

B₂R and AT_{1a}R in BHK cells, I observed that B₂R was localized in the plasma membrane in coexpressing cells while it was retained intracellularly when expressed alone. This coexpression of AT_{1a}R with B₂R resulted in a four-fold increase in [³H] bradykinin binding sites on the cell surface. In addition, these two receptors were cointernalized in response to their individual specific ligands. Interestingly, colocalization of B₂R and AT_{1a}R was also found in human foreskin fibroblasts (which endogenously express both receptors), in line with the possibility that heterodimerization may be required for surface localization of B₂R in native tissues as well. This is the first report where surface localization of a peptide GPCR is triggered by a distantly related peptide GPCR. These data support the hypothesis that heterodimerization may be a prerequisite for cell surface localization of some GPCRs.

A second approach that I followed to stabilize the purified B₂R was to reconstitute the B₂R-β-arrestin complex. β-arrestin is a cytosolic protein that participates in agonist mediated desensitization of GPCRs and therefore dampens the cellular responses initiated by the activation of GPCRs. I tried to reconstitute B₂R-β-arrestin complex *in vitro* by mixing purified B₂R and purified β-arrestin. But, no interaction of these two proteins was observed in the pull-down assays. However, a C-terminal mutant of B₂R (where a part of the C-terminus of the B₂R is exchanged with that of the vasopressin receptor) was found to interact with β-arrestin *in vitro* as revealed by pull-down assays.

In conclusion, this work establishes the production, characterization and isolation of three recombinant human GPCRs. Recombinant receptors were produced in milligram amounts and therefore, pave the way for structural analysis. The heterodimer complex of B₂R-AT_{1a}R and B₂R-β-arrestin complex can be of great help during crystallization. In addition, it was also found for the first time that the surface localization of a peptide GPCR can be triggered by heterodimerization with a distantly related peptide GPCR.

Chapter 1: Introduction

1.1 G protein-coupled receptors

G protein-coupled receptors (GPCRs) constitute the largest family of cell surface receptors involved in signalling across biological membranes. Approximately, 1-5% of the vertebrate genomes encode for GPCRs. In human genome, there are 800-1000 genes, which encode for receptors of this superfamily (Takeda *et al.*, 2002). GPCRs modulate a wide range of physiological processes and represent the largest class of therapeutic targets (reviewed in Wise *et al.*, 2002). Despite large variations in their stimuli, all GPCRs share a common seven α -helix transmembrane architecture and presumably perform signal transduction by a common mechanism via heterotrimeric guanyl nucleotide-binding proteins (G proteins) (reviewed in Okada *et al.*, 2001).

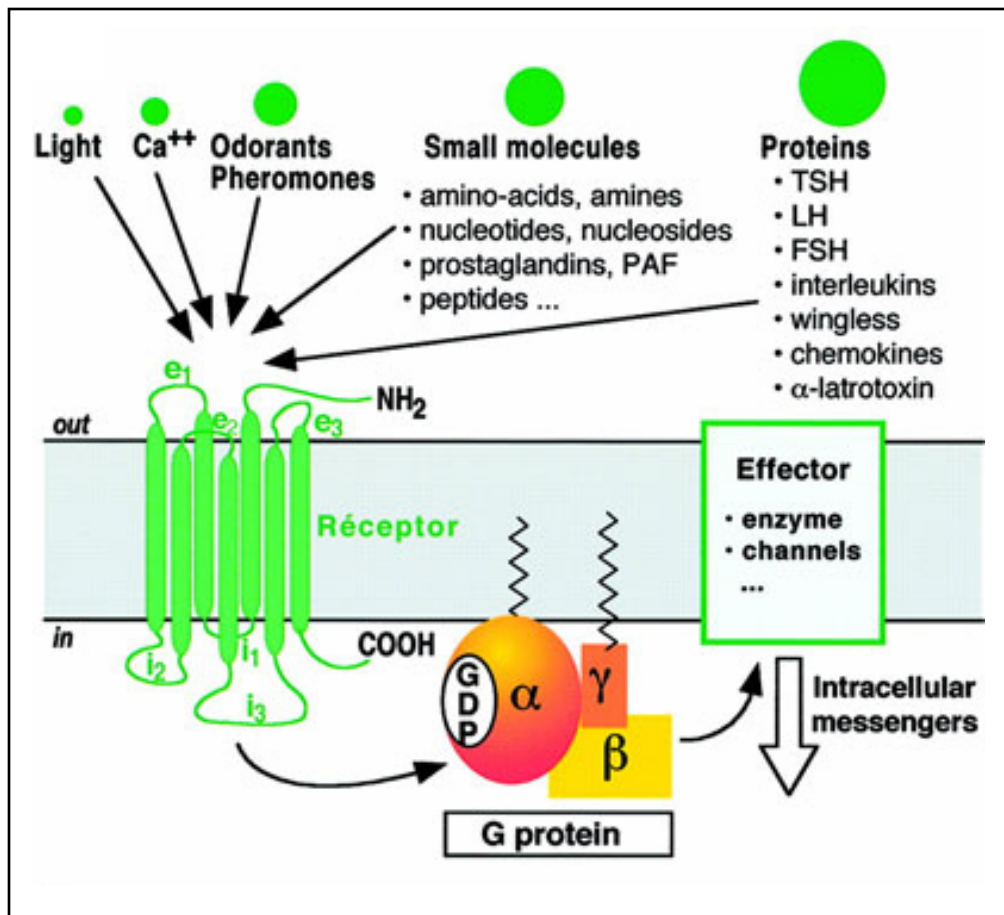
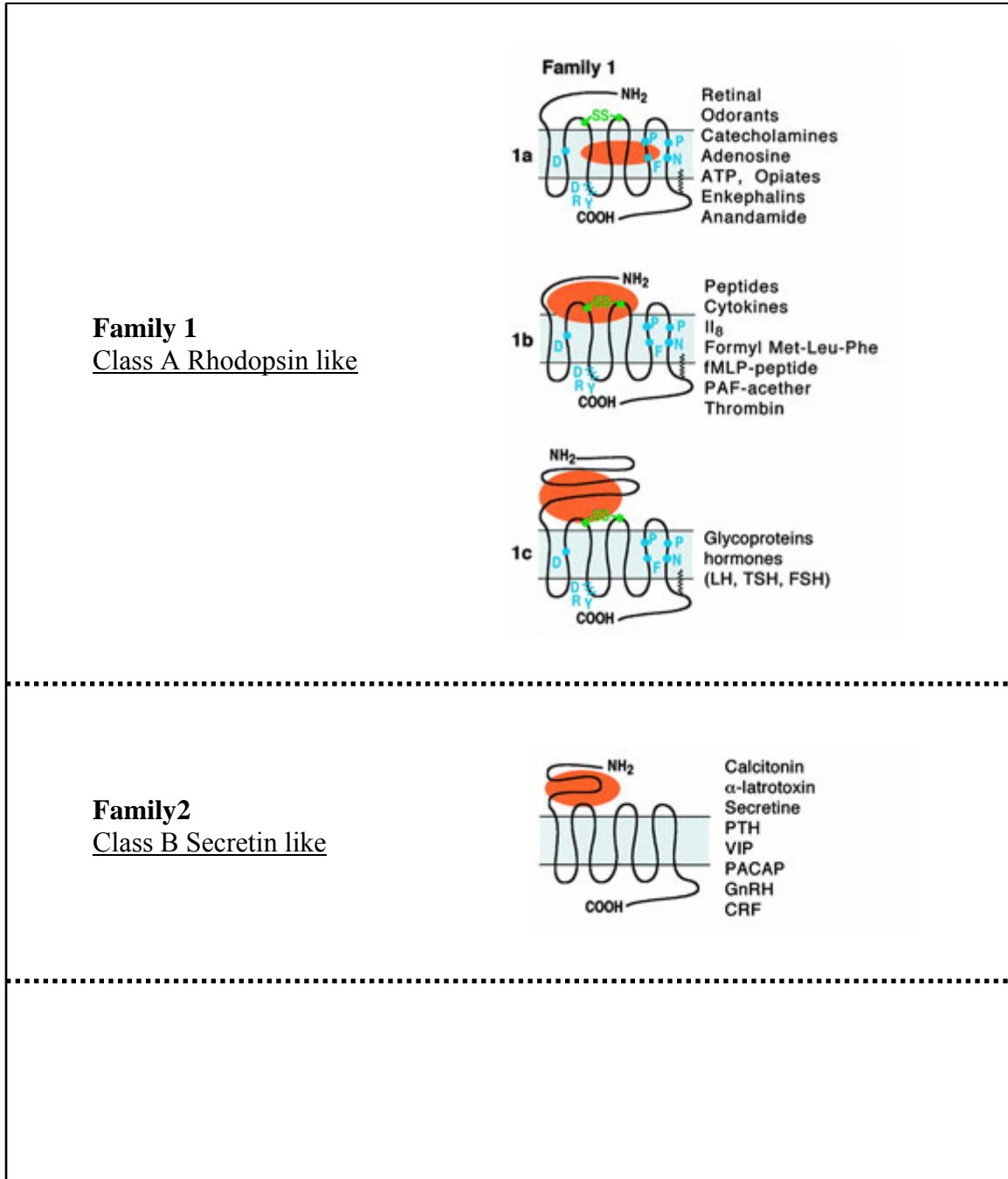


Fig. 1.1 All GPCRs contain a central common core of seven transmembrane helices. These helices are connected by three intracellular (i_1 , i_2 , i_3) and three extracellular (e_1 , e_2 , e_3) loops (from Bockaert *et al.*, 1999).

1.2 GPCR classification

Based on the amino acid sequence comparison, GPCRs can be classified in five main families (Fig. 1.2). No significant sequence similarity is observed among the receptors from different families, representing a remarkable example of molecular convergence (Bockaert *et al.*, 1999).



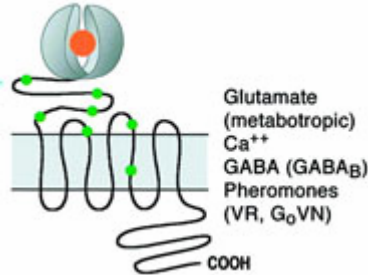
<p>Family 3 <u>Class C Metabotropic glutamate / pheromone</u></p>	
<p>Family 4 <u>Class D Fungal pheromone</u></p>	<p>Fungal pheromone A-Factor like (STE2, STE3), fungal pheromone B like (BAR, BBR, RCB, PRA), fungal pheromone M- and P-Factor receptors</p>
<p>Family 5 <u>Frizzled/Smoothened family</u></p>	<p>Frizzled and Smoothened receptors</p>
<p>cAMP Family <u>Class E cAMP receptors</u></p>	<p><i>Dictyostelium discoideum</i> receptors</p>

Fig. 1.2 Classification of GPCRs based on the amino acid sequence comparison (modified from Bockaert *et al.*, 1999).

1.3 GPCR activation (G protein cycle)

Agonist activation of receptors leads to conformational changes, which are not well understood. These changes probably involve rearrangements of transmembrane helices 3 and 6 (Ballesteros *et al.*, 2001). The activated receptor interacts with the heterotrimeric G protein (α , β and γ subunits) and serves as a guanine nucleotide exchange factor (GEF) to promote GDP dissociation and GTP binding. It has been proposed that the critical event in agonist activation of GPCR is the stabilization of the ternary complex of agonist/receptor/G protein. The activated G protein heterotrimer (i.e. GTP bound form) dissociates into α subunit and a $\beta\gamma$ dimer, both of which can regulate separate effectors.

Afterwards, hydrolysis of GTP to GDP occurs by the enzymatic activity of G_{α} subunit itself (known as GTPase activity of G_{α}). This leads to reassociation of the G protein heterotrimer and termination of the activation cycle (Fig.1.3).

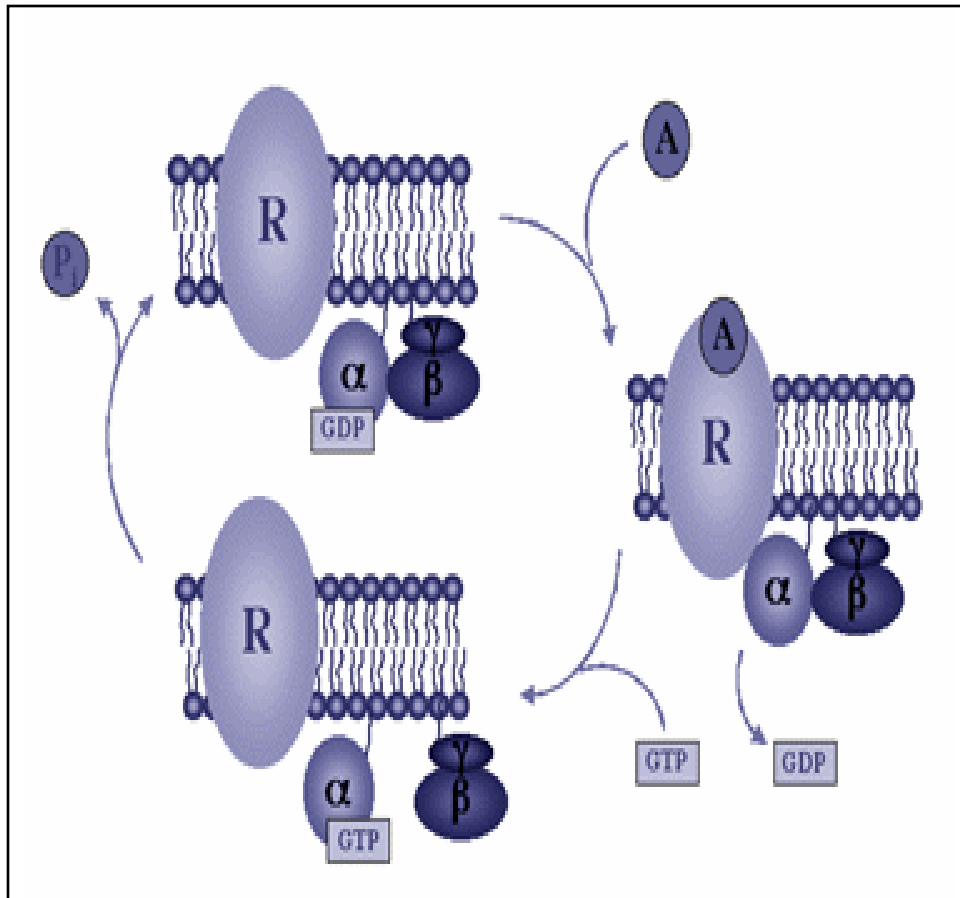


Fig. 1.3 Schematic representation of GPCR activation (G protein cycle).

It has also been found that the process of GTP hydrolysis is regulated by RGS proteins (regulator of G protein signalling) (De Vries *et al.*, 2000 & Ross *et al.*, 2000). More importantly, many GPCRs exhibit agonist independent coupling to G proteins, which is termed as constitutive activity of GPCRs.

The repertoire of heterotrimeric G Proteins consists of 21 different G_{α} subunits, 5 β subunits and 11 different γ subunits in humans (Helper *et al.*, 1992). The α subunit is a GTPase and functions as a molecular switch that can flip between two states i.e. active, when GTP is bound and inactive, when GDP is bound. β and γ subunits are associated in

a tightly linked $\beta\gamma$ complex (Gilman *et al.*, 1987). Both, the α subunit and the $\beta\gamma$ dimer, signal through the activation or inhibition of a broad range of effectors (Fig. 1.4).

G-protein subunits	Effectors
$G\alpha_s$ $G\alpha_{olf}$	\uparrow Adenylyl cyclase RGS-PX1 (GAP, sorting nexin) Calcium channels c-Src tyrosine kinases
$G\alpha_T$ (transducin) $G\alpha_{gust}$ (gustducin)	\uparrow cGMP phosphodiesterase Phosphodiesterase (bitter, sweet taste)
$G\alpha_{1,2,3}$ $G\alpha_o$ $G\alpha_z$	\downarrow Adenylyl cyclase, \uparrow c-Src tyrosine kinases Rap1GAP1
$G\alpha_q, G\alpha_{11}, G\alpha_{14,15,16}$	\uparrow Phospholipase C LARG RhoGEF
$G\alpha_{12}, G\alpha_{13}$	p115 RhoGEF, PDZ-RhoGEF, LARG RhoGEF (Rho activation, stress-fibre formation) E-Cadherin (β -catenin release)
$G\beta\gamma$	KIR3.1–3.4 (GIRK K^+ channels) GRKs \uparrow Adenylyl cyclases (ACII, ACM) \uparrow Phospholipases (PLC $\beta_1, \beta_2, \beta_3$) PI3K γ

cGMP, cyclic GMP; GAP, GTPase-activating protein; GEF, guanine-nucleotide exchange factor; GIRK, G-protein-regulated inwardly rectifying potassium channel; PI3K, phosphatidylinositol 3-kinase; RGS, regulator of G-protein signalling.

Fig. 1.4. Examples of some effectors, which are activated or inhibited by G proteins (from Lefkowitz *et al.*, 2002).

The combinatorial complexity of $\alpha\beta\gamma$ heterotrimers is enormous and relatively little is known about the specificity of subunit composition involved in specific pathways. Most GPCRs can couple to more than one type of G protein and therefore, several intracellular signalling pathways can be activated by the stimulation of just one particular

receptor. In addition, as the numbers of effectors, which are regulated by GPCRs, are relatively smaller in comparison to the large number of GPCRs, cross-regulation of the signalling pathways has also been observed.

In addition to G proteins, a number of other cellular proteins also interact with GPCRs (reviewed in Brady *et al.*, 2002). These proteins include GPCRs themselves as homo or heterodimers (described in detail in the section 1.5), molecular chaperones (e.g. Calnexin, Nina A etc.), receptor activity modifying proteins (RAMPs), PDZ domain containing proteins (e.g. Spinophilin, Homer etc.), arrestins, calmodulin and G protein-coupled receptor kinases (GRKs). Interaction of these accessory proteins with GPCRs has implications in ligand recognition, signalling specificity and receptor trafficking.

1.4 Receptor desensitization and internalization

In order to protect the cells from receptor overstimulation, many mechanisms have evolved, which are crucial for fine-tuning and regulating receptor signalling. Such mechanisms operate at the level of receptors as well as at the level of downstream effectors. Receptor desensitization is one of these mechanisms, which downregulates signalling, even in the presence of continuing agonist stimulation (reviewed in Ferguson *et al.*, 2001). Rapid desensitization of receptors is generally controlled by G protein-coupled receptor kinases (GRKs), which selectively phosphorylate agonist activated receptor. Subsequently, β -arrestin (a cytosolic protein) binds to the phosphorylated receptor. Binding of β -arrestin uncouples the receptor from the G protein and the receptor is targeted for endocytosis and subsequent degradation or recycling. Desensitization process at the level of downstream effectors is mediated by second messenger kinases such as protein kinase A and protein kinase C (Lawler *et al.*, 2001).

1.5 Dimerization of GPCRs

In the classical view of GPCR signalling, a single receptor is activated by the agonist. This activated receptor can activate many G proteins but one at a time. However, recent

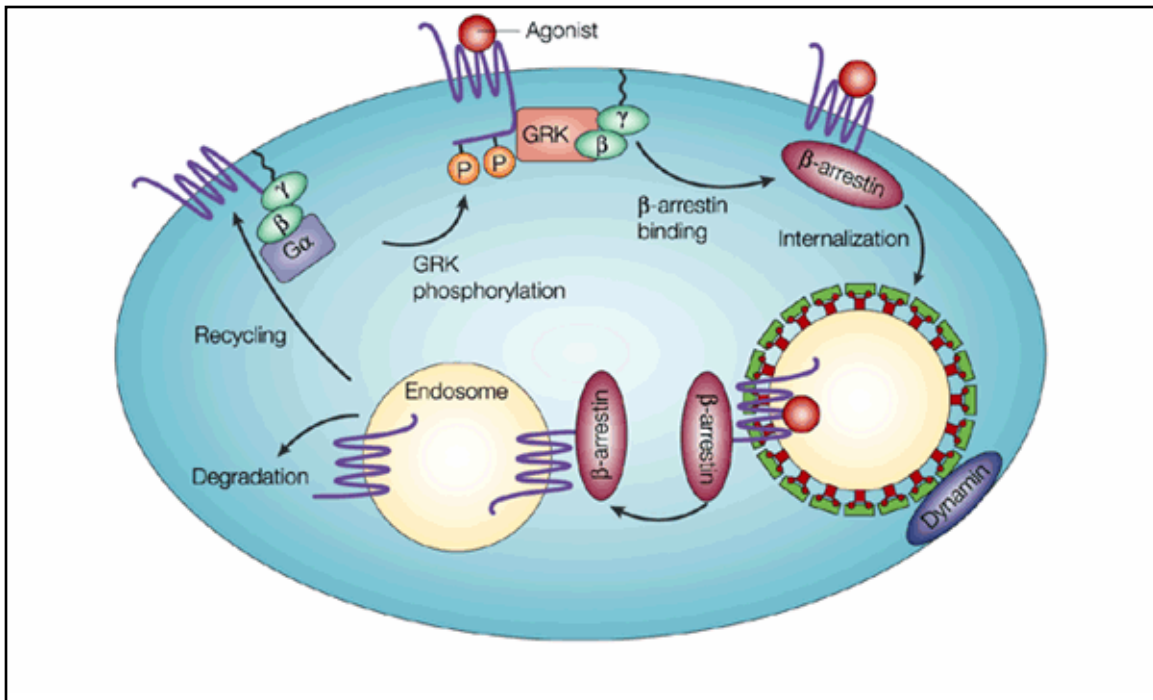


Fig. 1.5 Trafficking of GPCRs during downregulation process (from Lefkowitz *et al.*, 2002)

studies have established that many GPCRs, like other membrane receptors, can form both homo and heterodimers (reviewed in Bouvier *et al.*, 2001 & George *et al.*, 2002). Various functions have been attributed to the dimerization between different receptor subtypes. For example, heterodimerization has been proposed to promote the formation of receptors with unique pharmacological properties, which contributes to the pharmacological diversity of GPCRs (Jordan *et al.*, 1999, Jordan *et al.*, 2001 & Levac *et al.*, 2002). In addition, changes in the G protein coupling specificity (George *et al.*, 2000) and altered receptor endocytosis (Terillon *et al.*, 2004) have also been reported to occur upon receptor heterodimerization. For the metabotropic GABA_b receptor, heterodimerization between two subtypes (GABA_b-R₁ and GABA_b-R₂) is an obligatory step for cell surface expression of a functional receptor (White *et al.*, 1998 & Ng *et al.*, 1999). This surface translocation results from the masking of an endoplasmic reticulum (ER) retention signal present in the C-terminus of GABA_b-R₁, through the formation of a coiled-coil domain between the C-termini of the two receptor subtypes (Margeta-Mitrovic *et al.*, 2000). Until recently, effect of heterodimerization on cell surface trafficking was considered to be

confined to the GABA_b receptor. However, a recent study suggests that the heterodimerization between the α -adrenergic-1D and α -adrenergic-1B receptors is a prerequisite for the cell surface localization of the α -1D receptor (Hague *et al.*, 2004). It has also been published that the cell surface trafficking of mouse olfactory receptor is promoted by heterodimerization with β_2 -adrenergic receptor (Hague *et al.*, 2005). Recently, a heterodimer selective ligand has been identified (Waldhoer *et al.*, 2005) that has the unique property of selectively activating opioid receptor heterodimers but not monomers. These results firmly establish the physiological significance of GPCR heterodimerization.

On the other hand, the evidence for biological significance of GPCR homodimerization remains circumstantial despite numerous examples of receptor homodimerization reported in the literature (Angers *et al.*, 2002 & Terillon *et al.*, 2004). This is probably due to the technical limitations in differentiating the properties of a homodimer from that of a monomer. Several reports suggest constitutive homodimerization of GPCRs in the endoplasmic reticulum (ER) and indicate a role of homodimerization in quality control and ER export of these receptors (Ayoub *et al.*, 2002, Issafras *et al.*, 2002 & Terrillon *et al.*, 2003). Experimental support for this hypothesis is provided by a report describing homodimerization of β -2 adrenergic receptor as a prerequisite for its surface trafficking (Salahpour *et al.*, 2004).

1.6 Structural studies on GPCRs

Despite their importance as drug targets, little is known about the structure of GPCRs. The only GPCR structure currently available is that of bovine rhodopsin (Palczewski *et al.*, 2000). Although a number of different techniques have been applied to GPCR research, the GPCR activation mechanism still remains poorly understood.

1.6.1 Biophysical approaches

Electron paramagnetic resonance (EPR) spectroscopy and cys-crosslinking experiments have been used to study the orientation of helices and light induced conformational

changes in rhodopsin (Altenbach *et al.*, 1999 and reviewed in Columbus *et al.*, 2002). Zinc (II) binding sites were introduced in the neurokinin and κ -opioid receptors, which have provided some insight into the distance and orientation of different transmembrane helices (Elling *et al.*, 1996 and Thirstrup *et al.*, 1996).

1.6.2 Nuclear Magnetic Resonance (NMR) studies on GPCRs

Solution-state NMR spectroscopy has now been established as a promising method for the structure determination of polytopic membrane proteins (MacKenzie *et al.*, 1997, Girvin *et al.*, 1998 and Arora *et al.*, 2001). However, the feasibility of this approach remains unclear for GPCRs. Until now, solution-state NMR has been mainly used for studying GPCR fragments (Demene *et al.*, 2003, Grace *et al.*, 2004), isolated extramembrane domains (Estephan *et al.*, 2005) and dynamics of rhodopsin (Klein-Seetharaman *et al.*, 2002 and Klein-Seetharaman *et al.*, 2004). Only recently, attempts have been made to study a uniformly isotopically labeled full length GPCR (Tian *et al.*, 2005).

1.6.2.1 Solid-state NMR to study receptor-ligand interaction

High resolution solid-state NMR (ss-NMR) based on rapid rotation of sample at magic angle spinning (MAS) under ultrahigh magnetic field provides a unique opportunity to study receptor-ligand systems (reviewed in Luca *et al.*, 2005). In order to investigate GPCR-ligand system by ss-NMR, isotopic labeling of ligand is required. This is to detect the ligand signal in a highly sensitive and specific way while the background signals are suppressed. Although the natural abundance of the NMR active nucleus ^{13}C is only 1%, in detergent purified GPCR samples, the background is much higher due to high concentration of detergents and lipids. To circumvent this problem, two-dimensional double-quantum filtering techniques (Bax *et al.*, 1980) are used. In the resulting spectra, only those NMR active nuclei give rise to the overall signal, which are in the direct neighbourhood of another NMR active nucleus. This approach has already been

successfully used to investigate the structural changes in neurotensin upon binding to its cognate GPCR, the neurotensin receptor (Luca *et al.*, 2003).

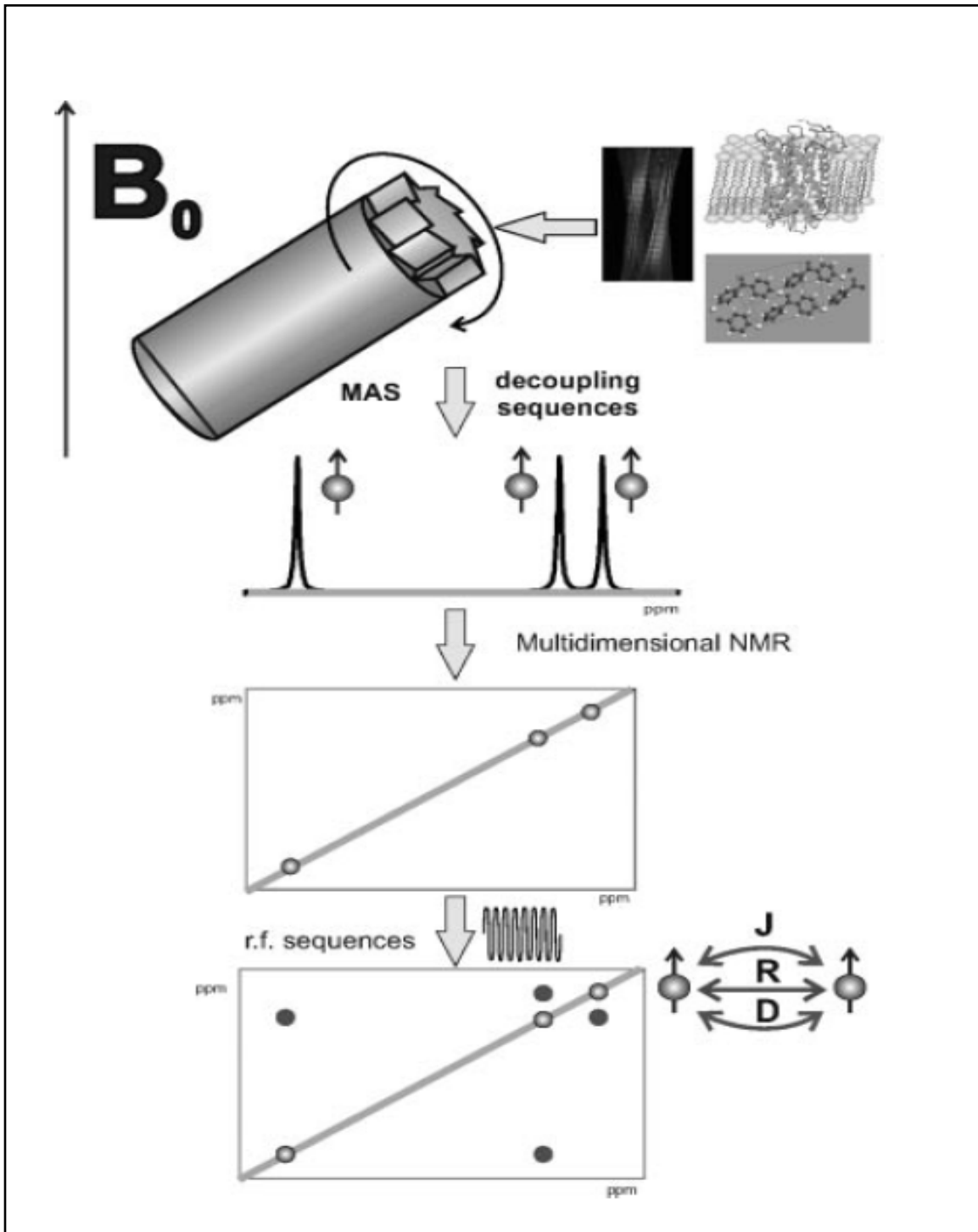


Fig. 1.6 ss-NMR set up to study molecular dynamics and structure (from Luca *et al.*, 2005).

1.6.3 Three-dimensional crystallization

The only GPCR structure currently available is that of the bovine rhodopsin (Palczewski *et al.*, 2000) (Fig. 1.7). Rhodopsin is unique among GPCRs for having its ligand 11-cis-retinal covalently attached to it. It can be isolated in large quantities directly from cow retina. On the contrary, most other GPCRs are present in tiny amounts in native tissues. Therefore, a lot of efforts have been put into developing different expression systems for GPCRs in the last decade. As a result, a number of recombinant GPCRs can now be produced using different heterologous expression systems (reviewed in Lundstrom *et al.*, 2005). As a next step, the major emphasis is on large-scale production and isolation of functional, homogenous and stable GPCR samples for three-dimensional crystallization attempts.

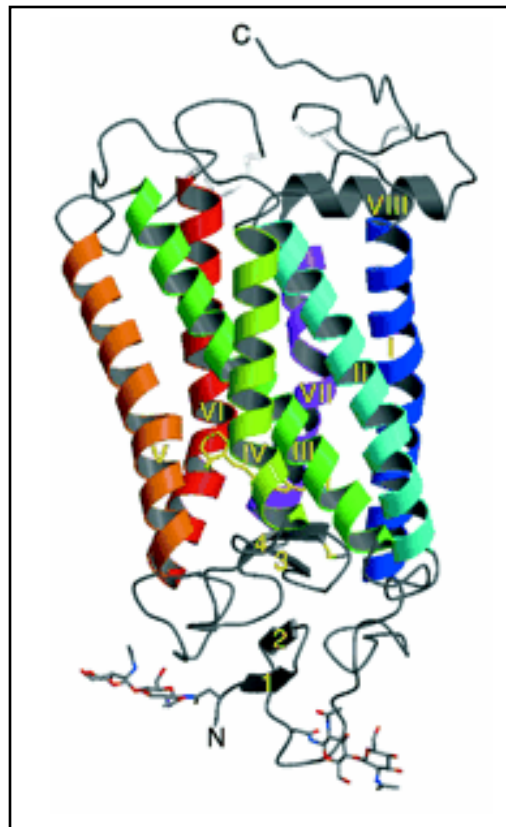


Fig. 1.7 Three-dimensional structure of bovine rhodopsin (parallel to the plane of the membrane) (from Palczewski *et al.*, 2000).

1.7 Renin-angiotensin-kinin system

The renin-angiotensin-kinin system (Fig. 1.8) is a hormone system that plays a crucial role in the long term regulation of blood pressure and blood volume in the body. This system is activated in the case of loss of blood volume or decrease in blood pressure. The pathways of the renin-angiotensin-kinin systems are active in a wide range of tissues, kidney being the most important site of renin release. Due to the direct involvement of these pathways in a number of physiological processes, this system represents an important target for therapeutic manipulation. Angiotensin converting enzyme (ACE) inhibitors and angiotensin II receptor blockers are widely used in the treatment of hypertension, heart failure and kidney disorders. B₂R and AT_{1a}R are two important signalling receptors involved in this system. Understanding the structure and function of these two GPCRs may help in designing potent and specific drugs that can be used in the treatment of cardiovascular diseases.

1.7.1 Kinins and their receptors

Kinins are small peptides that are present in blood plasma and affect smooth muscle contraction, blood pressure, blood flow throughout the body and permeability of small capillaries. Kinins are generated from kininogens by the action of plasma kallikrein. Two receptor subtypes (B₁R and B₂R) for kinins have been identified and characterized. These receptors belong to the rhodopsin family of G protein-coupled receptors (Regoli *et al.*, 1977). Bradykinin (BK) and lysyl-bradykinin (lys-BK) are the first set of bioactive kinins that are derived from kininogen in response to tissues injury. The action of BK and lys-BK are mediated by the activation of B₂R. Through the actions of carboxypeptidases on BK and lys-BK respectively, new set of kinin peptides (des-Arg⁹-BK and Lys-des-Arg⁹-BK) are derived and they activate B₁R (Blaukat *et al.*, 2003).

The genes of B₁R and B₂R are located on chromosome 14q32.1-q32.2. The B₂R gene is proximal to the B₁R receptor gene. These two genes are separated by an

intergenic region of only 12 kb (Cayla *et al.*, 2002). The close proximity of these two genes suggests that they evolved from a common ancestor by a gene duplication event.

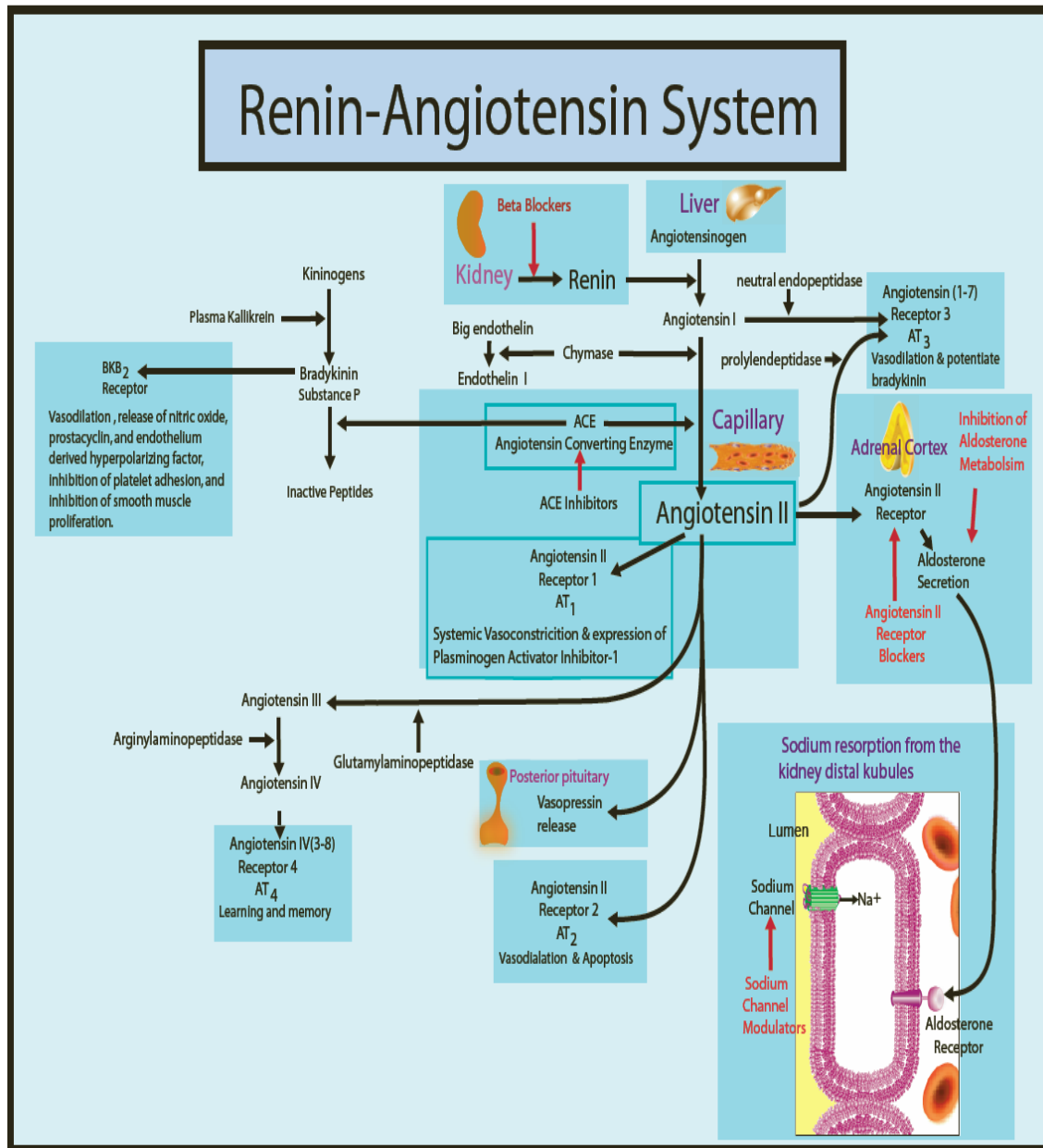


Fig. 1.8 Components and pathways involved in renin-angiotensin-kinin system.

1.7.2 Bradykinin B₂ receptor (B₂R)

B₂R is distributed in endothelial cells, vascular smooth muscle cells and cardiomyocytes. It mediates many physiological functions such as vasodilation, increased vascular permeability and cardiovascular protective mechanisms.

1.7.2.1 Ligand binding region of B₂R

Based on site-directed mutagenesis, ligand receptor cross-linking experiments and using anti-peptide antibodies against extracellular receptor domains, several residues have been identified that appear to be important for the binding of agonist and antagonist to the B₂R. These residues are depicted in Table 1.

Domain	Agonist		Antagonist		
	BK	FR190997	NPC/Icatib	LF16-0335	FR173657
N-terminus	Cys ²⁰				
TM2		Trp ⁸⁶			
TM3	Ser ¹¹¹	Ile ¹¹⁰	Ser ¹¹¹	Ile ¹¹⁰	Ile ¹¹⁰
TM4	Lys ¹⁷²				
TM6	Phe ²⁵⁹ , Thr ²⁶³	Phe ²⁵⁹		Trp ²⁵⁶	
EC3	Cys ²⁷⁷ , Asp ²⁶⁶ , Asp ²⁸⁴				
TM7	Gln ²⁸⁸				Gln ²⁸⁸ , Tyr ²⁹⁵

Table 1. Amino acids of B₂R, which are important for ligand binding (Leeb-Lundberg *et al.*, 2005).

1.7.2.2 Post-translational modifications of B₂R

Post-translational modifications of B₂R include glycosylation, disulfide bridge formation in the extracellular domains, palmitoylation and phosphorylation.

1.7.2.2.1 Glycosylation

B₂R has three potential N-linked glycosylation sites. These are N³ and N¹² at the N-terminus of the receptor and N¹⁸⁰ in the second extracellular loop. A previous study has shown that all three asparagines are glycosylated when the recombinant receptor was expressed in mammalian cells (Michineau *et al.*, 2004). However, the glycosylation is not required for receptor function.

1.7.2.2.2. Disulfide bridging

There are four cysteines in the extracellular loops of B₂R. These include C²⁰ (in the N-terminus), C¹⁰³ (in extracellular loop 1), C¹⁸⁴ (in extracellular loop 2), and C²⁷⁷ (in extracellular loop 3). Most members of GPCR superfamily have conserved cysteines in the extracellular loop 1 and 2. The crystal structure of rhodopsin revealed that these conserved cysteines are involved in a disulfide bridge formation. Although, there is indirect evidence of a disulfide bond between Cys¹⁰³ and Cys¹⁸⁴ in B₂R (Leeb-Lundberg *et al.*, 1995), reducing agents e.g. DTT, do not affect the binding of bradykinin to the B₂R.

1.7.2.2.3. Palmitoylation

The C-terminus of B₂R contains two potential sites for acylation (C³²⁴ and C³²⁹). A previous study has shown that both sites are palmitoylated (Pizard *et al.*, 2001). Mutation

of these sites has a negative effect on agonist induced receptor internalization but it does not affect ligand binding properties of the receptor.

1.7.2.2.4. Phosphorylation

Metabolic ^{32}P labeling experiments and phosphopeptide sequencing has identified three serine residues (Ser³³⁹, Ser³⁴⁶, and Ser³⁴⁸) at the C-terminus of B₂R which are major phosphorylation sites (Blaukat *et al.*, 2001). Ser³⁴⁸ shows constitutive phosphorylation while Ser³³⁹ and Ser³⁴⁶ are phosphorylated upon agonist stimulation. In addition, Thr³⁴² and Thr³⁴⁵ have also been identified as minor phosphorylation sites. Agonist induced phosphorylation of B₂R plays a role in receptor sequestration.

1.7.2.3 B₂R interactome

B₂R interacts with a number of proteins *in vivo* (Table 2). In addition to these proteins, B₂R is also known to form agonist induced homodimers (Abdalla *et al.*, 1999).

Interacting partner	Physiological significance	Reference
B ₁ R	- Increased constitutive and agonist stimulated receptor signalling. - Proteolytic degradation of B ₂ R	Kang <i>et al.</i> , 2004
AT1aR	- Enhanced G protein activation and altered receptor sequestration	Abdalla <i>et al.</i> , 2000
SHP2	- Antiproliferative effect	Duchene <i>et al.</i> , 2002
G(q/11) alpha	- G protein signalling	Kang <i>et al.</i> , 2000
Nitric oxide synthase 1 & 3	- Inhibition of receptor activation	Ju <i>et al.</i> , 1998

Table 2. Interacting partners of B₂R and physiological significance of their interactions.

1.7.3 Angiotensin II and its receptors

Angiotensin II is a potent vasoconstrictor. Its physiological functions include regulation of blood pressure, increased secretion of vasopressin and aldosterone, increased sodium resorption at the proximal tubules and cardiac muscle hypertrophy. Angiotensin II exerts its physiological effects mainly via two G protein-coupled receptors, AT₁R and AT₂R. The AT₁R and AT₂R are only ~30-35% homologous in the amino acid sequence but they have similar affinity for their endogenous ligand, angiotensin II. AT₁R has two distinct subtypes termed as AT_{1a}R and AT_{1b}R. These two receptor subtypes are ~95% identical in their amino acid sequences (Gou *et al.*, 1994). Although they have similar ligand binding and activation properties, they differ in their tissue distribution, chromosomal localization, genomic structure and transcriptional regulation.

1.7.4 Angiotensin II type 1 receptor (AT_{1a}R)

The human AT_{1a}R contains 359 amino acids and the gene is located on the q22 band of chromosome 3 (Tissir *et al.*, 1995). AT_{1a}R is expressed in a variety of cells including endometrial blood vessels, placenta, components of the renin-angiotensin system, vascular endothelial cells, renal vasculature and glomeruli. Activation of AT_{1a}R regulates smooth muscle contraction, aldosterone secretion, neuronal activation, neurosecretion, ion transport and cell growth.

1.7.4.1 Ligand binding region of AT_{1a}R

Based on site-directed mutagenesis and other biochemical experiments, a number of residues have been found to play important role in agonist and antagonist binding of AT_{1a}R (Fig. 1.9).

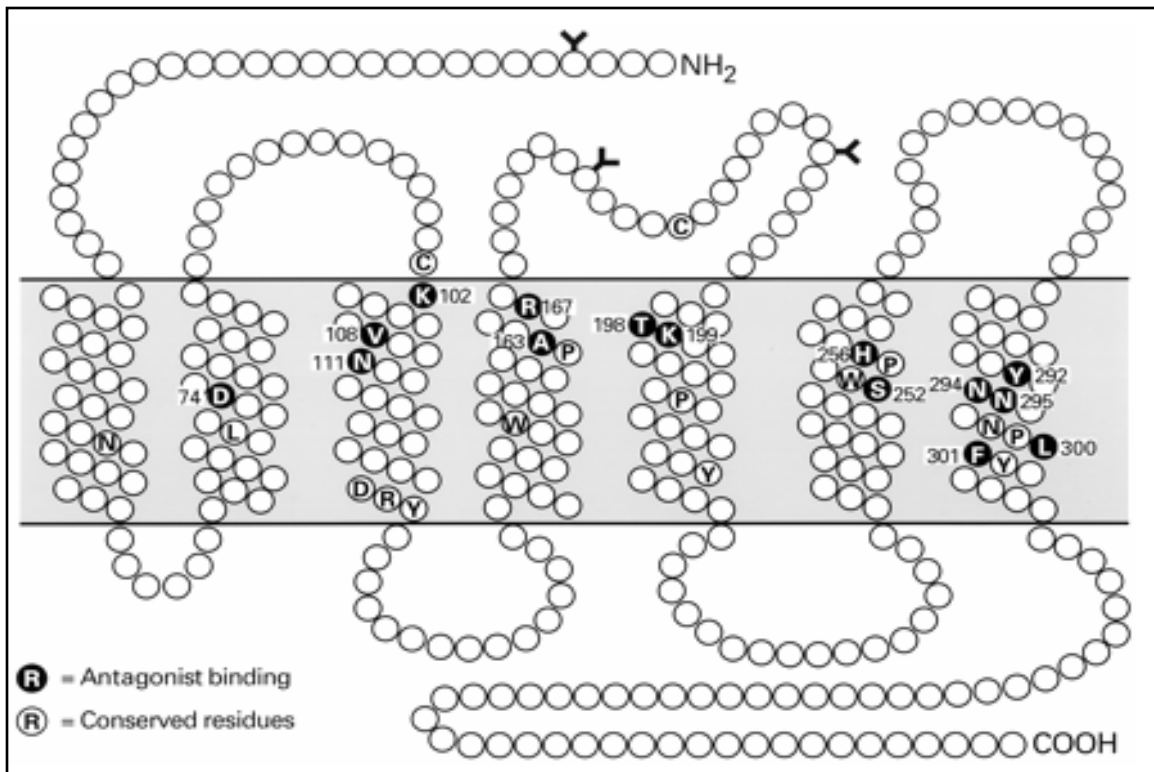
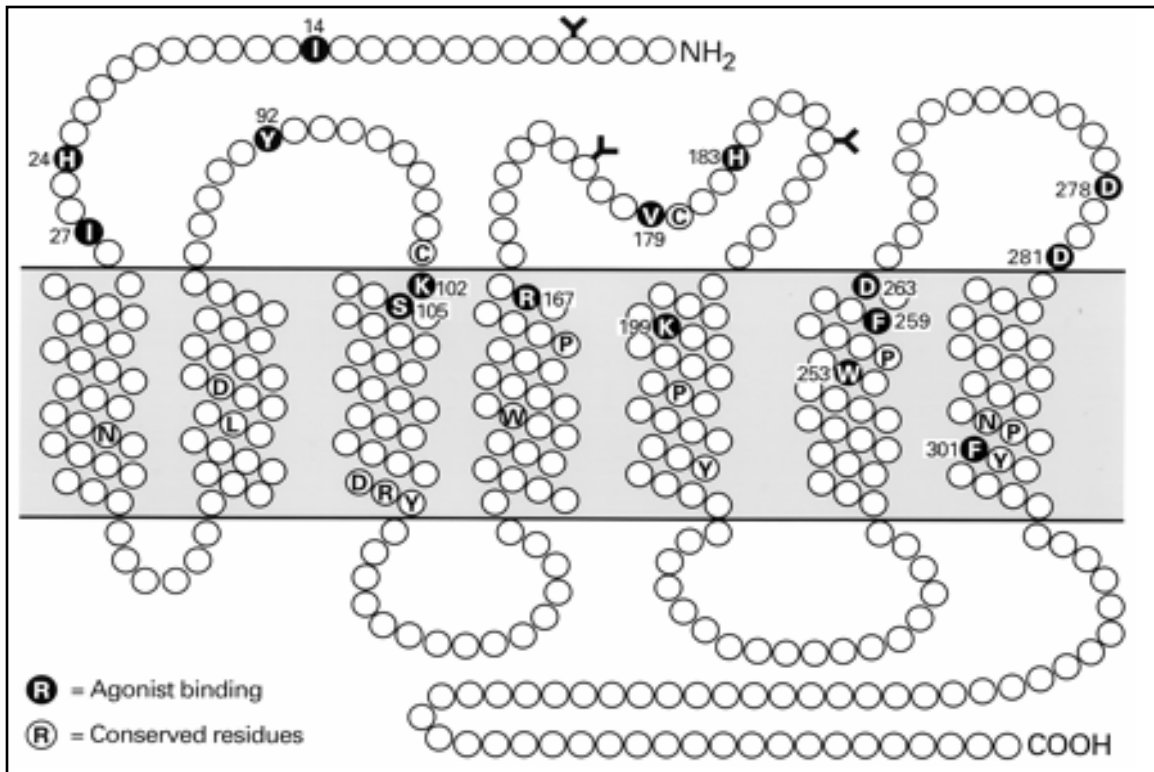


Fig. 1.9 Amino acids (shown in black) which contribute to the agonist binding site (top) and antagonist binding site of AT_{1a}R (bottom) (from De Gasparo *et al.*, 2000).

1.7.4.2 Post-translational modifications of AT_{1a}R

Post-translational modifications of AT_{1a}R include glycosylation, disulfide bond formation and phosphorylation.

1.7.4.2.1. Glycosylation

Human AT_{1a}R has three putative glycosylation sites (N⁴ at the N-terminus, N¹⁷⁶ and N¹⁸⁸ in second extracellular loop). A previous study has shown that all three sites are glycosylated when the recombinant receptor is expressed in mammalian cells (Jayadev *et al.*, 1999). Glycosylation of AT_{1a}R is crucial for its surface localization but does not affect ligand binding properties (Lancot *et al.*, 1999).

1.7.4.2.2 Disulfide bridge

Like other GPCRs, AT_{1a}R also has conserved cysteines in the extracellular loop 1 and 2. Reducing agents such as DTT, inhibit angiotensin II binding to the receptor (Chang *et al.*, 1982). This suggests that these cysteines are involved in a disulphide bridge formation, which is crucial for binding of the agonist to the receptor.

1.7.4.2.3. Phosphorylation

Based on site-directed mutagenesis experiments (Hunyady *et al.*, 1994), a cluster of serines has been identified in the c-terminus of AT_{1a}R that undergoes agonist induced phosphorylation (Fig.1.10).

1.7.4.3 AT_{1a}R interactome

AT_{1a}R interacts with a variety of intracellular proteins, which are listed in Table 3. In addition, agonist induced homodimerization of AT_{1a}R has also been reported (Abdalla *et al.*, 2004).

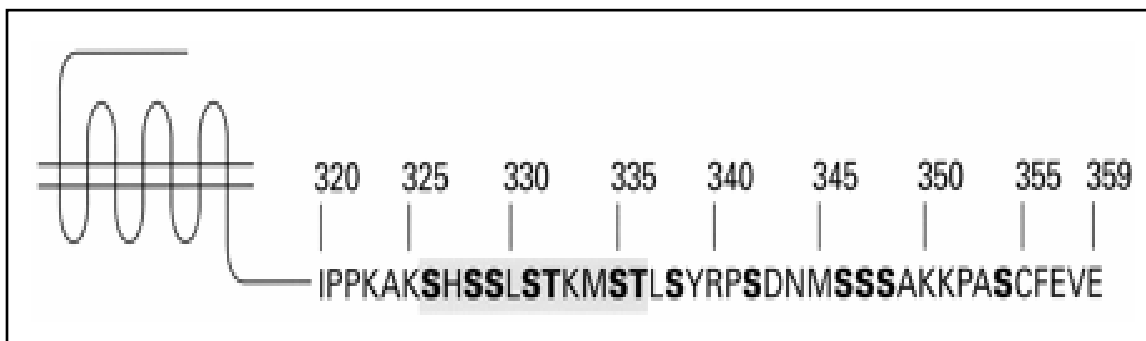


Fig. 1.11 The potential serine and threonine phosphorylation sites (shown in bold letters) in AT_{1a}R (from de Gasparo *et al.*, 2000).

Interacting partner	Physiological significance	Reference
G _{q/11} , G _{12/13} and G _{i/o}	- G protein signaling	Tian <i>et al.</i> , 1996 & Marcez <i>et al.</i> , 1997
B ₂ R	- Enhanced G protein activation and altered receptor sequestration	Abdalla <i>et al.</i> , 2000
Angiotensin II receptor associated protein	- Enhances internalization of AT _{1a} R	Cui <i>et al.</i> , 2000
Beta-arrestin 2	- Receptor downregulation	Oakley <i>et al.</i> , 2001
Janus kinase 2	- Stimulation of Jak/STAT pathway	Marrero <i>et al.</i> , 1995

Table 3. Interacting partners of AT_{1a}R & physiological significance of these interactions.

1.8 Neuromedin U and its receptors

Neuromedin U (NmU) is a neuropeptide that is found in almost all tissues with high levels in gastrointestinal tract and pituitary. NmU was originally isolated from porcine spinal cord (Kangawa *et al.*, 1983). Since then, NmU has been isolated and sequenced from many different species. NmU isoforms range from 8-25 amino acids but the C-terminal heptapeptide (Phe-Leu-Phe-Arg-Pro-Arg-Asn-NH₂) is entirely conserved (Fig.1.11). Asparagine-linked amidation at the C-terminus of NmU is crucial for its

bioactivity. Physiological roles of NmU include regulation of smooth-muscle contraction, blood pressure and local blood flow, ion transport in the gut, stress responses, cancer, gastric acid secretion, nociception and feeding behavior. NmU activates two G protein-coupled receptors, NmU₁R and NmU₂R. These receptors were orphanized recently (Howard *et al.*, 2000). Although these two receptors share 45 to 50% homology at the amino acid sequence level and bind to NmU with almost similar affinity, their tissue distribution differs significantly.

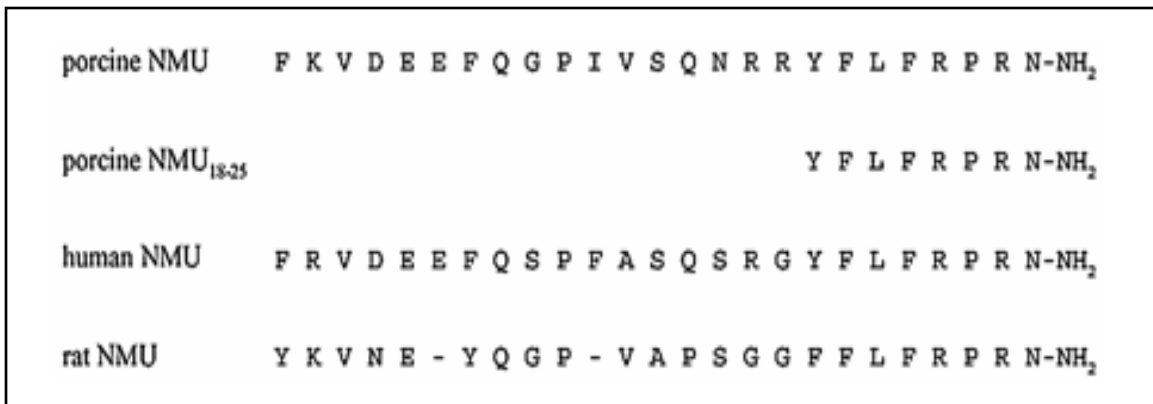


Fig. 1.12 Sequence alignment of NmU from different species (Brighton *et al.*, 2004) showing a conserved heptapeptide at the C-terminus.

1.8.1 Neuromedin U type 2 receptor (NmU₂R)

The gene for human NmU₂R is localized on chromosome 5q31.1-q31.3 (Raddatz *et al.*, 2000). NmU₂R is expressed in brain, spinal cord, thymus, thyroid and testis and mediate a variety of physiological roles of NmU.

1.8.2 Signalling pathway of NmU₂R

A recent study suggests that recombinant NmU₂R can couple to both G_{αq/11} and G_{αi} when expressed in HEK-293 cells (Brighton *et al.*, 2004). Receptor activation leads to pertussis toxin-insensitive activation of phospholipase C as well as pertussis toxin-sensitive inhibition of adenylyl cyclase.

1.8.3 Post-translational modification and receptor interactome

NmU₂R was identified only recently and there have not been many studies to characterize the post-translational modifications of this receptor. Based on the conserved sequence of the N-linked glycosylation motif, three putative glycosylation sites, two at the N-terminus (N⁹, N²⁷) and one in the third extracellular loop (N¹⁸⁰) have been predicted. Also, interactions of NmU₂R with other proteins as well as its dimerization properties have not yet been studied in detail.

1.9 Heterologous expression systems for GPCRs

Structural studies on membrane proteins require milligram quantities of pure, homogenous and stable samples. Initially, the structure determination was limited to naturally abundant membrane proteins. However, the development of molecular cloning and recombinant gene expression techniques has allowed large-scale production of recombinant membrane proteins. GPCRs are expressed in very low amounts in native tissues except rhodopsin, which is highly expressed and densely packed in the retinal membranes. Therefore, a number of expression systems have been used for heterologous expression of GPCRs. In some cases, large amounts of receptors have been produced and isolated for structural analysis. However, the choice of a suitable host is the crucial step. GPCRs, like many other membrane proteins, are largely hydrophobic and require proper lipid surrounding for correct folding and insertion into the membrane. GPCRs undergo a number of post-translational modifications such as glycosylation, palmitoylation and phosphorylation, which might be crucial for their proper function. All of these factors should be considered when selecting the appropriate host for overexpression of GPCRs.

1.9.1 *E. coli* expression system

There are several reports of successful overproduction of functional GPCRs in *E. coli*. These include the neurotensin receptor (Tucker *et al.*, 1996), the adenosine A_{2A} receptor (Weiss *et al.*, 2002), the muscarinic M₁ receptor (Hulme *et al.*, 1998), the opioid receptor

(Stanasila *et al.*, 1999), the substance K receptor (Muench *et al.*, 1995), the neuropeptide Y receptor (Hampe *et al.*, 2000) and the beta-2 adrenergic receptor (Grisshammer *et al.*, 1994). It has been possible to isolate large amounts of the neurotensin receptor and the adenosine A_{2A} receptor from *E. coli* using affinity chromatography (White *et al.*, 2004 and Weiss *et al.*, 2002). *E. coli* based expression is fast, easy, safe and scaleable. However, post-translational modifications of some GPCRs are required for their proper functioning e.g. the human prostacyclin receptor (Miggin *et al.*, 2003), the chemokine CCR8 receptor (Gutierrez *et al.*, 2004) etc. Therefore, this system can not be used for all GPCRs.

1.9.2 *Pichia pastoris* expression system

Pichia pastoris, a methylotrophic yeast, is capable of metabolizing methanol as its sole carbon source. The enzyme alcohol oxidase catalyzes the oxidation of methanol to formaldehyde and hydrogen peroxide. Due to the poor affinity of this enzyme for oxygen (K_m 0.1-1.0 mM) the yeast cells generate large amounts of this enzyme. In *Pichia pastoris*, two genes namely AOX1 and AOX2 code for alcohol oxidase. The AOX1 gene is responsible for approximately 95% of this enzyme in the cell. Expression of the AOX1 gene is tightly regulated and strongly induced by methanol. Therefore, the AOX1 promoter is widely used for heterologous expression of proteins in *Pichia pastoris*. Additionally, H₂O₂ produced during oxidation of methanol is highly toxic and in order to protect the cells, this oxidation of methanol takes place in the peroxisomes. The α -factor prepro-peptide (a secretion signal peptide from the *Saccharomyces cerevisiae*) is most commonly used for membrane insertion of recombinant membrane proteins. Major advantages of *Pichia pastoris* as an expression system are the strong AOX1 promoter, high cell mass generated by fermentation, stable insertion of heterologous genes in *Pichia pastoris* genome and the ability of *Pichia pastoris* to perform post-translational modifications such as glycosylation, phosphorylation, palmitoylation and disulphide bond formation (reviewed in Macauley-Patrick *et al.*, 2005).

GPCRs that have been produced successfully in *Pichia pastoris* include the human dopamine D_{2S} receptor (Grünewald *et al.*, 2004), the CB₂ cannabinoid receptor

(Feng *et al.*, 2002), the μ -opioid receptor (Sarramegna *et al.*, 2002), and the endothelin-B receptor (Schiller *et al.*, 2000). The main problems associated with this system are proteolytic degradation of the target protein in some cases, mistargeting of the recombinant membrane proteins and different glycosylation (Cereghino *et al.*, 2000) compared to the mammalian cells.

1.9.3 Baculovirus expression system

In this system, protein production results from the infection of insect cells by recombinant baculovirus encoding the gene(s) that has to be expressed. The gene of interest is inserted into a plasmid transfer vector that is introduced into the genome of a baculovirus by homologous recombination. In most cases, a very strong polyhedrin promoter is used for recombinant protein expression. Recent development of the MultiBac system (Berger *et al.*, 2004) offers the possibility of heterologous production of multiple subunits of membrane protein complexes in this system. Insect cells are semi-adherent, can grow in suspension and they can be adapted to serum-free media for large-scale production of recombinant proteins using bioreactors. Cells derived from *Spodoptera frugiperda* ovarian tissue (Sf9 and Sf21) are the most widely used cell lines. High Five™ cells from *Trichoplusia ni* grow faster than Sf9/Sf21 cells and now they are also being used for rapid production of recombinant proteins. Insect cells are able to perform post-translational modifications identical to those of mammalian cells and in most cases, the recombinant proteins exhibit characteristics very similar to their native counterparts.

Several GPCRs have been produced using the baculovirus system (Akermoun *et al.*, 2005, Sarramegna *et al.*, 2003 and reviewed in Massotte *et al.*, 2003). One of the problems associated with this expression system is the lipid composition of the plasma membranes of insect cells. The plasma membrane of these cells contains mainly unsaturated lipids and only low amounts of cholesterol. This is probably to ensure the membrane fluidity as the growth temperature ranges from 27 to 28 °C. However, for some GPCRs, membrane lipid composition is crucial for ligand binding. In case of the human oxytocin receptor (Gimpl *et al.*, 1995) and the human histamine H₂ receptor

(Beukers *et al.*, 1997), it was found that recombinant receptors were expressed in a low-affinity state in Sf9 cells. Addition of cholesterol to the isolated membranes increased the ligand binding affinity of these receptors. Also, in some cases, overexpression of GPCRs leads to their intracellular retention and accumulation of inactive receptors (Vasudevan *et al.*, 1991, and Grünewald *et al.*, 1996).

1.9.4 Semliki Forest Virus (SFV) system:

SFV is an enveloped single stranded RNA virus and a member of the alpha virus family. This expression system is based on a modified cDNA copy of the SFV viral genome where the genome is split and introduced into two plasmid vectors (Liljestrom *et al.*, 1991). The first plasmid is the cloning vector and contains the four non-structural SFV genes (nsP1-4). The subgenomic 26S promoter is located at the 3' end of the nsP4 gene and drives the expression of the foreign gene that is placed downstream of the nsP4. The second plasmid is the helper vector that contains the SFV structural genes. Structural genes are translated as a polyprotein (C-E3-E2-6K-E1) where C refers to the capsid protein and E3, E2, 6K and E1 refer to the envelope proteins. The E3 and E2 proteins are derived from their precursor (p62) by the activity of the host cell protease (Liljestrom *et al.*, 1994). For the expression of recombinant protein, mRNA from the two vectors (from the cloning vector and the helper vector) is synthesized by *in vitro* transcription and transfected into BHK cells by electroporation. Coelectroporation of these two RNA species leads to *in vivo* packaging of recombinant SFV particles. However, only the replicase-containing RNA i.e. RNA derived from cloning vector is packaged into viral particles, as the helper vector does not contain the packaging signal. As a result, upon infection of the host cells, only heterologous gene products are expressed and no new virus particles are generated. In the helper vector, three point mutations have been introduced in the p62 gene, which do not allow its intracellular cleavage (Smerdou *et al.*, 1999). This leads to conditionally infectious virus particles, which require *in vitro* activation by α -chymotrypsin treatment.

Mammalian cells provide most natural environment for the expression of recombinant human GPCRs. In these cells, the post-translational modifications are

efficiently performed and a relatively high percentage of the total recombinant protein is functional. Several GPCRs have been produced in mammalian cells using the SFV system (reviewed in Lundstrom *et al.*, 2003 and Hassaine *et al.*, 2005).

However, safety concerns and high costs of virus production limit the use of this system for large-scale expression of GPCRs in general.

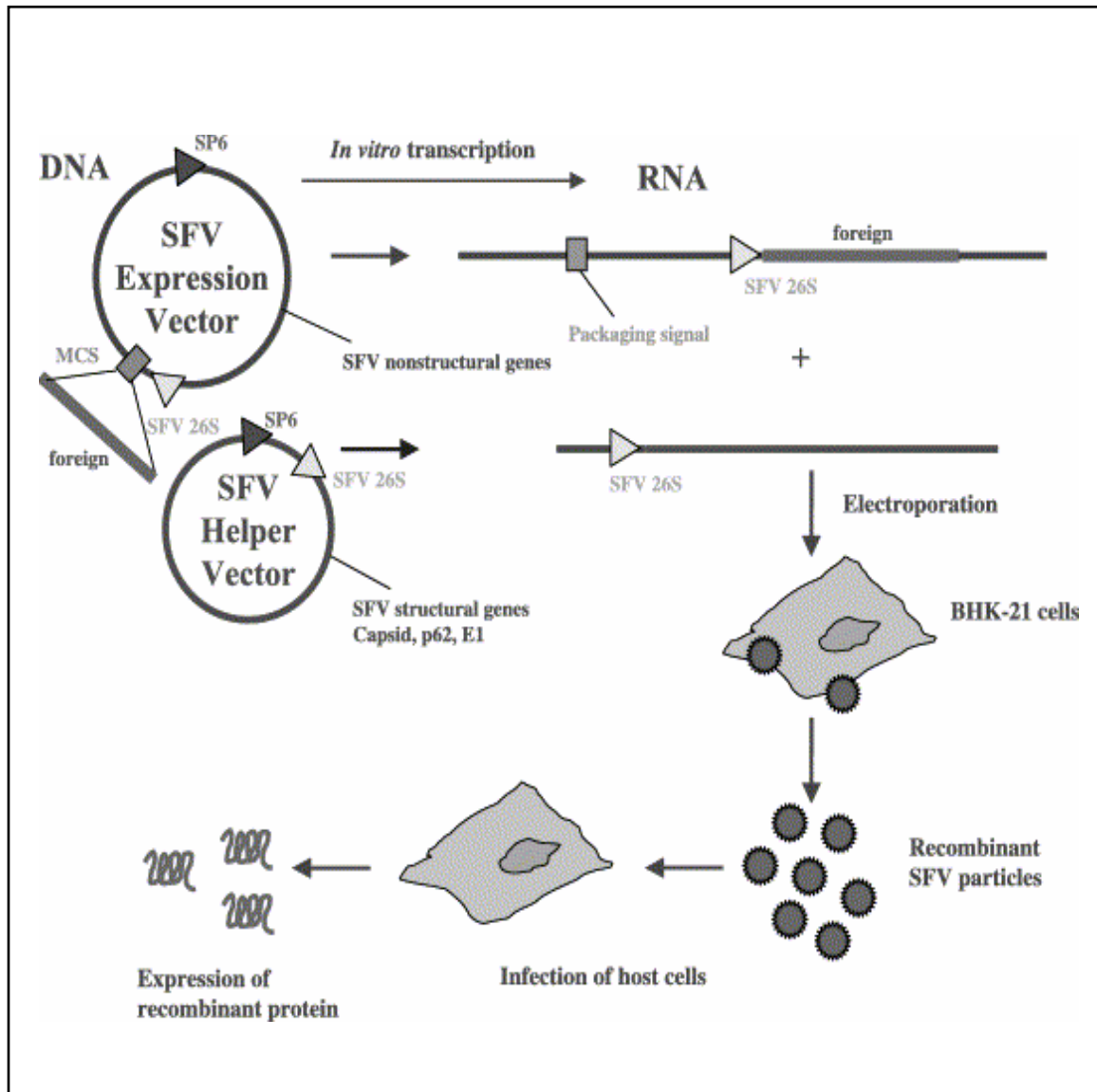


Fig. 1.13 Schematic representation of recombinant protein expression using SFV system (from Lundstrom *et al.*, 2003).

1.10 Aim of the project

1.10.1 Production, characterization and isolation of recombinant GPCRs

The aim of this project was to produce and isolate large amounts of three different G protein-coupled receptors namely the human bradykinin B₂ receptor (B₂R), the human angiotensin II type1 receptor (AT_{1a}R) and the human neuromedin NmU₂ receptor (NmU₂R). Three different host systems (i.e. *Pichia pastoris*, Baculovirus system and Semliki Forest Virus system) should be tested in order to select the most suitable system for the production of functional recombinant receptors. Recombinant receptors should be biochemically characterized in terms of their ligand binding capacity, glycosylation and localization in the host cells. Subsequently, the recombinant receptors should be functionally solubilized and purified by affinity chromatography. Homogeneity and stability of the purified receptors should also be evaluated.

1.10.2 Structural characterization of recombinant GPCRs

Isolated receptor samples should be used for structural characterizations that include three-dimensional crystallization trials and solid-state NMR studies. 3-Dimensional crystallization attempts aim to determine the structure of receptors while solid-state NMR experiments should provide insights into the receptor bound conformation of peptide ligands.

1.10.3 Interaction of recombinant GPCRs with their binding partners

Interaction of recombinant receptors with their binding partners should be investigated in order to reconstitute a complex of the receptor with an interacting protein. This attempt aims to stabilize the receptors and to increase their polar surface area that is available to make crystal contacts.

Chapter 2: Materials and Methods

2.1 Materials

2.1.1 General chemicals

General chemicals which are not listed below were purchased from the companies Sigma-Aldrich Chemie GmbH, Deisenhofen, Carl Roth & Co. KG, Karlsruhe or Merck KgaA, Darmstadt.

Acrylamide ready-made solution for polyacrylamide gels	Carl Roth GmbH&Co. KG, Karlsruhe
Agarose, electrophoresis grade	Bethesda Research Laboratories GmbH, Neu Isenburg
Ammonium-persulfate (APS)	Serva Elektrophoresis GmbH, Heidelberg
Ampicillin, sodium salt	Carl Roth GmbH&Co. KG, Karlsruhe
Bacto agar	Difco Laboratories, Detroit, Michigan, USA
Bacto tryptone	Difco Laboratories, Detroit, Michigan, USA
Bacto yeast extract	Difco Laboratories, Detroit, Michigan, USA
Biotin	Serva Elektrophoresis GmbH, Heidelberg
Bovine serum albumin (BSA)	Sigma-Aldrich Chemie GmbH, Deisenhofen
5-Bromo-4-chloro-3-indolylphosphate 4-toluidine salt (BCIP)	Biomol Feinchemikalien GmbH, Hamburg
Bromophenol blue	Sigma-Aldrich Chemie GmbH, Deisenhofen
Coomassie brilliant blue R-250	Serva Elektrophoresis GmbH, Heidelberg
Deoxynucleoside-5'-triphosphates (dATP, dGTP, dTTP, dCTP)	MBI Fermentas GmbH, St. Leon-Rot
1,4-dithiothreitol (DTT)	Serva Elektrophoresis GmbH, Heidelberg
Ethidium bromide	Bio-Rad Laboratories GmbH, Munich
Ethylene diamine tetra acetic Acid (disodium salt) (EDTA)	GERBU Biotechnik GmbH, Gaiberg
Genitacin sulfate G418	Novabiochem GmbH, Bad Soden/Ts.
Glass beads (0.5 mm)	Biomatik GmbH, Frankfurt
Glutaraldehyde	Sigma-Aldrich Chemie GmbH, Deisenhofen

Glycine	Serva Elektrophoresis GmbH, Heidelberg
Kanamycin	Carl Roth GmbH&Co. KG, Karlsruhe
Non-fat milk powder	Carl Roth GmbH&Co. KG, Karlsruhe
N,N,N',N'-tetramethylethyldiamine (TEMED)	Sigma-Aldrich Chemie GmbH, Deisenhofen
Nitrobluetetrazolium, toluidine salt (NBT)	Biomol Feinchemikalien GmbH, Hamburg
Peptone	Sigma-Aldrich Chemie GmbH, Deisenhofen
Phenol	Carl Roth GmbH&Co. KG, Karlsruhe
Polyethyleneglycol 400	Serva Elektrophoresis GmbH, Heidelberg
Polyethyleneglycol 4000	Serva Elektrophoresis GmbH, Heidelberg
Polyethyleneimine (PEI)	Sigma-Aldrich Chemie GmbH, Deisenhofen
Silver nitrate (AgNO ₃)	Sigma-Aldrich Chemie GmbH, Deisenhofen
Tetracycline-hydrochloride	Sigma-Aldrich Chemie GmbH, Deisenhofen
Tris-(hydroxymethyl)-aminomethane	Carl Roth GmbH&Co. KG, Karlsruhe
Tunicamycin	Sigma-Aldrich Chemie GmbH, Deisenhofen
Yeast nitrogen base (YNB), w/o amino acids, w/o ammonium-sulfate	Difco Laboratories, Detroit, Michigan, USA

2.1.2 Radioactive labeled chemicals

[³ H] bradykinin	NEN Life Science Products, Boston, USA
[³ H] angiotensin II	Amersham Biosciences, USA
[¹²⁵ I] neuromedin U	Amersham Biosciences, USA
[³ H] inositol phosphate	NEN Life Science Products, Boston, USA

2.1.3 Detergents

Sodium-dodecyl-sulfate (SDS)	Carl Roth GmbH&Co. KG, Karlsruhe
Digitonin	Sigma-Aldrich Chemie GmbH, Deisenhofen

Deoxycholate, sodium salt	Sigma-Aldrich Chemie GmbH, Deisenhofen
n-Dodecyl- β -D-maltoside (LM)	Glycon Biochemicals, Luckenwalde
n-Decyl- β -D-maltoside (DM)	Glycon Biochemicals, Luckenwalde
n-Undecyl- β -D-maltoside (UM)	Glycon Biochemicals, Luckenwalde
n-Octyl- β -D-glucoopyranoside (OG)	Glycon Biochemicals, Luckenwalde
n-nonyl- β -D-glucoopyranoside (NG)	Glycon Biochemicals, Luckenwalde
n-Dodecylphosphocholine, Fos12	Anatrace, Maumee, OH, USA
n-Tetradecylphosphocholine, Fos14	Anatrace, Maumee, OH, USA
n-Hexadecylphosphocholine, Fos16	Anatrace, Maumee, OH, USA
Tween 20	Koch-Light Ltd., Haverhill, England

2.1.4 Protease inhibitors

Aprotinin	Biomol Feinchemikalien GmbH, Hamburg
Benzamidine	Sigma-Aldrich Chemie GmbH, Deisenhofen
Leupeptin	Calbiochem GmbH, Bad Soden
Pepstatin A	Serva Elektrophoresis GmbH, Heidelberg
Phenylmethylsulfonylfluoride (PMSF)	Carl Roth GmbH&Co. KG, Karlsruhe
Complete (EDTA free)	Roche Diagnostis GmbH, Mannheim
E64	Biomol Feinchemikalien GmbH, Hamburg

2.1.5 Chromatographic matrices and prepacked columns

Anti-Flag M1/M2 affinity resin	Sigma-Aldrich Chemie GmbH, Deisenhofen
ImmunoPure immobilized monomeric avidin gel	Pierce, Rockford, USA
Ni-NTA matrix	Qiagen GmbH, Hilden
Streptactin agarose	IBA, Göttingen, Germany
Superose TM 6 PC 3.2/30	Amersham Pharmacia Biotech, Freiburg
Dowex AG1-X8 columns	Bio-Rad Laboratories GmbH, Munich

2.1.6 Enzymes

Restriction endonucleases	MBI Fermentas GmbH, St. Leon-Rot New England Biolabs GmbH, Schwalbach
<i>Pfu</i> DNA polymerase	Stratagene GmbH
DNA ligase	New England Biolabs GmbH, Schwalbach
SP6 RNA polymerase	MBI Fermentas GmbH, St. Leon-Rot

2.1.7 Antibodies

Anti-Flag M2 monoclonal antibody	Sigma-Aldrich Chemie GmbH, Deisenhofen
Anti-his monoclonal antibody	Sigma-Aldrich Chemie GmbH, Deisenhofen
AP conjugated streptavidin	Sigma-Aldrich Chemie GmbH, Deisenhofen
Anti-mouse IgG, AP conjugated	Sigma-Aldrich Chemie GmbH, Deisenhofen
Anti-B ₂ R antibody	Calbiochem GmbH, Bad Soden
Anti-AT ₁ R antibody	Calbiochem GmbH, Bad Soden
Anti-rabbit IgG, HRP conjugated	Sigma-Aldrich Chemie GmbH, Deisenhofen

2.1.8 Kits

Qiagen plasmid mini and maxiprep kit	Qiagen GmbH, Hilden
Qiaquick gel extraction kit	Qiagen GmbH, Hilden
Qiaquick PCR purification kit	Qiagen GmbH, Hilden
BCA protein assay kit	Pierce, Rockford, USA

2.1.9 Marker proteins

Pre-stained protein marker	New England Biolabs GmbH, Schwalbach
Lambda DNA (for <i>Eco</i> RI+ <i>Hind</i> III DNA marker)	New England Biolabs GmbH, Schwalbach

2.1.10 Buffers and Solutions

Agarose gel (1%)	1.0 g agarose 100 ml 1xTAE buffer 2.5 µl EtBr (10mg/ml)
Ampicillin stock solution (1000x)	100 mg/ml in H ₂ O (sterile filtered, stored at -20°C)
AP buffer	100 mM Tris/HCl, pH 9.5 100 mM NaCl 5 mM MgCl ₂
Aprotinin (40x)	20 mg/ml in PBS
APS	10% (w/v) in H ₂ O
BCIP-solution	50 mg BCIP/ml DMF (stored at -20°C)
Benzamidine (100x)	100 mM in H ₂ O
Binding assay buffer	50 mM Hepes, pH 7.4 100 mM NaCl 2 mM EDTA, 0.1% BSA
Breaking buffer	50 mM Na ₂ HPO ₄ , pH 7.4 100 mM NaCl 5 mM EDTA Protease inhibitors
Coomassie solution	1.25 g Coomassie brilliant blue R250 200 ml H ₂ O 50 ml acetic acid 250 ml methanol
Conditioner (silver gels)	400 mM sodium-acetate, pH 6.0 0.5 % (v/v) glutaraldehyde 0.1% (w/v) Na ₂ S ₂ O ₃ 30% (v/v) ethanol

Destaining solution (coomassie gels)	40% methanol 10% acetic acid 50% H ₂ O
Developer (silver gels)	2.5% (w/v) Na ₂ CO ₃ 0.04% (v/v) formaldehyde
Fixer (silver gels)	30% ethanol 10% acetic acid
Kanamycin stock solution	30 mg/ml in H ₂ O, stored at -20°C
Leupeptin (500X)	0.25 mg/ml in H ₂ O
Loading buffer 4X (SDS-PAGE)	0.25 mM Tris/HCl, pH 6.8 40% (w/v) glycerol 20% (v/v) β-mercaptoethanol 8% (w/v) SDS 0.004% (w/v) bromophenol blue
Loading buffer (DNA)	50 mM Tris/HCl, pH 7.4 5 mM EDTA 50% (v/v) glycerol 0.05% (w/v) bromophenol blue
NBT solution	50 mg NBT/ml in 70% DMF, stored at 4°C
Pepstatin A (500X)	0.35 mg/ml in methanol
PMSF (200X)	200 mM in isopropanol
Running buffer 10X (SDS -PAGE)	500 mM Tris/HCl 1.92 M glycine 1% (w/v) SDS
NTP mix (<i>in vitro</i> transcription)	10 mM ATP 10 mM CTP 10 mM UTP 5 mM GTP
Staining solution (silver gels)	0.1% (w/v) AgNO ₃ 0.025% (v/v) formaldehyde

TAE buffer (50X)	2 M Tris/HCl 1 M acetic acid 50 mM EDTA, disodium salt
TBST buffer	10 mM Tris/HCl, pH 8.0 150 mM NaCl 0.1% Tween-20
Tetracycline stock solution	12.5 mg/ml in 50% ethanol, stored at -20°C
Transfer buffer 5X (Immunoblot)	190 mM glycine 50 mM Tris
Transfer buffer 1X (Immunoblot)	38 mM glycine 10 mM Tris 20% (v/v) methanol
Solubilization buffer	50 mM Hepes, pH 7.4 100 mM NaCl Protease inhibitors Detergents (as indicated in the results section)

2.1.10.1 Buffers for purification

Equilibration buffer (Ni-NTA)	50 mM Hepes, pH 7.4 100 mM NaCl Detergent (3-5x cmc) 5-10 mM Imidazole, pH 7.4
Washing buffer (Ni-NTA)	50 mM Hepes, pH 7.4 100 mM NaCl Detergent (3-5x cmc) 40-60 mM Imidazole
Elution buffer (Ni-NTA)	50 mM Hepes, pH 7.4 100 mM NaCl Detergent (3-5x cmc) 200 mM Imidazole

Equilibration buffer &	50 mM Hepes, pH 7.4
Washing buffer (Mono. avidin)	100 mM NaCl Detergent (3-5x cmc) 2-5 mM EDTA, pH 7.4
Elution buffer (Mono. avidin)	Washing buffer + 2-5 mM Biotin
Equilibration buffer &	50 mM Hepes, pH 7.4
Washing buffer (Streptactin)	150 mM NaCl Detergent (3-5x cmc) 1-2 mM EDTA, pH 7.4
Elution buffer (Streptactin)	Washing buffer + 2.5-5.0 mM desthiobiotin
Equilibration buffer &	50 mM Hepes, pH 7.4
Washing buffer	100 mM NaCl
(Anti-Flag matrix)	Detergent (3-5x cmc) 2-5 mM EDTA, pH 7.4
Elution buffer	10 mM Glycine, pH 2.8
(Anti-Flag matrix)	100 mM NaCl, 2-5 mM EDTA, pH 7.4 Detergent (3-5x cmc)
Regeneration buffer	10 mM Glycine, pH 2.8

2.1.11 *E. coli* strain and culture medium

E. coli strain XL1-blue

endA1, hsdR17 (rk-, mk+), supE44, thi-1, λ^- , recA1, gyrA96, relA1, Δ (lacZYA-argF) U169 [F': proAB, lacI^q Z Δ M15, Tn10(Tet^r)]. Stratagene GmbH, Heidelberg.

E. coli strain DH5-alpha

F'phi80lacZ, delta(lacZYA-argF)U169, deoR, recA1, endA1, supE 44, λ -thi-1, gyrA96, relA1/F', proAB+, lacIqZdeltaM15 Tn10(tetr). Stratagene GmbH, Heidelberg.

LB medium

Bacto tryptone	10 g/l
Bacto yeast extract	5 g/l
NaCl	5 g/l
Bacto agar	15 g/l (for the plates)

SOB medium

Bacto tryptone	20 g/l
Bacto yeast extract	5 g/l
NaCl	10 mM
KCl	2.5 mM

SOC medium

Bacto tryptone	20 g/l
Bacto yeast extract	5 g/l
NaCl	10 mM
KCl	2.5 mM
MgCl ₂	10 mM
MgSO ₄	10 mM
Glucose	20 mM

FSB (Frozen storage buffer)

Sodium-acetate	10 mM
Glycerol	10% (w/v)
KCl	100 mM
MnCl ₂ x4H ₂ O	45 mM
CaCl ₂ x2H ₂ O	10 mM
HACoCl ₃	3 mM

2.1.12 *Pichia pastoris* strain and culture medium

SMD1163: Mut⁺, His⁻, protease-deficient (his4, pep4, prb). Invitrogen Inc., San Diego
Culture media as described in Multi-Copy *Pichia* expression kit (K1750-01).

2.1.13 Insect cell lines and culture medium

Sf9 cells	American Type Tissue Collection, USA
Sf21 cells	Aventis Pharma, Frankfurt am Main
High Five™ cells	Aventis Pharma, Frankfurt am Main
TNM-FH medium	ccPro, Neustadt
FKS	GibcoBRL, Life Technologies GmbH,
L-glutamine	GibcoBRL, Life Technologies GmbH,
Gentamycin	ccPro, Neustadt
Vitamin B12	Sigma Chemie GmbH, Deisenhofen
Pluronic-68	Sigma Chemie GmbH, Deisenhofen

2.1.14 Mammalian cell lines and culture medium

BHK cells	European Collection of Cell Cultures, UK
CHO cells	Aventis Pharma, Frankfurt am Main
HEK-293 cells	Aventis Pharma, Frankfurt am Main
HF-15 cells	Dr. Werner Mueller-Esterl, Frankfurt
Dulbecco's modified eagle's medium (DMEM)	Cell Concepts, Umkirch, Germany
Iscove's medium	Cell Concepts, Umkirch, Germany
Trypsin-EDTA	Cell Concepts, Umkirch, Germany

2.1.15 General apparatus

Cell mill	BioMatik GmbH, Germany
Electroporation device	Bio-Rad, Munich
Microscope	Olympus Inc., Japan
Shakers	Infors AG, Bottmingen, Switzerland
Spectrophotometer	Thermo Spectronic, Cambridge, UK
Vortexer	Bender&Hobein AG, Zürich, Switzerland
Thermomixer 5436	Eppendorf GmbH, Hamburg

2.1.16 Centrifuges

Sorvall RC-5B	Sorvall, Bad Homburg
Avanti J-20 XPI	Beckman-Coulter, Fullerton, CA, USA
Optima LE-80K ultracentrifuge	Beckman-Coulter, Fullerton, CA, USA
Tabletop ultracentrifuge TL100	Beckman Instruments Inc., Palo Alto, USA
Microfuge 5415D	Eppendorf GmbH, Hamburg
Sigma tabletop centrifuge	Sigma-Aldrich Chemie GmbH, Deisenhofen

2.1.17 Filters & membranes

GF/C filters for binding assay	Whatman Intl. Ltd, Maidstone, England
1,2 µM membranes RA	Millipore GmbH, Eschborn
0,45 µM membranes HA	Millipore GmbH, Eschborn
Small filters 0,22 µm and 0,45 µm	Schleicher&Schuell GmbH, Dassel
Immobilon-P poly vinylidene difluoride (PVDF) membranes	Millipore GmbH, Eschborn

2.1.18 Primers

2.1.18.1 For cloning

B₂R_Pichia_Fw	5'-CGGGATCCCTCAATGTCACCTTGCAAGGGCCCA-3'
B₂R_Pichia_Rv	5'-CGGAATTCCTGTCTGCTCCCTGCCCAGTCCT-3'
B₂R_Baculo_Fw	5'-CGGGATCCCCTCAATGTCACCTTGCAAGGGCCC-3'
B₂R_Baculo_Rv	5'-CGGAATTCCTGTCTGCTCCCTGCCCAGTCCT-3'
B₂R_SFV_Fw	5'-CGGGATCCCTCAATGTCACCTTGCAAGGGCCC-3'
B₂R_SFV_Rv	5'-CGATCAGTCTGTCTGCTCCCTGCCCAGTCCT-3'
NmU₂R_Pichia_Fw	5'-CGACTAGTTCAG GGATGGAAAACTTCAGAA-3'
NmU₂R_Pichia_Rv	5'-GG GAATTCGGTTTTGTAAAGTGGAAGCT TTG-3'
NmU₂R_SFV_Fw	5'-CGGGGCCTCAG GGATGGAAAACTTCAGAA-3'
NmU₂R_SFV_Rv	5'-GGACTAGGGTTTTGTAAAGTGGAAGCT TTG-3'
AT_{1a}R_Pichia_Fw	5'-CGGGATCCCATTCTCAACTCTTCTACTGAAG-3'
AT_{1a}R_Pichia_Rv	5'-CGGAATTCCTCAACCTCAAAACATGGTGC-3'
AT_{1a}R_Baculo_Fw	5'-CGGGATCCCCATTCTCAACTCTTCTACTGAAG-3'
AT_{1a}R_Baculo_Rv	5'-CGGAATTCCTCAACCTCAAAACATGGTGC-3'
AT_{1a}R_SFV_Fw	5'-CGGGATCCCATTCTCAACTCTTCTACTGAAG-3'
AT_{1a}R_SFV_Rv	5'-CGACTAGTCTCAACCTCAAAACATGGTGC-3'

2.1.18.2 For sequencing

pPIC9K based constructs

Alpha_Fw	5'-CTACTATTG CCAGCATTGCTGC-3'
AOX1_Rv	5'-GGCAAATGGCATTCTGACATCC-3'

SFV constructs

CAP_Fw	5'-CTG TCGGTG GTCACC TGG-3'
CAP_Rv	5'-CGCGGGCGCCACCGGCGG-3'

Baculovirus constructs

Bac_Fw 5'-AATGATAACCATCTCGCAAATAAATAAG-3'

Bac_Rv 5'-GAGGAACTTCAAAGGGACCACAAGTTTC-3'

2.2 Methods

2.2.1 *E. coli* cultivation and preparation of competent cells

A single colony of *E. coli* XL1-blue or DH5-alpha was inoculated into 3-5 ml of LB medium with appropriate antibiotic. The culture was incubated overnight at 37°C and 225 rpm. Large (50-100 mL) *E. coli* cultures were started from the small overnight pre-culture. Competent *E. coli* cells were prepared according to the TFB (transformation buffer) based chemical transformation protocol (Hanahan *et al.*, 1991). The *E. coli* cells were grown in LB medium overnight. The cells were then cooled on ice for 15 min, pelleted for 15 min at 1000 g and resuspended in 1/3 of the culture volume of TFB. Following resuspension, the cells were incubated on ice. Afterwards, the cells were pelleted (1000 g, 4°C, 15 min), and resuspended in 1/12.5 of the original culture volume of FSB (frozen storage buffer). DMSO was added (7 µl to 200 µl suspension) and the suspension was swirled with a pipette. The cells were incubated on ice for 5 min, a second aliquot of DMSO was added, followed by 15 min incubation on ice. The suspension was aliquoted 200 µl each in pre-cooled eppendorf tubes and flash frozen in liquid nitrogen. The aliquots were stored at -80°C.

2.2.2 DNA transformation and isolation

Competent *E. coli* cells were thawed on ice and 200 µl of cell suspension was mixed with 10 µl of the ligation reaction or plasmid DNA. After 30 min incubation on ice, the cells were subjected to heat shock at 42°C for 2 min. Cells were incubated on ice for 5 min after the heat shock. Subsequently, 800 µl of SOC medium was added and the cells were incubated for 45-60 min at 37°C with shaking. 100 µl of the suspension was plated on an LB plate containing the appropriate antibiotic and the plate was incubated overnight at

37° C. Isolation of plasmid DNA from *E. coli*, purification of PCR products and extraction of DNA fragments from the agarose gel were carried out according to the instructions in the relevant Qiagen kits.

2.2.3 Restriction digestion of DNA and ligation

Restriction digestions of plasmid DNA were performed according to the specifications of restriction endonucleases (as mentioned in manufacturer's protocol). Ligation of DNA fragments and vectors were carried out using T4 DNA ligase following the instructions in manufacturer's protocol.

2.2.4 *Pichia pastoris* culture, preparation of competent cells and transformation

As described in Multi-Copy *Pichia* expression kit (K1750-01, Invitrogen).

2.2.5 Clone selection and expression in *Pichia pastoris*

Selection of *Pichia* clones on G 418 plates were done as described in Multi-Copy *Pichia* expression kit (K1750-01) but lower concentrations of G 418 was used (0.025 mg/ml-0.5 mg/ml). For test expression, pre-cultures were inoculated in BMGY from single colony and grown overnight at 30°C. Secondary cultures were inoculated (starting O.D. 1) in BMMY, grown at indicated temperatures (22°C or 30°C) and 0.5% methanol was added 6 h before harvesting.

2.2.6 Insect cell culture

Monolayers of Sf9 and Sf21 cells were grown in TNM-FH medium supplemented with 5% FKS, 2 mM glutamine and vitamin B₁₂. For suspension culture, 0.1% pluronic was added to the culture medium. High Five™ cells were grown in Express Five™ medium supplemented with 100 ml glutamine (100X). Cells were maintained at 27°C. Suspension cultures were grown in Erlenmeyer flasks at 27°C with shaking at 125 rpm.

2.2.6.1 Transfection

Transfection reaction was set up as follows:

Expression vector DNA	0.5 µg (5µl)
BacuGold DNA	0.1 µg (1µl)
Lipofectin	30 µg (5 µl)
H ₂ O	39µl

Reaction mixture was incubated at room temperature for 15 minutes and then 1 ml medium (without FKS) was added to this reaction. Subsequently, the reaction mix was added to Sf9 cells (approximately 1.28×10^6 cells, in medium with no FKS) in six well plates. After 4 hours, medium with 10% FKS was added to the cells. Supernatant was collected after 7 days, centrifuged down and used for plaque assay.

2.2.6.2 Plaque assay

Supernatant was diluted (10^{-1} - 10^{-6}) and added to the Sf9 cells (2.0×10^6) in Petri dishes. After 1 h incubation, supernatant was removed and 4 ml of 1:1 mixture of low melting agarose and culture medium (with 10% FKS) was added to the cells. Once the agarose was solidified, 1-2 ml medium (with 5% FKS) was added and plates were incubated for 4-5 days at 27°C. Afterwards, medium was removed and 1-2 ml of 1:1 mixture of low melting agarose and culture medium (with 10% FKS) was added to the plates. In this step X-gal was also added in order to differentiate between wild type and recombinant plaques. Next day, plaques were picked and added to Sf9 cells (2.0×10^6) in six well plates. After 6-7 days, supernatant was collected (main virus stock), centrifuged and used for preparing new virus stocks.

2.2.6.3 Preparation of virus stocks and titer determination

100 µl of main virus stock was added to a monolayer culture of Sf9 cells (in 15 ml flask, 75-80% confluency). After one week, cells were separated by centrifugation at 6000 g for 10 min, and supernatant was collected. 100-200 µl of this virus stock was added to a 100 ml suspension culture of Sf9 cells (0.5×10^6 /ml) for preparing large amounts of virus.

Virus titer was determined by end point dilution method (Reed *et al.*, 1938) and expressed as the number of plaque-forming units (p.f.u.)/ml.

2.2.6.4 Protein expression in Sf9 cells

Cells were grown in suspension culture at 27°C and infected at density of 2x10⁶ cells/ml. For optimization, different MOI and expression time was used. For large-scale expression, cells were grown in wave bioreactor, infected at MOI 10 and harvested after 72-96 hours post-infection.

2.2.7 Mammalian cell culture

Monolayer of mammalian cells were maintained in 1:1 mixture of DMEM (Dulbecco's modified eagles medium) and Iscove's modified medium supplemented with 10% FKS and 2 mM glutamine. Suspension culture of BHK cells were grown in Glasgow minimum essential medium (GMEM) supplemented with 2 mM glutamine, 5% FKS and 10% tryptose phosphate broth solution. Cells were maintained at 37°C with 5% CO₂ in a humidified chamber.

2.2.7.1 *In vitro* transcription

Plasmid DNA was linearized with appropriate restriction enzyme (*Nru*I for pSFV2 based expression vectors and *Spe*I for pSFV-helper2 vector) for 2 h at 37°C. Restriction digestion of plasmid DNA was checked on 1% agarose gel. Linearized DNA was purified using Qiaquick PCR purification kit (Qiagen) and used for *in vitro* transcription. *In vitro* transcription reaction was set up as follows:

5 µl linearized DNA (5 µg)

10 µl reaction buffer (5X)

5 µl CAP (10 mM)

5 µl DTT (50 mM)

5 µl NTP mix

2 µl RNAase inhibitor (40 units)

3 μ l SP6 RNA polymerase (60 units)

15 μ l H₂O

Reaction mix was incubated at 37°C for 60 min and afterwards electroporated into BHK cells.

2.2.7.2 Electroporation of mRNA into BHK cells

BHK Cells ($1-2 \times 10^7$) were washed twice with PBS, detached with trypsin/EDTA and resuspended in 30 ml of growth medium. Cell suspension was spun down at 1200 g for 5 min. Subsequently, medium was removed and the cells were resuspended in PBS. The centrifugation was repeated as described before and the cells were finally resuspended in 0.4 ml PBS. Cells were transferred to a 0.2 cm electroporation cuvette. Meanwhile, 25 μ l of helper mRNA reaction was added into receptor mRNA reaction, mixed and immediately added to the cuvette. Cells were electroporated with two pulses under the following settings,

Capacitance 25 μ F

Resistance ∞

Voltage 1.5 kV

A typical time constant of 0.7-0.8 was observed. Cells were transferred to a 25 cm² flask containing 10 ml of growth medium and incubated for 24 h at 37°C.

2.2.7.3 Collection and activation of virus

Recombinant virus was collected by filtering the supernatant of the cells through a 0.22 μ M filter. Virus was activated by α -chymotrypsin (final concentration 0.5 mg/ml) treatment at room temperature for 20-30 minutes. To stop the reaction, aprotinin (final concentration 0.25 mg/ml) was added and incubated further for 5-10 minutes. Activated virus was used to infect the cells or stored at -80°C until used.

2.2.7.4 Protein expression in mammalian cells

Cells were infected at a density of $1-2 \times 10^6$ cells/ml and incubated at 37°C for defined time periods. Subsequently, the cells were harvested and membranes were prepared.

2.2.8 Membrane preparation of *Pichia pastoris*

2.2.8.1 Analytical scale:

For small scale (20 ml culture), cells were centrifuged and the pellet was resuspended in 1 ml of breaking buffer. Equal volume of acid washed glass beads (0.5 mm in diameter) were added to the cells and vortexed for 10 min at 4°C. This leads to mechanical disruption of the cells. Glass beads, unbroken cells and cell debris were separated by centrifugation in plastic columns with filter. The supernatant was used for ultracentrifugation at 100,000 g (4°C) for 40 min. Subsequently, the pellet was resuspended in 500 µl of storage buffer and homogenized. Aliquots were flash frozen and stored at -80°C until used.

2.2.8.2 Preparative scale

For large-scale membrane preparation, *Pichia* cells were broken using a cell mill by mechanical disruption. Cells (from 6 liter culture) were pelleted and resuspended in breaking buffer (30% of their wet weight, e.g. 100 g cells in 300 ml breaking buffer). 100 ml of acid washed, pre cooled glass beads (0.5 mm) were added to the cells. Cell suspension was passed three times through the mill and the cell breakage was checked under the microscope. The glass beads were washed with 100 ml of breaking buffer and separated from broken cells by vacuum filtration. Broken cells were spun down at 3500 g (4°C) for 20 min in order to remove cell debris and unbroken cells. The supernatant was subjected to ultracentrifugation at 100,000 g (4°C) for 1.5-2 h. The pellet was resuspended in storage buffer and homogenized until it became completely homogenous. It was further diluted to 75-100 ml with the storage buffer, aliquots were made and flash frozen. Membranes were stored at -80°C until further use.

2.2.9 Membrane preparation from insect cells and mammalian cells

Cells were washed and resuspended in breaking buffer at a density of $5-6 \times 10^6$ cells/ml. The cells were broken by using nitrogen cavitation procedure. In this method, first the

cells were equilibrated under a high pressure (500 psi) of nitrogen gas for 0.5-1 hour in “parr bomb”. During this incubation at high pressure, nitrogen dissolves into the aqueous buffers and into the cells. After incubation, the pressure was released from the pressurized “parr bomb”. The nitrogen rapidly converts back into the gas and disrupts the cells as it leaves (Broekma *et al.*, 1992). The lysate was spun down at 3000 g (4°C) for 10 min to remove the cell debris and unbroken cells. The supernatant was subjected to centrifugation at 100000 g for 1-2 h at 4°C. The pelleted membrane fraction was resuspended and homogenized in storage buffer. Membranes were aliquoted and frozen in liquid nitrogen. Aliquots were stored at -80°C until further use.

2.2.10 Determination of protein concentration

For the determination of protein concentration, the BCA protein assay was used (Smith *et al.*, 1985) following the instructions of BCA protein assay kit (Pierce).

2.2.11 SDS-PAGE analysis

Analytical separation of proteins was carried out on denaturing polyacrylamide gels (10-15%) following the standard protocol (Fling *et al.*, 1986). But the samples were not subjected to heat denaturation, as it may result in aggregation of membrane proteins. The proteins in the gel were either stained with coomassie brilliant blue, silver nitrate or electrotransferred to PVDF membranes for Western blot analysis.

2.2.12 Western blot analysis

After electrophoresis, the proteins were transferred to a PVDF membrane by electroblotting following the standard procedure (Towbin *et al.*, 1979). Protein transfer was carried out at the constant current of 50-60 mA per gel for 1.5-2 h. After the transfer, antibody staining was carried out according to the manufacturer’s protocol. Briefly, the PVDF membrane was blocked for 1-2 h at room temperature in TBST buffer and subsequently, washed three times (5 min each) with TBST buffer. Afterwards, the membrane was incubated with appropriate antibodies for 0.5-1 h at room temperature. Again, the membrane was washed three times with TBST buffer and then incubated in

secondary antibody (Alkaline Phosphatase/Horse Raddish Peroxidase conjugated goat anti-mouse IgG) for 0.5-1 h at room temperature. The membrane was then washed three times with TBST buffer. Finally, 10 ml of alkaline phosphatase buffer containing 66 μ l of NBT solution and 33 μ l of BCIP solution was added to the membrane and incubated till the bands appeared. The reaction was stopped by washing the membrane with water.

2.2.13 Radioligand binding assays

Radioligand binding assays were carried out to check the functionality of recombinant receptors.

2.2.13.1 Binding assay on membranes

For ligand binding assay, membranes were diluted in binding buffer. 5-20 μ g of total protein/assay point was used. Membranes were incubated for 45-60 min at 4°C/25°C with radioactive ligand (at a concentration of approximately 10x K_d). Non-specific binding was determined in the presence of 1 μ M non-radioactive ligand. For saturation binding experiments, different concentrations of radioactive ligands (0.1 nM-50 nM) were used. After incubation, the reaction was terminated by rapid filtration through GF/C glass-fiber filters (presoaked in 0.3% polyethyleneimine). These filters were washed four times with cold binding buffer or water. Subsequently, the filters were transferred to the counting vials. Radioactivity was measured using a Wallac microbeta counter or gamma counter (for 125 I NmU). Dissociation constants (K_d) and B_{max} values were calculated using “KaleidaGraph” software by non-linear regression and a single site model.

2.2.13.2 Binding assay on solubilized and purified receptors

Ligand binding of solubilized and purified receptor was measured by calcium phosphate precipitation method. Samples were incubated for 40-45 min at 4°C with radioactive ligand (as described above) and after incubation, 200 μ l of $Ca_3(PO_4)_2$ was added. Bound ligand was separated from free ligand in three washing steps using centrifugation at 2000 rpm (4°C). Finally, the precipitate was resuspended in washing buffer and transferred to

the counting vials. Non-specific binding was determined in the presence of 1-10 μM of non-radioactive ligand.

2.2.14 G protein coupling assay (inositol phosphate release)

BHK cells expressing B_2R were incubated with [^3H] myoinositol (0.25 $\mu\text{Ci}/\text{well}$) for 16 h in 6 well plates. Following incubation, cells were washed twice with PBS, resuspended in PBS containing 10 mM LiCl and incubated for 10 min at 37 $^\circ\text{C}$. Cells were then incubated either with 1 μM bradykinin for different time intervals (5-20 min) or with different concentrations of bradykinin (1 pM-0.1 mM) for 10 min. The reaction was terminated by the addition of 0.1% trichloroacetic acid (TCA). Afterwards, the cells were lysed and total inositol phosphate was isolated using ion-exchange column (Dowex AG1-X8, pre-washed with 20 mM ammonium formate). [^3H] inositol phosphates were eluted with 1 M ammonium formate/0.1 M formic acid solution and radioactivity was determined by liquid scintillation counting.

2.2.15 Localization of recombinant receptors

Localization of the recombinant receptors in the host cells was investigated by either confocal microscopy (using eGFP fusion construct) or immunogold labeling experiment (using Flag-tagged construct).

2.2.15.1 Confocal Microscopy

For localization experiments, cells were grown on sterile cover slips, infected with virus and 16-24 h post infection, fixed for 15 min at room temperature (RT) with 4% paraformaldehyde. Subsequently, the cells were rinsed three times with PBS, permeabilized with digitonin (50 $\mu\text{g}/\text{ml}$ in DMSO) for 15 min at RT. Then the cells were washed and incubated with either anti-Flag/anti-Myc monoclonal antibodies (in BHK cells) or with receptor specific antibodies (in HF-15 cells) for 1 h at RT. Afterwards, the

cells were rinsed with PBS and incubated with Cy3/cy5 coupled Goat anti-mouse or Goat anti-rabbit IgG secondary antibody for 1 h at RT. The cells were washed three times with PBS and then mounted onto slides by using Gel Mount aqueous mounting medium. For internalization experiments, the cells were stimulated with appropriate ligands at 37°C for indicated time. Subsequently, the cells were fixed, permeabilized and stained for confocal microscopy as described above. Cells were scanned with a Zeiss LSM 510 laser scanning confocal microscope. eGFP, Cy3 and Cy5 were detected at wavelengths of 488 nm, 550 nm and 650 nm, respectively.

2.2.15.2 Electron microscopy (fixation, embedding and immunogold staining)

For immunogold labeling experiments, cells were fixed with sodium phosphate buffer containing 4% (v/v) paraformaldehyde for 2 h at room temperature. After incubation, cells were washed and then treated with 2% (w/v) glycine in sodium phosphate buffer in order to block unreacted aldehyde groups. For post-embedding immunostaining, glycine-treated cells were dehydrated with ethanol, embedded in LR White resin, and samples were polymerized at 58°C. Immunogold staining was performed on thin sections using the anti-Flag M2 antibody (1:300 dilution). A gold-coupled goat anti-mouse Ig (1:60 dilution, 90 min room temperature) was used as secondary antibody.

For pre-embedding immunostaining, fixed and glycine treated cells were incubated first with 1% (w/v) BSA, then with 0.1% (w/v) BSA and finally incubated with the anti-Flag M2 antibody at 4°C overnight. Subsequently, cells were washed and incubated with gold-coupled goat anti-mouse Ig for 90 min at room temperature. After immunogold labeling, the cells were washed and fixed with 1% (v/v) glutardialdehyde for 30 min and subsequently treated with 1% (w/v) OsO₄ in 100 mM sodium cacodylate buffer. Cells were further treated with 2% (w/v) uranyl acetate, dehydrated with ethanol, embedded in Spurr's resin, and polymerized at 70 °C. Thin sections were analyzed by electron microscopy (EM 208S, Philips, the Netherlands).

2.2.16 Solubilization of receptors from the membranes

In order to solubilize the receptors, membranes (at a concentration of 5 mg/ml) were resuspended in the solubilization buffer containing appropriate detergent (as indicated in results section) and 0.2% cholesterol hemisuccinate (CHS). The suspension was incubated for 2 hours with gentle mixing at 4°C. Following solubilization, the suspension was subjected to ultracentrifugation at 100,000 g for 1-2 h, and the supernatant containing solubilized receptor was used for receptor purification.

2.2.17 Purification of recombinant receptor

Recombinant receptors were purified by affinity chromatography using different affinity tags fused to the receptors.

2.2.17.1 Immobilized metal affinity chromatography (IMAC)

Solubilizate (20-200 ml) was filtered through 0.65 µm filter and mixed with previously equilibrated (1-10 ml) Ni-NTA matrix. Binding to the affinity resin was carried out at 4°C for two hours. The mixture was packed into a column and washed with 10-15 column volumes of the washing buffer. Receptor protein was eluted with 5-10 column volumes of the elution buffer. Ni-NTA matrix was regenerated with the regeneration buffer, washed with water and stored in 20% ethanol.

2.2.17.2 Purification on monomeric avidin matrix

Non-specific binding sites on monomeric avidin resin were blocked according to the manufacturer's protocol. Subsequently, the matrix was equilibrated with 5-10 column volumes of the equilibration buffer. The elution fraction from the Ni-NTA matrix was applied to this pre-equilibrated monomeric avidin matrix. The column was washed with 10-15 column volumes of the washing buffer and the receptor protein was eluted by 5-10 column volumes of the elution buffer. Monomeric avidin resin was regenerated with the regeneration buffer and stored in 20% ethanol.

2.2.17.3 Purification on anti-Flag antibody matrix

Anti-Flag antibody matrix was pre-equilibrated according to the manufacturer's protocol. The eluate from Ni-NTA column was applied to this pre-equilibrated anti-Flag antibody matrix, washed with 5-6 column volumes of the washing buffer and finally, the receptor protein was eluted with 5 column volumes of the elution buffer. For purification on M1 matrix, 5 mM CaCl₂ was added in all the buffers as the binding of Flag-tagged protein to this matrix is calcium dependent. The matrix was regenerated with the regeneration buffer and stored in 20% ethanol.

2.2.17.4 Purification on streptactin matrix

Pre-equilibrated streptactin resin was mixed with the eluate from Ni-NTA column and incubated for 1-2 h at 4°C on the rolling wheel. Subsequently, the material was packed into the column and washed with 6-10 column volumes of the washing buffer. Receptor protein was eluted with the elution buffer containing 2.5-5.0 mM desthiobiotin.

2.2.18 Concentration of proteins

Purified protein was concentrated using Vivaspin concentration tubes (cut off 50 kDa). The tubes with the protein solution were spun down at 3000 g at 4°C until the desired concentration of purified protein was achieved. Alternatively, proteins were concentrated by using TCA precipitation method (Tornqvist *et al.*, 1976).

2.2.19 Coomassie and silver staining of proteins

For Coomassie staining, the gels were incubated for 1 h in Coomassie Brilliant Blue solution. Afterwards, the gels were placed into the destaining solution (changed 2-3 times) until the bands became clearly visible.

For silver staining, the gels were fixed for 15 min in the fixer followed by 15 minute incubation in the conditioner. Then, the gels were washed 3 times (5 min each) in water. After washing, the gels were incubated in the silver nitrate solution for 10 min,

washed twice in water (30 sec each) and developed using the developer solution. The reaction was stopped by adding 50 mM EDTA solution.

2.2.20 Analytical gel filtration

Molecular sieve chromatography (gel filtration or size-exclusion) was used to separate the proteins based on their molecular mass and to check the dispersity (homogeneity) of the purified receptors. For this purpose mainly Superose 6 PC 3.2/30 column (Pharmacia) was used on a Smart Chromatography station. Purified protein in 50-100 μ l (5-10 mg/ml) was applied to the pre-equilibrated column. The flow rate was set to 50 μ l/min and temperature was set to 4°C.

2.2.21 Sample preparation for ss-NMR analysis

Recombinant B₂R was purified from BHK cells or Sf9 cells using affinity chromatography. Either of the three ¹³C/¹⁵N variants of bradykinin was added to the elution fraction and incubated for 2-3 hour at 4°C. Subsequently, the eluate was concentrated as described in section 2.2.18. In order to remove extra detergent and free peptide, repeated dilution and concentration was performed using a detergent free buffer. Subsequently, the receptor-ligand complex was transferred to a 4 mm MAS rotor, flash frozen and stored at -80°C until further use.

2.2.22 Three-dimensional crystallization trials

Purified receptor samples were concentrated up to 10 mg/ml and then used for 3-D crystallization screening in 300 nl drops (using Cartesian Crystallization Robot). Initially, a wide range of pH (4.0-9.0), precipitants (PEG 400 and PEG 4000), salts (acetate, sulphate and malonate) and two different temperatures (4°C and 18°C) were tested (detail scheme is shown in appendix). Commercially available crystallization kits (from Sigma and Jena Biosciences) were also used.

Chapter 3: Production, characterization and isolation of
 B_2R

3.1 Production and isolation of B₂R from *Pichia pastoris*

3.1.1 Sub-cloning of B₂R gene in *Pichia* expression vector

The coding region of B₂R gene was amplified from cDNA vector (pB₂R from Aventis) with the primers B₂R_ *Pichia*_Fw/Rv using the *Pfu* DNA polymerase. PCR products were checked on a 1% agarose gel (Fig. 3.1), purified using a PCR purification kit and then digested with *Bam*HI and *Eco*RI enzymes. After restriction digestion, PCR product was ligated to *Bam*HI-*Eco*RI digested pPIC9K (modified) vector.

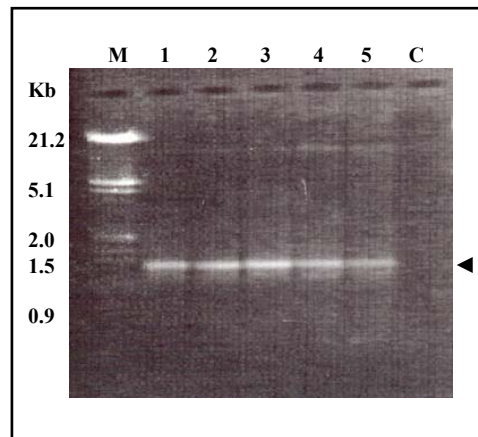


Fig. 3.1 Amplification of B₂R gene from cDNA vector by PCR under the following conditions: 94°C = 5 min, 94°C = 40 sec, 66°C = 40 sec, 72°C = 90 sec and 72°C = 10 min. Total 30 cycles (from step 2 to step 4) were used for amplification. PCR products were analyzed on 1% agarose gel. M = Lambda DNA marker (*Eco*RI + *Hind*III), C = control (no template), 1-5 = different amounts (50 ng-200 ng) of template DNA.

3.1.2 Expression construct

A modified pPIC9K expression vector (Fig. 3.2) was used for the production of B₂R in *Pichia pastoris*. This vector contains the alcohol-oxidase I (AOXI) promoter for heterologous production of recombinant proteins and a coding region for the α -mating factor prepro-peptide (α -factor) of *Saccharomyces cerevisiae*. The α -factor is used as a secretion signal for soluble proteins. It was previously reported that an N-terminal fusion of this factor enhances the production of GPCRs in *Pichia pastoris* (Weiss *et al.*, 1998).

The protease-cleavage site, inserted between the α -factor sequence and the receptor, is recognized by the Kex-2 protease of *Pichia pastoris* and should lead to an efficient cleavage of the α -factor. The coding region of B₂R receptor gene was cloned into the Multiple Cloning Site (MCS) of the modified pPIC9K vector (modified from original pPIC9K vector by Markus Weiss). The modified pPIC9K vector contains a Flag tag and a Histidine₁₀ tag at the N-terminus of the MCS and a biotinylation domain of *Propionibacterium shermanii* transcarboxylase (Cronan *et al.*, 1990) at the C-terminus of the MCS. The tags were separated from the receptor coding region by a TEV protease cleavage site. The Flag and His₁₀ tags can be used for immunological detection and receptor purification. Previous studies have shown a positive effect of biotinylation domain on recombinant expression of GPCRs in *Pichia pastoris* (Weiss *et al.*, 1998). Additionally, this domain also serves as an affinity tag for receptor purification via monomeric avidin matrix.

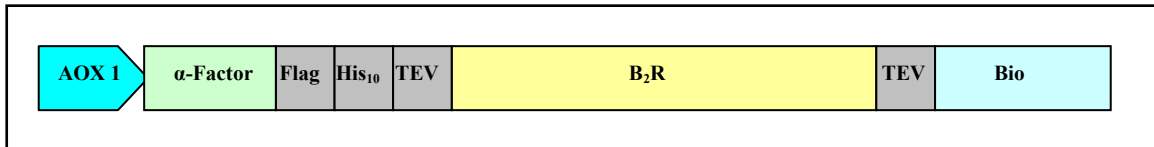


Fig. 3.2 Expression construct for production of recombinant B₂R in *Pichia pastoris*. AOX1 = alcohol oxidase 1 promoter, α -factor = α -mating factor prepro-peptide of *S. cerevisiae*, Flag = coding sequence for Flag epitope, His₁₀ = coding sequence for histidine 10 tag, B₂R = coding sequence of B₂R gene, TEV = cleavage site for TEV protease, Bio = biotinylation domain of *Propionibacterium shermanii* transcarboxylase.

3.1.3 Production of recombinant receptor

Pichia cultures were grown in shake flasks (as described in Multi-Copy *Pichia* expression kit, Invitrogen), membranes were prepared (after 24 h of induction with methanol) and subjected to Western blot analysis and ligand binding assay.

3.1.3.1 Western blot analysis

Western blot with anti-Flag M2 antibody was performed to check the expression of recombinant receptor. As shown in Fig. 3.3, a band of approximately 55 kDa was seen in

membranes from *Pichia* cells expressing B₂R. This corresponds well with the calculated size of the recombinant receptor fusion protein (50.7 kDa). An additional band of approximately 75 kDa was also observed that probably represents the unprocessed[#] receptor.

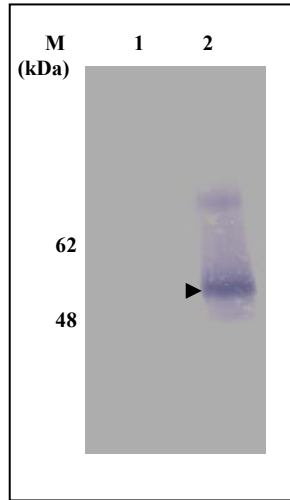


Fig. 3.3 Western blot analysis of the recombinant B₂R produced in *Pichia pastoris*. Proteins were separated using 10% SDS-PAGE and probed with anti-Flag M2 antibody. Lane 1 = 10 µg of control *Pichia* membranes and lane 2 = 10 µg of membranes from *Pichia* cells expressing FlagHis₁₀B₂RBio fusion protein.

3.1.3.2 [³H] bradykinin binding

In order to check the functionality of the recombinant receptor and to calculate the total amount of functional receptor in membranes, a saturation binding experiment using [³H] bradykinin was performed. [³H] bradykinin binding was saturable and revealed a B_{max} value of 0.5 pmol recombinant B₂R per mg membrane protein (Fig. 3.4). A high affinity binding of [³H] bradykinin to the recombinant receptor was observed with a K_d value of 0.87 nM. This K_d value is similar to that reported for B₂R in native tissues (see appendix).

[#]Unprocessed receptor represents the fusion of recombinant receptor and α-factor as Kex-2 endopeptidase of *Pichia* failed to cleave the α-factor completely.

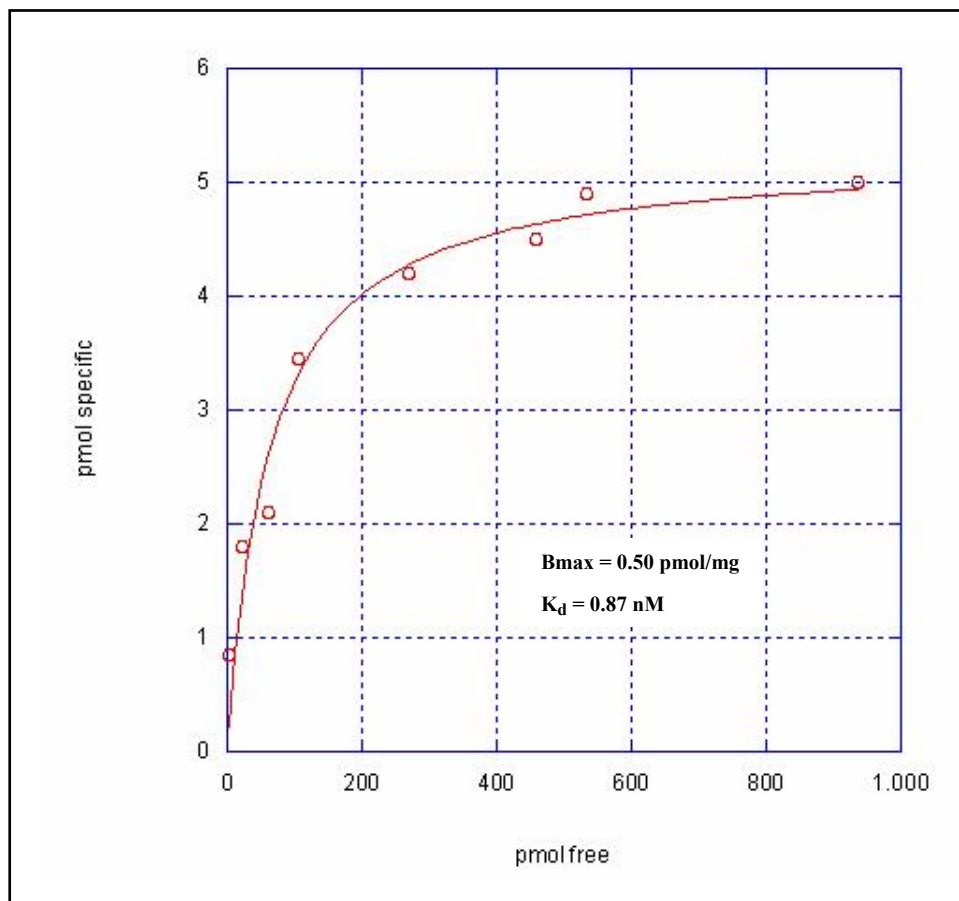


Fig. 3.4 Saturation curve for $[^3\text{H}]$ bradykinin binding to the recombinant B_2R produced in *Pichia pastoris*. Graph was generated using the single site model in KaleidaGraph software.

3.1.4 Optimization of functional expression of B_2R

It has been reported previously (Aleksandra Ivanovic, PhD thesis) that the addition of DMSO (dimethylsulphoxide) during expression of recombinant GPCR in *Pichia pastoris* results in significant increase in the amount of functional receptor. Therefore, in order to increase the functional expression of B_2R , DMSO was added to the *Pichia* cultures during the methanol induction step. As shown in Fig. 3.5, approximately seven-fold increases in the functional expression of recombinant B_2R was observed by the addition of DMSO. Maximum expression level was obtained in presence of 2% DMSO and it

corresponds to 3.5 pmol of recombinant B₂R per mg of membrane protein (~0.1 mg of receptor per liter culture).

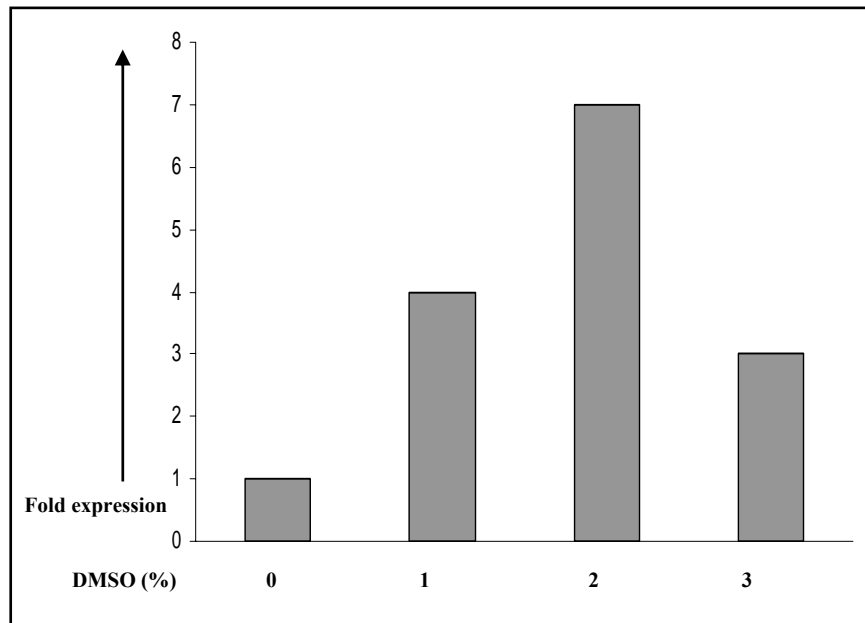


Fig. 3.5 Effect of DMSO on the expression level of recombinant B₂R in *Pichia pastoris*. DMSO was added to the cultures, membranes were prepared and [³H] bradykinin binding was measured.

3.1.5 Glycosylation analysis

There are three putative glycosylation sites[#] in B₂R, two at the N-terminus (N³, N¹²) and one in the third extracellular loop (N¹⁸⁰). In order to analyze the glycosylation state of the recombinant receptor, enzymatic deglycosylation using PNGaseF and EndoH was performed on *Pichia* membranes expressing B₂R, followed by Western blot analysis. As shown in Fig. 3.6, the recombinant receptor band was shifted to lower molecular weight size upon enzymatic deglycosylation. This reveals that the recombinant B₂R produced in *Pichia* was glycosylated. The band corresponding to the unprocessed receptor was also reduced in size upon enzymatic deglycosylation.

[#]These sites are predicted on the basis of conserved N-linked glycosylation motif (Asn-Xaa-Ser/Thr).

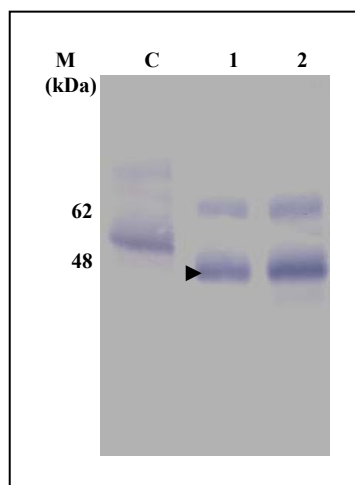


Fig. 3.6 Glycosylation analysis of the recombinant B₂R produced in *Pichia*. 10 µg of *Pichia* membranes expressing B₂R were treated with 0.5 units of PNGaseF (lane 2) or 0.5 units of EndoH (lane 3) at 4°C for 2 h. The lane “C” is untreated control *Pichia* membranes (10 µg). Proteins were separated by 10% SDS-PAGE and Western blot analysis was performed using anti-Flag M2 antibody.

3.1.6 Solubilization of recombinant B₂R

In order to solubilize the recombinant B₂R from *Pichia* membranes, different detergents were tested. As shown in Fig. 3.7, B₂R was solubilized with most of the detergents. However, proteolytic degradation of B₂R during solubilization was also observed (bands at approximately 40 kDa). [³H] bradykinin binding on solubilizate was used to monitor the functional solubilization of B₂R from *Pichia* membranes. It revealed that approximately 20-25 % of the [³H] bradykinin binding sites were solubilized with n-dodecyl-β-D-maltoside (LM) and Foscholine14. Recovery with other detergents was lower. It has been previously reported (Markus Weiss, Ph.D. thesis and Weiss *et al.*, 2002) that addition of Cholesterol hemisuccinate (CHS) exerts a positive effect on functional solubilization of GPCRs from *Pichia* membranes. Therefore, 0.2% CHS was added during solubilization. As shown in Fig. 3.8, addition of CHS resulted in a significant increase in the solubilization of functional B₂R.

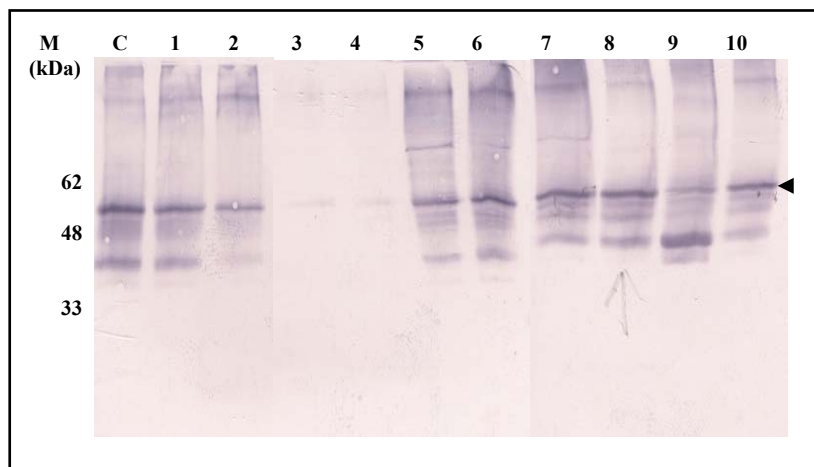


Fig. 3.7 Solubilization of recombinant B₂R from *Pichia* membranes (5 mg/ml). Lane 1-10 = LM, UM, DM, NG, OG, Fos12, Fos14, Fos 16, CHAPS, Digitonin and LDAO. All the detergents were used at the concentration of 1% except OG (2%). Proteins in the supernatant were separated by 10% SDS-PAGE and Western blot analysis was performed using anti-Flag M2 antibody.

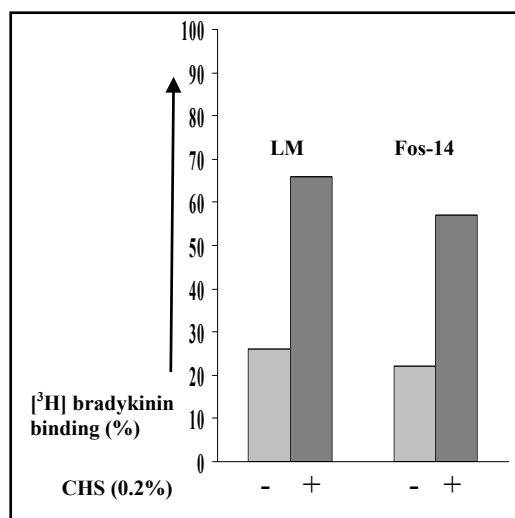


Fig. 3.8 Effect of CHS on solubilization of [³H] bradykinin binding sites from *Pichia* membranes.

3.1.7 Purification of recombinant B₂R

The N-terminal His₁₀ tag enabled the purification of the recombinant receptor by Ni-NTA resin. Receptor was solubilized from the membranes (5 mg/ml) with 1% LM in presence of 0.2% CHS. Solubilizate was applied to Ni-NTA matrix (batch binding). Subsequently,

the column was washed with washing buffer (see materials and methods) and finally the receptor was eluted with elution buffer containing 200 mM imidazole. As a second step of purification, Ni-NTA eluate was then applied to monomeric avidin matrix. The recombinant receptor binds to this matrix via its biotinylated bio tag. B₂R from this column was eluted with 2 mM biotin. The eluates from Ni-NTA and monomeric avidin were analyzed on a 10% silver stained SDS-polyacrylamide gel. As depicted in Fig. 3.9 (lane 1), after two-step affinity purification, the recombinant receptor was >85 % pure (band at 55 kDa, indicated by the arrow head).

In order to check the homogeneity of purified B₂R, eluate from monomeric avidin column was analyzed by gel filtration using a superose 6 column (PC3.2/30) in the SMART chromatography system. A main peak at the retention volume of 1.60 ml (indicated by the arrow head) was observed. It corresponds to the homogenous population of purified B₂R. In addition to this main peak, some aggregated receptor (peak at retention volume of 0.89 ml and 1.3 ml) was also observed.

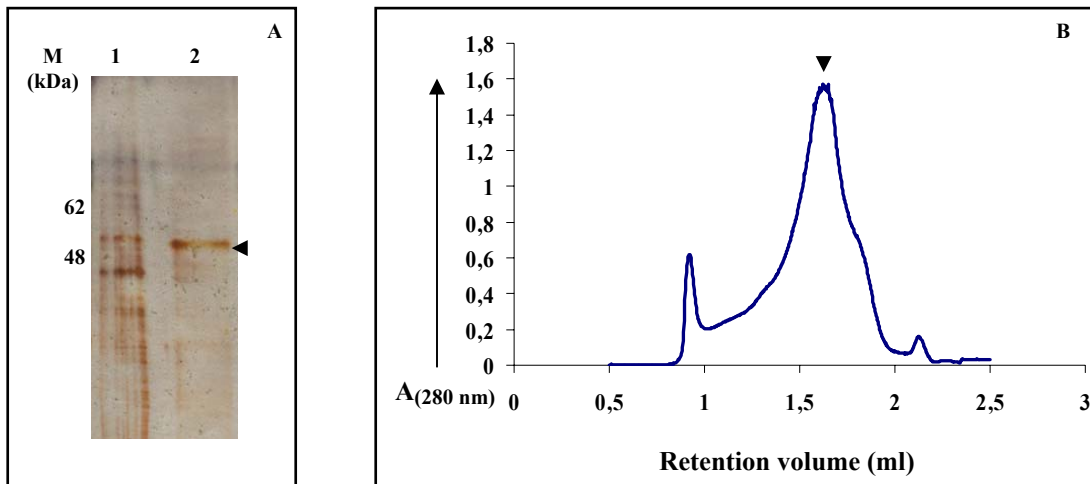


Fig. 3.9 Purification of recombinant B₂R from *Pichia pastoris*. **A.** Silver stained 10% SDS-PAGE showing the eluate from Ni-NTA (lane 1, 1 μ g) and monomeric avidin (lane 2, 0.5 μ g). **B.** Analytical gel filtration of purified B₂R (eluate from monomeric avidin column, 0.5 mg at a concentration of 10 mg/ml) using superose 6 column.

[³H] bradykinin binding was also measured on different fractions during purification. As shown in Table 3.1, recovery of the active receptor was approximately 20% after two-step purification.

	[³ H]bradykinin binding (nmol)	Specific activity (nmol/mg)	Total protein (mg) BCA/[³ H]BK binding	Recovery (%)
Membrane	9.00	0.0030	3000/(0.45)	100
Solubilisate	6.72	0.0041	1640/(0.33)	74
Ni-NTA eluate	3.51	0.417	8.41/(0.18)	39
Mon.Avidin eluate	1.71	0.987	1.71/(0.09)	19

Table 3.1. Recovery of functional B₂R during different steps of purification based on [³H] bradykinin binding analysis and BCA quantification.

Due to the low production level of receptor in *Pichia pastoris*, baculovirus mediated expression of B₂R in insect cells was tested.

3.2 Production and isolation of B₂R from insect cells using the baculovirus system

3.2.1 Sub-cloning of the B₂R gene in the baculovirus expression vectors

The coding region of B₂R gene was cloned into the MCS of modified pVL vectors (the original pVL1392 vector was a kind gift from Max D. Summers, Texas, USA) between *Bam*HI and *Eco*RI enzyme sites. Amplification of the receptor gene (with B₂R_Baculo_Fw/Rv primers using *Pfu* DNA polymerase) and ligation to the expression vectors was carried out as described in section 3.1.1.

3.2.2 Expression constructs

The baculovirus constructs used for the expression of B₂R in insect cells are shown in Fig. 3.10. The first construct was made by Dr. Helmut Reiländer (in collaboration with Dr. Schroeder, University of Mainz, Germany) and the modified pVL1392 vectors for the other two constructs were provided by Gabi Maul. In the baculovirus constructs, the

receptor expression was driven by a polyhedrin promoter and a prepro-mellitin sequence from honey bee was used as a signal peptide. This signal sequence is expected to drive the recombinant receptor to the plasma membrane and later it gets cleaved off by an insect cell signal peptidase (Tessier *et al.*, 1991). For detection and purification of recombinant receptor, Flag and His₁₀ tag at the N-terminus and a biotinylation domain at the C-terminus of the MCS were engineered. The construct with an eGFP fusion at the C-terminus of the receptor was also made that can be used for receptor localization studies using confocal microscopy.

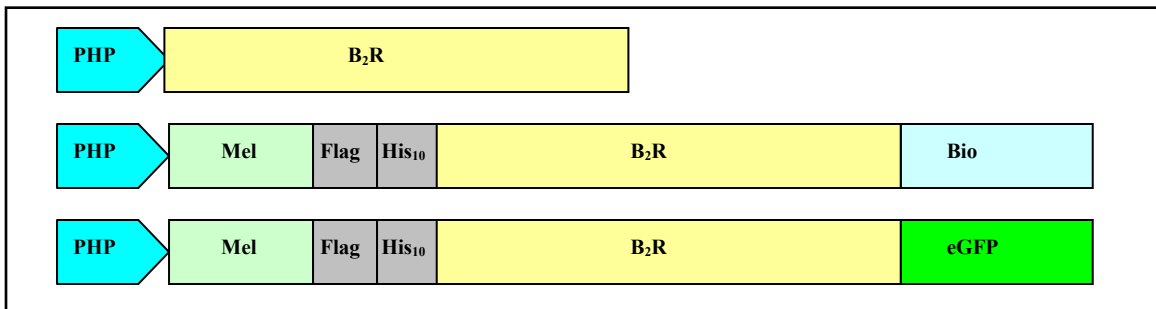


Fig. 3.10 Expression constructs for production of the recombinant B₂R in insect cells. PHP = polyhedrin promoter, Mel = prepro-mellitin signal sequence of honey bee, Flag = coding sequence for Flag epitope, His₁₀ = coding sequence for histidine 10 tag, B₂R = coding sequence for B₂R gene, Bio = biotinylation domain of *Propionibacterium shermanii* transcarboxylase and eGFP = coding sequence of enhanced green fluorescent protein.

3.2.3 Production of the recombinant receptor

In order to check the expression of B₂R, Sf9 cells were infected at MOI 10 with one of the recombinant baculovirus constructs (pVLMelFlagHis₁₀B₂RBio). 72 h post-infection, membranes were prepared and subjected to Western blot analysis and [³H] bradykinin binding analysis.

3.2.3.1 Western blot analysis

Western blots with anti-Flag M2 antibody and alkaline phosphate-coupled streptavidin were performed to check the expression of recombinant receptor. As shown in Fig. 3.11, a band of approximately 55 kDa was seen in Sf9 membranes expressing B₂R. This apparent molecular mass closely corresponds to the calculated size of the receptor fusion protein (49.3 kDa). However, on anti-Flag M2 immunoblot (Fig. 3.11 A), in addition to the full length receptor band, another band of approximately 40 kDa was also observed. This band probably represents a proteolytic degradation product of B₂R. Interestingly, this band was not observed on anti-strep blot (Fig. 3.11 B). Therefore, this band represents an N-terminal fragment of B₂R.

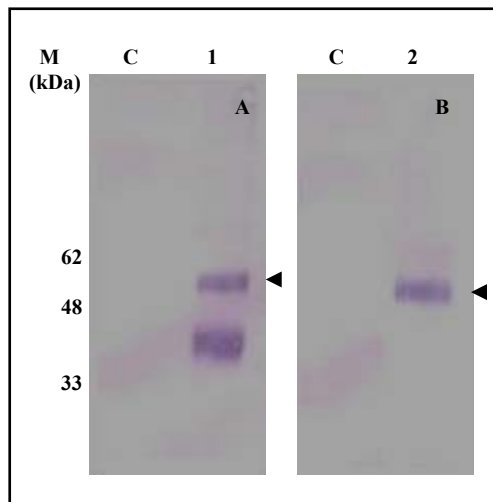


Fig. 3.11 Western blot analysis of the FlagHis₁₀B₂RBio construct produced in Sf9 cells using 10% SDS-PAGE. C = 10 µg membranes from non-infected Sf9 cell, lane 1 & 2 = 10 µg membranes from Sf9 cells expressing FlagHis₁₀B₂RBio fusion protein. **A** = anti-Flag M2 blot, **B** = anti-strep blot.

3.2.3.2 [³H] bradykinin binding

In order to check the functionality of the recombinant receptor and to calculate the total amount of functional receptor in membranes, a saturation binding experiment using [³H] bradykinin was performed. Suspension culture of Sf9 was grown and infected with baculovirus corresponding to three different constructs (shown in Fig. 3.10) at an MOI of

10. 72 h post-infection, membranes were prepared and saturation binding was performed using [³H] bradykinin. As shown in Fig. 3.12, the construct pVLMelFlagHis₁₀B₂RBio exhibited the highest expression level and therefore it was used for further studies.

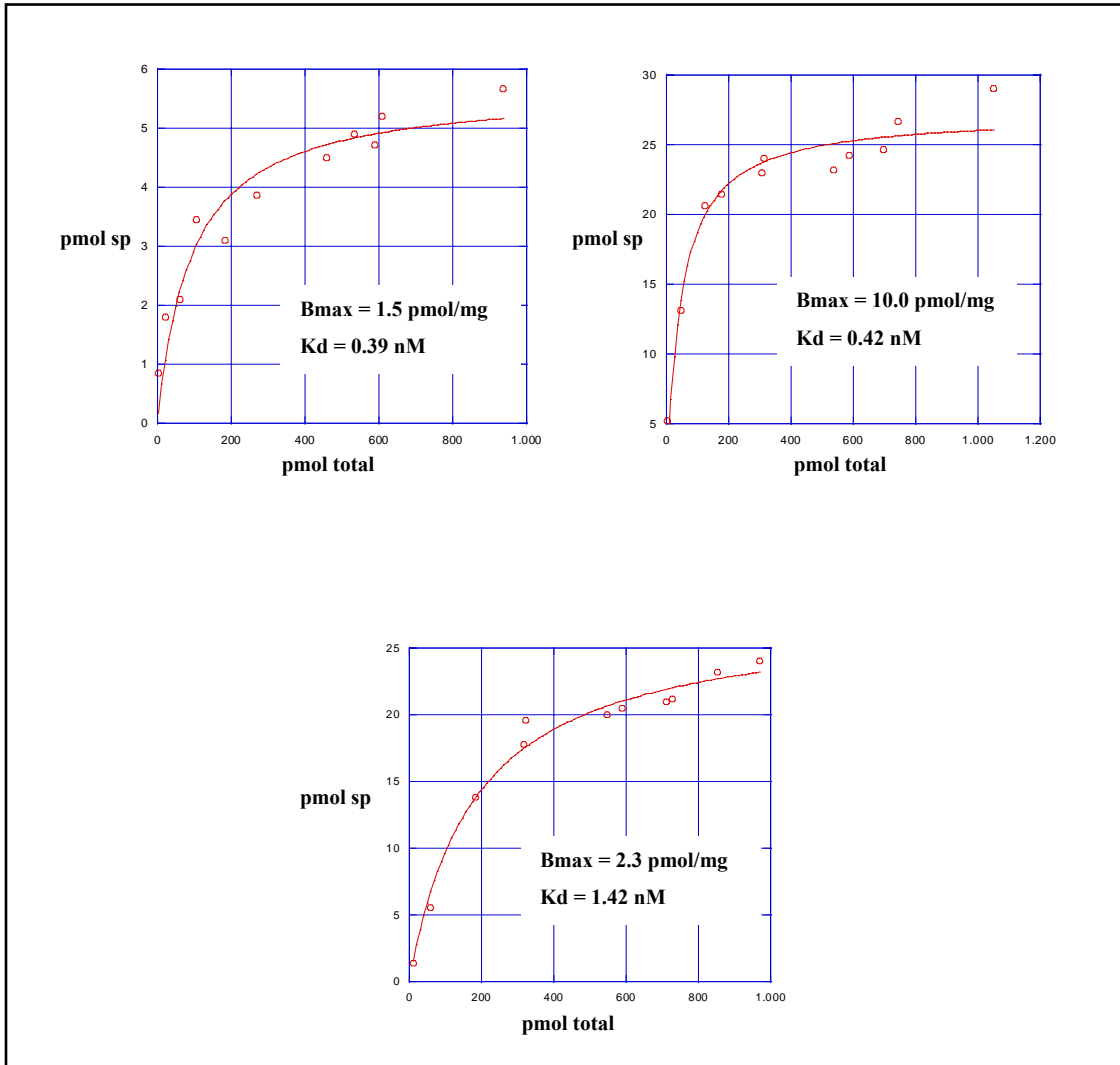


Fig. 3.12 Saturation curves for [³H] bradykinin binding to recombinant B₂R produced in Sf9 cells[#]. **A:** pVLB₂R, **B:** pVLMelFlagHis₁₀B₂RBio and **C:** pVLMelFlagHis₁₀B₂ReGFP. (C). Graphs were made using the single site model in Kaleidagraph software.

[#]For receptor expression studies, Sf9/Sf21 cells were infected at a density of 2.5x10⁶ cells/ml and H5 cells at 2.0x10⁶ cells/ml.

3.2.4 Optimization of functional production level of B₂R

The expression conditions (such as MOI, cell line and expression time) are known to influence the production of recombinant GPCRs in the baculovirus system (reviewed in Massotte *et al.*, 2003). Therefore, in order to maximize the expression level of B₂R in this system, three different parameters, namely cell type, MOI and expression time were investigated. The results are shown in Fig. 3.13. Significant effect of expression time on functional expression of B₂R was observed. [³H] bradykinin binding was detected as early as 24 h after infection and it reached to a maximum level 96 h post-infection (in Sf9 cells). A similar time course of CXCR₁ expression in insect cells has been reported earlier (Maeda *et al.*, 2005). Effect of MOI on B₂R expression was moderate in Sf9 cells but more significant in H5 cells. However, the maximum expression level in Sf9 cells using MOI 5 or 10 was almost similar. Use of low MOI for receptor expression makes the scale-up feasible. Sf9 cells showed maximal expression of B₂R among the three different cell lines that were tested. Although, in some cases the production level of recombinant proteins is better in H5 cells compared to Sf9 cells (personal communication, Ingo Focken, Aventis), it was not observed for B₂R.

For further characterization and large-scale production, Sf9 cells were infected at MOI of 5 and harvested 96 h post-infection. Under these expression conditions, a typical expression level of 10 pmol/mg for B₂R (0.3 mg/liter culture) was obtained.

3.2.5 Glycosylation analysis of recombinant B₂R

In order to analyze the glycosylation state of the recombinant receptor, either enzymatic deglycosylation (using PNGaseF or EndoH) was performed on Sf9 membranes or tunicamycin was added to the culture medium, followed by Western blot analysis. As shown in Fig. 3.14, the recombinant receptor band was shifted to a lower molecular weight size upon deglycosylation. This reveals that the recombinant B₂R produced in Sf9 cells was glycosylated. In addition, size of the degradation product was also reduced indicating that it represents an N-terminal fragment of B₂R.

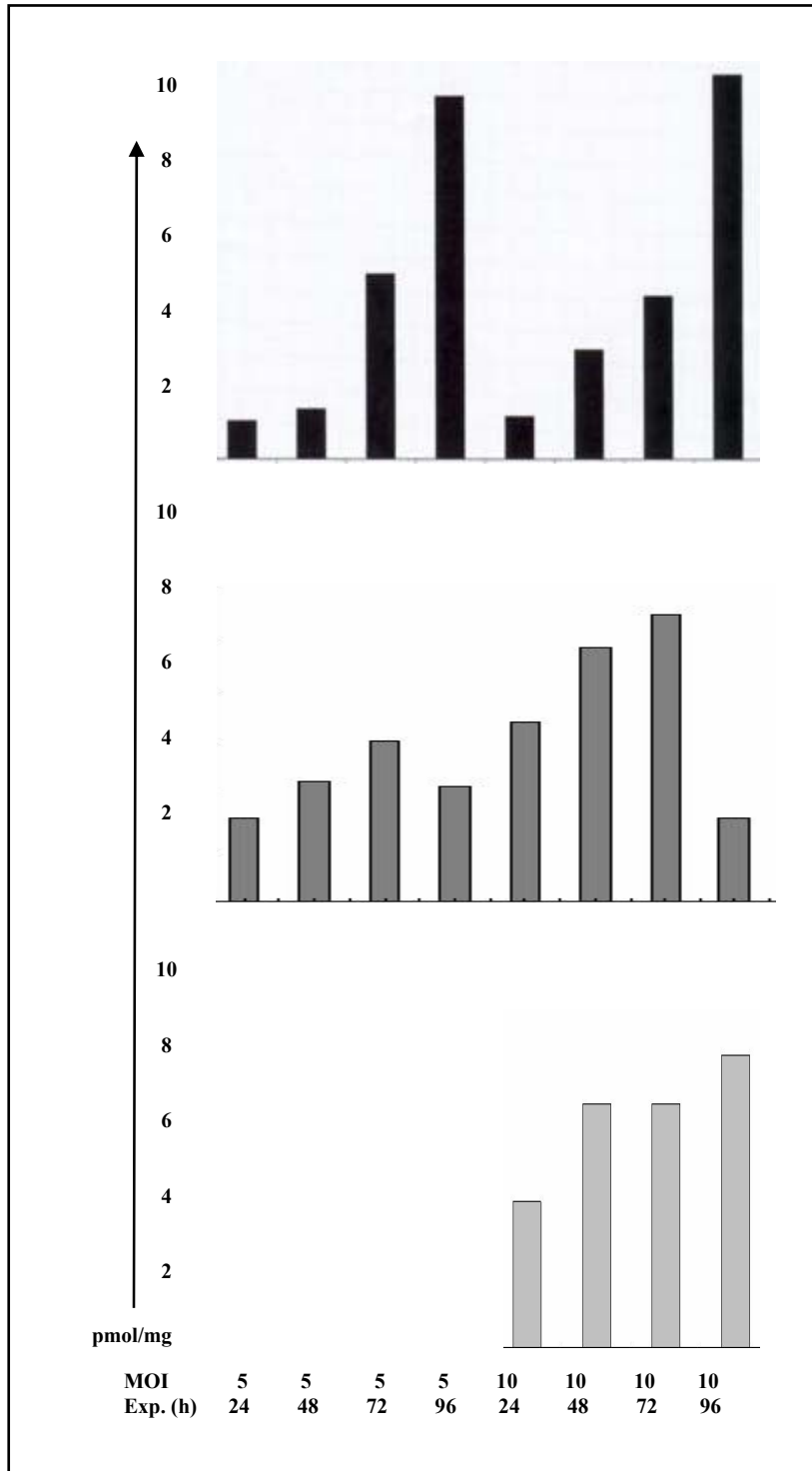


Fig. 3.13 Effect of cell type, MOI and expression time on the expression of recombinant B₂R in baculovirus system. Upper panel = Sf9 cells, middle panel = H5 cells and lower panel = Sf21 cells.

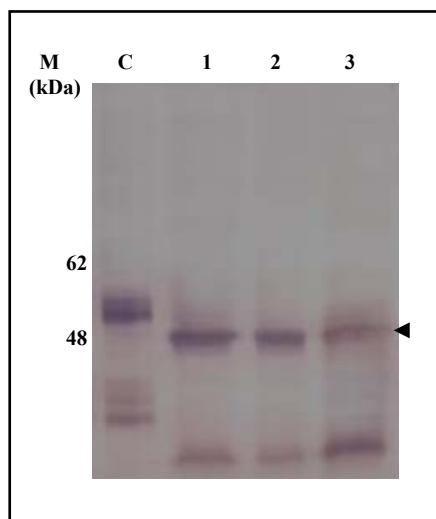


Fig. 3.14 Glycosylation analysis of the recombinant B₂R produced in Sf9 cells. 10 µg of membranes from Sf9 cells expressing B₂R were treated with 0.5 units of PNGaseF (lane 1) or 0.5 units of EndoH (lane 2) at 4°C for 2 h. Tunicamycin (10 mg/ml) was added to the Sf9 cell cultures. The lane “C” is untreated control Sf9 membranes (10 µg). Proteins were separated by 10% SDS-PAGE and Western blot analysis was performed using anti-Flag M2 antibody.

3.2.6 Localization of the recombinant B₂R

In order to check the localization of recombinant receptor, immunogold labeling experiments were carried out using the pVLMelFlagHis₁₀B₂RBio construct. Additionally, confocal microscopy using the pVLMelFlagHis₁₀B₂ReGFP construct was also performed.

3.2.6.1 Immunogold labeling experiment

Sf9 cells expressing B₂R were analyzed by pre- and post-embedding as described in materials and methods section. As shown in Fig. 3.15, most of the recombinant receptors were localized in intracellular membranes, probably in the endoplasmic reticulum. Only few receptor molecules were found in the plasma membrane.

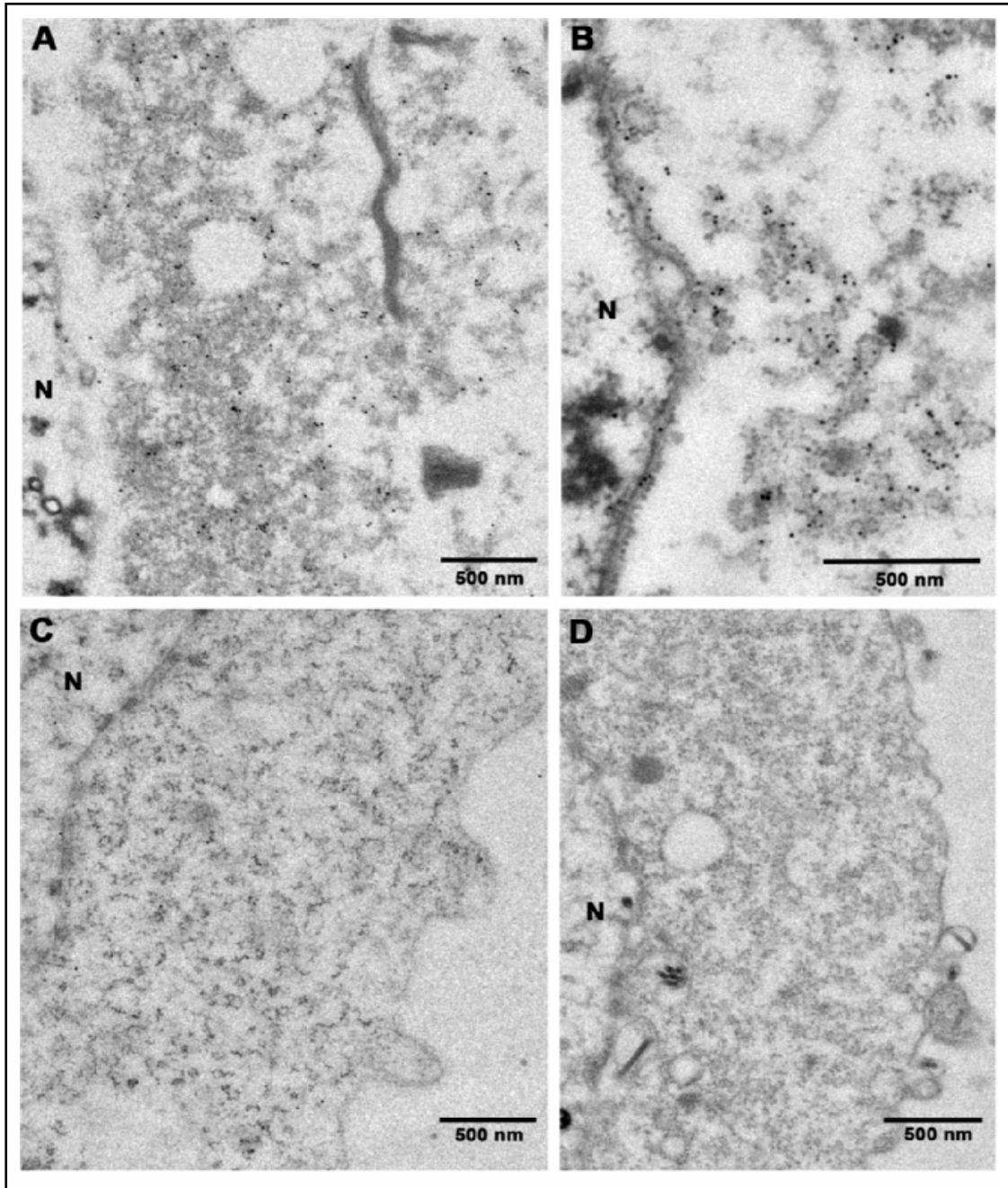


Fig. 3.15 Localization of the recombinant B₂R in insect cells using immunogold labeling experiment[#]. A&B = post-embedding labeling, C&D = control non-infected cells.

[#]This experiment was performed by Dr. Winfried Haase.

3.2.6.2 Localization analysis of B₂R by confocal microscopy

Receptor-eGFP fusion protein is a fast and efficient tool to check the receptor expression and localization in the host cells. Confocal microscopy was performed on Sf9 cells and H5 cells expressing the pVLMelFlagHis10B2ReGFP construct. The recombinant receptor appeared to be localized mainly in the perinuclear membranes (Fig. 3.16), most probably in the endoplasmic reticulum. Only little fluorescence was observed on the plasma membrane.

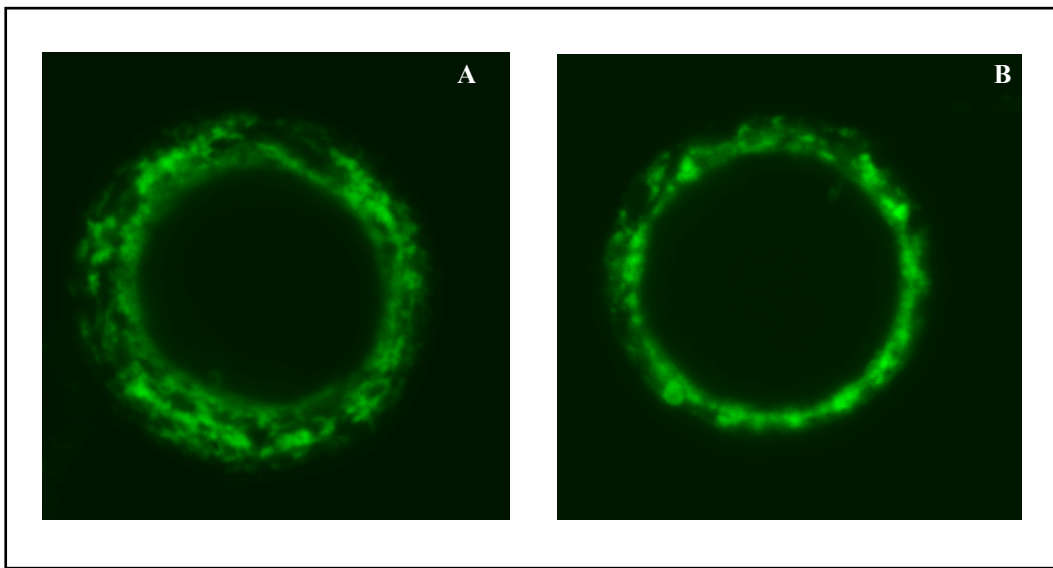


Fig. 3.16 Confocal imaging of Sf9 (A) & H5 (B) cells expressing B₂R-eGFP. The cells were grown and infected on cover slips. 48 h post-infection, cells were fixed and scanned (488 nm) with a Zeiss laser scanning confocal microscope.

3.2.7 Large-scale production of recombinant B₂R

For structural studies, large amounts of receptor are needed. Therefore, a 25 liter wave bioreactor (shown in Fig. 3.17) was used for large-scale culture of Sf9 cells. Cells were initially grown in shake flasks and later transferred to the wave bioreactor. Cells were infected at a density of $2-2.5 \times 10^6$ cells/ml and harvested 96 h post-infection. Membranes were prepared using the nitrogen cavitation method and the amount of recombinant

receptor was estimated by [³H] bradykinin binding assay. Later, the membranes were used for isolation of the recombinant receptor.

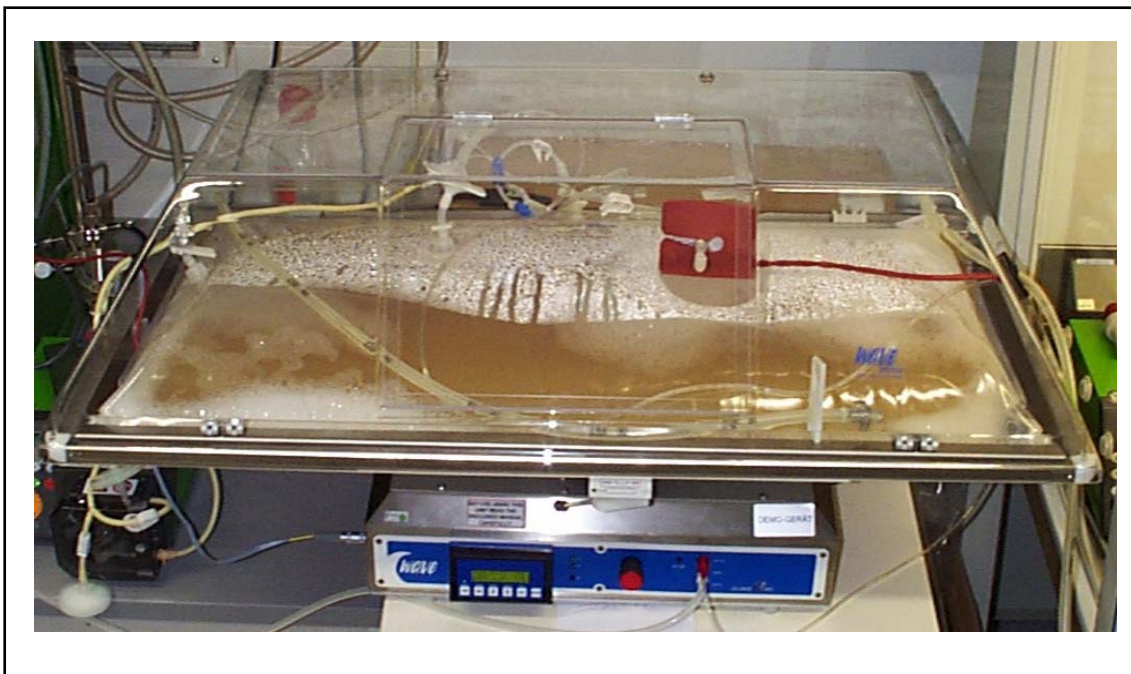


Fig. 3.17 Wave bioreactor (SYSTEM20/50 from WAVE BIOTECH) used for large-scale culture of Sf9 cells. Production of B₂R in wave bioreactor was carried out by Ingo Focken at Sanofi-Aventis.

From a 25 liter Sf9 cell culture, approximately 15 g of membrane was obtained. [³H] bradykinin binding on the membranes from the bioreactor was similar to that of small cultures in Erlenmeyer flasks. As estimated from [³H] bradykinin binding analysis, a total of 7-8 mg of recombinant B₂R was obtained in membranes (Table 3.2)

Culture volume (L)	Total membrane (mg) (BCA)	[³ H] bradykinin binding (pmol/mg)	Total functional B ₂ R in membranes (mg)
25	12-15x10 ³	8-10	7-8

Table 3.2: Estimation of functional B₂R produced in Sf9 cells using the wave bioreactor.

3.2.8 Solubilization and purification of B₂R

LM and Fos14 were the most effective detergents for the solubilization of B₂R from *Pichia* membranes (see section 3.1.6). Therefore, to solubilize B₂R from Sf9 membranes, either of these two detergents was used. Solubilization efficiency, as assessed by [³H] bradykinin binding, was approximately 65-70%.

3.2.8.1 Purification of B₂R via Ni-NTA and monomeric avidin

It has been reported earlier that addition of a high affinity ligand (endothelin) during solubilization and purification stabilizes the endothelin B receptor (Danka Elez, PhD thesis). Therefore, membranes from Sf9 cells expressing B₂R were incubated with bradykinin (1 μM) for two hours. Subsequently, membranes were solubilized and applied to Ni-NTA resin. Eluate from Ni-NTA column was analyzed by silver stained 10% SDS-PAGE. Recombinant receptor band at 55 kDa was enriched (Fig. 3.18 A, lane 4). However, other impurities were also detected. As a second step of purification, the eluate from Ni-NTA was loaded on to the monomeric avidin column. The eluate from monomeric avidin column (lane 5) revealed mainly two bands on silver stained SDS-polyacrylamide gel, one at 55 kDa that represents B₂R and another band at approximately 65 kDa. Purified B₂R was present in homogenous form (Fig. 3.18 B, peak at 1.61 ml) as revealed by analytical gel filtration.

3.2.8.2 Purification of B₂R via Ni-NTA and anti-Flag antibody matrix

Alternatively, the eluate from Ni-NTA column was applied to anti-Flag M1 or M2 antibody resins. As shown in Fig. 3.19 (A), in addition to the recombinant B₂R at 55 kDa, two more bands (65 kDa and 35 kDa respectively) were also observed in the eluates of M1 and M2 resins (lane 2 & 3). The band at 65 kDa was also observed in the eluate of monomeric avidin (Fig 3.18, lane 5). However, the 35 kDa band probably represents the proteolytic cleavage product of B₂R. Western blot (with alkaline phosphatase-coupled

streptavidin) of the eluate from M2 resin revealed a single band at approximately 55 kDa corresponding to B₂R (Fig. 3.19B).[#]

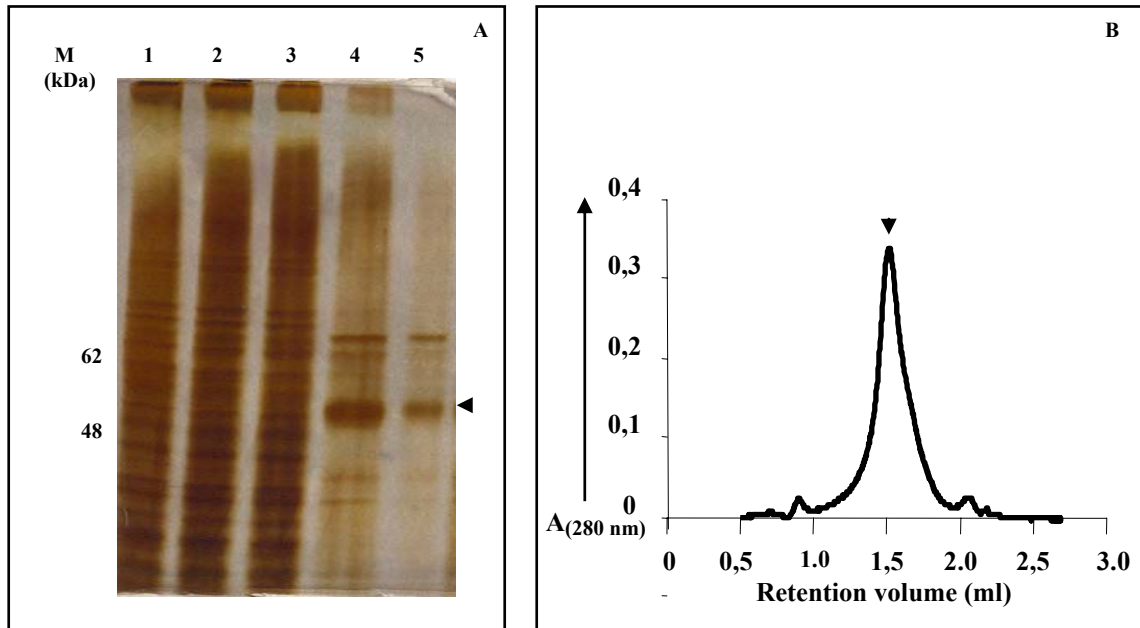


Fig. 3.18 Purification of recombinant B₂R from Sf9 cells. **A.** Silver stained 10% SDS-PAGE showing membranes (lane 1, 0.2 µg), solubilisate (lane 2, 0.2 µg), flow through (lane 3, 0.2 µg), eluate from Ni-NTA (lane 4, 1 µg) and monomeric avidin (lane 5, 0.5 µg). **B.** Analytical gel filtration of purified B₂R (eluate from monomeric avidin column, 0.15 mg at a concentration of 3 mg/ml) using superose 6 column.

[#]The band of approximately 35 kDa was stained with anti-Flag antibody on the Western blot (see section 3.2.3.1) but not with AP-conjugated streptavidin. As described before, this represents an N-terminal fragment of B₂R. The C-terminal fragment after proteolytic degradation is not seen on the gel as it is smaller in size (10-12 kDa).

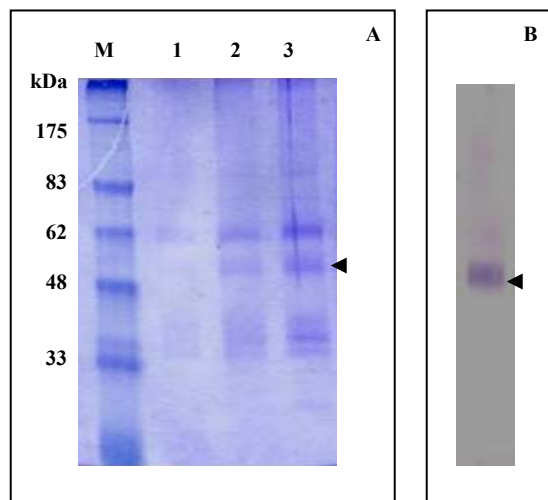


Fig. 3.19 Purification of recombinant B₂R from Sf9 cells. **A.** Coomassie stained 10% SDS-PAGE showing the eluate from anti Flag M1 resin (lane 1 and 2, 0.5 and 1 µg respectively) and anti-Flag M2 resin (lane 3, 1 µg). **B.** Western blot analysis of the eluate from M2 resin using AP-conjugated streptavidin.

Here, it was not possible to follow receptor purification by ligand binding (receptor was purified with high affinity ligand bradykinin). Therefore, estimation of purification yield is based on the total protein quantification by BCA assay. It was estimated that the receptor yield after two-step purification was 15-20% (BCA quantification) of the starting amount in membranes (based on ligand binding).

3.2.8.3 Identification of 65 kDa band as a protein tyrosine phosphatase

As shown in Fig. 3.18 and 3.19, a 65 kDa protein was copurified with the recombinant B₂R on three different affinity resins (Ni-NTA, monomeric avidin and anti-Flag antibody resins). It is likely that this band is just not a contamination but rather a specific interaction partner of B₂R. In order to identify this protein, mass spectrometric analysis was performed. The peaks obtained (shown in Table 3.3) during mass spectrometric analysis were analyzed by PeptIdent programme (EXPASY tools, www.expasy.org/tools/peptident). In this analysis, the 65 kDa band was identified as protein-tyrosine phosphatase SHP-2. Interaction of this protein with B₂R has been documented earlier by using surface plasmon resonance technique. Interaction of B₂R and SHP-2 is important in

the anti-proliferative effect of bradykinin in primary culture renal mesangial cells (Duchene *et al.*, 2002).

Peaks obtained (Da)	Corresponding peptide
919.66	MEQRAER
887.65	QQCELLK
865.60	FKYCQAK
774.90	EFDKQAK
693.86	
676.49	WSDLR

Table 3.3 Peaks obtained during mass spectrometry analysis of the 65 kDa protein and corresponding peptides (analyzed by EXPASY tools, www.expasy.org/tools/peptident).

It is important to mention that the copurification of this receptor tyrosine phosphate was observed only during purification of B₂R from insect cells in the presence of bradykinin (receptor agonist). This protein gets copurified with B₂R even after three affinity columns suggesting a strong interaction with the receptor. Therefore, it can be advantageous during the crystallization of B₂R.

3.3 Production and isolation of the B₂R from mammalian cells

Next, SFV based expression of B₂R in mammalian cells was tested. Mammalian cells provide the most natural environment for heterologous expression of recombinant human GPCRs.

3.3.1 Sub-cloning of B₂R gene in SFV expression vectors

B₂R gene was amplified with the primers B₂R_SFV_Fw/Rv and ligated to modified SFV vectors between *Bam*HI and *Spe*I site using standard cloning procedure.

3.3.2 Expression constructs

For expression of B₂R in mammalian cells, the modified SFV expression vectors were provided by Christoph Reinhart. In this system, expression of recombinant proteins is driven by a subgenomic 26 S promoter. These vectors contain either a Kozak sequence (K) and a self-cleavable signal sequence from influenza haemagglutinin (HA) gene or a capsid sequence (a translation enhancer element from 5' end of capsid gene from SFV) at the N-terminus. Additionally, these vectors also contain affinity tags as described before in section 3.1.2. An e-GFP fusion construct of B₂R was also made for localization analysis.

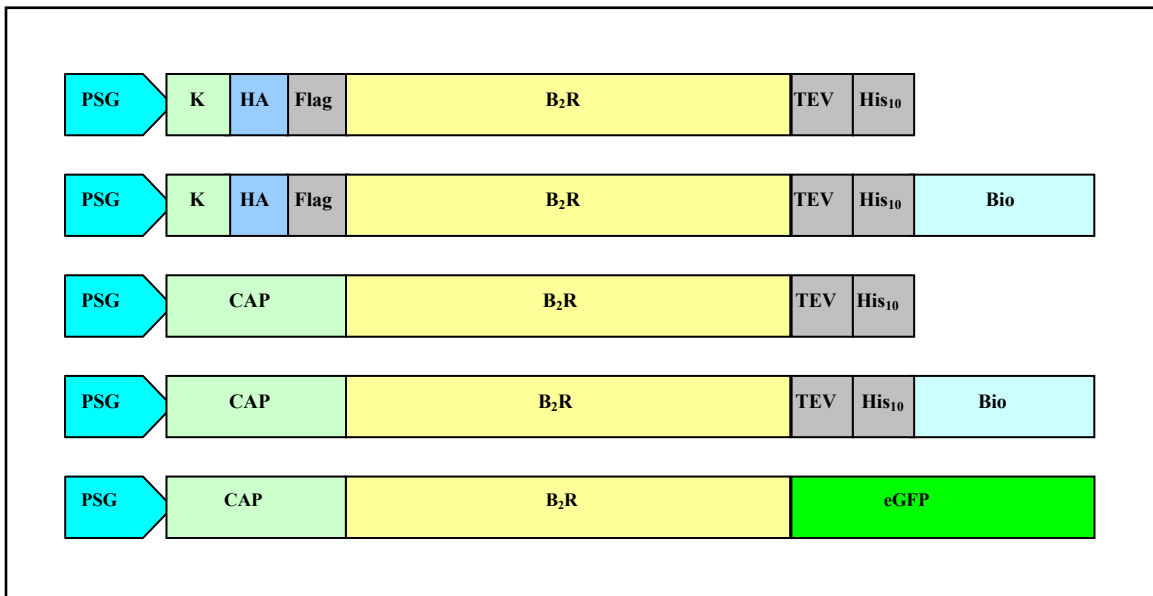


Fig. 3.20 Expression constructs for production of recombinant B₂R in mammalian cells. PSG = subgenomic 26S promoter, K = Kozak sequence, HA = signal sequence from influenza haemagglutinin (HA) gene, Flag = coding sequence for Flag epitope, CAP = capsid sequence, B₂R = coding sequence for B₂R gene, His₁₀ = coding sequence for histidine 10 tag, TEV = cleavage site for TEV protease, Bio = biotinylation domain of *Propionibacterium shermanii* transcarboxylase, eGFP = enhanced green fluorescent protein.

3.3.3 Production of the recombinant receptor

Recombinant virus particles were generated and activated as described in materials and methods section. Monolayer cultures of BHK cells were grown and infected at approximately 75-80 % confluency.

3.3.3.1 Comparison of different construct for B₂R production in BHK cells

In order to select the best construct, [³H] bradykinin binding was performed on membranes from BHK cells expressing different constructs. As shown in Fig. 3.21, best expression of B₂R was observed in the membranes from BHK cells expressing the pSFVCAPB₂RTEVHis₁₀Bio construct. Therefore, this construct was used for further studies. A positive effect of the biotinylation domain (Grunewald *et al.*, 1996) and capsid sequence (Lundstrom *et al.*, 2001) on the expression of recombinant GPCRs has been reported. Also in this study, a significant effect of the biotinylation domain and capsid sequence on expression of B₂R was observed (construct 1 vs. construct 2 and construct 3 vs. construct 4).

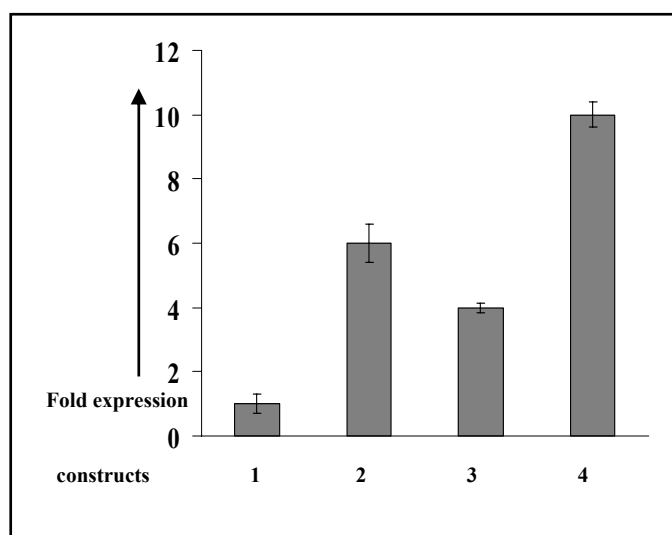


Fig. 3.21 [³H] bradykinin binding on BHK cell membranes expressing different constructs of B₂R. **1** = pSFVGenFlagB₂RTEVHis₁₀, **2** = pSFVGenFlagB₂RTEVHis₁₀Bio, **3** = pSFVCAPB₂RTEVHis₁₀ and **4** = pSFVCAPB₂RTEVHis₁₀Bio.

3.3.3.2 Western blot analysis of B₂R

Western blot analysis of membranes from BHK cells expressing B₂R using anti-his antibody revealed a major band of approximately 50 kDa (Fig. 3.22). It corresponds well to the calculated size of recombinant receptor fusion protein (50.1 kDa). An additional band of approximately 75 kDa was also observed. This probably represents a fusion of recombinant B₂R with capsid protein although an efficient cleavage of capsid protein from the recombinant protein is generally expected (Lundstrom *et al.*, 2003). This band of 75 kDa was not always observed on the Western blots and its presence probably depends on expression conditions.

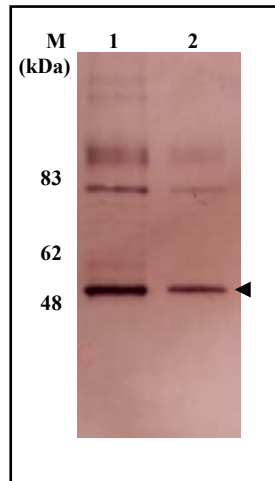


Fig. 3.22 Western blot analysis of the recombinant B₂R produced in BHK cells. Proteins were separated by 10% SDS-PAGE and probed with anti-his antibody. Lane 1 = 10 μ g of BHK membranes expressing B₂R, lane 2 = 5 μ g of BHK membranes expressing B₂R.

3.3.3.3 [³H] bradykinin binding

In order to calculate the total amount of functional receptor in membranes, a saturation binding experiment using [³H] bradykinin was performed. As shown in Fig. 3.23, [³H] bradykinin binding was saturable and revealed a B_{max} value of 5 pmol recombinant B₂R per mg membrane protein. A high affinity binding of [³H] bradykinin to the recombinant receptor was observed with a K_d value of 0.12 nM. This K_d value is similar to those

reported for B₂R in native tissues (see appendix). The non-specific binding was determined in presence of 1 μM bradykinin and it was less than 10% of total binding.

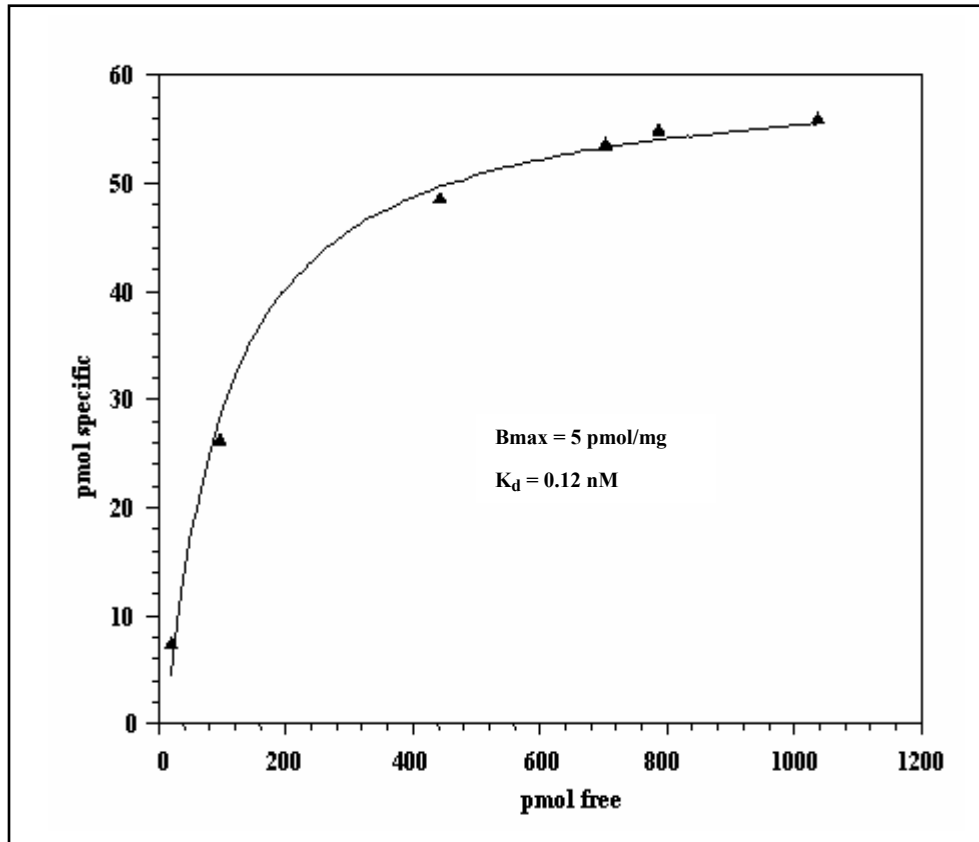


Fig. 3.23 Saturation curve for [³H] bradykinin to recombinant B₂R produced in BHK cells. The graph was generated using single site model in Kaleidagraph software.

3.3.4 Optimization of functional expression of B₂R

In an attempt to optimize the expression level of B₂R in mammalian cells, following parameters were tested.

3.2.4.1 Adherent cells vs. suspension culture

For large-scale production of recombinant receptor, a suspension culture is needed. Therefore, BHK cells were grown in suspension culture and infected at a density of 1-

2×10^6 cells/ml. Interestingly, [^3H] bradykinin binding on membranes of BHK cells grown in suspension culture revealed an expression level of 11 pmol/mg (compared to 5 pmol/mg with adherent BHK cells). Further expression studies were carried out using suspension cultures of BHK cells.

3.2.4.2 Time scale of B₂R expression in BHK cells

In order to find an optimal time point for B₂R expression in BHK cells, time dependence of B₂R expression was determined. BHK cells were grown and infected as described before. Subsequently, the cells were harvested at different time intervals, membranes were prepared and [^3H] bradykinin binding was measured. As shown in Fig. 3.24, there was only a moderate effect of expression time on B₂R expression level in BHK cells. For further experiments, cells were harvested 24 h post-infection.

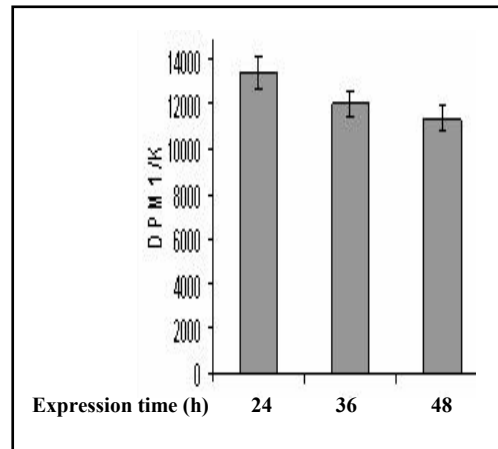


Fig. 3.24 Effect of expression time on recombinant B₂R expression in BHK cells as measured by [^3H] bradykinin binding assay.

3.3.4.3 Effect of DMSO on B₂R expression

In an attempt to further increase the functional expression of B₂R, DMSO was added to the BHK cell cultures during expression. 24 h post-infection, membranes were prepared and subjected to [^3H] bradykinin binding analysis. As shown in Fig. 3.25, a five-fold

increase in functional expression of recombinant B₂R was achieved by the addition of 2% DMSO. A maximum expression level of 55-60 pmol/mg for recombinant B₂R (0.3 mg/liter culture) was observed.

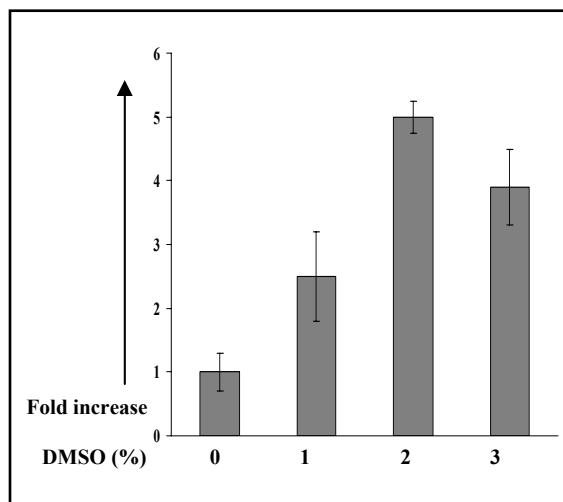


Fig. 3.25 Effect of DMSO on the expression level of recombinant B₂R in BHK cells. DMSO was added to the cultures, membranes were prepared and [³H] bradykinin binding was measured.

3.3.4.4 Effect of cell type on B₂R expression

It has been previously reported that expression level of a recombinant GPCR may vary among different cell lines (Lundstrom *et al.*, 2003). Four different cell lines (BHK-21, CHO-K1, Cos-7 and HEK-293) were tested for B₂R expression. However, no significant difference in the expression level of B₂R was observed in these cell lines. Therefore, for large-scale production, BHK cells were used.

3.3.5 Glycosylation analysis of recombinant B₂R

To check the glycosylation state of the recombinant receptor in BHK cells, enzymatic deglycosylation using PNGaseF or EndoH was performed. As shown in Fig. 3.26, there was no change in the migration of the recombinant B₂R suggesting that the receptor was not glycosylated in BHK cells.

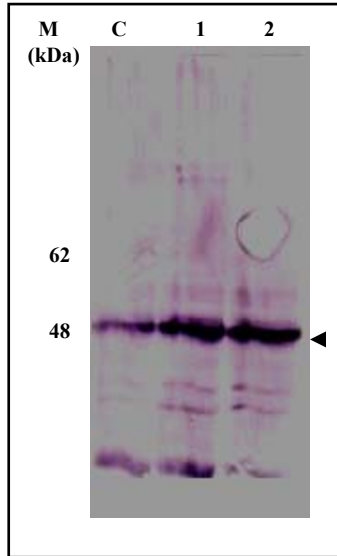


Fig. 3.26 Glycosylation analysis of the recombinant B₂R produced in BHK cells. 10 µg of membranes from BHK cells expressing B₂R were treated with 0.5 units of PNGase F (lane 1) or 0.5 units of EndoH (lane 2) at 4°C for 2h. The lane “C” is untreated control membranes from BHK cells (5 µg). The proteins were separated using 10% SDS-PAGE and probed with anti-his antibody.

3.3.6 Localization of recombinant B₂R

In order to check the localization of recombinant B₂R, immunogold labeling experiments were carried out using BHK cells expressing pSFVGenFlagB₂RHis₁₀Bio construct. Additionally, B₂R-eGFP fusion protein was used to check the receptor localization by confocal microscopy.

3.3.6.1 Immunogold labeling experiment

BHK cells expressing B₂R were fixed for pre- and post-embedding as described (see materials and methods). As shown in Fig. 3.27, most of the recombinant receptors were localized in the intracellular membranes (most probably in the endoplasmic reticulum). Only very few receptor molecules were found in the plasma membrane (Fig. 3.27 D&F). Similar intracellular localization of recombinant beta-2 adrenergic receptor was observed in BHK cells (Darui Huo, Ph.D. thesis).

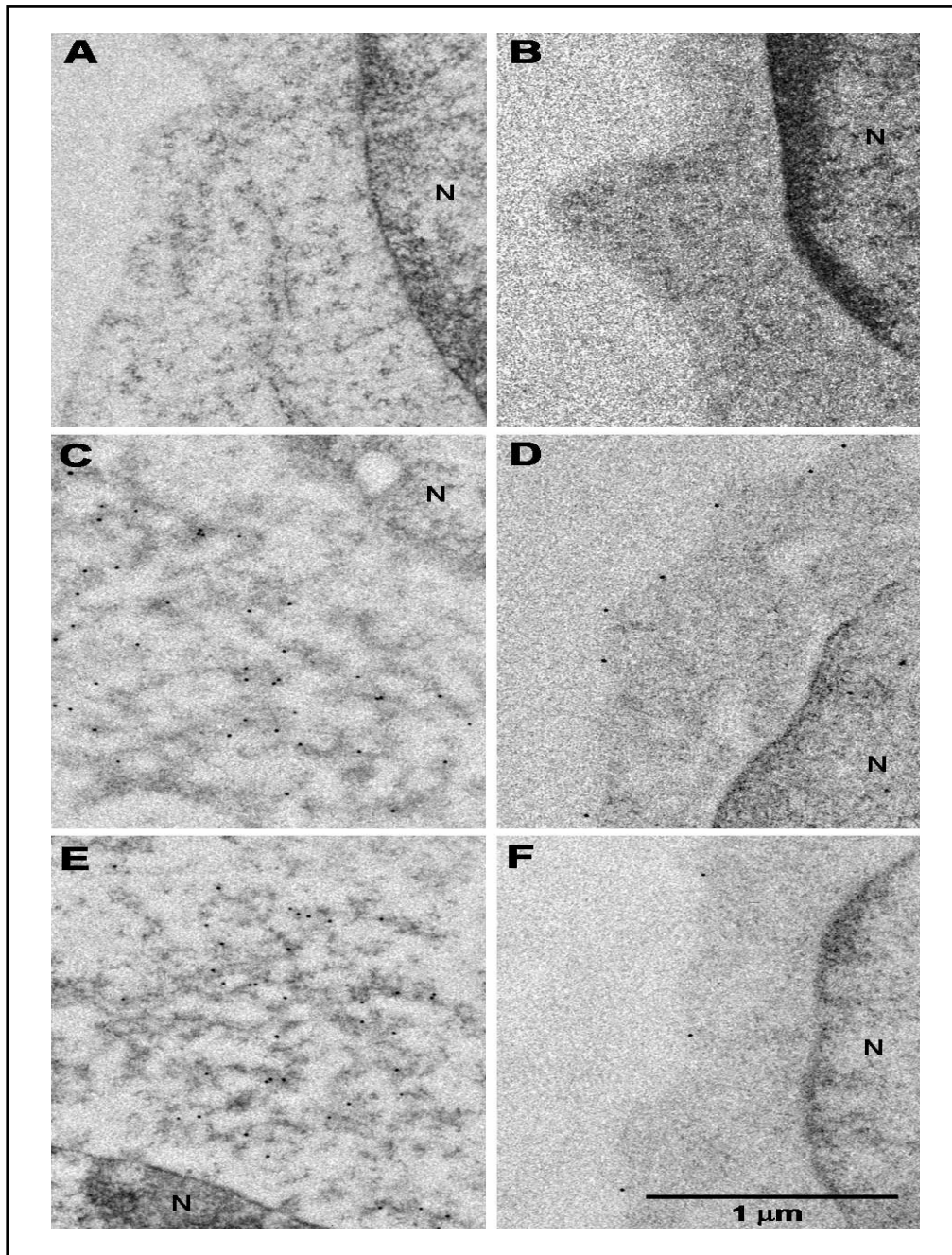


Fig. 3.27 Localization of recombinant B₂R in BHK cells using immunogold labeling experiment. A&B = control BHK cells, C&E = post-embedding labeling of BHK cells expressing B₂R and D&F = pre-embedding labeling of BHK cells expressing B₂R. This experiment was performed by Dr. Winfried Haase.

3.3.6.2 Localization analysis of B₂R by confocal microscopy

Localization of B₂R-eGFP fusion protein was checked by confocal microscopy. As shown in Fig. 3.28, recombinant B₂R was mainly localized in the perinuclear membranes (most probably in the endoplasmic reticulum). Only low levels of fluorescence were observed on the plasma membrane. A similar intracellular retention has been observed in BHK cells for the overexpressed alpha-2B adrenergic receptor (Sen *et al.*, 2003).

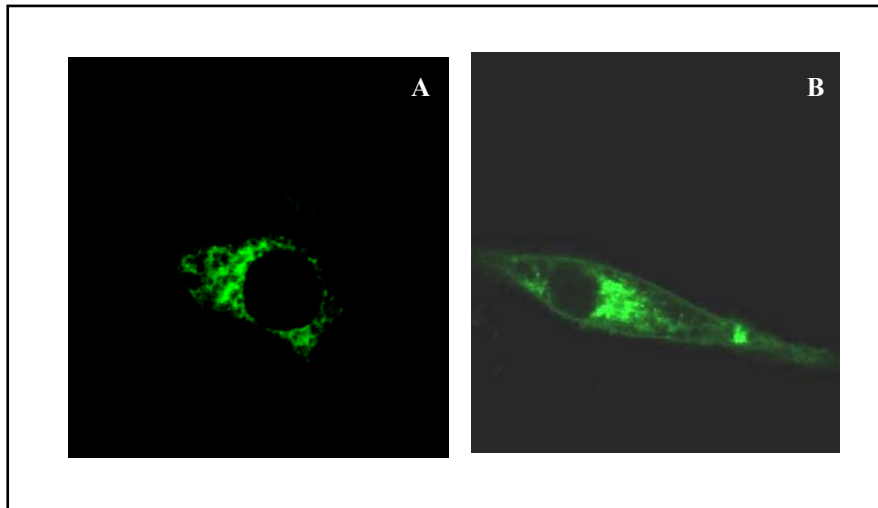


Fig. 3.28 Confocal imaging of BHK cell (A) or CHO cell (B) expressing B₂R-eGFP. Cells were grown and infected on cover slips. 24 h post-infection, cells were fixed and scanned (488 nm) with a Zeiss laser scanning confocal microscope.

3.3.7 G protein coupling (inositol phosphate release assay) of B₂R

In order to check the G protein coupling of recombinant B₂R, bradykinin induced phosphatidyl inositol turnover was measured. BHK cells expressing B₂R were pre-labeled with [³H] inositol and then stimulated with 1 μM of bradykinin for different time intervals. Also, the effect of bradykinin concentration on IP₃ accumulation was analyzed by stimulating the BHK cells expressing B₂R with different concentrations of bradykinin (1 pM-0.1mM) for 10 min and subsequently, IP₃ accumulation was monitored. As shown in Fig. 3.29, rapid accumulation of IP₃ was observed in response to bradykinin.

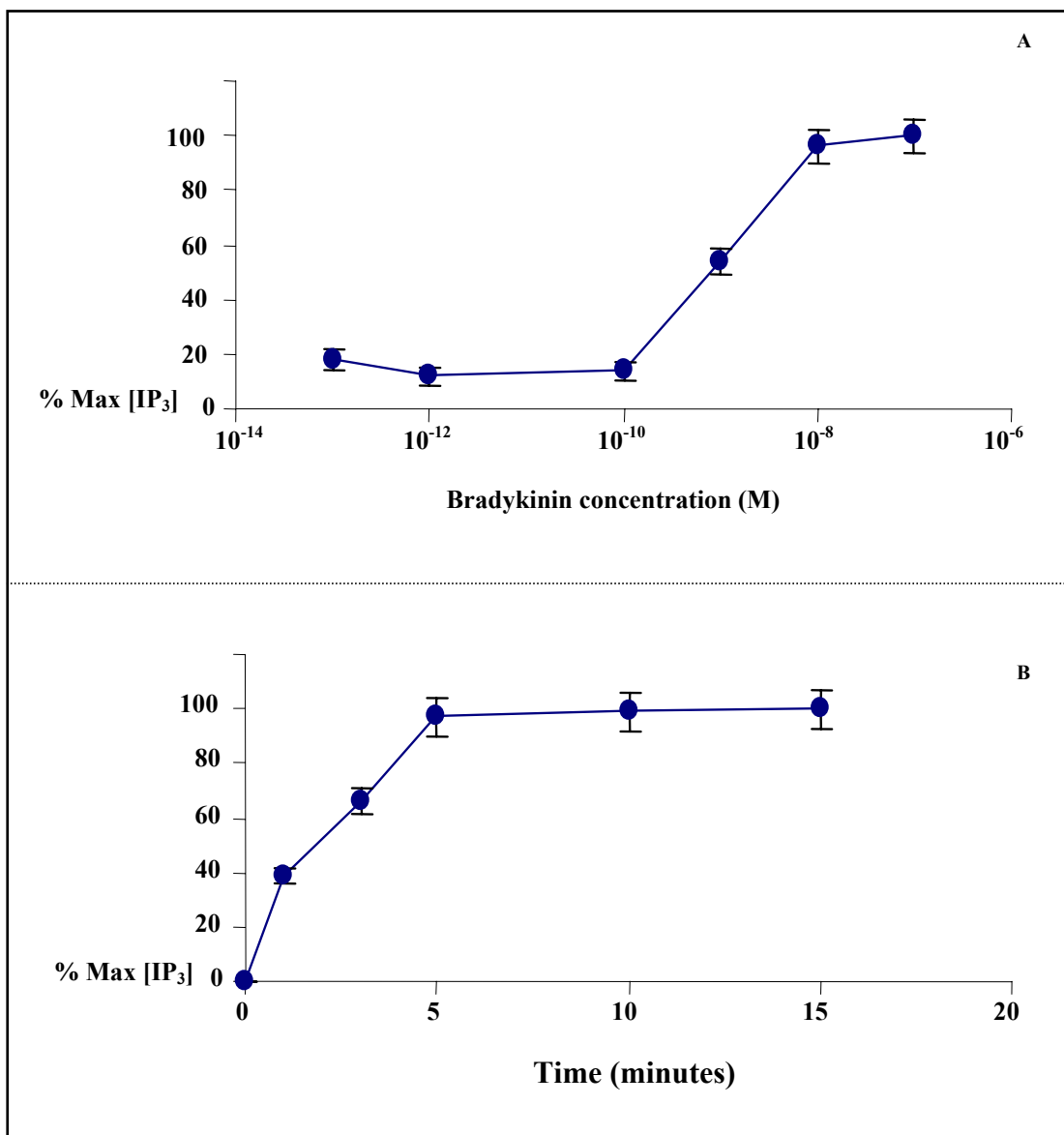


Fig. 3.29 G-protein coupling of recombinant B₂R. **A.** Concentration dependence (bradykinin) of IP₃ accumulation in BHK cells expressing B₂R. **B.** Time course of bradykinin (1 μM) induced IP₃ response in BHK cells expressing B₂R.

3.3.8 Solubilization and purification of B₂R

Recombinant B₂R was solubilized from membranes (5 mg/ml) using 1% LM or Fos-14 in presence of 0.2% CHS. Approximately, 65-70% of [³H] bradykinin binding sites were

solubilized from membranes. Solubilized receptor was purified using Ni-NTA resin. Eluate from Ni-NTA column was analyzed by silver stained 10% SDS-PAGE. As shown in Fig. 3.30 (A), >80% pure receptor was obtained after Ni-NTA purification. In order to check the homogeneity of purified receptor, the eluate from Ni-NTA column was analyzed by gel filtration on a superose 6 column. As revealed in Fig. 3.30 (B), purified B₂R was present mainly in homogenous form (peak at 1.61 ml). In addition to the main peak, some aggregation of purified B₂R was also observed (the peaks at 0.9 ml and 1.2 ml). However, when B₂R was purified in presence of bradykinin, no aggregation of the receptor was observed (Fig. 3.31).

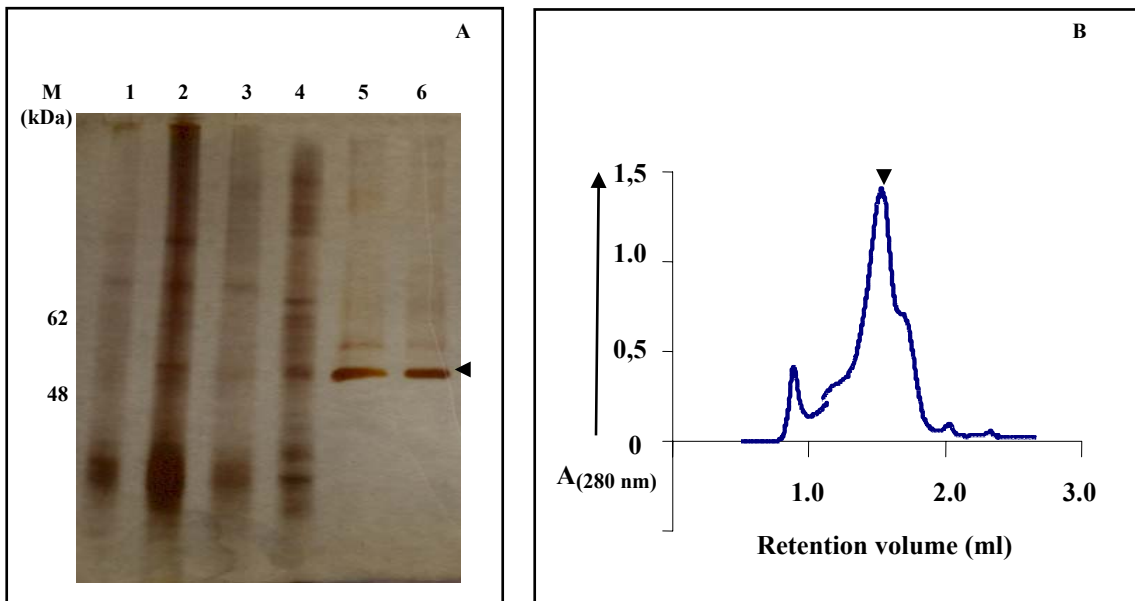


Fig. 3.30 Purification of recombinant B₂R from BHK cells. **A.** Silver stained 10% SDS-PAGE showing membranes (lane 1, 0.2 µg), solubilisate (lane 2, 0.2 µg), flow through (lane 3, 0.2µg), wash (lane 4, 0.2 µg), eluate from Ni-NTA (lane 5, 0.8 µg) and gel filtration fraction (lane 6, 0.8 µg). **B.** Analytical gel filtration of purified B₂R (eluate from Ni-NTA column, 0.5 mg at a concentration of 10 mg/ml) using superose 6 column.

[³H] bradykinin binding was measured on different fractions during purification steps. As shown in Table 3.4, recovery of the active receptor was approximately 32% after Ni-NTA purification. A similar purification profile was observed when the recombinant receptor was solubilized and purified with Foscholine 12 or Foscholine 14.

	[³ H]bradykinin binding (nmol)	Specific activity (nmol/mg)	Total protein (mg) BCA/[³ H]BK binding	Yield (%)
Membrane	61.8	0.032	1932 (3.09)	100
Solubilisate	43.5	0.037	1176 (2.16)	69
Ni-NTA eluate	19.6	10.3	1.9 (0.98)	32

Table 3.4 Recovery of functional B₂R during different steps of purification based on [³H] bradykinin binding analysis.

3.3.9 Stability analysis of purified B₂R

In order to check the long-term stability, recombinant B₂R was purified (in the presence of bradykinin) and stored at 4°C. After a defined time period, homogeneity of the receptor was investigated by analytical gel filtration. Purified receptor was stable for at least two weeks as shown in Fig. 3.31. Therefore, it can be used for three-dimensional crystallization attempts.

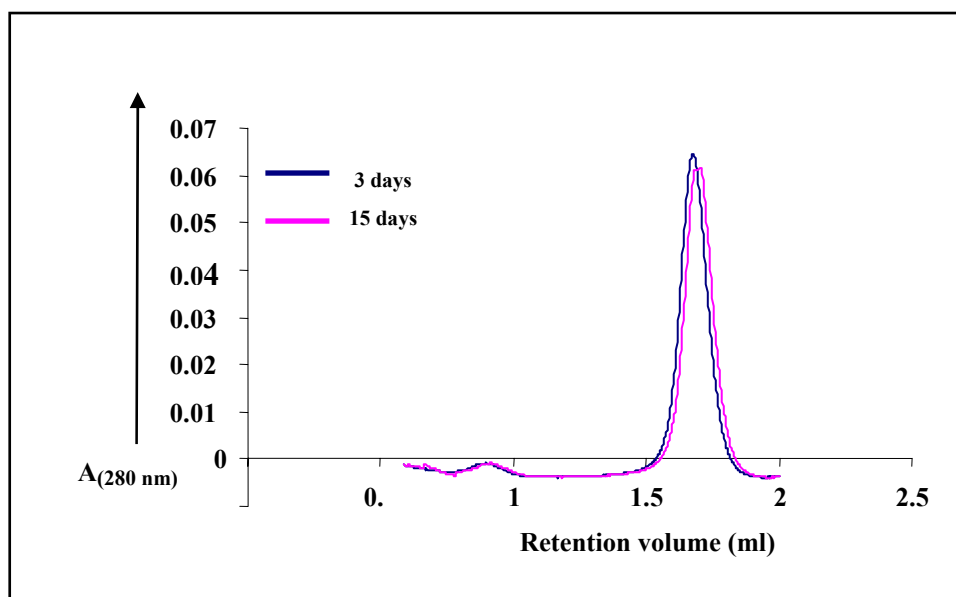


Fig. 3.31 Stability analysis of purified B₂R by analytical gel filtration. Purified B₂R was stored at 4°C for 3 or 15 days and subsequently analyzed by using superpose 6 column (50 µg at a concentration of 1 mg/ml).

Chapter 4: Structural studies with $\mathcal{B}_2\mathcal{R}$

4.1 Solid-state NMR analysis of receptor bound conformation of bradykinin[#]

High resolution solid-state NMR techniques based on rapid sample rotation about the magic angle (magic angle spinning, MAS) under ultra high magnetic fields provide an excellent tool to study ligand-receptor systems. It has already been used successfully to investigate the backbone structure of neurotensin when bound to its cognate GPCR, the neurotensin receptor (Luca *et al.*, 2003). The active conformation of a GPCR ligand may provide useful information for designing potent and specific drugs acting on that particular receptor. As shown in section 3.2.5 and 3.3.5, recombinant B₂R can be isolated in milligram quantities. Therefore, in parallel to crystallization trials, a part of isolated B₂R was used for ss-NMR studies in order to understand the conformation of receptor bound bradykinin.

4.1.1 Sample preparation (peptides and receptor)

Three differently labeled variants of bradykinin (¹³C/¹⁵N labeled peptides[!]) have been used for ss-NMR experiments. These peptides are shown in Fig. 4.1. Selectively labeled peptides (R¹F⁵ and F⁸R⁹) are required in order to differentiate between individual arginines and phenyl alanines in the 2-dimensional spectra.

U ¹	R-P*-P*-G*-F*-S*-P*-F*-R
R ¹ F ⁵	R*-P-P-G-F*-S-P-F-R
F ⁸ R ⁹	R-P-P-G-F-S-P-F*-R*

Fig. 4.1 Differently labeled bradykinin variants that are being used in ss-NMR study. The asterisks represent ¹³C/¹⁵N labeled amino acids.

[#]These experiments are carried out by Jakob Lopez and Clemens Glaubitz at the Center for Biomolecular Magnetic Resonance, Frankfurt.

[!]The ¹³C/¹⁵N labeled peptides are synthesized and characterized by Karin Heidemann (in the group of Harald Schwalbe) at the Center for Biomolecular Magnetic Resonance, Frankfurt.

The receptor was isolated as described in sections 3.2.8 and 3.3.8. Purified B₂R was incubated with ¹³C/¹⁵N labeled peptides in a molar ratio of 1:10. Subsequently, the receptor was concentrated to 50-60 μl (at 18-20 mg/ml). In order to remove the free ligand, repeated dilution (up to 1:100, in detergent free buffer) and concentration was performed. This complex of B₂R-bradykinin was transferred to a 4 mm MAS rotor and used for ss-NMR measurements. As control experiments, ss-NMR measurements were also performed on lyophilized bradykinin and bradykinin in detergent solution.

4.1.2 ¹³C-Cross-polarization spectrum of lyophilized bradykinin

Fig. 4.2 shows ¹³C-CP spectrum of uniformly labeled bradykinin (U¹). Assignments were carried out with the help of previous measurements and double quantum/single quantum spectroscopy. Double quantum filtering (DQF) was used in order to measure only those signals which belong to two adjacent ¹³C nuclei, eliminating the large background signal due to detergent and the protein.

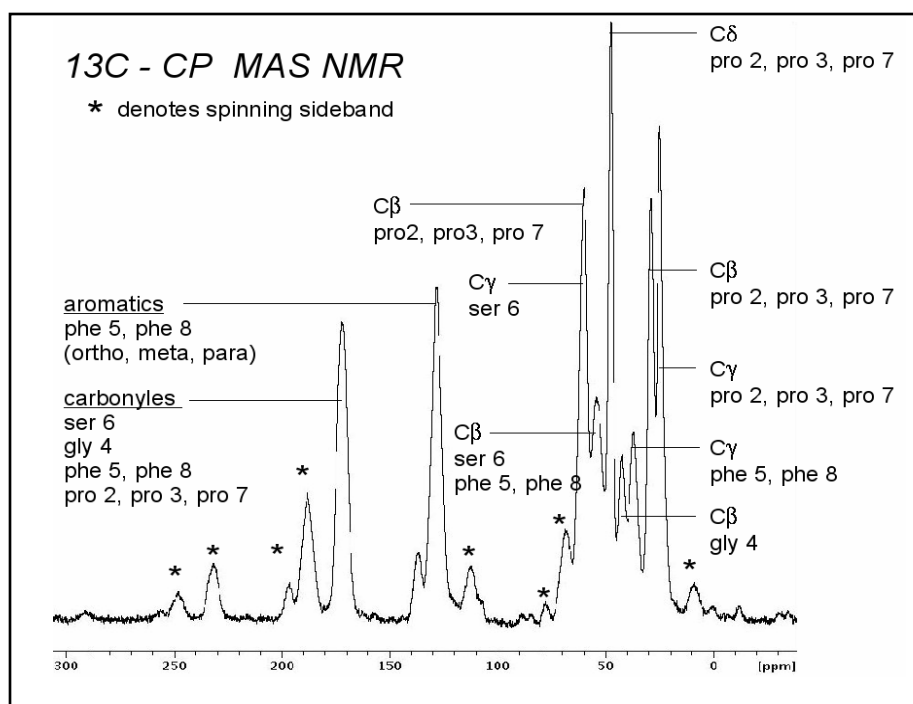


Fig. 4.2 ¹³C-CP spectrum and assignments using lyophilized bradykinin (2 mg of ¹³C/¹⁵N labeled bradykinin in a 4 mm MAS rotor).

4.1.3 Two-dimensional double quantum/single quantum ^{13}C NMR spectrum

Next, two-dimensional double quantum/single quantum experiments were performed using lyophilized bradykinin (U^1). Here, the assignments were carried out by starting with a known peak and assigning peaks at the same horizontal chemical shift coordinate to nuclei which are known to be covalent neighbors of the first peak's nucleus. One assignment walk for a proline residue is indicated in the Fig. 4.3.

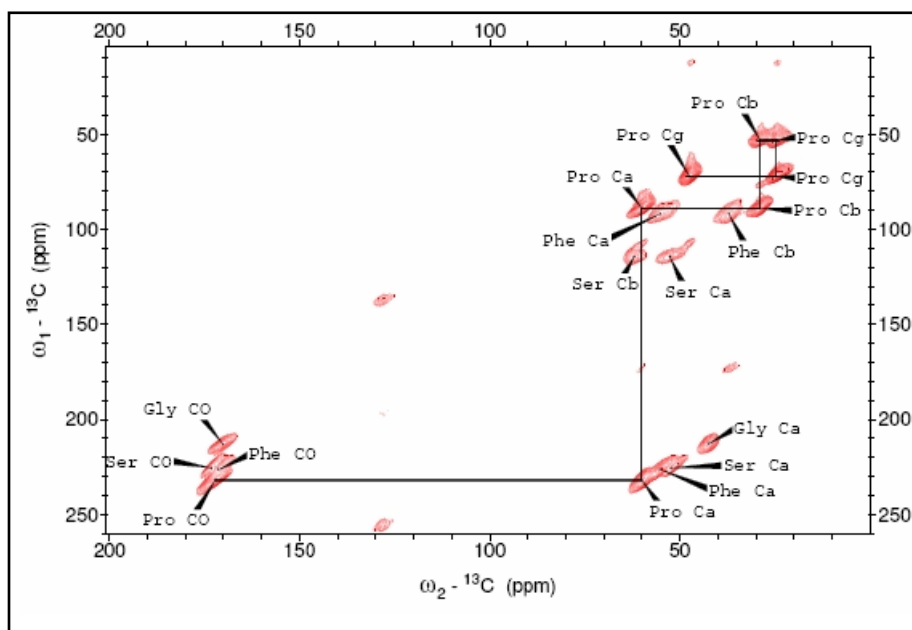


Fig. 4.3 2-D double quantum/single quantum ^{13}C NMR spectrum of bradykinin (U^1 , 2 mg of peptide).

4.1.4 Comparison of 1-dimensional spectra of bradykinin in different states

The main goal of this study was to monitor the conformational changes in bradykinin upon binding to B_2R in order to obtain the backbone structure of receptor bound bradykinin. Therefore, the one-dimensional spectrum of $^{13}\text{C}/^{15}\text{N}$ labeled lyophilized bradykinin was compared to that of bradykinin in detergent solution and bradykinin in receptor bound state. As indicated in Fig. 4.4, significant changes in the chemical shifts were observed for bradykinin after binding to the receptor.

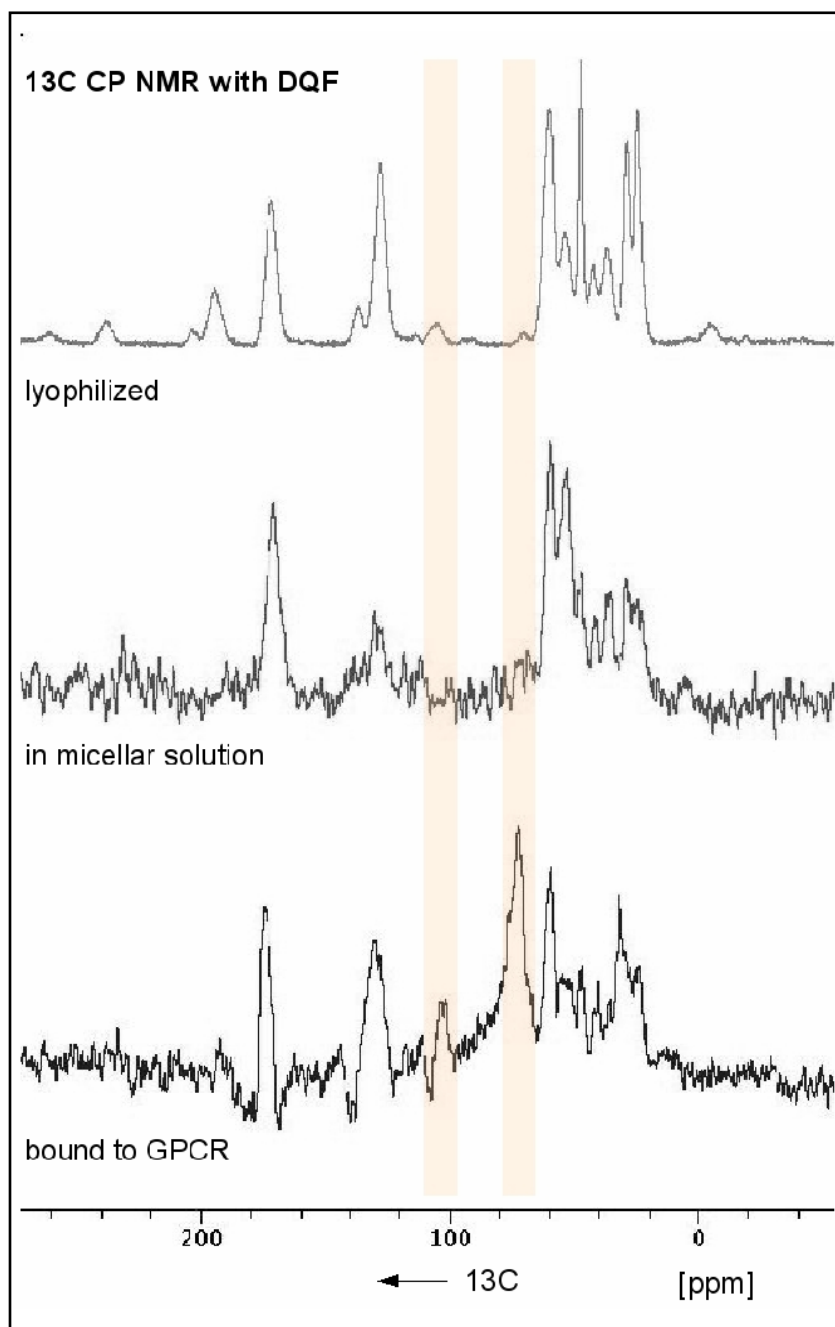


Fig. 4.4 1-D spectra of lyophilized bradykinin, bradykinin in detergent solution and bradykinin bound to B₂R. The shaded part shows some of the changes in chemical shifts that occur upon binding of bradykinin to B₂R.

4.1.5 Reducing the measurement time

In order to translate the chemical shifts observed in 1-D spectra into the structural constraints, 2-D NMR analysis is necessary. However, 1 mg of B₂R will bind to approximately 25 µg of ¹³C/¹⁵N bradykinin. Therefore, it requires long measurement times to get a good signal/noise ratio in 2-D spectra. In order to reduce the measurement time, either the receptor amount was increased to 2.5 mg (thus increasing the amount of bound ¹³C/¹⁵N bradykinin) or measurements were carried out at low temperature (180 K).

4.1.5.1 Receptor aggregation at high concentration

One of the limitations of ss-NMR is the small volume (50-60 µl) of MAS rotors. Therefore, in order to increase the amount of receptor in the rotor, it should be highly concentrated (e.g. up to 50 mg/ml for 2.5 mg of receptor). Unfortunately, the purified B₂R aggregated (as revealed by gel filtration analysis) when concentrated to 45 mg/ml (Fig. 4.5).

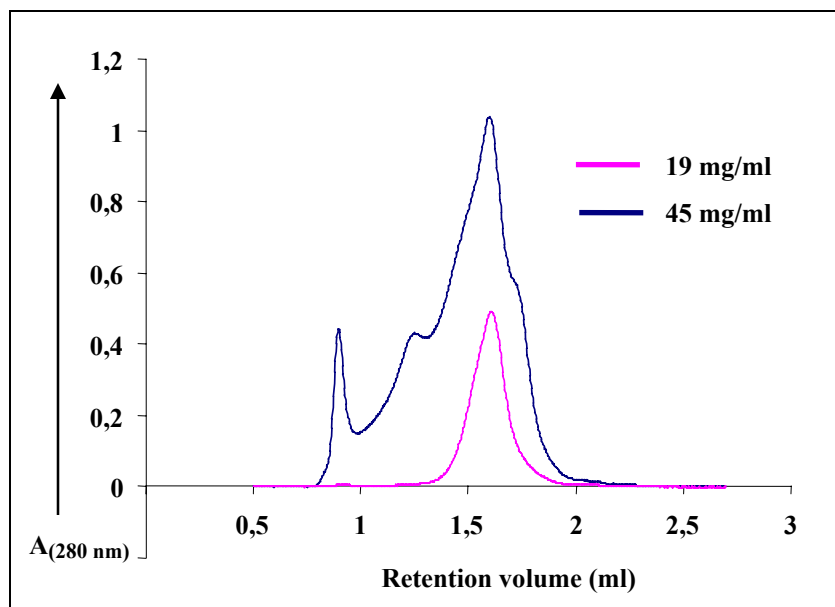


Fig. 4.5 Purified B₂R aggregates at high concentration. Receptor homogeneity was analyzed at indicated concentrations by gel filtration using superose 6 column. The peaks at 0.90 ml and 1.3 ml represent aggregated receptor while the peak at 1.6 ml shows homogenous receptor.

4.1.5.2 Effect of temperature on signal/noise ratio

Performing ss-NMR measurements at low temperatures (<200K) results in a better signal/noise ratio, presumably due to a better magnetization from ^1H to ^{13}C via cross-polarization and reduces the chances of overheating the samples. Therefore, effect of lowering the temperature on the signal to noise ratio in 1-D ^{13}C DQF spectra was examined. As depicted in Fig. 4.6, approximately four-fold improvement in overall signal/noise ratio was observed when the temperature was lowered from 210 K to 180 K.

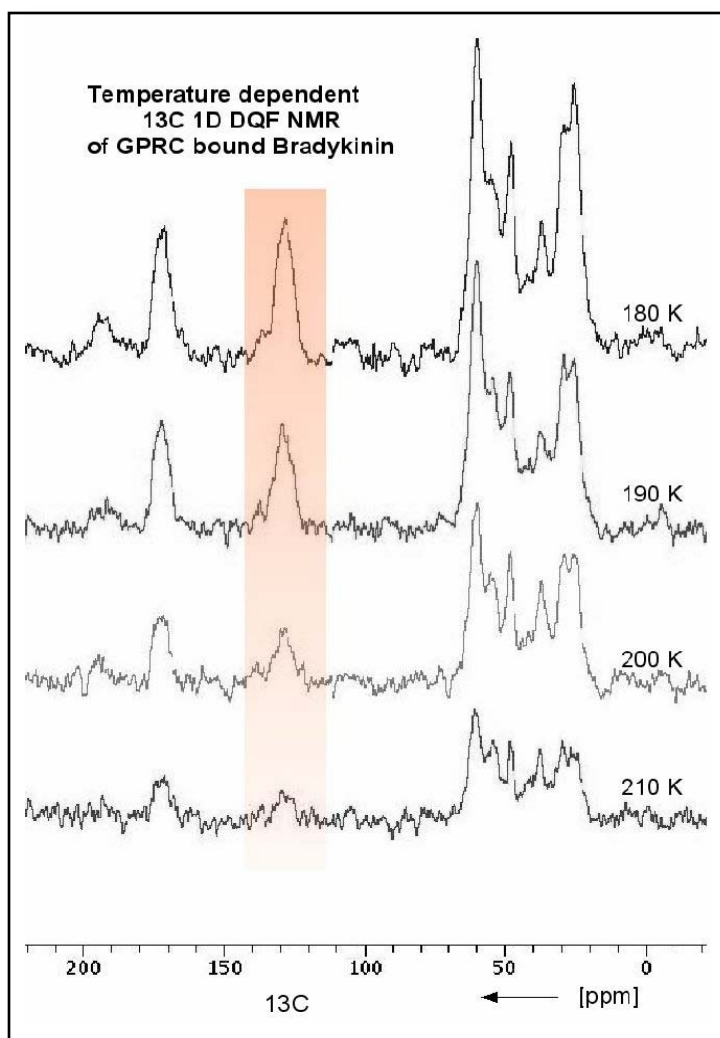


Fig. 4.6 Improvement of signal/noise ratio in 1-D ^{13}C DQF spectra ($^{13}\text{C}/^{15}\text{N}$ bradykinin bound to B_2R) at lower temperature. The shaded part shows increased intensity of one of the peaks in 1-D spectra.

4.1.6 Two-dimensional spectrum of $^{13}\text{C}/^{15}\text{N}$ bradykinin bound to B_2R

Under optimized conditions (25 μg bound to 1 mg B_2R , 180K), the two dimensional double quantum ^{13}C NMR spectrum of $^{13}\text{C}/^{15}\text{N}$ bradykinin (U^1) bound to B_2R can be measured within three days (Fig. 4.7). Similar experiments with selectively labeled bradykinin variants (R^1F^5 and F^8R^9) are in progress.

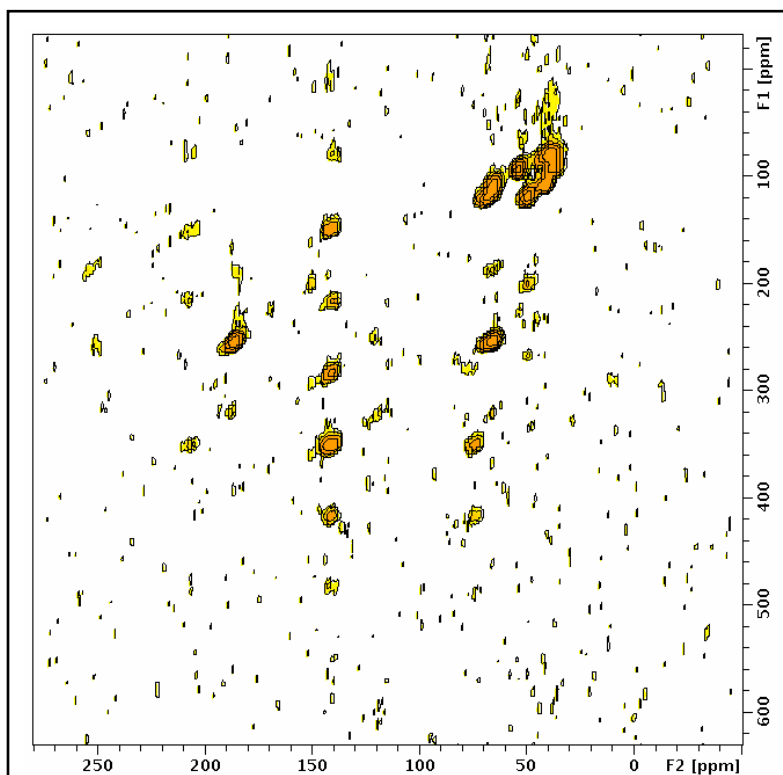


Fig. 4.7 Two-dimensional double quantum/single quantum ^{13}C NMR spectrum of bradykinin (U^1) bound to B_2R . A typical experiment requires a measurement time of approximately 3 days.

4.2 Three-dimensional crystallization trials of B_2R

For 3-dimensional crystallization screening, B_2R was purified as described in sections 3.2.8 and 3.3.8. The purified B_2R was concentrated up to 10 mg/ml. In order to remove the free detergent micelles, gel filtration was performed. The initial screening scheme has

been given in the appendix. Initially, a pH (4-9) and temperature (4°C and 18°C) screen combined with different PEGs (as precipitant) was used. The protein in crystallization drops was stable over a wide range of pH and some microcrystalline precipitates were obtained with PEG 400 (concentration 12-18%, w/v). With PEG 4000, the crystallization drops remained mostly clear and no protein precipitation was observed even at high concentrations (20-22%, w/v) and over a long period of time (3-4 weeks). Commercially available screening kits (from SIGMA and Jena Biosciences) were also used in order to screen the combinations of different precipitants and buffers. As shown in Fig. 4.8, some crystalline structures were observed. However, these are too small to verify either by Western blot analysis or by X-ray beam. It has not been possible so far to reproduce them under the same conditions. Further crystallization screening is ongoing to obtain reproducible and bigger crystals.

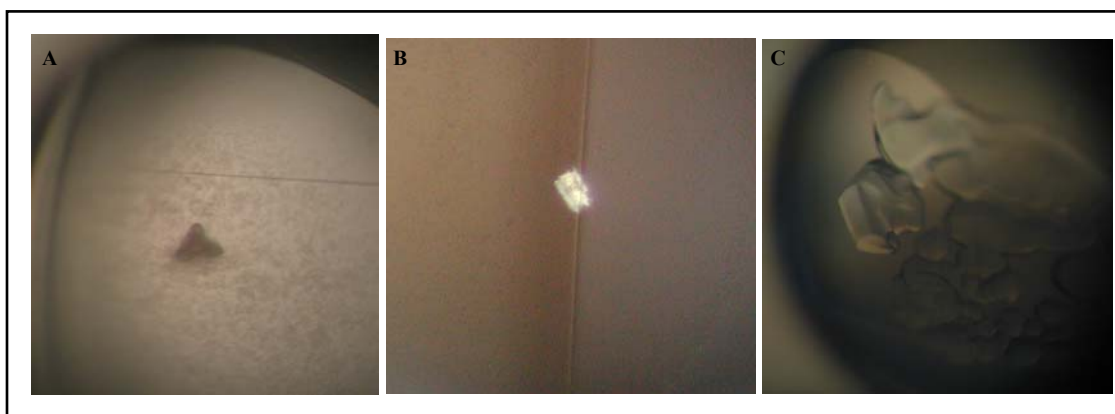


Fig. 4.8 Some crystal-like structures (A & B) obtained during 3-D crystallization attempts of B₂R. Often, heavy detergent crystallization was observed (C).

4.3 Interaction of B₂R with β -arrestin

β -arrestin is a soluble protein that binds to the agonist activated GPCRs and blocks the G protein coupling. This results in downregulation of G protein dependent signalling pathways mediated via GPCRs. A complex of GPCR- β -arrestin might be useful for cocrystallization attempts. Purified B₂R from BHK cells was mixed with purified β -arrestin-2 in a molar ratio of 1:10 and incubated at room temperature for 2 h. Subsequently, a pull-down assay was performed using Ni-NTA resin. The flow through

and elution fractions were analyzed by 10% silver stained SDS-PAGE. As shown in Fig. 4.9 (A), β -arrestin was present in the flow through fraction and was not observed in the elution fraction with B_2R . This indicates that there was no interaction between purified B_2R and β -arrestin *in vitro*.

Recently, it was observed that B_2R - V_2R chimera binds to β -arrestin with high affinity *in vivo* (Simaan et al., 2005). This B_2R - V_2CT chimera contains the first 324 amino acids of the human B_2R (Met-1 to Cys-324) fused to the last 29 amino acids of the V_2R (Ala-343 to Ser-371). Therefore, attempts were made to reconstitute the B_2R - V_2R chimera with β -arrestin *in vitro*. As shown in Fig. 4.9 (B), β -arrestin was present with B_2R - V_2R in the elution fraction of Ni-NTA resin. No binding of purified β -arrestin alone to the Ni-NTA resin was detected (Fig. 4.9 C). Further studies are ongoing to examine the stability of this complex by analytical gel filtration.

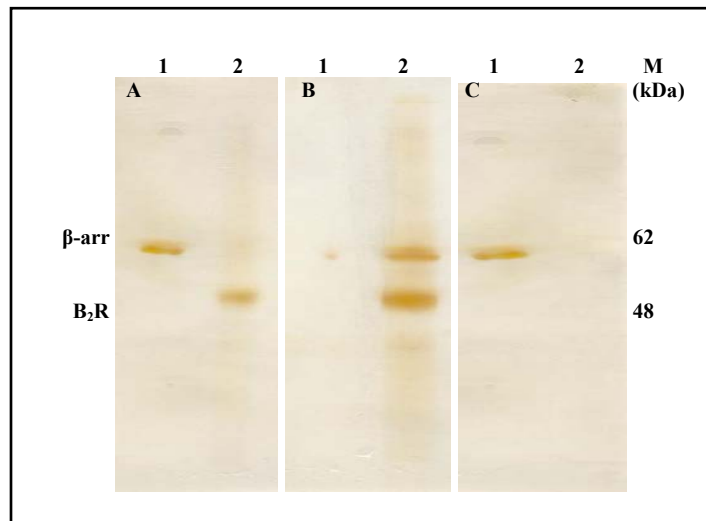


Fig. 4.9 Interaction of B_2R - β -arrestin[#] by pull down assay using Ni-NTA resin followed by 10% silver stained SDS-PAGE. **A.** Using wild type B_2R , flow through (lane 1, 0.3 μ g) and elution (lane 2, 0.3 μ g). **B.** Using B_2R - V_2R mutant^{*}, flow through (lane 1, 0.2 μ g) and elution (lane 2, 0.4 μ g). **C.** Using β -arrestin alone, flow through (lane 1, 0.2 μ g) and elution (lane 2, 0.3 μ g).

[#]Purified β -arrestin-2 was provided by Jan Griesbach, MPI Biophysics, Frankfurt.

^{*}The gene for B_2R - V_2R mutant was a kind gift from Dr. S.A. Laporte (Montreal, Canada). This mutant was expressed and purified similar to the wild type B_2R .

*Chapter 5: Production, characterization and isolation of
 $AT_{1a}R$*

5.1 Production and isolation of the AT_{1a}R using *Pichia pastoris*

5.1.1 Sub-cloning of the AT_{1a}R gene in *Pichia* expression vector

The coding region of AT_{1a}R gene was amplified from cDNA vector (pAT_{1a}R from Aventis) with the primers AT_{1a}R_*Pichia*_Fw/Rv (Fig. 5.1) and ligated into the pPIC9K (modified) vector between *Bam*HI and *Eco*RI sites using the standard cloning techniques.

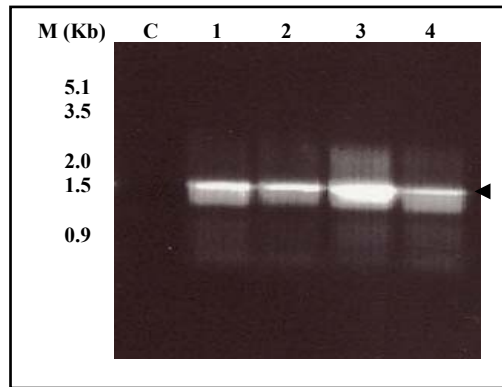


Fig. 5.1 Amplification of the AT_{1a}R gene from the cDNA vector by PCR under following conditions: 94°C = 5 min, 94°C = 40 sec, 69°C = 40 sec, 72°C = 90 sec and 72°C = 10 min. Total 30 cycles (step 2 to step 4) were used for amplification. PCR products were analyzed on 1% agarose gel. M= Lambda DNA (*Eco*RI + *Hind*III) marker, C= control (no template), 1-4 = different amounts (50 ng-200 ng) of template DNA.

5.1.2 Expression constructs

A modified pPIC9K expression vector was used for the production of the AT_{1a}R in *Pichia pastoris*. This vector has been described earlier in section 3.1.2. In some cases, it has been observed that the elution of recombinant proteins from monomeric avidin column is not very efficient[#] (personal experience and communication with other colleagues). Therefore, an expression construct with a Strep II tag (instead of Bio tag) was also made (Fig. 5.2). Strep II tag allows purification of the recombinant receptor on streptactin agarose resins.

[#]After repeated use of monomeric avidin resin, the recovery of bound proteins goes down and the binding capacity of the resin also decreases.

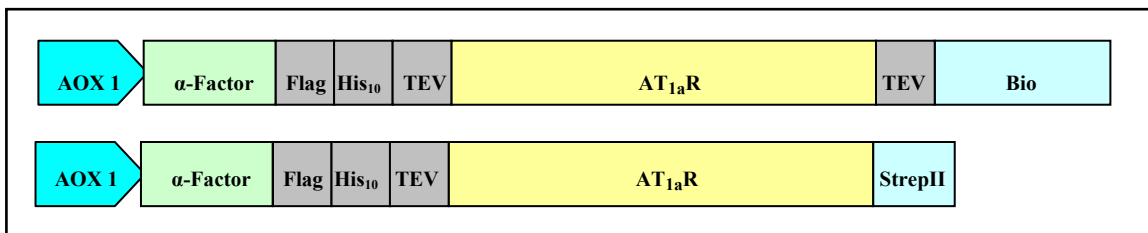


Fig. 5.2 Expression construct for production of recombinant AT_{1a}R in *Pichia pastoris*. AOX1 = alcohol oxidase 1 promoter, α -factor = α -mating factor prepro-peptide of *S. cerevisiae*, Flag = coding sequence for Flag epitope, His₁₀ = coding sequence for histidine 10 tag, TEV = cleavage site for TEV protease, AT_{1a}R = coding sequence for AT_{1a}R, Bio = biotinylation domain of *Propionibacterium shermanii* transcarboxylase, StrepII = coding region of strep II tag.

5.1.3 Production of the recombinant receptor

Pichia cultures were grown in shake flasks (as described in Multi-Copy *Pichia* Expression Kit, Invitrogen), membranes were prepared (after 24 h of induction with methanol) and subjected to Western blot analysis and ligand binding assay.

5.1.3.1 Western blot analysis

Western blot with anti-Flag M2 antibody was performed to check the expression of recombinant receptor. As shown in Fig. 5.3, a band of approximately 55 kDa was observed in membranes from *Pichia* cells expressing AT_{1a}R. This corresponds well with the calculated size of recombinant receptor fusion protein (52.9 kDa).

5.1.3.2 [³H] angiotensin II binding

In order to check the functionality of the recombinant receptor and to calculate the total amount of functional receptor in membranes, a saturation binding experiment using [³H] angiotensin II was performed. [³H] angiotensin II binding was saturable and revealed a B_{max} value of 57 pmol recombinant AT_{1a}R per mg membrane protein (Fig. 5.4). A high affinity binding of [³H] angiotensin II to the recombinant receptor was observed with a K_d value of 1.3 nM. This K_d value is similar to those reported for AT_{1a}R in native tissues (see appendix).

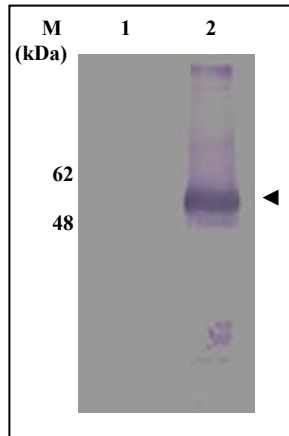


Fig. 5.3 Western blot analysis of the FlagHis₁₀AT_{1a}RBio construct produced in *P. pastoris*. Proteins were separated using 10% SDS-PAGE and probed with anti-Flag M2 antibody. Lane 1: 10 µg of control *Pichia* membranes, lane 2: 10 µg of membranes from *Pichia* cells expressing FlagHis₁₀B₂RBio fusion protein.

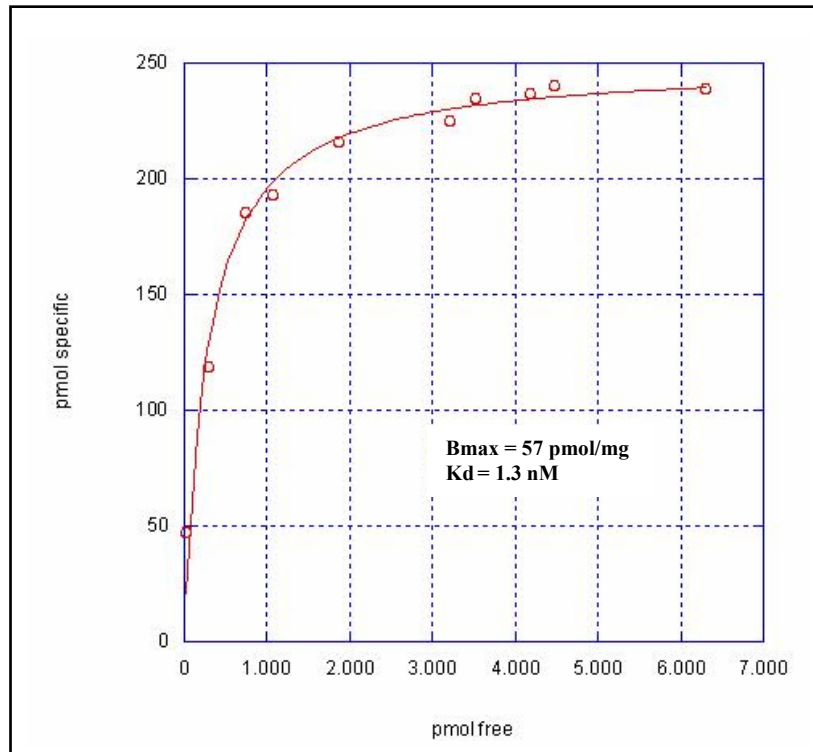


Fig. 5.4 Saturation curve for [³H] angiotensin II binding to recombinant AT_{1a}R produced in *Pichia pastoris*. The graph was generated using the single site model in KaleidaGraph software.

5.1.4 Optimization of functional production level of AT_{1a}R

In order to increase the functional expression of AT_{1a}R, DMSO was added to the *Pichia* cultures during methanol induction step. As shown in Fig. 5.5, approximately three-fold increase in the functional expression of recombinant AT_{1a}R was observed by the addition of DMSO. Maximum expression level was obtained by the addition of 2% DMSO and it corresponds to 167 pmol/mg of recombinant AT_{1a}R (3-4 mg/liter culture).

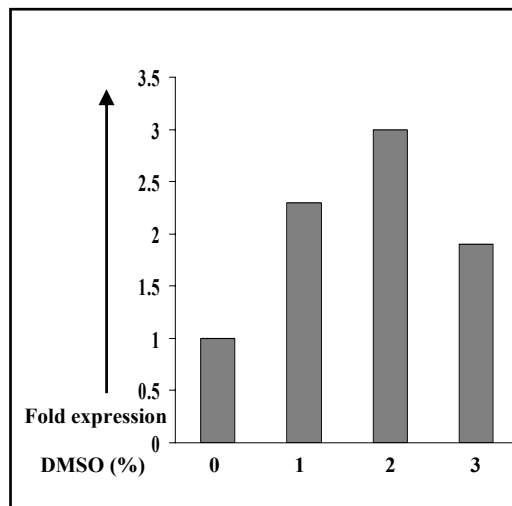


Fig. 5.5 Effect of DMSO on expression levels of recombinant AT_{1a}R in *Pichia pastoris*. DMSO was added to the cultures, membranes were prepared and [³H] angiotensin II binding was measured.

[³H] angiotensin II binding revealed an expression level of 30 pmol/mg for the FlagHis₁₀AT_{1a}RStrep II construct. Low expression level has been observed for the strep-tagged constructs in comparison to the bio-tagged constructs for several other GPCRs (Christoph Reinhart, personal communication).

5.1.5 Glycosylation analysis

There are three putative glycosylation sites[#] in AT_{1a}R, one at the N-terminus (N⁴), and two in the second extracellular domain (N¹⁷⁶ and N¹⁸⁸). In order to analyze the glycosylation state of the recombinant receptor, enzymatic deglycosylation using PNGaseF or EndoH was performed on *Pichia* membranes expressing AT_{1a}R, followed by Western blot analysis. As shown in Fig. 5.6, the recombinant receptor band was shifted to lower molecular weight size upon enzymatic deglycosylation. This result reveals that the recombinant B₂R produced in *Pichia* was glycosylated.

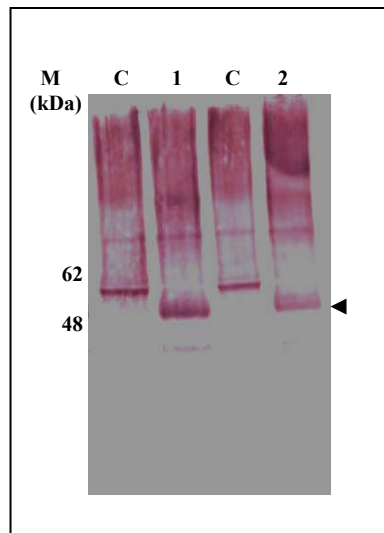


Fig. 5.6 Glycosylation analysis of the recombinant AT_{1a}R produced in *Pichia*. 10 µg of *Pichia* membranes expressing AT_{1a}R were treated with 0.5 units of PNGaseF (lane 1) or 0.5 units of EndoH (lane 2) at 4°C for 2 h. The lane “C” is untreated control *Pichia* membranes (10 µg). The proteins were separated by 10% SDS-PAGE and Western blot analysis was performed using anti-Flag M2 antibody.

[#]These sites are predicted based on conserved N-linked glycosylation motif (Asn-Xaa-Ser/Thr). Previous reports suggest that these sites are glycosylated when the recombinant AT_{1a}R is expressed in mammalian cells and play a significant role in trafficking of the receptor (Lanctot *et al.*, 1999 and Jayadev *et al.*, 1999).

5.1.6 Solubilization of recombinant AT_{1a}R

In order to solubilize the recombinant AT_{1a}R from *Pichia* membranes, different detergents (in presence of 0.2% CHS) were tested. As shown in Fig. 5.7, AT_{1a}R was solubilized with most detergents.

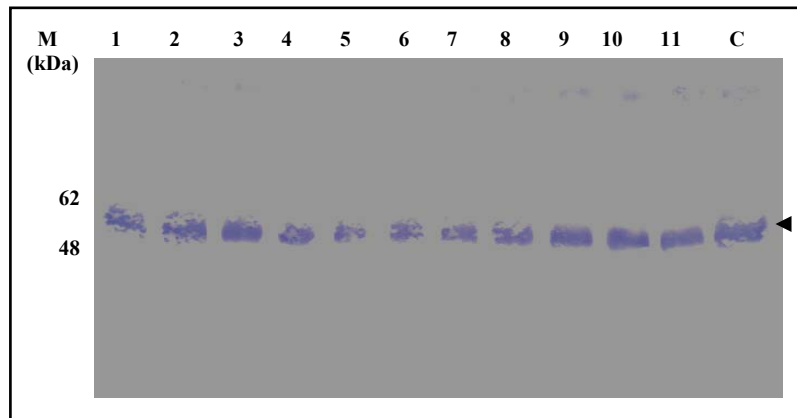


Fig. 5.7 Solubilization of the recombinant AT_{1a}R from *Pichia* membranes (5 mg/ml). Lane 1-11 = DM, UM, LM, DG, NG, OG, CHAPS, LDAO, Fos12, Fos14, and Fos16. All the detergents were used at a concentration of 1% except OG (2%). Solubilizate was loaded on a 10% SDS-polyacrylamide gel and Western blot analysis was performed using anti-Flag M2 antibody.

[³H] angiotensin II binding on solubilizate was used to monitor the functional solubilization of the AT_{1a}R from *Pichia* membranes. Best functional solubilization (60-70%) was observed with LM. Therefore, the recombinant AT_{1a}R was solubilized with LM for further purification.

5.1.7 Purification of the recombinant AT_{1a}R

In order to stabilize the active conformation of the receptor, angiotensin II (1 μM) was added to the *Pichia* membranes expressing AT_{1a}R. Subsequently, the receptor was solubilized with 1% LM in the presence of 0.2% CHS.

5.1.7.1 AT_{1a}R purification using Ni-NTA and monomeric avidin

Recombinant AT_{1a}R (FlagHis₁₀AT_{1a}RBio fusion protein) was purified from *Pichia* membranes by a combination of Ni-NTA and monomeric avidin resins. In the first step, solubilizate was applied to Ni-NTA resin. Subsequently, the column was washed with washing buffer (see materials and methods) and finally the receptor was eluted with elution buffer containing 200 mM imidazole. As a second step of purification, Ni-NTA eluate was applied to monomeric avidin matrix. The recombinant receptor binds to this matrix via its biotinylated bio tag. The receptor was eluted with 2 mM biotin and analyzed by 10% silver stained SDS-PAGE. As shown in Fig. 5.8 (lane 2), the recombinant receptor was >85 % pure.

In order to check the homogeneity of purified AT_{1a}R, the eluate from the monomeric avidin column was analyzed by gel filtration on a superose 6 column in the SMART chromatography system. A main peak was observed at a retention volume of 1.61 ml (indicated by the arrow head). It corresponds to the homogenous population of purified AT_{1a}R. In addition to this main peak, some aggregated receptor (peak at retention volume of 0.89 ml) was also observed. An additional peak at a retention volume of 1.8 ml was also observed that probably represents the free detergent micelles.

5.1.7.2 AT_{1a}R purification using Ni-NTA and streptactin

The recombinant AT_{1a}R from the membranes of *Pichia* cells expressing FlagHis₁₀AT_{1a}RStrepII construct, was purified using two-step affinity purification (Ni-NTA and streptactin agarose) procedure. As shown in Fig 5.9, after streptactin purification, recombinant receptor was >90 % pure.

As the receptor was purified in presence of the high affinity ligand angiotensin II, it was not possible to measure [³H] angiotensin II binding on purified fractions. Based on BCA quantification, approximately, 25-30% yield was obtained i.e. approximately 3 mg of recombinant AT_{1a}R in membrane (based on ligand binding) yielded roughly 1 mg of pure AT_{1a}R (based on BCA quantification) after two-step affinity purification.

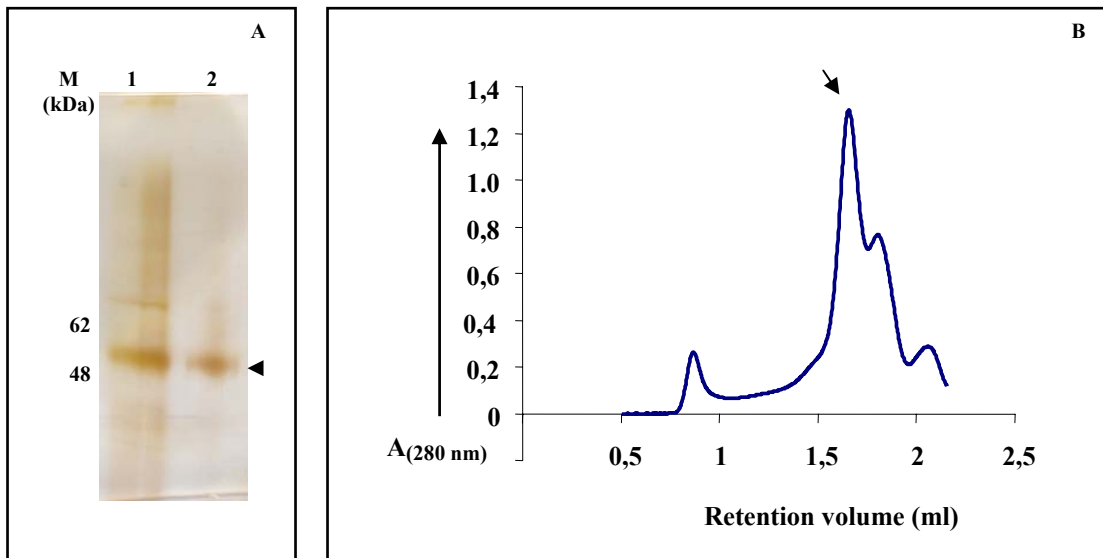


Fig. 5.8 Purification of the recombinant AT_{1a}R from *Pichia pastoris*. Samples were analyzed by silver stained 10% SDS-PAGE. **A.** The eluate from Ni-NTA (lane 1, 1 µg) and monomeric avidin (lane 2, 0.5 µg). **B.** Analytical gel filtration of purified B₂R (eluate from monomeric avidin column, 0.4 mg at a concentration of 10 mg/ml) using superose 6 column.

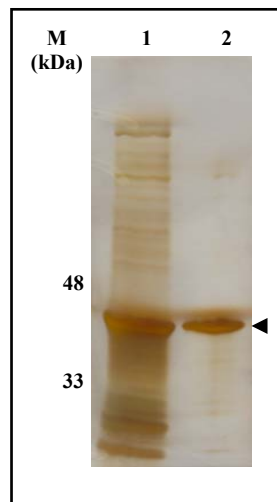


Fig. 5.9 Purification of the recombinant AT_{1a}R from *Pichia pastoris*. Purified fractions were analyzed by silver stained 10% SDS-PAGE. Lane 1 = eluate from Ni-NTA (1.2 µg) and lane 2 = eluate from streptactin (0.6 µg).

5.1.7.3 Fluorescein labeled angiotensin II as a probe to monitor AT_{1a}R purification

In order to determine whether angiotensin II remains bound to AT_{1a}R during purification steps, fluorescein labeled angiotensin II was used during purification. Membranes were incubated with fluorescent angiotensin II (1 μ M) for two hours, subsequently solubilized and purified by a combination of Ni-NTA and streptactin resins. Purified receptor was analyzed by gel filtration analysis. As shown in Fig. 5.10, absorbance peak of the fluorescent angiotensin II (490 nm) was aligned with AT_{1a}R peak (280 nm). This shows that fluorescein angiotensin II remains bound to AT_{1a}R during purification. A complex of AT_{1a}R-fluorescein angiotensin II provides an efficient tool for identifying protein crystals in the crystallization drops.

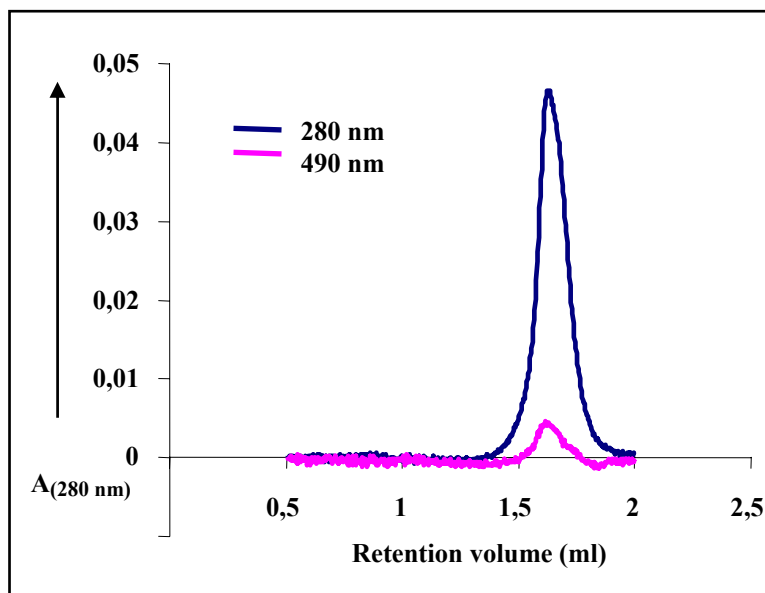


Fig. 5.10 Analytical gel filtration of AT_{1a}R purified in the presence of fluorescent-angiotensin II. The eluate from streptactin column (50 μ g at a concentration of 1 mg/ml) was analyzed by using a superose 6 column.

5.1.8 Stability of the purified receptor

Stability of the purified protein is a crucial point before it can be subjected to crystallization trials. In order to check the long-term stability, recombinant AT_{1a}R was

purified and stored at 4°C. After a defined time period, the homogeneity of receptor was investigated by analytical gel filtration. Purified receptor was stable for at least two weeks as shown in Fig. 5.11. Therefore, it can be used for three-dimensional crystallization attempts.

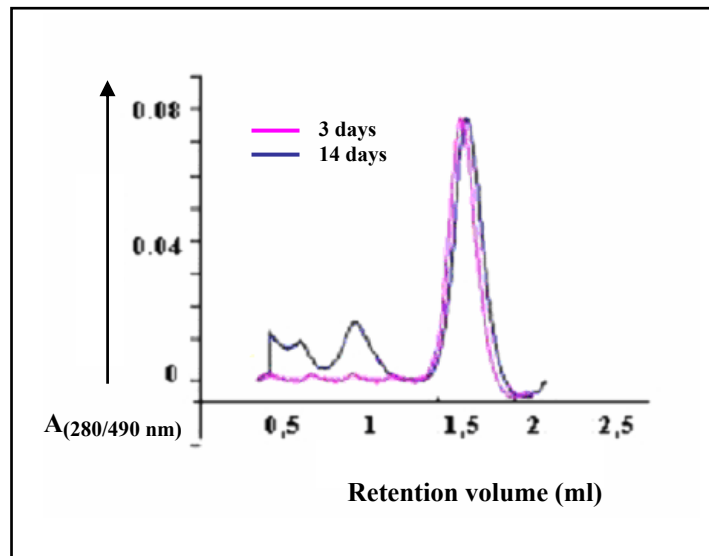


Fig. 5.11 Stability analysis of purified AT_{1a}R by analytical gel filtration. Purified AT_{1a}R was stored at 4°C for 3 or 15 days and subsequently analyzed using superose 6 column (100 µg at a concentration of 2 mg/ml).

Although AT_{1a}R was expressed in *Pichia* at high level, for reasons of comparison AT_{1a}R was also expressed in Sf9 cells and BHK cells.

5.2 Production and isolation of AT_{1a}R from insect cells using the baculovirus system

5.2.1 Sub-cloning of AT_{1a}R gene in baculovirus expression vectors

The coding region of AT_{1a}R gene was cloned into the MCS of modified pVL vectors between *Bam*HI and *Eco*RI enzyme sites. Amplification of receptor gene (with AT_{1a}R_Baculo_Fw/Rv primers using *Pfu* DNA polymerase) and ligation to the expression vectors was carried out using the standard cloning procedures.

5.2.2 Expression constructs

The baculovirus constructs used for the expression of AT_{1a}R in insect cells are shown in Fig. 5.12. The modified pVL vectors were provided by Gabi Maul. The first construct was used for isolation of recombinant receptor using Flag and His₁₀ tag at the N-terminus and a bio tag at the C-terminus while the construct with eGFP fusion at the C-terminus can be used for receptor localization studies using confocal microscopy.

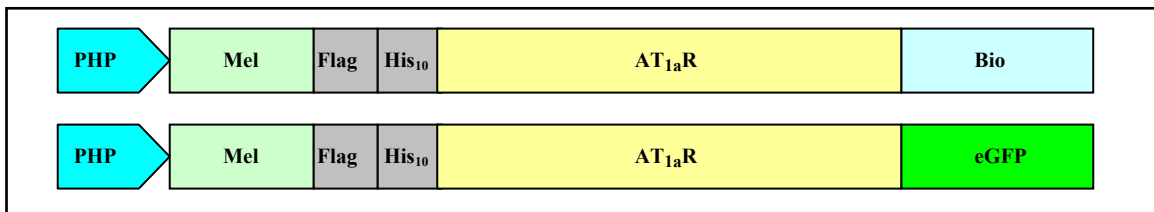


Fig. 5.12 Expression constructs for production of the recombinant AT_{1a}R in insect cells. PHP = polyhedrin promoter, Mel = prepro-mellitin signal sequence of honey bee, Flag = coding sequence for Flag epitope, His₁₀ = coding sequence for histidine 10 tag, AT_{1a}R = coding region of AT_{1a}R, Bio = biotinylation domain of *Propionibacterium shermanii* transcarboxylase and eGFP = coding sequence of enhanced green fluorescent protein.

5.2.3 Production of the recombinant receptor

In order to check the expression of AT_{1a}R, Sf9 cells were infected at MOI 10 with the recombinant baculovirus constructs (pVLMelFlagHis₁₀AT_{1a}RBio). 72 h post-infection, membranes were prepared and subjected to Western blot analysis and [³H] angiotensin II binding analysis.

5.2.3.1 Western blot analysis

Western blot with anti-Flag M2 antibody was performed to check the expression of recombinant receptor. As shown in Fig. 5.13, a major band of approximately 55 kDa was seen in the membranes from Sf9 cells expressing AT_{1a}R. This apparent molecular mass closely corresponds with the calculated size of AT_{1a}R fusion protein (51.5 kDa). In

addition to the main receptor band, some proteolytic degradation products of smaller sizes were also observed.

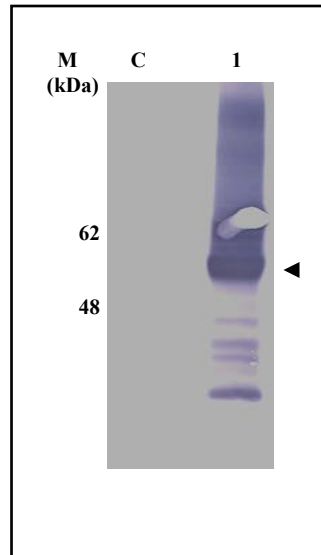


Fig. 5.13 Western blot analysis of the FlagHis₁₀AT_{1a}RBio construct produced in Sf9 cells. Proteins were separated by 10% SDS-PAGE and probed with anti-Flag M2 antibody. C = 10 μ g of membranes from non-infected Sf9 cells, lane 1 = 10 μ g of membranes from Sf9 cells expressing the FlagHis₁₀AT_{1a}RBio fusion protein.

5.2.3.2 [³H] angiotensin II binding

In order to check the functionality of the recombinant receptor and to calculate the total amount of functional receptor in membranes, a saturation binding experiment using [³H] angiotensin II was performed. A suspension culture of Sf9 was grown and infected with baculovirus corresponding to FlagHis₁₀AT_{1a}RBio construct (shown in Fig. 5.12) at MOI 10. 72 h post-infection, membranes were prepared and saturation binding was performed using [³H] angiotensin II. [³H] angiotensin II binding was saturable and revealed a B_{max} value of 29 pmol recombinant AT_{1a}R per mg membrane protein (Fig. 5.14). A high affinity binding of [³H] angiotensin II to the recombinant receptor was observed with a K_d value of 0.98 nM. This K_d value is similar to those reported for AT_{1a}R in native tissues (see appendix).

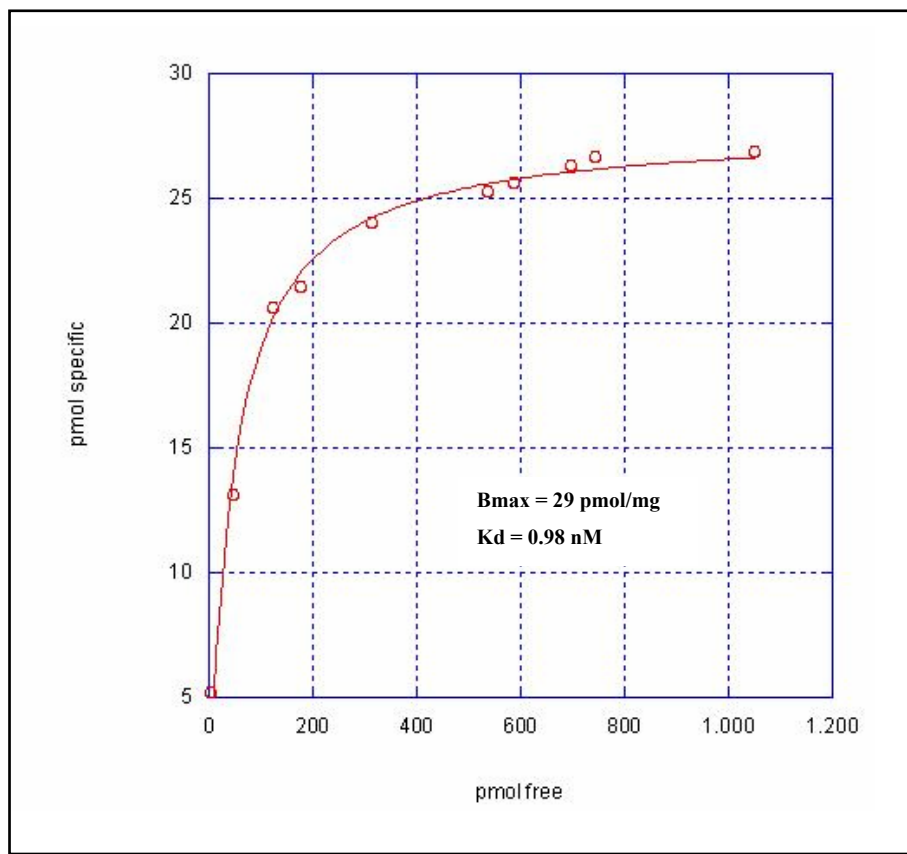


Fig. 5.14 Saturation curve for [³H] angiotensin II binding to recombinant AT_{1a}R (pVLMelFlagHis₁₀AT_{1a}RBio) produced in Sf9 cells. Graph was generated using the single site model in Kaleidagraph software.

5.2.4 Glycosylation analysis of the recombinant AT_{1a}R

In order to analyze the glycosylation state of the recombinant receptor, enzymatic deglycosylation using PNGaseF or EndoH was performed on Sf9 membranes expressing AT_{1a}R. As shown in Fig. 5.15, the recombinant receptor band was shifted to a lower molecular weight size upon deglycosylation. This reveals that the recombinant AT_{1a}R produced in Sf9 cells was glycosylated. However, complete deglycosylation did not occur (a band of higher molecular size than the completely deglycosylated AT_{1a}R was also observed, shown by asterisk).

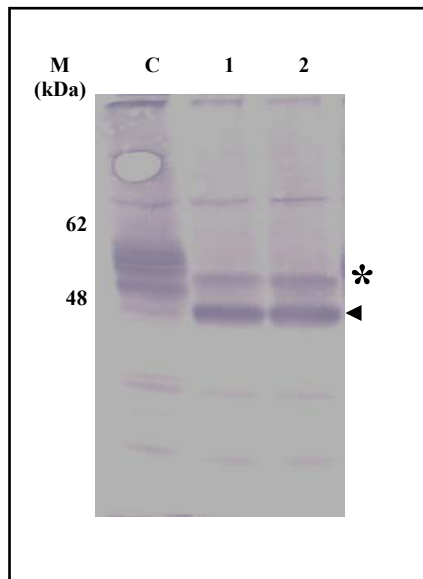


Fig. 5.15 Glycosylation analysis of the recombinant AT_{1a}R produced in Sf9 cells. 10 µg of Sf9 membranes expressing AT_{1a}R were treated with 0.5 units of PNGaseF (lane 1) or 0.5 units of EndoH (lane 2) at 4°C for 2h. The lane “C” is untreated control SF9 membranes (10 µg). The proteins were separated by 10% SDS-PAGE and Western blot analysis was performed using anti-Flag M2 antibody.

5.2.5 Solubilization and purification of AT_{1a}R

Recombinant receptor was solubilized from the membranes (5 mg/ml) using 1% LM in the presence of 0.2% CHS. Solubilization efficiency, as assessed by [³H] angiotensin II binding, was approximately 60-70%. For purification, membranes from Sf9 cells expressing AT_{1a}R were incubated with angiotensin II (1 µM) for two hours. Subsequently, the receptor was solubilized and purified by a combination of Ni-NTA and monomeric avidin. The eluate from monomeric avidin revealed >90% pure receptor (Fig. 5.16). Further studies are ongoing to evaluate the homogeneity and stability of purified AT_{1a}R.

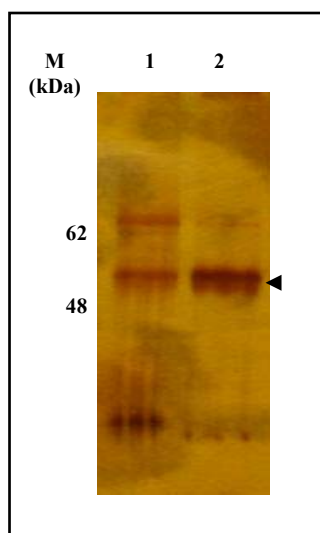


Fig. 5.16 Purification of recombinant AT_{1a}R from Sf9 cells. Silver stained 10% SDS-polyacrylamide gel showing the eluate from Ni-NTA (lane 1, 0.7 µg) and monomeric avidin (lane 2, 0.5 µg).

5.3 Production and isolation of AT_{1a}R from BHK cells

Next, the SFV based expression of AT_{1a}R in BHK cells was performed. Mammalian cells provide most natural environment for heterologous expression of recombinant human GPCRs.

5.3.1 Sub-cloning of AT_{1a}R gene in SFV expression vectors

AT_{1a}R gene was amplified with the primers AT_{1a}R_SFV_Fw/Rv and cloned into the MCS of modified SFV vectors between *Bam*HI and *Spe*I enzyme sites using the standard cloning procedure.

5.3.2 Constructs

Expression constructs for production of AT_{1a}R in mammalian cells are shown in Fig. 5.17. The first construct was used for isolation of the recombinant receptor while the

second construct was used for investigating the localization of recombinant receptor by confocal microscopy.

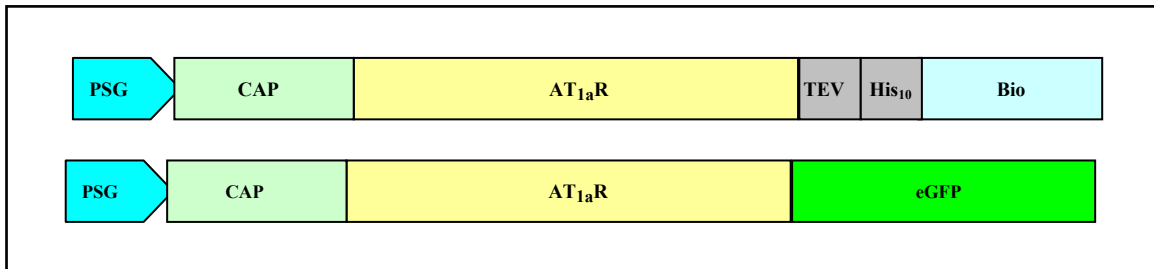


Fig. 5.17 Expression constructs for the production of recombinant AT_{1a}R in mammalian cells. PSG = subgenomic 26 S promoter, CAP = capsid sequence, AT_{1a}R = coding sequence for AT_{1a}R gene, His₁₀ = coding sequence for histidine 10 tag, TEV = cleavage site for TEV protease, Bio = biotinylation domain of *Propionibacterium shermanii* transcarboxylase, eGFP = enhanced green fluorescent protein.

5.3.3 Production of the recombinant AT_{1a}R in BHK cells

Recombinant virus particles were generated and activated as described in the materials and methods section. Suspension cultures of BHK cells were grown in spinner flasks and infected at a density of $1-2 \times 10^6$ cells/ml. During infection 2% DMSO was added[#]. 24 h post-infection, membranes were prepared and subjected to Western blot analysis and [³H] angiotensin II binding assay.

5.3.3.1 Western blot analysis of AT_{1a}R produced in BHK cells

Western blot analysis of BHK cell membranes expressing AT_{1a}R using anti-his antibody revealed a major band of 55 kDa (Fig. 5.18). This corresponds well with the calculated size of recombinant receptor fusion protein (51.6 kDa).

[#]Addition of 2% DMSO was found to increase the expression level of recombinant B₂R and NmU₂R (see sections 3.3.4.3 and 7.3.3.3, respectively).

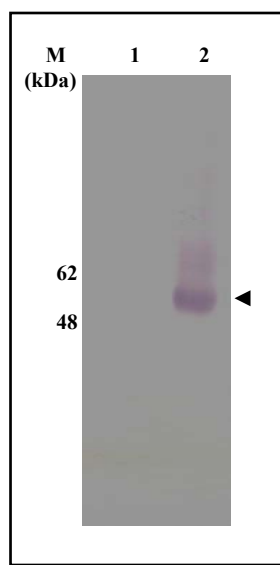


Fig. 5.18 Western blot analysis of the recombinant AT_{1a}R produced in BHK cells. Proteins were separated by 10% SDS-PAGE and probed with anti-his antibody. Lane 1 = 10 μ g of membranes from non-infected BHK cells, lane 2 = 10 μ g of membranes from BHK cells expressing AT_{1a}R.

5.3.3.2 [³H] angiotensin II binding

In order to calculate the total amount of functional receptor in membranes, a saturation binding experiment using [³H] angiotensin II was performed. As shown in Fig. 5.19, [³H] angiotensin II binding was saturable and revealed a B_{max} value of 32 pmol recombinant receptor per mg membrane protein. A high affinity binding of [³H] angiotensin II to the recombinant receptor was observed with a K_d value of 1.1 nM. This K_d value is similar to those reported for AT_{1a}R in native tissues (see appendix). The non-specific binding was determined in presence of 1 μ M angiotensin II and it was less than 20% of total binding.

5.3.4 Glycosylation analysis of the recombinant AT_{1a}R in BHK cells

To check the glycosylation state of the recombinant receptor in BHK cells, enzymatic deglycosylation using PNGaseF or EndoH was performed. As shown in Fig. 5.20, the recombinant receptor band was shifted to lower molecular weight size upon

deglycosylation. This reveals that the recombinant AT_{1a}R produced in BHK cells was glycosylated. Interestingly, B₂R and NmU₂R were not glycosylated when expressed in BHK cells using SFV vectors.

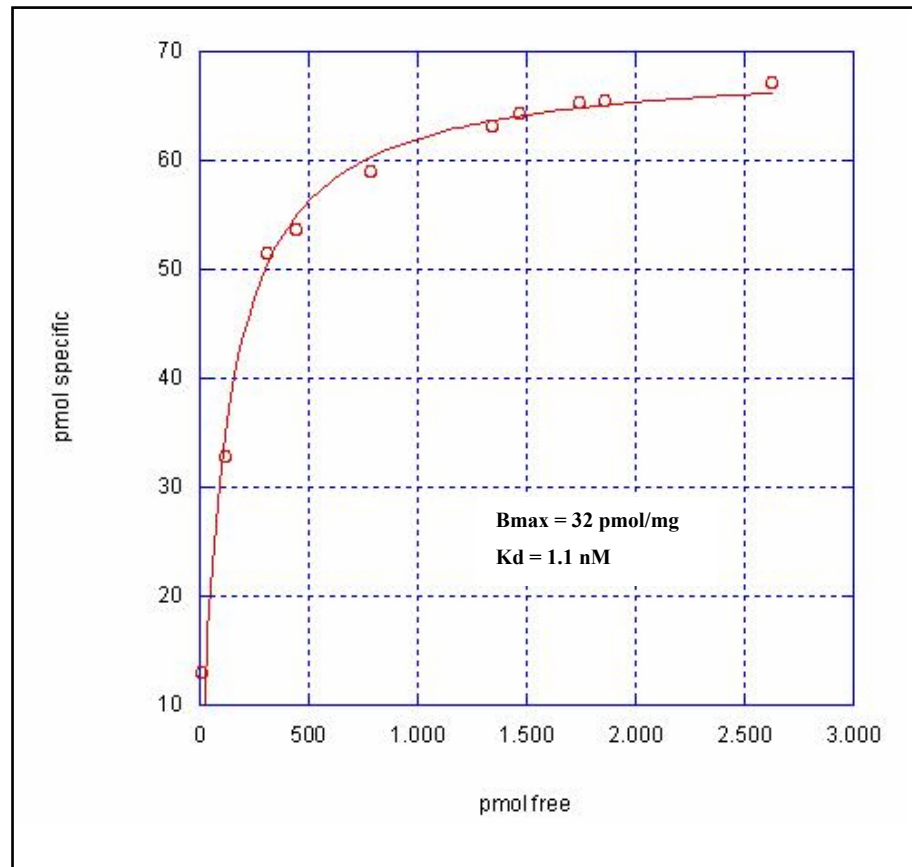


Fig. 5.19 Saturation curve for [³H] angiotensin II binding to the recombinant AT_{1a}R produced in BHK cells. The graph was generated using single site model in Kaleidagraph software.

5.3.5 Localization of the recombinant AT_{1a}R by confocal microscopy

In order to check the localization of recombinant receptor, BHK cells were infected with recombinant virus coding for AT_{1a}R-eGFP fusion protein. 16 h post-infection cells were fixed and analyzed by confocal microscopy. As shown in Fig. 5.21, recombinant AT_{1a}R appeared to be localized predominantly in the plasma membrane.

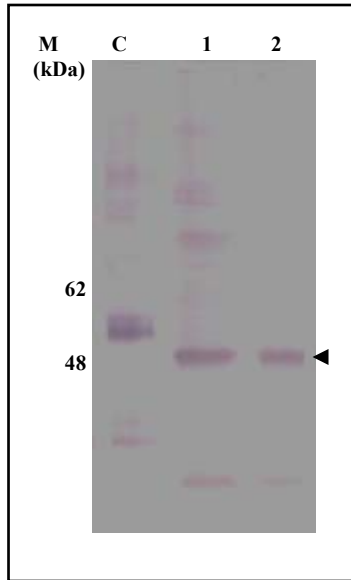


Fig. 5.20 Glycosylation analysis of the recombinant AT_{1a}R produced in BHK cells. 10 μ g of membranes from BHK cells expressing AT_{1a}R were treated with 0.5 units of PNGaseF (lane 2) or 0.5 units of EndoH (lane 3) at 4°C for 2 h. Lane “C” is untreated control membranes (5 μ g). Proteins were separated by 10% SDS-PAGE and Western blot analysis was performed using anti-his antibody.

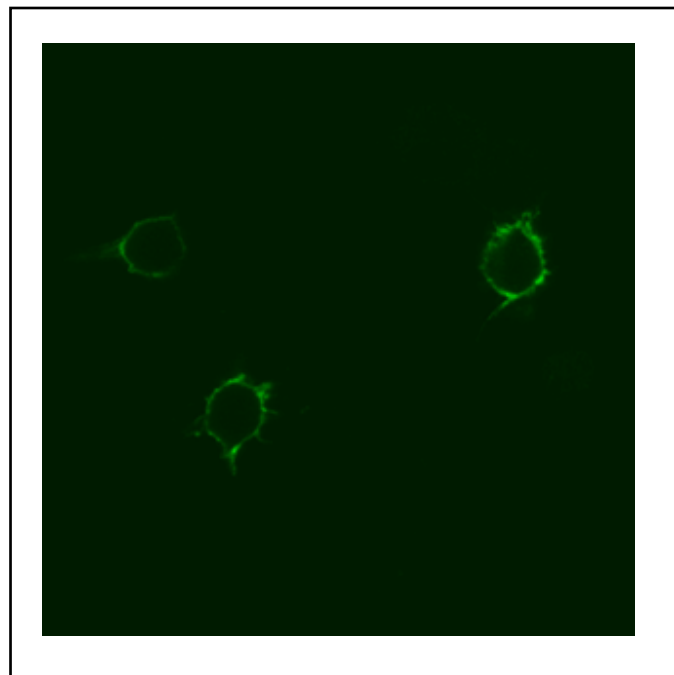


Fig. 5.21 Confocal imaging of BHK cells expressing AT_{1a}R-eGFP. Cells were grown and infected on sterile cover-slips. 16 h post-infection, cells were fixed and scanned (488 nM) with a Zeiss laser scanning confocal microscope.

5.3.6 Solubilization and purification of AT_{1a}R from BHK cells

Recombinant AT_{1a}R was solubilized from membranes (5 mg/ml) using 1% LM in the presence of 0.2% CHS. Approximately, 75-80 % of [³H] angiotensin II binding sites were solubilized from membranes. Solubilized receptor was purified using Ni-NTA resin. The eluate from Ni-NTA column was analyzed by silver stained 10% SDS-PAGE. As shown in Fig. 5.22 (A), >70% pure receptor was obtained after Ni-NTA purification. In order to check the homogeneity of the purified receptor, the eluate from Ni-NTA column was analyzed by gel filtration on a Superose 6 column. As revealed in Fig. 5.22 (B), purified AT_{1a}R was present in a nearly homogenous form (peak at 1.61 ml), although significant aggregation was also detected (peak at 0.91 ml). It has been observed previously that the biotinylation of the bio domain is not complete in mammalian cells (Helmut Reiländer, personal communication). Therefore, purification via monomeric avidin was not tried as it may result in significant loss of the receptor in flow through fraction.

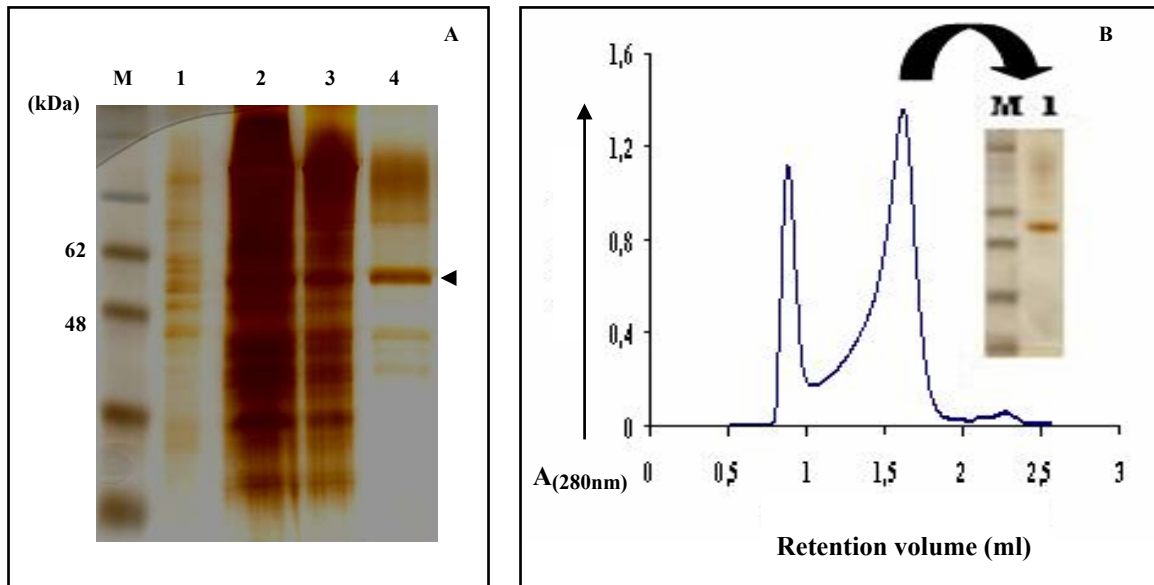


Fig. 5.22 Purification of recombinant AT_{1a}R from BHK cells. **A.** Silver stained 10% SDS-PAGE showing membranes (lane 1, 0.2 µg), solubilize (lane 2, 1 µg), flow through (lane 3, 1 µg), and eluate from Ni-NTA (lane 4, 0.5 µg). **B.** Analytical gel filtration of purified AT_{1a}R (eluate from Ni-NTA column, 0.4 mg at a concentration of 10 mg/ml) using a superose 6 column, inset shows main peak of the gel filtration analyzed by 10% silver stained SDS-PAGE (M = marker and lane 1 = 0.2 µg AT_{1a}R after gel filtration).

5.3.7 Proteolytic degradation of purified AT_{1a}R

The purified AT_{1a}R showed proteolytic degradation when stored at 4°C for three days (Fig. 5.23). It may be due to copurification of a protease with AT_{1a}R. This problem of proteolytic degradation was not addressed in detail as sufficient amount of stable AT_{1a}R could be obtained from *Pichia* (section 5.1.8).

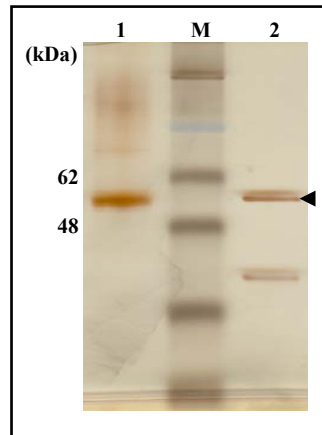


Fig. 5.23 Proteolytic degradation of AT_{1a}R after purification. Purified AT_{1a}R was stored at 4°C and subsequently analyzed by 10% silver stained SDS-PAGE. Lane 1 = AT_{1a}R immediately after purification (0.3 µg) and lane 2 = AT_{1a}R after three days at 4°C (0.3 µg).

5.3.8 Three-dimensional crystallization trials of AT_{1a}R

Purified AT_{1a}R from *Pichia pastoris* was used for 3-D crystallization attempts. As shown in Fig. 5.24, some crystalline structures were observed. However, these are too small to verify either by Western blot analysis or by X-ray beam. It has not been possible so far to reproduce them under the same conditions. Further crystallization screening is ongoing to obtain reproducible and bigger crystals.

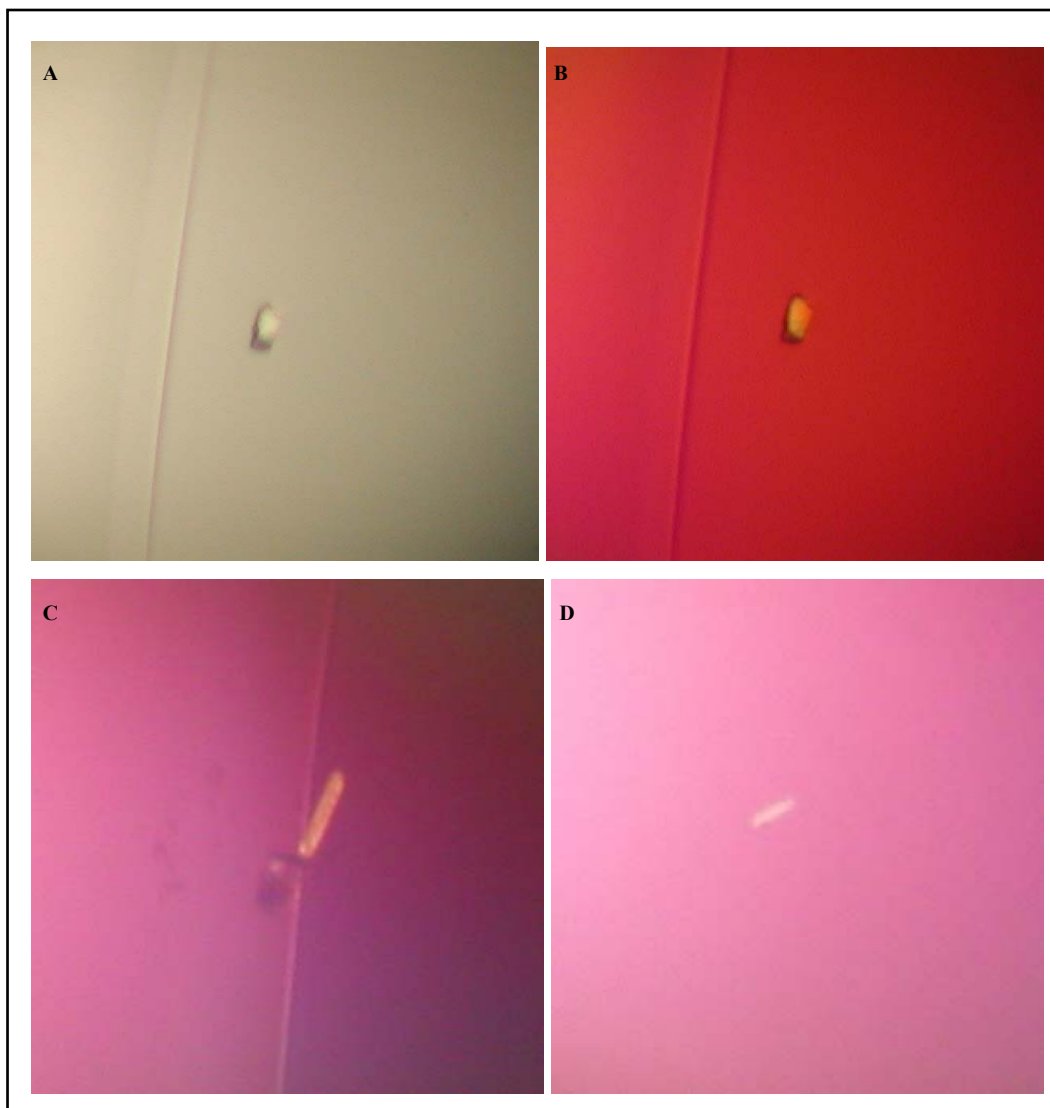


Fig. 5.24 Crystal like structures obtained during 3-D crystallization attempts of AT_{1a}R.

Chapter 6: Coexpression of B_2R and $AT_{1a}R$ and isolation of the heterodimer complex

6.1 Coexpression of B₂R and AT_{1a}R

Human B₂R is known to form a stable heterodimer with human AT_{1a}R (Abdalla *et al.*, 2000). Coexpression of B₂R and AT_{1a}R was performed in order to isolate the heterodimer complex for crystallization. The heterodimer complex should have an extended polar surface area compared to the monomer and thus represents a better object for 3-D crystallization. Additionally, the three-dimensional structure of a heterodimer should lead to a better understanding of the dimerization interface. SFV based expression is an efficient way of coexpressing two or more proteins in mammalian cells. Coexpression of a GPCR (α -1b-AR) and G-proteins using SFV system has already been described (Scheer *et al.*, 1999). In this study, coexpression of B₂R and AT_{1a}R in BHK cell was performed using the SFV system.

6.1.1 Constructs for coexpression of B₂R and AT_{1a}R

The genes for B₂R and AT_{1a}R were amplified from respective cDNA vectors by PCR and cloned into modified SFV expression vectors (see section 3.3.2). The resulting constructs are shown in Fig. 6.1. Other constructs used in this study have already been described in chapter 3 and chapter 5 (see sections 3.3.2 and 5.3.2).

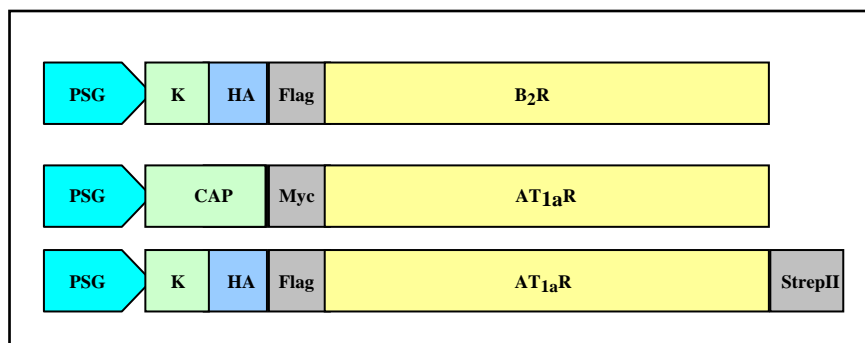


Fig. 6.1 Expression constructs for coexpression of recombinant B₂R and AT_{1a}R in BHK cells. PSG = promoter, K = Kozak sequence, HA = signal sequence from influenza haemagglutinin (HA) gene, Flag = coding sequence for Flag epitope, B₂R = coding sequence for B₂R gene, AT_{1a}R = coding sequence for AT_{1a}R gene, Strep II = coding sequence for strep tag II.

6.1.2 Coinfection of BHK cells with B₂R and AT_{1a}R virus

Virus particles were generated and activated as described in the materials and methods section. The amount of virus used for coexpression was optimized in order to obtain a 1:1 expression ratio of both receptors (based on radioligand binding assay).

6.2 Coexpression with AT_{1a}R results in trafficking of B₂R to the plasma membrane

As shown in section 3.3.6.2, the B₂R-eGFP fusion protein shows intracellular retention when expressed in BHK cells. During coexpression of B₂R and AT_{1a}R it was noticed that heterodimerization of B₂R and AT_{1a}R leads to surface trafficking of B₂R. This effect of heterodimerization was investigated using radioligand binding assay, confocal microscopy and cointernalization of the two receptors. Although heterodimerization of B₂R and AT_{1a}R has been reported previously (Abdalla *et al.*, 2000), the effect of heterodimerization on surface trafficking of individual receptors was not addressed.

6.2.1 Surface expression analysis based on radioligand binding assay

In order to check the expression of receptors, [³H] bradykinin and or [³H] angiotensin II binding assay was performed on intact cells. Surprisingly, it was found that when AT_{1a}R was coexpressed with B₂R, the number of [³H] bradykinin binding sites on the surface of intact cells was increased four times compared to the expression of B₂R alone (Fig. 6.2). In order to confirm that the increase in [³H] bradykinin binding is specific to coexpression of AT_{1a}R, coexpression of B₂R with AT₂R was also performed. AT₂R is 30-35% identical to AT_{1a}R in amino acid sequence and binds to angiotensin II with almost the same affinity. However, coexpression of AT₂R did not lead to an increase in [³H] bradykinin binding sites on the cell surface. This finding indicates that the increase in surface expression of B₂R is specific to AT_{1a}R coexpression. Surface expression of AT_{1a}R or AT₂R, as measured by [³H] angiotensin II binding assay, remains unaltered by coexpression of B₂R. There was no significant [³H] bradykinin or [³H] angiotensin II binding in non-infected BHK cells.

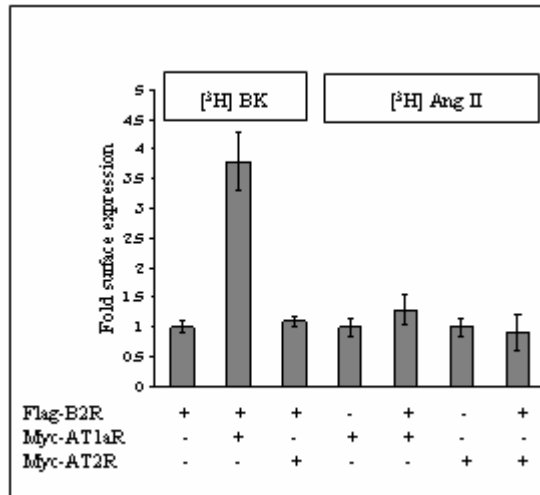


Fig. 6.2 Coexpression of the AT_{1a}R increases cell surface binding sites of [³H] bradykinin. BHK cells were infected with virus encoding Flag-B₂R, Myc-AT_{1a}R and Myc-AT₂R separately or together (Flag-B₂R with either Myc-AT_{1a}R or Myc-AT₂R). 24 h post-infection ligand binding assay was performed on the intact cells using [³H] bradykinin or [³H] angiotensin II.

6.2.2 Surface expression analysis based on confocal microscopy

In order to determine if the increase in [³H] bradykinin binding sites was due to surface translocation of B₂R in response to heterodimerization with AT_{1a}R, BHK cells coexpressing B₂R-eGFP[#] and Myc-AT_{1a}R were examined by confocal microscopy. As shown in Fig 6.3, B₂R was translocated to the plasma membrane when coexpressed with AT_{1a}R. Again, coexpression of AT₂R had no effect on the localization of B₂R (Fig. 6.3 C) revealing specificity of B₂R-AT_{1a}R interaction. B₂R and AT_{1a}R were found to exhibit clear colocalization when coexpressed (Fig. 6.3 D-F). Flag-B₂R also exhibited intracellular localization like B₂R-eGFP, while AT_{1a}R-eGFP and Myc-AT_{1a}R were localized on the cell surface (Fig. 6.3 G-I).

[#]As described in section 3.3.6.2, B₂R-eGFP was mainly localized intracellularly when expressed alone in BHK or CHO cells.

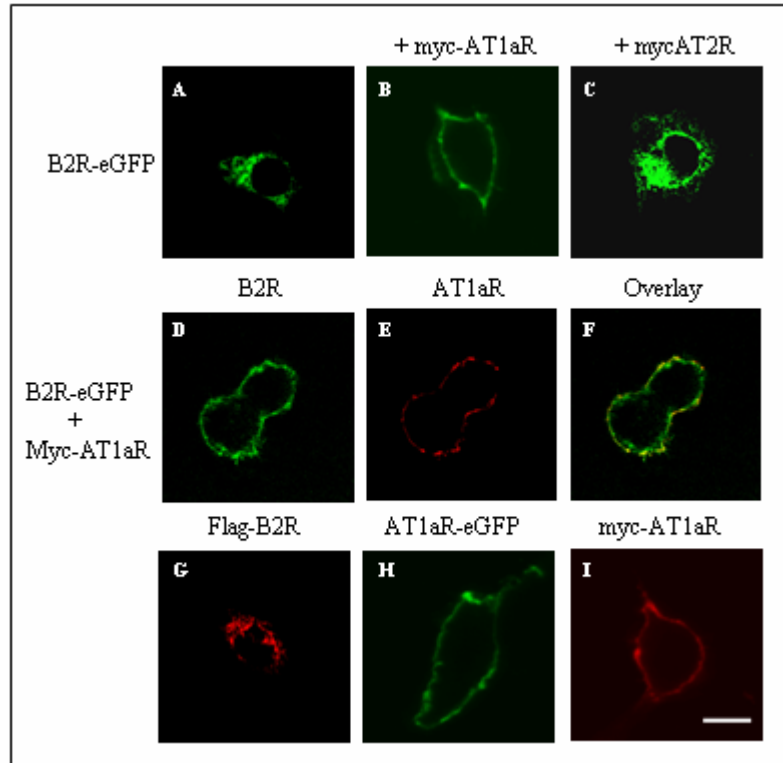


Fig. 6.3 Coexpression of $AT_{1a}R$ and B_2R translocates B_2R to the plasma membrane as revealed by confocal microscopy. B_2R -eGFP was intracellularly retained when expressed alone (A), while it reached the cell surface upon coexpression with myc- $AT_{1a}R$ (B). Coexpression of myc- AT_{2R} (C) had no effect on the trafficking of B_2R . Clear colocalization of B_2R and $AT_{1a}R$ was observed (D-F) in BHK cells coexpressing both receptors. Flag-tagged B_2R also exhibited intracellular localization (G) when expressed alone, while $AT_{1a}R$ -eGFP (H) and Myc- $AT_{1a}R$ (I) were localized on the cell surface. The scale bar represents 10 μ m.

6.3 Selective agonist induced cointernalization of B_2R and $AT_{1a}R$

After agonist stimulation, both B_2R and $AT_{1a}R$ are known to internalize rapidly (Kule *et al.*, 2004 and Bachvarov *et al.*, 2001). To determine whether B_2R and $AT_{1a}R$ remain physically associated throughout this process, agonist induced internalization of these receptors was monitored. As shown in Fig. 6.4 D-F, stimulation of BHK cells coexpressing B_2R -eGFP and Myc- $AT_{1a}R$ with 1 μ M bradykinin resulted in significant internalization of B_2R -eGFP as well as Myc- $AT_{1a}R$. Internalized receptors exhibited clear colocalization. Similarly, stimulation of BHK cells coexpressing Flag- B_2R and $AT_{1a}R$ -

eGFP with 1 μ M angiotensin II resulted in robust internalization of Flag-B₂R in addition to AT_{1a}R-eGFP (Fig. 6.4 G-H). Again, internalized B₂R and AT_{1a}R were found to be colocalized. These studies suggest that B₂R and AT_{1a}R persistently associate on the cell surface as well as during the endocytic process that follows agonist stimulation. Non-stimulated BHK cells expressing B₂R-eGFP and Myc-AT_{1a}R are shown as control (Fig. 6.4 A-C)

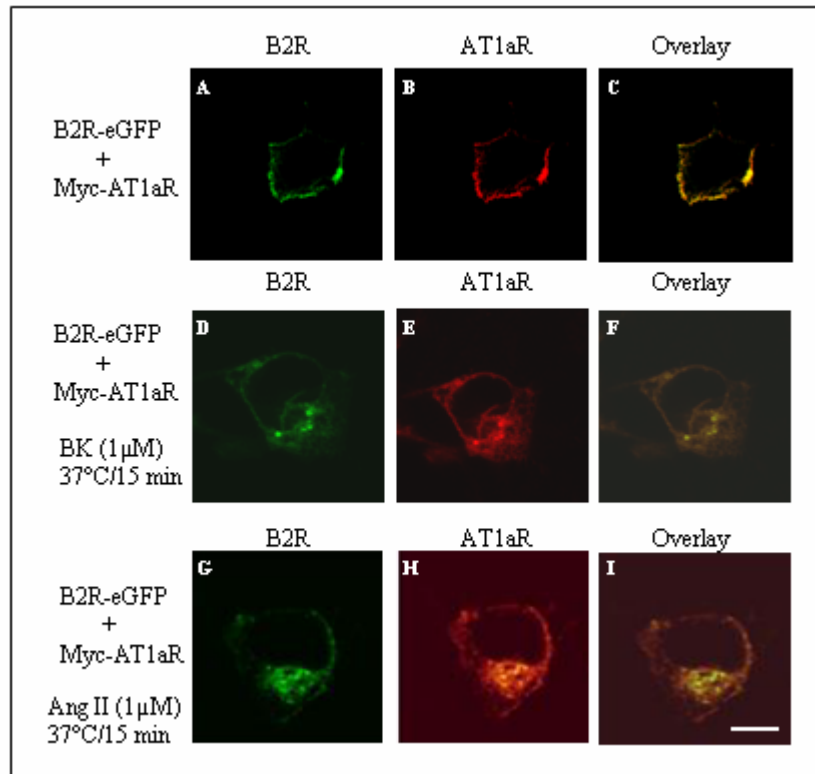


Fig. 6.4 Cointernalization of B₂R and AT_{1a}R in response to individual agonist ligands. Non-stimulated cells are shown as control (A-C). BHK cells coexpressing B₂R-eGFP and Myc-AT_{1a}R were stimulated either with 1 μ M bradykinin (D-F) or 1 μ M angiotensin II (G-I), for 15 min at 37°C. Subsequently, the cells were fixed, permeabilized and stained with either anti-Flag M2 monoclonal antibody or anti-Myc monoclonal antibody followed by Cy3/Cy5 coupled anti-mouse/anti-rabbit IgG secondary antibody. The cells were visualized by confocal microscopy (488 nm for eGFP, 550 nm for Cy3 and 650 nm for Cy5). The scale bar represents 5 μ m.

6.4 B₂R and AT_{1a}R colocalize in human foreskin fibroblasts

Human foreskin fibroblasts are known to express both B₂R (Ochsenbein *et al.*, 1999) and AT_{1a}R (Nickenig *et al.*, 1997). To determine whether B₂R and AT_{1a}R are colocalized in these cells, human foreskin fibroblasts were incubated with antibodies directed against the C-terminus of B₂R and AT_{1a}R. Afterwards, the cells were stained with Cy3/Cy5-coupled secondary antibodies, fixed and subsequently used for confocal microscopy. As shown in Fig. 6.5, B₂R and AT_{1a}R were found to be colocalized in line with the possibility that heterodimerization also drives surface localization of B₂R in native tissues.

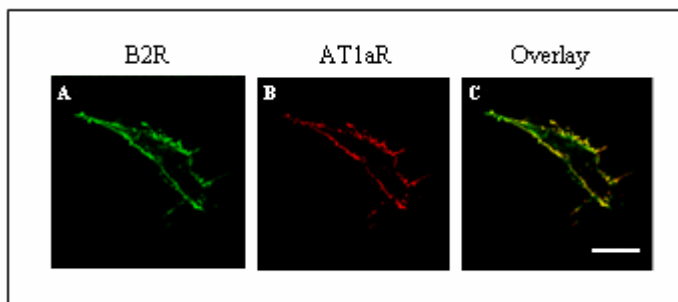


Fig. 6.5 Endogenously expressed B₂R and AT_{1a}R are colocalized at the plasma membrane in human foreskin fibroblasts. The cells were grown on sterile cover slips, fixed and permeabilized with digitonin. Subsequently, the endogenous receptors were stained with B₂R and AT_{1a}R specific monoclonal antibodies followed by Cy3/Cy5 coupled anti-mouse/ant-rabbit IgG secondary antibody. Receptors were visualized by confocal microscopy (A-C) at the wavelengths of 550 nm (Cy3) and 650 nm (Cy5). The scale bar represents 10 μ m.

6.5 Isolation of the heterodimer complex

For the isolation of the heterodimer complex, BHK cells were infected with recombinant SFV coding for B₂R-His₁₀ and AT_{1a}R-strepII. 24 h post-infection, membranes were prepared and receptors were solubilized with 1% LM in presence of 0.2% CHS. A two-step procedure comprising Ni-NTA followed by streptactin column was used for the purification.

6.5.1 Analysis by silver stained SDS-PAGE and Western blot

The eluate from streptactin column was analyzed by 10% silver stained SDS-PAGE. As shown in Fig. 6.6 (A), two major bands of 45 kDa and 40 kDa were observed. These bands correspond well with the size of AT_{1a}R and B₂R, respectively. The eluate from streptactin column was also analyzed by anti-his antibody and AP-conjugated streptavidin. As shown in Fig. 6.6 (B-C), a band of approximately 40 kDa was observed in anti-his blot that represents the B₂R-His₁₀ fusion protein and a band of 45 kDa was seen in an anti-strep blot that represents the AT_{1a}R-strepII fusion protein.

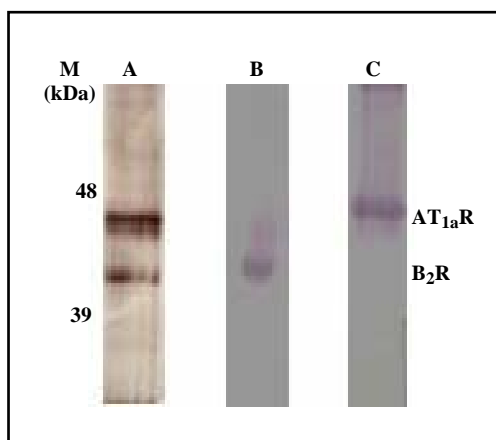


Fig. 6.6 Purification of B₂R-AT_{1a}R heterodimer complex from BHK cells. The eluate from streptactin was loaded on a 15% SDS-polyacrylamide gel. **A.** Silver staining of the gel (1 μ g). **B.** Western blot with anti-his antibody. **C.** Western blot with anti-strep antibody.

6.5.2 Analysis by gel filtration

In order to check the integrity and homogeneity of the purified heterodimer complex, the eluate from streptactin matrix was analyzed by gel filtration on a superose 6 column in the SMART chromatography system. A main peak at a retention volume of 1.50 ml was observed (Fig. 6.7). This peak was analyzed by silver staining on a 15% SDS-polyacrylamide gel. It showed two bands corresponding to AT_{1a}R and B₂R (as in Fig. 6.6). In addition to this main peak, two additional peaks (at retention volume 1.2 ml and 1.3 ml) were also observed, which probably represent aggregated material.

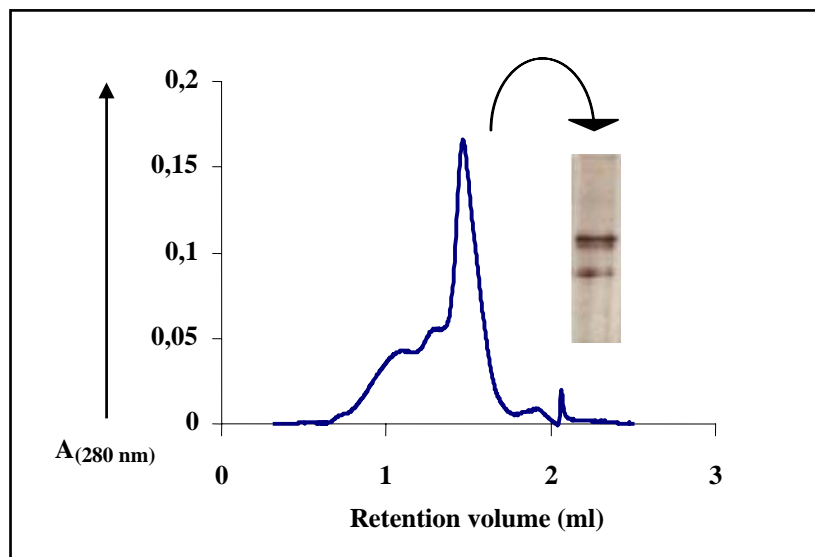


Fig. 6.7 Analytical gel filtration of purified AT_{1a}R-B₂R heterodimer complex (eluate from streptactin column, 0.1 mg at a concentration of 2 mg/ml) using superose 6 column.

6.5.3 Ligand binding analysis of heterodimer complex

Radioactive ligand assay was performed on the eluates from Ni-NTA and streptactin columns. As shown in Fig. 6.8, [³H] angiotensin II binding on Ni-NTA eluate and [³H] bradykinin binding on streptactin eluate was detected. The eluate after two columns (Ni-NTA followed by streptactin) revealed approximately 1:1 binding of [³H] angiotensin II and [³H] bradykinin. These data agree with the isolation of a B₂R-AT_{1a}R heterodimer complex.

6.6 Stability analysis of the heterodimer complex

In order to check the stability of B₂R-AT_{1a}R complex over time, the complex was stored at 4°C and after three days, a pull down assay was performed using either Ni-NTA resin or streptactin resin. Unfortunately, AT_{1a}R was found in the flow through of Ni-NTA resin and B₂R was present in the flow through of streptactin resin (Fig. 6.9). This indicates that the complex dissociates when stored after purification. Further attempts to stabilize the complex are underway.

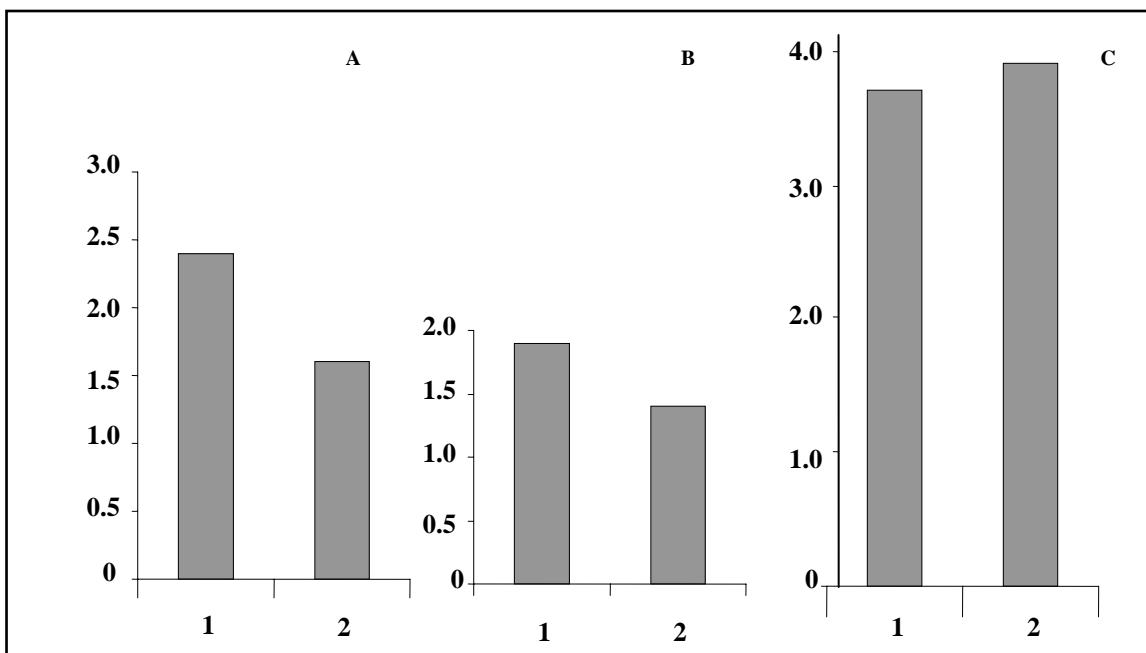


Fig. 6.8 Radioligand binding analysis during isolation of heterodimer complex. **A.** [³H] bradykinin binding (1) and [³H] angiotensin II binding (2) on the eluate from Ni-NTA column, **B.** [³H] angiotensin II binding (1) and [³H] bradykinin binding (2) on streptactin eluate, and **C.** [³H] bradykinin binding (1) and [³H] angiotensin II binding (2) after two steps of purification.

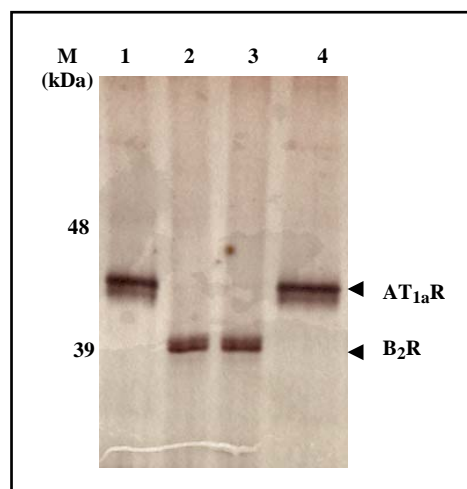


Fig. 6.9 Analysis of the B₂R-AT_{1a}R heterodimer complex stability over time. After purification, the B₂R-AT_{1a}R heterodimer complex was stored at 4°C followed by a pull down assay using either Ni-NTA or streptactin resin. A 15% silver stained SDS-polyacrylamide gel showing flow through of Ni-NTA (lane 1, 0.4 µg), eluate of Ni-NTA (lane 2, 0.4 µg), flow through streptactin (lane 3, 0.4 µg), and eluate from streptactin resin (lane 4, 0.4 µg).

*Chapter 7: Production, characterization and isolation of
 NmU_2R*

7.1 Production and isolation of NmU₂R from *Pichia pastoris*

7.1.1 Sub-cloning of NmU₂R gene in *Pichia* expression vector

The coding region of NmU₂R gene was amplified from cDNA vector (pNmU₂R, from Aventis) with the primers NmU₂R_ *Pichia*_Fw/Rv using *Pfu* DNA polymerase. PCR products were checked on 1% agarose gel (Fig.7.1), purified using PCR purification kit and then digested with *Spe*I and *Eco*RI enzymes. After restriction digestion, the PCR product was ligated to *Spe*I-*Eco*RI digested pPIC9K (modified) vector. The resulting construct was verified by DNA sequencing.

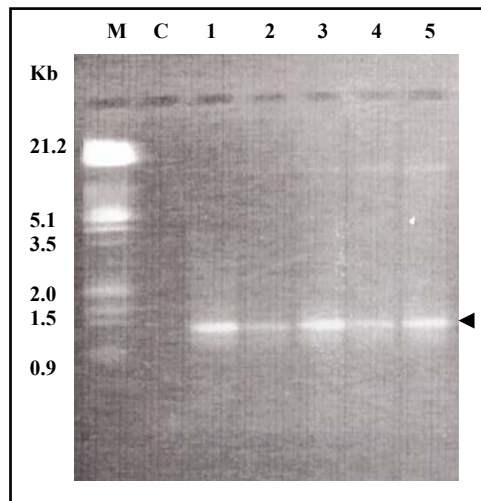


Fig. 7.1 Amplification of NmU₂R gene from cDNA vector by PCR under following conditions: 94°C = 5 min, 94°C = 40 sec, 68°C = 40 sec, 72°C = 90 sec and 72°C = 10 min. Total 30 cycles (step 2 to step 4) were used for amplification. PCR products were analyzed on 1% agarose gel. M = Lambda DNA (*Eco*RI + *Hind*III) marker, C= control (no template DNA), 1-5 = different amounts (50 ng-200 ng) of template DNA.

7.1.2 Expression construct

The modified pPIC9K expression vector used for production of NmU₂R in *Pichia pastoris* has been described before (section 3.1.2). This vector contains a Flag tag and a histidine 10 tag at the N-terminus and a biotinylation domain of *Propionibacterium shermanii* transcarboxylase at the C-terminus. The resulting construct is shown in Fig. 7.2

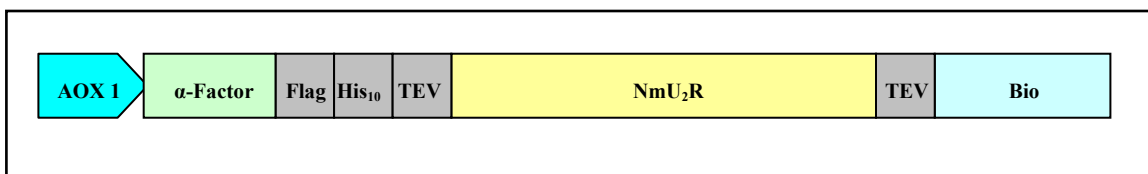


Fig. 7.2 Expression construct for production of recombinant NmU₂R in *Pichia pastoris*. AOX1 = alcohol oxidase 1 promoter, α -factor = α -mating factor prepro-peptide of *S. cerevisiae*, Flag = coding sequence for Flag epitope, His₁₀ = coding sequence for histidine 10 tag, NmU₂R = coding sequence of NmU₂R gene, TEV = cleavage site for TEV protease, Bio = biotinylation domain of *Propionibacterium shermanii* transcarboxylase.

7.1.3 Production of the recombinant receptor

Pichia cultures were grown in shake flasks (as described in Multi-Copy *Pichia* expression kit, Invitrogen), membranes were prepared (after 24 h of induction with methanol) and subjected to Western blot analysis and ligand binding assay.

7.1.3.1 Western blot analysis

Western blot with anti-Flag M2 antibody was performed to check the expression of recombinant receptor. As shown in Fig. 7.3, a band of approximately 55 kDa was seen in the membranes of *Pichia* cells expressing NmU₂R. The size of this band corresponds well to the calculated size of recombinant receptor fusion protein (52.3 kDa). An additional band of approximately 75 kDa was also seen which probably represents unprocessed receptor. The unprocessed receptor is the fusion of recombinant receptor and alpha-factor as Kex-2 endopeptidase of *Pichia pastoris* failed to cleave the alpha-factor completely.

7.1.3.2 [¹²⁵I] NmU binding

In order to check the functionality of the recombinant receptor and to calculate the total amount of functional receptor in membranes, a saturation binding experiment using [¹²⁵I] NmU was performed. [¹²⁵I] NmU binding was saturable and revealed a B_{max} value of 1.5 pmol recombinant NmU₂R per mg membrane protein (Fig. 7.4). A high affinity binding

of [125 I] NmU to the recombinant receptor was observed with a K_d value of 0.79 nM. This K_d is similar to a previously reported value for NmU₂R in COS-7 cell (see appendix).

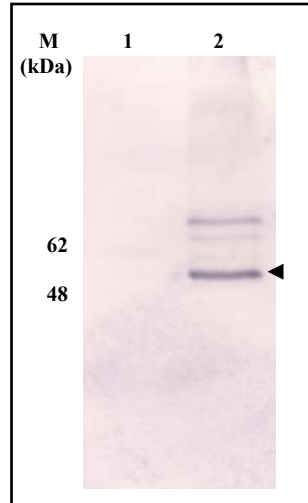


Fig. 7.3 Western blot analysis of the FlagHis₁₀NmU₂RBio construct produced in *P. pastoris*. Proteins were separated by 10% SDS-PAGE and probed with anti-Flag M2 antibody. Lane 1 = 5 μ g of membranes from *Pichia pastoris* expressing FlagHis₁₀NmU₂RBio protein and lane 2 = 5 μ g of control *Pichia* membranes.

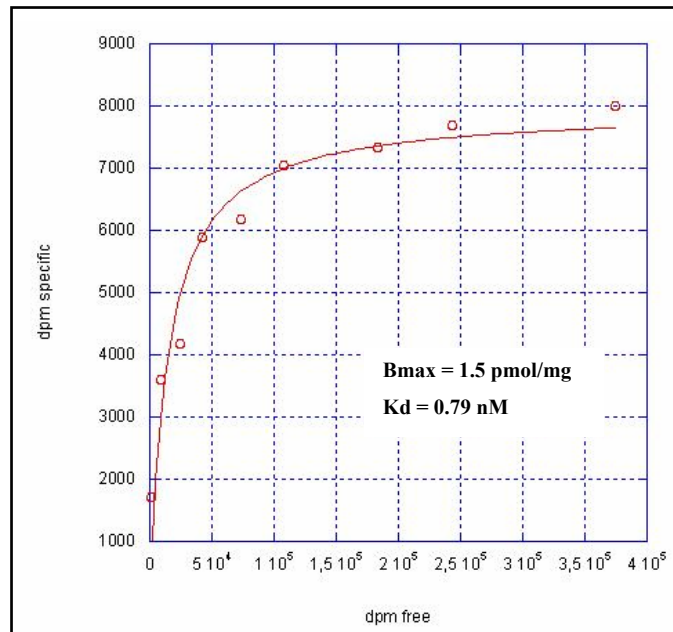


Fig. 7.4 Saturation curve for [125 I] NmU binding to the recombinant NmU₂R produced in *Pichia*. The Graph was generated using a single site model in KaleidaGraph software.

7.1.4 Optimization of functional production level of NmU₂R

In order to increase the functional expression of NmU₂R, DMSO was added to the *Pichia* cultures during the methanol induction step. As shown in Fig. 7.5, approximately four-fold increase in functional expression of recombinant NmU₂R was observed upon addition of DMSO. Maximum expression level was obtained in presence of 2% DMSO and it corresponds to approximately 6 pmol/mg (0.2 mg/l culture) of recombinant NmU₂R.

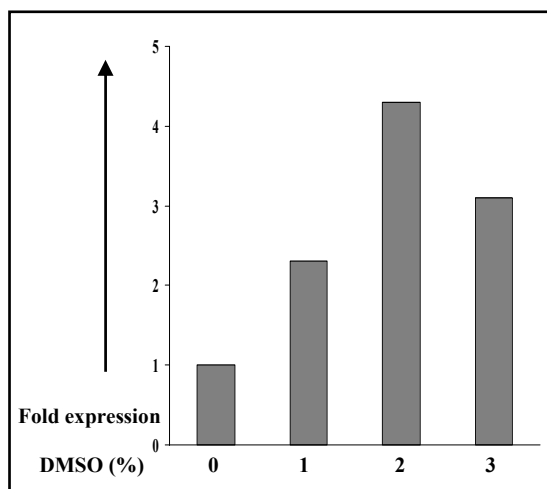


Fig. 7.5 Effect of DMSO on the expression level of recombinant NmU₂R in *Pichia pastoris*. DMSO was added to the cultures, membranes were prepared and [¹²⁵I] NmU binding was measured.

7.1.5 Glycosylation analysis

There are three putative glycosylation sites[#] in NmU₂R, two at the N-terminus (N⁹, N²⁷) and one in the third extracellular loop (N¹⁸⁰). In order to analyze the glycosylation state of the recombinant receptor, enzymatic deglycosylation using PNGaseF or EndoH was performed on *Pichia* membranes expressing NmU₂R, followed by Western blot analysis.

[#]These sites are predicted based on the conserved N-linked glycosylation motif (Asn-Xaa-Ser/Thr).

As shown in Fig. 7.6, the recombinant receptor band was shifted to lower molecular weight size upon enzymatic deglycosylation. This result reveals that the recombinant NmU₂R produced in *Pichia* was glycosylated.

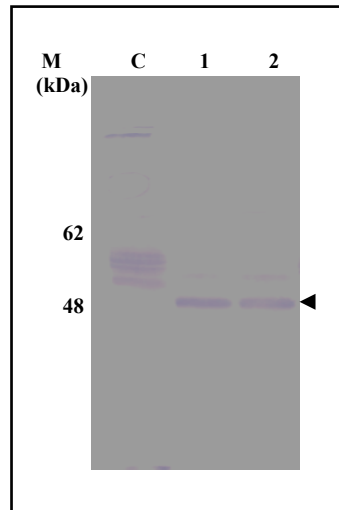


Fig. 7.6 Glycosylation analysis of the recombinant NmU₂R produced in *Pichia*. 5 µg of *Pichia* membranes expressing NmU₂R were treated with 0.5 units of PNGaseF (lane 1) or 0.5 units of EndoH (lane 2) at 4°C for 2h. The lane “C” is untreated control *Pichia* membranes (5 µg). The proteins were separated by 10% SDS-PAGE and Western blot analysis was performed using anti-Flag M2 antibody.

7.1.6 Solubilization of the recombinant NmU₂R

In order to solubilize the recombinant NmU₂R from *Pichia* membranes, different detergents (with 0.2 % CHS) were tested. As shown in Fig. 7.7, NmU₂R was solubilized with most of the detergents. [¹²⁵I] NmU binding on solubilizate was used to monitor the functional solubilization of NmU₂R from *Pichia* membranes. It revealed that approximately 50-60 % of the [¹²⁵I] NmU binding sites were solubilized with maltoside detergents (LM, UM and DM). The recovery with other detergents was lower. Therefore, for further studies, NmU₂R was solubilized with 1% LM in presence of 0.2% CHS.

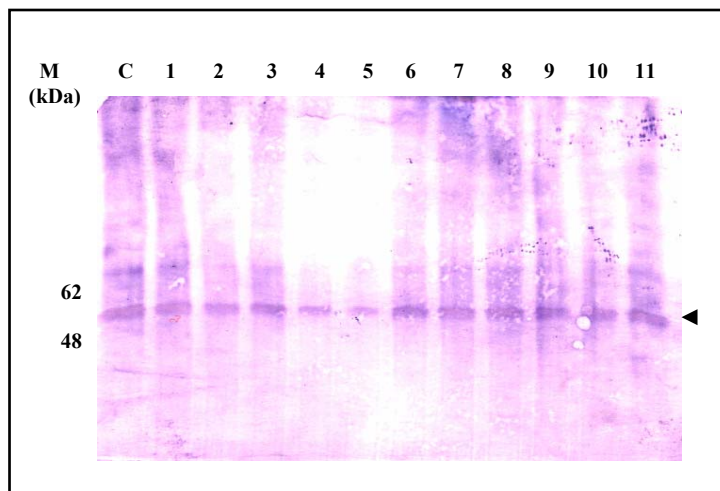


Fig. 7.7 Solubilization of the recombinant NmU₂R from *Pichia* membranes (5 mg/ml). Lane 1-11 = LM, UM, DM, NG, OG, Fos12, Fos14, Fos16, CHAPS, LDAO, digitonin. All the detergents were used at the concentration of 1% except OG (2%). Solubilizate was loaded on a 10% SDS-polyacrylamide and Western blot analysis was performed using anti-Flag M2 antibody.

7.1.7 Purification of recombinant NmU₂R

Pichia membranes expressing NmU₂R were saturated with NmU (1 μM) in order to stabilize the active conformation of the receptor. Subsequently, the receptor was solubilized and purified on Ni-NTA resin. As a second step of purification, the eluate from Ni-NTA was applied to monomeric avidin matrix. The recombinant receptor from this column was eluted with 2 mM biotin. The eluates from Ni-NTA and monomeric avidin columns were analyzed by 10% silver stained SDS-PAGE. As shown in Fig. 7.8 A, the recombinant receptor was >75 % pure after monomeric avidin purification.

In order to check the homogeneity of purified NmU₂R, the eluate from monomeric avidin column was analyzed by gel filtration on a Superose 6 column in the SMART chromatography system. A main peak at a retention volume of 1.60 ml (indicated by the arrow head) was observed (Fig. 7.8 B). It corresponds to a homogenous population of purified NmU₂R. In addition to this main peak, some aggregated receptor (peak at retention volume of 0.89 and shoulder at 1.4-1.5 ml) and a peak at a retention volume of 1.79 ml was also observed. The peak at 1.79 ml contained no protein (as analyzed by silver stained SDS-PAGE) and probably represents free detergent micelles.

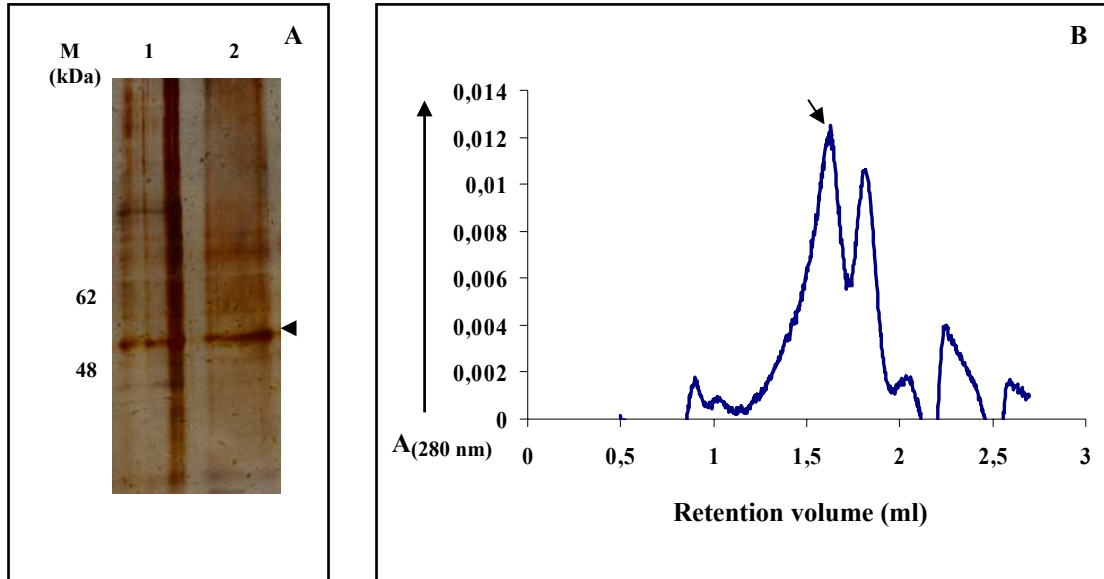


Fig. 7.8 Purification of the recombinant NmU₂R from *Pichia pastoris*. **A.** Silver stained 10% SDS-polyacrylamide gel showing the eluate from Ni-NTA (lane 1, 1 µg) and monomeric avidin (lane 2, 0.8 µg). **B.** Analytical gel filtration of purified NmU₂R (eluate from monomeric avidin column, 25 µg at a concentration of 0.5 mg/ml) using superose 6 column.

Here, it was not possible to follow the receptor purification by ligand binding (receptor was purified with high affinity ligand NmU). Therefore, the estimation of purification yield is based on the total protein quantification by BCA assay. It was estimated that the receptor yield after two-step affinity purification was 20-25% (BCA quantification) of the starting amount in membranes (based on ligand binding).

7.2 Production and isolation of the NmU₂R from BHK cells

7.2.1 Sub-cloning of NmU₂R gene in SFV expression vectors

The coding region of NmU₂R gene was amplified with the primers NmU₂R_SFV_Fw/Rv and ligated into the modified SFV vector between *Sma*I and *Spe*I enzyme sites, using the standard cloning procedure.

7.2.2 Expression construct

For the expression of NmU₂R in mammalian cells, the modified SFV expression vector (described in section 3.3.2) was provided by Christoph Reinhart. The expression construct of NmU₂R is shown in Fig. 7.9. Here, expression of the recombinant NmU₂R protein is driven by a subgenomic 26S promoter. This vector contains a capsid sequence (a translation enhancer element from 5' end of the capsid gene from SFV) and affinity tags for detection and purification of NmU₂R.

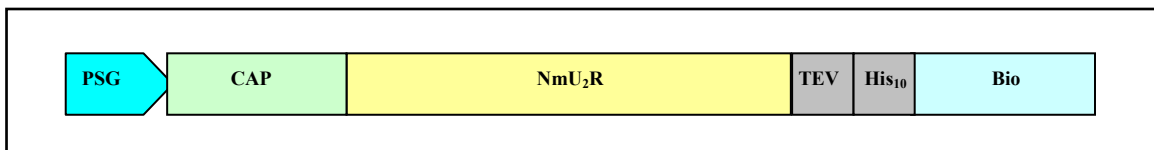


Fig. 7.9 Expression constructs for production of recombinant NmU₂R in mammalian cells. PSG = subgenomic 26S promoter, CAP = capsid sequence, NmU₂R = coding sequence for NmU₂R gene, His₁₀ = coding sequence for histidine 10 tag, TEV = cleavage site for TEV protease, Bio = biotinylation domain of *Propionibacterium shermanii* transcarboxylase.

7.2.3 Production of recombinant NmU₂R in BHK cells

Recombinant virus particles were generated and activated as described in the materials and methods. Suspension cultures of BHK cells were grown and infected at a density of 1-2x10⁶ cells/ml. 24 h post-infection, membranes were prepared and subjected to Western blot analysis and [¹²⁵I] NmU binding analysis.

7.2.3.1 Western blot analysis of NmU₂R

Western blot analysis of membranes from BHK cells expressing NmU₂R revealed a band of approximately 55 kDa (Fig. 7.10). It corresponds well with the calculated size of recombinant receptor fusion protein (50.1 kDa).

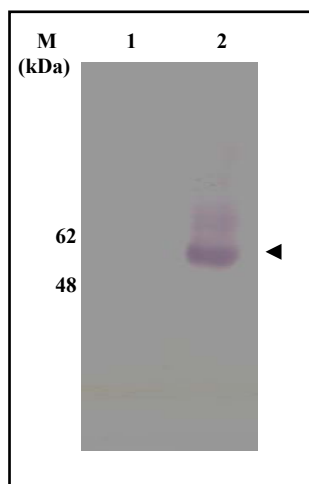


Fig. 7.10 Western blot analysis of the recombinant NmU₂R produced in BHK cells. Proteins were separated by 10% SDS-PAGE and probed with anti-his antibody. Lane 1 = 10 μg of membranes from non-infected BHK cells and lane 2 = 10 μg of membranes from BHK cells expressing NmU₂R.

7.2.3.2 [¹²⁵I] NmU binding analysis

In order to calculate the total amount of functional receptor in membranes, a saturation binding experiment using [¹²⁵I] NmU was performed. [¹²⁵I] NmU binding was saturable and revealed a B_{max} value of 2.3 pmol recombinant NmU₂R per mg membrane protein (Fig. 7.11). A high affinity binding of [¹²⁵I] NmU to the recombinant receptor was observed with a K_d value of 1.2 nM. This K_d is similar to a previously reported value for NmU₂R in COS-7 (see appendix). The non-specific binding was determined in presence of 1 μM NmU and it was less than 20% of total binding.

7.2.3.3 Effect of DMSO on NmU₂R expression

In an attempt to further increase the functional expression of NmU₂R, DMSO was added to the BHK cell cultures during expression step. 24 h post-infection, membranes were prepared and subjected to [¹²⁵I] NmU binding analysis. As shown in Fig. 7.12, approximately four-fold increases in functional expression of recombinant NmU₂R was

achieved in the presence of 2% DMSO and this corresponds to approximately 9 pmol/mg (0.1 mg/liter culture) of NmU₂R.

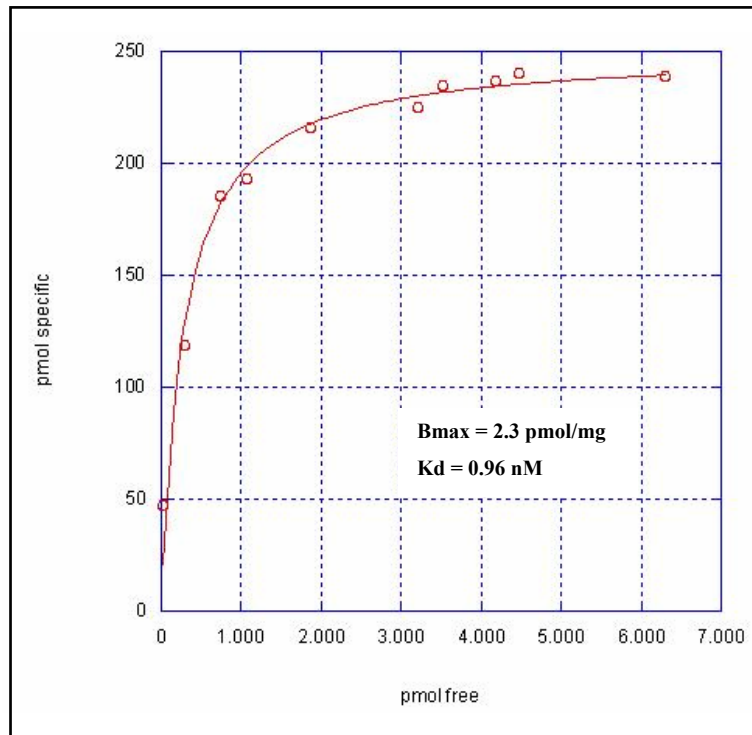


Fig. 7.11 Saturation curve for [¹²⁵I] NmU to recombinant NmU₂R produced in BHK cells. The graph was generated using the single site model in KaleidaGraph software.

7.2.4 Glycosylation analysis

In order to analyze the glycosylation state of the recombinant receptor, enzymatic deglycosylation using PNGaseF or EndoH was performed on membranes from BHK cells expressing NmU₂R, followed by Western blot analysis. As shown in Fig. 7.13, there was no change in the migration of the recombinant NmU₂R band suggesting that the receptor was not glycosylated. Similarly, recombinant B₂R, when produced in BHK cells, was also not glycosylated.

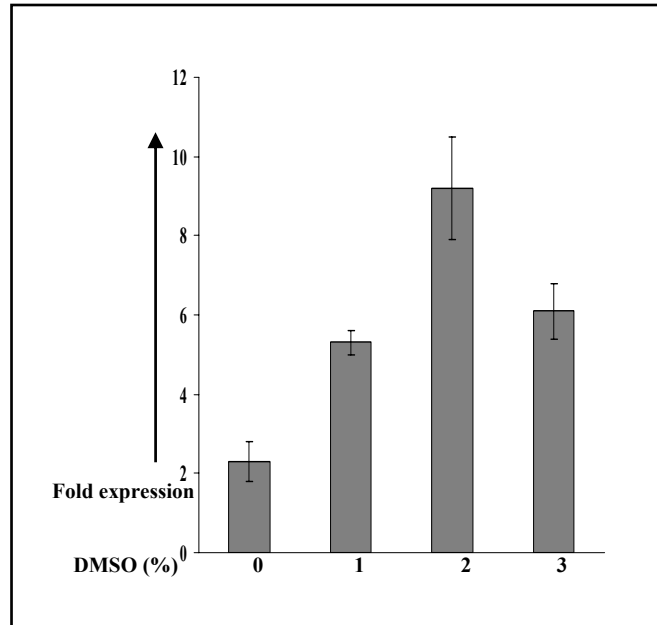


Fig. 7.12 Effect of DMSO on the expression level of recombinant NmU₂R in BHK cells. DMSO was added to the cultures, membranes were prepared and [¹²⁵I] NmU binding was measured.

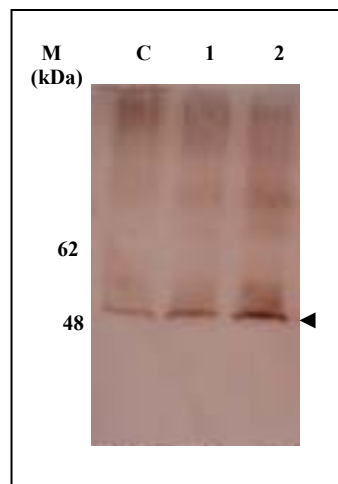


Fig. 7.13 Glycosylation analysis of the recombinant NmU₂R produced in BHK cells. 10 µg of membranes from BHK cells expressing NmU₂R were treated with 0.5 units of PNGaseF (lane 2) or 0.5 units of EndoH (lane 3) at 4°C for 2 h. The lane “C” is untreated control membranes (5 µg). The proteins were separated by 10% SDS-PAGE and Western blot analysis was performed using anti-his antibody.

7.2.5 Localization analysis of NmU₂R

Localization of NmU₂R in BHK cells (using fluorescein labeled NmU) was checked by confocal microscopy. As shown in Fig. 7.14, recombinant NmU₂R was mainly localized in the perinuclear membranes (most probably in the endoplasmic reticulum). Only low levels of fluorescence were observed on the plasma membrane. Similar intracellular retention of overexpressed alpha-2B adrenergic receptor (Sen *et al.*, 2003) and recombinant B₂R (this study, section 3.3.6.2) was observed in BHK cells.

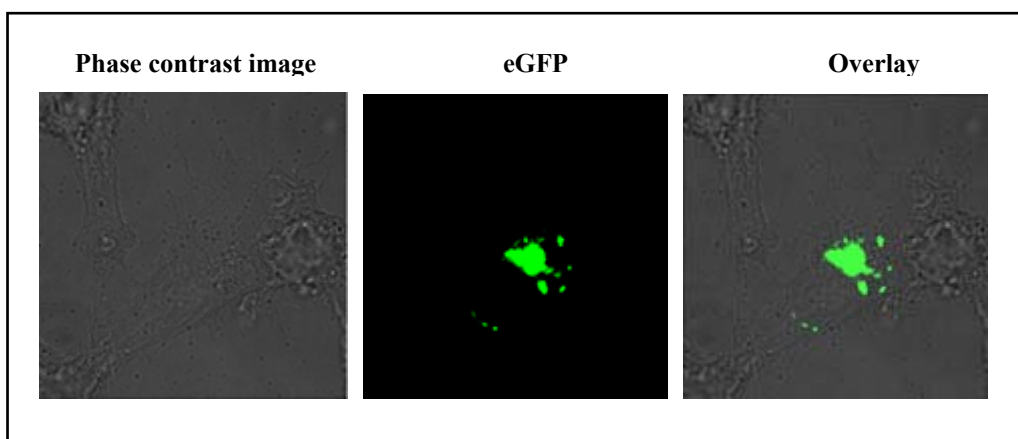


Fig. 7.14 Confocal imaging of BHK cell expressing NmU₂R. Cells were grown and infected on cover slips. 24 h post-infection, cells were permeabilized and stained with fluorescein labeled NmU. Subsequently, the cells were fixed and scanned (488 nm) with a Zeiss laser scanning confocal microscope.

7.2.6 Solubilization and purification of NmU₂R

Recombinant NmU₂R was solubilized from membranes (5 mg/ml) using 1% LM in the presence of 0.2% CHS. Approximately, 55-60% of the [¹²⁵I] NmU binding sites were solubilized from membranes.

For purification, membranes were first saturated with NmU (1 μM) in order to stabilize the active conformation of the receptor. Subsequently, the receptor was solubilized (1% LM in presence of 0.2% CHS) and purified using Ni-NTA resin. Eluate

from the Ni-NTA column was analyzed by silver stained 10% SDS-PAGE. As shown in Fig. 7.15 (A), >80% pure receptor was obtained after Ni-NTA purification.

In order to check the homogeneity of purified receptor, the eluate from Ni-NTA column was analyzed by gel filtration on a Superose 6 column. As shown in Fig. 7.15 (B), purified NmU₂R was present mainly in homogenous form (peak at 1.60 ml). Some aggregation of the purified NmU₂R was also detected (peak at 0.9 ml and shoulder at 1.2 ml). Additionally, a peak at a retention volume of 1.75 ml was also observed which possibly corresponds to the free detergent micelles.

It was estimated that receptor yield after Ni-NTA purification was 30-32% (BCA quantification) of the starting amount in membranes (based on ligand binding).

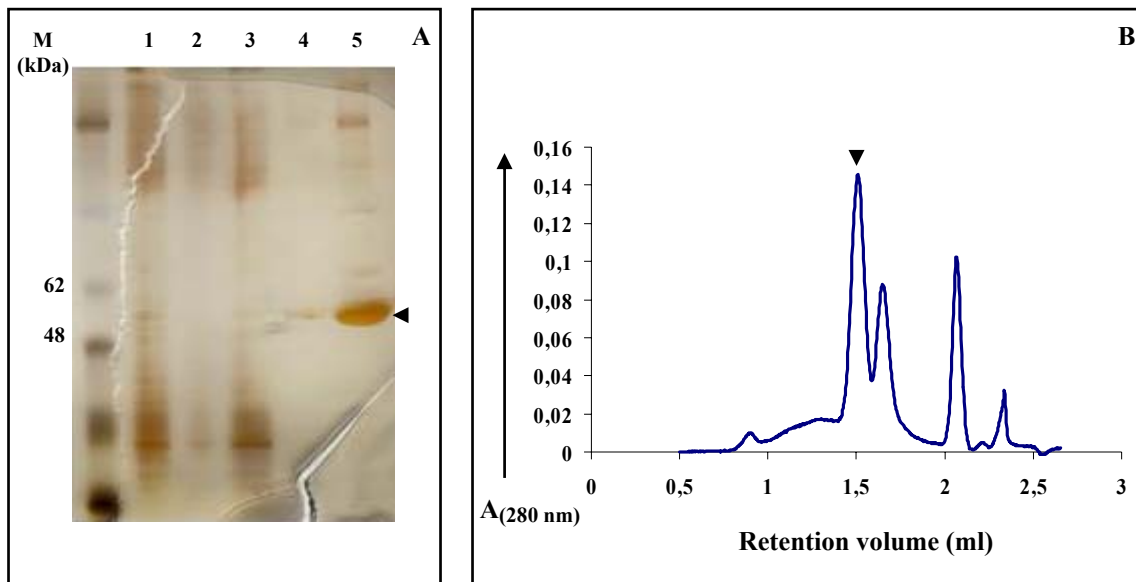


Fig. 7.15 Purification of recombinant NmU₂R from BHK cells. **A.** Silver stained 10% SDS-polyacrylamide gel showing membranes (lane 1, 0.2 µg), solubilizate (lane 2, 0.2 µg), flow through (lane 3, 0.2 µg), eluate from Ni-NTA (lane 4 & 5, 0.1 µg & 0.8 µg, respectively). **B.** Analytical gel filtration of purified B₂R (eluate from Ni-NTA column, 0.1 mg at a concentration of 2 mg/ml) using superose 6 column.

Chapter 8: Discussion

8.1 Structural studies on GPCRs

G protein-coupled receptors (GPCRs) are involved in many important cellular signal transduction processes such as differentiation, proliferation, angiogenesis, cancer, development and cell survival. GPCRs represent an important class of drug targets with proven therapeutic value. Over 200 major prescription drugs target GPCRs, representing over 30% of the total drugs on the market (Wise *et al.*, 2002). However, due to the lack of a three-dimensional structure (except bovine rhodopsin), structure-based drug design has not been possible. It should be noted that the only GPCR crystallized till date, the bovine rhodopsin (Palczewski *et al.*, 2000), was obtained from the natural source (bovine retina) where it is found in large amounts. The reasons for the extremely low success rate in structure determination of GPCRs are their low abundance in native tissues and the complications related to the expression of recombinant receptors in heterologous systems. These complications include inefficient transport and insertion in the plasma membrane as well as their toxic effect on the host cell. Additionally, isolation of large amounts of stable receptor proteins for structural characterization has also been a challenging task. Due to the lack of 3-D structures, a number of biochemical and biophysical techniques have been used to get some information about GPCRs. One of the most common approaches is site-directed mutagenesis coupled to functional analysis. Additionally, electron paramagnetic resonance (EPR) spectroscopy, NMR spectroscopy and Cys-crosslinking experiments have also been carried out on rhodopsin (see papers by Khorana and coworkers). These studies have resulted in some insights into the GPCR mechanism. More recently, the bovine rhodopsin structure has been used as a template for molecular modeling of other GPCRs. However, all the above mentioned studies do not provide sufficient details of GPCR activation and signalling mechanism. Therefore, it is necessary to obtain three-dimensional structures of GPCRs and more importantly, in different states (i.e. agonist/antagonist bound, in complex with G protein and in complex with beta-arrestin etc.). The first step towards this goal is to produce and isolate sufficient amounts of GPCRs that can be used for structural characterization. This has been the major focus during my PhD work. Although the number of structures of membrane proteins are growing (97 unique structures until October 2005), it is interesting to note

that the X-ray crystal structure of only one human recombinant membrane protein i.e. monoamine oxidase (MAO) has been determined until now (Binda *et al.*, 2000). Monoamine oxidase is a monotopic membrane protein and therefore, it has little hydrophobic surface (MAO has a single transmembrane helix that anchors it to the outer membrane). The bulk of this 520 residue protein, including the active site, is outside the membrane. This example reflects the fact that large-scale production and isolation of recombinant human membrane proteins has been a difficult task. It is not surprising that heterologous production of membrane proteins in general is more difficult than the cytoplasmic proteins. Membrane proteins require a complicated set of events for their targeting and insertion into the membrane. It may happen that when overproduced in a heterologous system, membrane proteins can saturate the secretory pathway of the cell. This might lead to the accumulation of unfolded and inactive protein inside the host cell. Therefore, overproduction and isolation of GPCRs represent the main bottlenecks for structural characterization. Once a given GPCR can be produced and isolated in sufficient quantities, the next focus should be long-term stability and trials to increase its polar surface area for making crystal contacts.

8.2 Heterologous production of B₂R in different host systems

B₂R plays a crucial role in cardiovascular system and it is a major target for the treatment of a wide spectrum of cardiovascular disorders. Understanding the receptor structure and the receptor bound conformation of bradykinin would be a great help in designing more specific and potent drugs to treat cardiovascular diseases. During this study, human B₂R was produced in three different hosts namely *Pichia pastoris*, insect cells and mammalian cells.

Among different heterologous expression systems for GPCR production, the methylotrophic yeast *Pichia pastoris* has been described as an efficient one. In this system, the genes coding for the heterologous proteins are placed under the control of alcohol oxidase-1 (AOX1) promoter (Cregg *et al.*, 1993). The AOX1 promoter is highly inducible by methanol and tightly regulated. In the presence of methanol, the promoter activity is maximal and it may contribute up to 30% of the total protein content of the cell

(Cregg *et al.*, 1993). Since, *P. pastoris* is a eukaryotic system, its intracellular environment is more suitable for expression and correct folding of eukaryotic proteins. Several GPCRs have been successfully expressed in *Pichia*, such as the β_2 -adrenergic receptor and the 5HT_{5A}-serotonergic receptor (Weiss *et al.* 1998), the human CB₁ cannabinoid receptor (Kim *et al.*, 2005), the human D_{2S} dopamine receptor (Grünewald *et al.*, 2004), the CB₂ cannabinoid receptor (Feng *et al.*, 2002), the human μ -opioid receptor (Sarramegna *et al.*, 2002), and the human ET_(b) endothelin receptor (Schiller *et al.*, 2000). Previous successes with GPCR production in *Pichia pastoris* make it the first choice for the production of a given GPCR. However, the expression level of recombinant B₂R in *Pichia pastoris* was low (0.3 pmol/mg) under basic culture conditions (see result section 3.1.3.2). By addition of DMSO, the expression level was increased up to 3.5 pmol/mg (0.1 mg of receptor in membrane per liter culture), but still too low for large-scale production. *Pichia pastoris* can be grown in the fermentor, which results in large biomass. This makes it possible to obtain significant amount of receptor despite its low expression level. However, it has also been noticed in some cases that expression level of GPCRs in *Pichia* decreases when fermentor is used (Christoph Krettler, personal communication). As mentioned before, the main goal of this study was to isolate large amounts of the receptor. With low expression level of the receptor, large amounts of detergent will be required during solubilization step. Therefore, production of B₂R in *Pichia* using fermentor was not considered and other expression systems were tested.

Among the different factors that may influence the ligand binding of a given receptor, the non-appropriate lipid environment is particularly relevant. It has already been reported that ligand binding of some GPCRs was significantly affected by the surrounding lipid environment (Burger *et al.*, 2000, Chattopadhyay *et al.*, 2005, and Lagane *et al.*, 2000). In yeast, the major sterol of the plasma membrane is ergosterol. A recent study suggests that cholesterol and ergosterol have quite opposite effects with respect to the ligand binding properties of the human μ -opioid receptor (Lagane *et al.*, 2000). Ergosterol was found to constrain the μ -opioid receptor in an inactive state and could not replace cholesterol in activating it. In view of these observations, it is likely

that due to inappropriate lipid environment, the recombinant B₂R produced in *Pichia* can not bind to its ligand. Additionally, it is also possible that B₂R requires certain molecular chaperones for proper folding and activity, which are not present in *Pichia pastoris*. Therefore, one can consider coexpressing the receptor with molecular chaperones such as calnexin and BiP. Although it has been found that the coexpression of calnexin improves the yield of functional Shaker potassium channel (Higgins *et al.*, 2003), coexpression of GPCRs (substance P receptor and adenosine A_{2a} receptor) with molecular chaperones did not improve their expression level in (Butz *et al.*, 2003).

Next, baculovirus mediated expression of B₂R in insect cells was tested. The baculovirus system has also been very efficient for heterologous production of several membrane proteins. Baculovirus based expression has resulted in functional production of several GPCRs such as the dopamine D₂ receptor (Grünwald *et al.*, 1996 and Javitch *et al.*, 1994), serotonin receptors (Parker *et al.*, 1994, Butkerait *et al.*, 1995 and Mulheron *et al.*, 1994), muscarinic receptors (Parker *et al.*, 1994 and Rincken *et al.*, 1991), the β₂-adrenergic receptor (Reiländer *et al.*, 1991), the adenosine A_{2a} receptor (Murphree *et al.*, 2002 and Robeva *et al.*, 1996), cannabinoid receptors (Glass *et al.*, 1999) and opioid receptors (Massotte *et al.*, 1997). It has been observed that post-translational modifications in insect cells are identical to mammalian cells. Therefore, this system is a good choice for those GPCRs where the receptor function is influenced by post-translation modifications.

The expression level of B₂R in insect cells using the baculovirus system was 10 pmol/mg (0.3 mg of the receptor per liter culture). Interestingly, there was no increase in the receptor expression level by addition of DMSO in cell culture medium. However, it was possible to obtain 6-8 mg of recombinant receptor in membranes by using a 25 liter wave bioreactor. Thus, the baculovirus mediated expression of B₂R in insect cells provides a suitable system for large-scale production and further characterization of this receptor.

For the heterologous production of human GPCRs, mammalian cells provide most natural environment. Therefore, SFV based expression of B₂R in mammalian cells

was also tested. It has been demonstrated that the SFV based system leads to high levels of expression (50–150 pmol/mg) of several GPCRs (Lundstrom *et al.*, 2003). The expression level of B₂R in mammalian cells was 10-11 pmol/mg under basic conditions (see result section 3.3.3), which was further increased to 60 pmol/mg (0.6 mg/liter) by the addition of DMSO in culture medium. This expression level of B₂R is the maximum reported so far in any expression system. Previous studies using stable or transient cell lines have resulted in only low (100-200 fmol/mg) or moderate expression levels (1-3 pmol/mg). Although it was observed that the expression level of B₂R in the bioreactor (30-32 pmol/mg) was relatively lower than in the spinner flasks (55-60 pmol/mg), it was possible to obtain up to 5-6 mg of receptor in membrane by using a 20 liter wave bioreactor. One advantage of using the SFV system is the broad range of host cells that can be infected by SFV. The choice of appropriate host cells has also been shown to play a significant role in the expression of some receptors. For example, rat odorant receptors were retained intracellularly when expressed in BHK cells but showed plasma membrane localization when expressed in olfactory epithelial cell line OLF442 (Monastyrskaia *et al.*, 1999). In some cases, the expression levels also vary depending on the host cell. For instance, the expression levels of the rat κ and μ opioid receptors were higher in rat C6 glioma cells compared to BHK or CHO cells (Simmen *et al.*, 1998). During this study, four different cell lines (BHK-21, CHO-K1, COS-7 and HEK-293) were tested for expression of B₂R but no significant difference was observed. Although, the expression level of B₂R is best in mammalian cells, the high cost of virus production does not allow the use of this system on a routine basis for large-scale production of the recombinant receptor.

8.3 Characterization of the recombinant B₂R

Immunoblot analysis of recombinant B₂R from *Pichia* and BHK cells showed a single band of 55 kDa and 50 kDa respectively. These sizes correspond well with the calculated molecular masses of the recombinant receptor with or without glycosylation. However, recombinant B₂R from insect cells showed two bands of 55 kDa and 35 kDa. While the major band of 55 kDa represents a full length receptor fusion protein, the smaller band of 35 kDa is a proteolytic degradation product. Due to the long expression time in the

baculovirus system and because it is a lytic system (i.e. producer cells are lysed at the end of the virus life cycle), proteins expressed in this system often show proteolytic cleavage. Similar proteolytic degradation of overexpressed rat thrombin receptor (Chinni *et al.*, 1998) and human histamine H₁ receptor (Ratnala *et al.*, 2004) in insect cells has been reported. However, unlike the H₁ receptor, addition of leupeptin in the culture medium did not prevent proteolytic cleavage of B₂R.

In human fibroblasts and platelets which naturally express B₂R, this receptor has been found to be a protein of 69 kDa (Blaukat *et al.*, 2003). This molecular weight is higher than predicted from the receptor coding region (40 kDa) and may represent a heavily glycosylated (at N³, N¹² and N¹⁸⁰) form of the receptor. The recombinant receptor produced in *Pichia* and insect cells was in glycosylated form, although heavy glycosylation like native tissue was not observed. During deglycosylation, size of the proteolytic cleavage product observed in Sf9 cells was also reduced, indicating that the degradation product is the N-terminal part of the recombinant receptor. It was surprising that recombinant B₂R was not glycosylated when produced using the SFV system. For some members of GPCR family, glycosylation is required for optimal cell surface expression and receptor function while for some other members, cell surface localization and function are not affected glycosylation state of the receptor (reviewed in Wu *et al.*, 2005). Interestingly, when murine CB₂ cannabinoid receptor was produced in the SFV system using similar constructs, it was only partially glycosylated (Olson *et al.*, 2003). The presence of non-glycosylated receptor molecules may represent the saturation of rate limiting step of carbohydrate processing in the host cells. Alternatively, fast replication of the recombinant virus may also interfere with the glycosylation machinery of the host cell.

Saturation binding analysis on membranes revealed that the ligand binding affinity of the recombinant B₂R from different host cells was similar to that of native tissues. High affinity of the recombinant B₂R for bradykinin provides a useful tool to stabilize the receptor during solubilization and purification steps, as the receptor-ligand complex should be more stable than the receptor alone.

8.4 Intracellular localization of recombinant B₂R

In order to check the localization of recombinant B₂R in insect cells and mammalian cells, confocal microscopy using eGFP fusion constructs and immunogold labeling experiments using Flag-tagged constructs were performed. Both methods revealed localization of B₂R in the intracellular membranes, probably representing the endoplasmic reticulum. Only a minor fraction of the recombinant receptor was detected on the plasma membrane. The baculovirus constructs contain a prepro-mellitin signal sequence, which is supposed to result in efficient targeting of the membrane proteins to the cell surface. But it was not the case for recombinant B₂R. However, previous reports also indicate intracellular retention of overexpressed GPCRs in insect cells (Blaukat *et al.*, 1999, Grünewald *et al.*, 1996, Maeda *et al.*, 2004 and Sen *et al.*, 2005).

In the constructs of SFV system, a signal sequence from influenza hemagglutinin (HA) gene was fused at the N-terminus of the receptor, still the receptor was retained intracellularly. Similar intracellular retention was observed for the beta-2 adrenergic receptor (Darui Huo, Ph.D. Thesis), human neurokinin 1 receptor (Lundstrom *et al.*, 2001) and human alpha-2b adrenergic receptor (Sen *et al.*, 2003), when expressed using SFV system. Nevertheless, as here, in many case even the intracellular retained receptor is capable of ligand binding. Localization of B₂R in *Pichia* was not checked. Previous reports strongly suggest intracellular localization of different GPCRs when expressed in *Pichia pastoris* (Grünewald *et al.*, 2004, Schiller *et al.*, 2000 and Weiss *et al.*, 1998).

It is generally assumed that over production of GPCRs or membrane proteins in general, saturates the secretion machinery of the host cell. This often leads to the accumulation of recombinant membrane proteins in the intracellular membrane compartments such as the endoplasmic reticulum and Golgi. However, as discussed later in this section, co-expression of B₂R and AT_{1a}R in BHK cells resulted in the cell surface targeting of the recombinant B₂R.

8.5 Isolation of recombinant B₂R

The most commonly used approach for purification of recombinant membrane proteins is affinity purification based on the affinity tags fused to the protein. Two-step purification based on affinity tags is a suitable approach for large-scale isolation of recombinant GPCRs. Immobilized metal affinity chromatography is most widely used as the first step because it is generally robust and inexpensive. Large amounts of solubilizate can be applied on these columns and the recombinant protein can be eluted with an excess of imidazole. As a second step, either monomeric avidin column or streptactin column can be used. Recombinant B₂R was successfully purified using a combination of Ni-NTA and monomeric avidin columns (from *Pichia* and Sf9) or in a single step by a Ni-NTA column (from BHK cells). Homogeneity of the purified membrane protein is an important issue before it can be subjected to the crystallization trails. Analytical gel filtration revealed that purified B₂R from *Pichia* was partially aggregated while it was mainly in homogenous state (at concentration of 10-20 mg/ml) when purified from BHK cells or Sf9 cells. However, purified B₂R from BHK cells showed aggregation at high concentrations (section 4.1.5.1). Aggregation of recombinant GPCRs upon purification is a common problem (personal communication with colleagues and Danka Elez, Ph.D. thesis). Non-specific interaction of hydrophobic domains can be one of the reasons for receptor aggregation. Leaking of some Ni⁺² ions from the Ni-NTA affinity matrix during purification may also lead to receptor aggregation (via binding to histidine tags). Another problem associated with purification of membrane protein purification is delipidation. Lipids can have a stabilizing effect on membrane proteins and severe delipidation during purification may result in instability and aggregation of these proteins.

An interesting observation during the purification of B₂R from Sf9 cells was copurification of a protein-tyrosine phosphatase SHP-2. Interaction of this protein with B₂R has been reported previously (Duchene *et al.*, 2002). This interaction is crucial for the anti-proliferative effect of bradykinin in primary culture renal mesangial cells. It is generally thought that a complex of a GPCR with one of its interacting partners may be a valuable tool for crystallization of the receptor. This is due to the fact that such a complex not only stabilizes the receptor in one conformation but also increases the polar surface

area of the receptor available for making crystal contacts. Therefore, the complex of B₂R and SHP-2 provides a unique opportunity for cocrystallization. However, the endogenous pool of the SHP-2 in Sf9 cells might be limited in comparison to the overexpressed B₂R. Therefore, coexpression of recombinant human SHP-2 and B₂R should be tested. By using different tags fused to B₂R and SHP-2, it should be possible to separate the complex of B₂R-endogenous SHP-2 and B₂R-recombinant SHP-2.

One problem associated with the baculovirus system is incomplete biotinylation of the biotinylation domain. It has been previously observed that only 30-40% of total recombinant receptor is botinylated in insect cells (Helmut Reiländer, personal communication). This results in a significant loss of recombinant receptor during purification on a monomeric avidin column. On the other hand, anti-Flag antibody matrix is expensive and can not be used repeatedly as its binding capacity decreases with repeated use. Therefore, an alternative strategy for purification of recombinant B₂R from insect cells should be explored. One possibility is a construct with Strep II tag and purification based on a combination of Ni-NTA and streptactin columns.

8.6 Structural studies with isolated B₂R

The main goal of this study was to use the isolated receptors for three-dimensional crystallization trials. However, as mentioned in the earlier, crystallization of recombinant human membrane proteins still remains a challenge. Therefore, a part of the isolated receptor was used for solid-state NMR studies and the other part for crystallization trials. Solid-state NMR studies aim to understand the receptor bound conformation of bradykinin as discussed later in this section.

8.6.1 Three-dimensional crystallization trails

The purified B₂R from BHK cells and Sf9 cells was used for three-dimensional crystallization screening. The protein in crystallization drops was stable over a wide range of pH and some microcrystalline precipitates were obtained with PEG 400. One of the major problems associated with crystallization trials was heavy detergent

crystallization. It often made analysis of the drops difficult. It can also be the case that tiny protein crystals are masked by the detergent crystals. Therefore, it is necessary to remove extra free detergent after purification. Dialysis is one of the most commonly used methods to remove detergents. However, due to low cmc of n-dodecyl- β -D-maltoside, dialysis may not be very efficient. Another option is removal of the detergent via Bio-Beads. For this method, a precise way to measure the detergent concentration is required. In addition, use of rhodamine labeled bradykinin during purification of the receptor can be helpful. It should result in colored protein crystals and therefore, it should be possible to differentiate the protein crystals from detergent crystals.

As discussed before, the complex of B₂R- β -arrestin, B₂R-SHP-2 or B₂R-AT_{1a}R represent valuable tools for cocrystallization of B₂R. Further attempts are required to characterize and stabilize these complexes before they can be used for crystallization attempts.

8.6.2 Solid-state NMR analysis of receptor bound bradykinin

Solid-state NMR is a general method to study molecular structure and dynamics in a non-crystalline environment. Recent progress in the field has led to the development of high resolution ss-NMR techniques (magic angle spinning, MAS) which are based on rapid rotation of the sample at a fixed angle under ultra high magnetic field. Although it has not been possible so far to study a full-length GPCR by ss-NMR, this technique offers a unique possibility to probe the conformational changes in the ligand upon binding to the receptor. In order to investigate the receptor bound conformation of bradykinin, ¹³C/¹⁵N uniformly labeled bradykinin variants were incubated with the purified B₂R. This receptor-ligand complex was then transferred to 4-mm MAS rotor, flash frozen and subjected to NMR analysis. It was possible to detect signals of ¹³C/¹⁵N labeled peptide (roughly 25 μ g) bound to just 1 mg of receptor. However, to get good signal/noise ratio, the experiments had to be carried out for long durations (9-10 days). Therefore, in order to increase the signal/noise, the amount of purified receptor was increased (this will increase the amount of bound ¹³C/¹⁵N labeled bradykinin). Unfortunately, it was not possible as the volume of MAS rotor is only 50 μ l and the purified receptor has a

tendency to aggregate at higher concentrations. Therefore, an alternative approach (i.e. measurements at low temperature) was used to shorten the measurement time. At 180 K, it became feasible to get sufficiently good signal /noise ratio within one day (compared to 3-5 days at 210 K). Interestingly, significant changes in the chemical shifts of receptor bound bradykinin were observed as compared to the lyophilized bradykinin or bradykinin in detergent micelles. Bradykinin has two arginines (R¹ and R⁹), three prolines (P², P³ and P⁷) and two phenylalanines (F⁵ and F⁸). The next step is to use selectively labeled bradykinin in order to assign the signals to individual amino acids. The information derived from these measurements will finally be used to generate a three-dimensional model of receptor bound bradykinin. It is expected that the receptor bound conformation of bradykinin will pave the way to design more specific and potent drugs acting on B₂R.

8.7 Coexpression of B₂R and AT_{1a}R

As mentioned before, GPCRs have a small polar surface area that can make crystal contacts. Therefore, a heterodimer complex of a given GPCR with another GPCR can be a more suitable object for crystallization. Human B₂R forms a stable heterodimer with human AT_{1a}R (Abdalla *et al.*, 2000) and this heterodimerization increases the activation of G_{αq} and G_{αi} proteins, the two major signalling G-proteins triggered by AT_{1a}R. Therefore, the coexpression of these two receptors was performed in order to isolate the heterodimer complex. Interestingly, it was found that the coexpression of B₂R with AT_{1a}R leads to cell surface translocation of B₂R.

8.7.1 Heterodimerization with AT_{1a}R promotes surface localization of B₂R

Several members of class I GPCRs, such as α_{1D}-AR (McCune *et al.*, 2000, Chalothorn *et al.*, 2002 and Hague *et al.*, 2004), α_{2C}-AR (Von Zastrow *et al.*, 1993), adenosine 2b receptor (Sitaraman *et al.*, 2002), and bitter-taste receptor (Chandrasekhar *et al.*, 2000) are known to be largely intracellular when expressed in heterologous system. Similarly, human B₂R, when overexpressed in BHK cells, was predominantly retained intracellularly with only a minor fraction reaching the plasma membrane (section 3.3.6.2). Effects of

homodimerization and heterodimerization on surface localization of GPCRs have been observed in some cases. It has been suggested that homo or heterodimerization may be a pre-requisite for certain GPCRs to be exported to the plasma membrane. In most cases, heterodimerization of two members of the same subfamily i.e. different subtypes has been shown to drive this phenomenon. The only published example where surface localization of a GPCR is driven by a distantly related GPCR is heterodimerization of mouse olfactory receptor with β 2-adrenergic receptor (Hague *et al.*, 2005). It is interesting that several other membrane proteins also need oligomerization for their cell surface targeting. These include shaker potassium channels (Gu *et al.*, 2003), the AMPA receptor (Dubel *et al.*, 2004), the transforming growth factor β receptor (De Crescenzo *et al.*, 2004), and the insulin receptor (Wu *et al.*, 2004). Similarly, coexpression of B₂R and AT_{1a}R in BHK cells resulted in cell surface localization of B₂R as revealed by confocal microscopy and ligand binding assay. Interestingly, coexpression of angiotensin II type 2 receptor (AT₂R) did not affect the surface expression of B₂R, revealing a specific interaction between AT_{1a}R and B₂R. Cointernalization of B₂R and AT_{1a}R after selective agonist stimulation was also observed which indicates that these two receptors remain associated during the endocytosis pathway. Additionally, colocalization of B₂R and AT_{1a}R in human foreskin fibroblast cells, which express both the receptors, was also observed. It supports the possibility that heterodimerization of these two receptors may result in surface localization of B₂R in native tissues as well. Infact, heterodimerization of these receptors has been shown to occur in platelets and omental vessels from preeclamptic women (Abdalla *et al.*, 2002). AT_{1a}R reversibly aggregates due to oxidative stress in normotensive pregnant women and signalling is blocked. However, AT_{1a}R-B₂R heterodimerization confers the AT_{1a}R resistance to inactivation by oxidative stress and maintains angiotensin II signalling in preeclampsia. This demonstrates a regulatory role of B₂R-AT_{1a}R heterodimerization under physiological condition. Although the mechanistic basis of GPCR dimerization is not well understood, recent studies suggest that the oligomerization of proteins may increase the avidity for dimeric molecular chaperones such as those of the 14-3-3 family. These chaperones mediate the release of maturing proteins from the ER (Yuan *et al.*, 2003). Surface translocation of B₂R as a result of heterodimerization, supports the hypothesis that for some GPCRs (such as

olfactory receptors and B₂R), interaction with other specific receptors is required for cell surface localization.

8.7.2 Isolation of B₂R-AT_{1a}R heterodimer complex

By employing a two-step affinity purification, it was possible to isolate the heterodimer complex of B₂R-AT_{1a}R (as shown by SDS-PAGE, analytical gel filtration and ligand binding analysis, see result section 6.5). Unfortunately, this heterodimer complex tends to dissociate over time when stored at 4°C. One of the problems associated with purification of membrane proteins is delipidation. Previous reports have shown that increased delipidation of the cytochrome bc₁ complex leads to a gradual decrease in activity up to complete loss of function and destabilization of this multisubunit complex (Yu *et al.*, 1980). Therefore, one can imagine that significant loss of some particular lipids, which are necessary to maintain the heterodimer complex, during purification steps, may lead to its dissociation over time. Additionally, choice of detergent is also crucial for long-term stability of membrane protein complexes. Therefore, addition of certain lipids during purification and screening a range of detergents for purification may be of particular importance for the long-term stability of this complex.

8.8 Production and isolation of AT_{1a}R

Human AT_{1a}R is one of the most studied GPCRs for its functional properties. However, there is no published report attempting heterologous production of this receptor for large-scale isolation. Although, several small molecule antagonist drugs acting on this receptor are already available (e.g. Losartan, Valsartan, Irbesartan and Candesartan), structural studies are mandatory in order to understand the ligand binding and receptor activation mechanism in detail. Therefore, this receptor was heterologously produced using *Pichia pastoris*, baculovirus system and SFV system. Expression level of AT_{1a}R in *Pichia pastoris* was high (3-4 mg/liter culture). A positive effect of biotinylation domain on receptor expression was observed (see section 7.1.4). Similar effect of biotinylation domain on GPCR expression in *Pichia* has already been found (Helmut Reiländer, personal communication and Grünewald *et al.*, 1996). Large-scale cultures in shake

flasks yielded milligram quantities of this receptor in membranes. The recombinant receptor showed similar ligand binding affinity to angiotensin II as the AT_{1a}R in native tissues. More importantly, the recombinant receptor was successfully isolated in homogenous form and it was stable at 4°C for at least two weeks (gel filtration analysis). Therefore, it was used for 3-D crystallization attempts. In order to stabilize the recombinant AT_{1a}R, angiotensin II was added during solubilization and purification. As discussed before, addition of colored ligands during receptor purification provides a useful tool to identify crystals in the crystallization drops. Use of fluorescein labeled angiotensin revealed that the ligand (angiotensin II) remains bound to the purified receptor. As fluorescent angiotensin II is inexpensive and easily available, it can also be used during large-scale purification of the recombinant receptor.

It should be possible to produce large amounts of recombinant receptor in *Pichia* by using fermentors. It has already been done successfully for the β-2 adrenergic receptor (Christoph Reinhart, PhD thesis) and the endothelin-b receptor (Schiller *et al.*, 2002). Angiotensin II is a small peptide with no repeated amino acids in its sequence. Therefore, it is a good candidate for solid-state NMR studies. In this case, a single uniformly labeled (¹³C/¹⁵N angiotensin II) peptide (as compared to three different variants of bradykinin) should provide sufficient information that is required to generate a model of the receptor bound conformation of angiotensin II.

Although AT_{1a}R could be successfully expressed and isolated from *Pichia*, for reasons of comparison, it was also produced in BHK cells and Sf9 cells. Moderate expression levels for recombinant AT_{1a}R were obtained in BHK cells and Sf9 cells. The binding affinity of the recombinant receptor in these cells was also comparable to that in native tissues. Interestingly, out of the three GPCRs produced in BHK cells during this study, only this receptor was glycosylated and was localized to the cell surface. Similar to *Pichia*, the recombinant receptor was successfully isolated from BHK and Sf9 cells. However, the purified receptor from BHK cells showed proteolytic degradation when stored at 4°C. It may be due to copurification of some protease, which leads to the receptor degradation over time. However, this problem was not addressed in detail as

large amounts of recombinant receptor could successfully be purified from *Pichia*. The stability of recombinant receptor from Sf9 cells has not been tested.

8.9 Production, characterization and isolation of NmU₂R

Two GPCR subtypes for neuromedin U in human were recently discovered (Raddatz *et al.*, 2000). Due to several physiological roles of neuromedin U (e.g. smooth muscle contraction, blood pressure control, stress response, feeding and energy homeostasis), these receptors are considered to be important drug targets. The two subtypes of this receptor share approximately 45-50% sequence homology. During this study, human NmU₂R was produced in *Pichia pastoris* and BHK cells. In both systems, moderate expression levels of this receptor were achieved. However, during its production in the SFV system, only BHK cells were tested so far. It would be interesting to compare its expression level in other cell lines such as HEK-293, CHO-K1 or COS-7. The recombinant NmU₂R produced in *Pichia* and BHK cells showed a similar ligand binding affinity to that of native tissues. Like recombinant B₂R, this receptor was also glycosylated in *Pichia* but not in BHK cells. It was possible to purify the recombinant receptor using affinity chromatography. Purified receptor from BHK cells revealed mainly homogenous population on gel filtration analysis. However, as mentioned before, the SFV system is not suited for large-scale production of the receptor (especially for those receptors, which have low expression levels) on a routine basis.

Expression of this receptor in baculovirus system was not tested. It has been found that the expression level of NmU₁R in insect cells is low (Hongyang Xia, personal communication). As mentioned before, NmU₁R and NmU₂R share high sequence similarity and bind to the ligand (NmU) with almost the same affinity. Therefore, in my opinion expression of NmU₂R may be similar to NmU₁R in insect cells. Therefore, further attempts to improve the expression and purification of this receptor from *Pichia* should be made.

8.10 Effect of DMSO on functional expression of recombinant receptors

Positive effect of DMSO on functional expression of recombinant GPCRs in *Pichia* has been reported earlier (Alexandra Ivanovic, PhD thesis). During this study also, positive effect of DMSO on expression level of three different recombinant GPCRs in *Pichia* was observed. Interestingly, expression of recombinant receptors in BHK cells was also increased by the addition of DMSO in the culture medium. However, no such effect was observed in Sf9 cells. The exact reason for this DMSO effect is not known yet. However, a previous study in *S. cerevisiae* showed that in response to DMSO, phospholipid biosynthesis was significantly increased via up-regulation of INO1 and OPI3 genes (Murata *et al.*, 2003). It was also observed that DMSO treatment leads to membrane proliferation and affects membrane integrity. Therefore, increased membrane permeability and altered protein-lipid interactions may be responsible for the effect of DMSO on the expression of recombinant receptors.

8.11 Future perspectives

During the course of this study, successful production and isolation strategies for recombinant B₂R have been established. The next steps should include long-term stabilization of the receptor, reconstituting the complex of B₂R with its interacting partner(s) to increase the polar surface area and to fix the receptor in one conformation. In this context, copurification of recombinant B₂R and endogenous SHP-2 from insect cells provides a unique opportunity. In comparison to overexpressed B₂R, the endogenous pool of SHP-2 in insect cells may be limited. Therefore, coexpression of recombinant B₂R and recombinant SHP-2 should be tested. By using two different tags on B₂R and SHP-2 respectively, it should be possible to isolate the complex of recombinant B₂R and recombinant SHP-2. Additionally, further attempts to stabilize the B₂R-AT_{1a}R heterodimer complex and B₂R-beta arrestin complex should be made. These complexes represent a physiologically relevant signalling state of B₂R and structural information on these complexes should lead to a better understanding of GPCR signalling mechanism. Interestingly, coexpression of AT_{1a}R with B₂R drives the later to the cell surface. When expressed individually, B₂R recycles back to the cell surface after agonist

induced endocytosis while the AT_{1a}R undergoes ubiquitination and degradation. It will be interesting to see how the ubiquitination machinery responds to this heterodimer complex. Also, the problem of proteolytic cleavage of B₂R in insect cells should be addressed further. The possibilities to overcome this problem include testing different protease inhibitors in the culture medium and to identify the cleavage site and to remove it by site-directed mutagenesis. Another problem associated with the baculovirus system is incomplete biotinylation of the biotinylation domain. To circumvent this problem, one can try to use constructs with strep II tag. It will also be interesting to coexpress B₂R in *Pichia* with G proteins, molecular chaperones or AT_{1a}R, in order to increase functional production level. Coexpression of G proteins with neurokinin receptor has already been tested in *Schizosaccharomyces pombe* (Arkininstall *et al.*, 1995). In order to get the receptor bound conformation of bradykinin, further solid-state NMR studies have to be done. This information may provide some new insight into the binding of endogenous ligand bradykinin to its cognate receptor. The receptor bound conformation of bradykinin can be used to design more potent and specific bradykinin analogs acting as therapeutic molecules on B₂R.

The recombinant AT_{1a}R was produced at high levels in *Pichia pastoris* and could be successfully purified. One of the future goals should be to use a fermentor for large-scale production of this receptor. It should be possible to get milligram quantities of the purified receptor and it can be used for crystallization trials and solid-state NMR studies. A previous report indicates a strong interaction of β -arrestin with AT_{1a}R (Wei *et al.*, 2004). Therefore, *in vitro* reconstitution of receptor- β -arrestin complex should also be tested.

Although the recombinant NmU₂R was expressed at moderate levels in *Pichia* and BHK cells, it could be easily purified. Therefore, a major focus should be on increasing the expression level of this receptor. As the endogenous peptide ligand (NmU-8) of NmU₂R binds the receptor with high affinity, it represents a potential candidate for solid-state NMR analysis. NmU₂R was identified only recently (Raddatz *et al.*, 2000) and only little is known about its interaction with other proteins (such as its homo and heterodimerization). It will be interesting to identify its interaction partners and to study the roles of these interactions in NmU₂R regulated signalling mechanisms.

References

AbdAlla, S., Zaki, E., Lothar, H., & Quitterer, U. (1999) Involvement of the amino terminus of the B(2) receptor in agonist-induced receptor dimerization. *J Biol Chem.* 274, 26079-26084.

AbdAlla, S., Lothar, H., el Massiery, A., & Quitterer, U. (2001) Increased AT(1) receptor heterodimers in preeclampsia mediate enhanced angiotensin II responsiveness. *Nat Med.* 7, 1003-1009.

AbdAlla, S., Lothar, H., Langer, A., el Faramawy, Y., & Quitterer, U. (2004) Factor XIIIa transglutaminase crosslinks AT1 receptor dimers of monocytes at the onset of atherosclerosis. *Cell* 119, 343-54.

Akermoun, M., Koglin, M., Zvalova-Iooss, D., Folschweiller, N., Dowell, S.J., & Gearing, K.L. (2005) Characterization of 16 human G protein-coupled receptors expressed in baculovirus-infected insect cells. *Protein Expr Purif.* 44, 65-74.

Altenbach, C., Cai, K., Khorana, H.G., & Hubbell, W.L. (1999) Structural features and light-dependent changes in the sequence 306-322 extending from helix VII to the palmitoylation sites in rhodopsin: A site- directed spin-labeling study. *Biochemistry* 38, 7931-7937.

Angers, S., Salahpour, A., & Bouvier, M. (2002) Dimerization: an emerging concept for G protein-coupled receptor ontogeny and function. *Annu Rev Pharmacol Toxicol.* 42, 409-435.

- Arkininstall, S., Edgerton, M., Payton, M., & Maundrell, K.** (1995) Co-expression of the neurokinin NK2 receptor and G-protein components in the fission yeast *Schizosaccharomyces pombe*. *FEBS Lett.* 375, 183-187.
- Arora, A., Abildgaard, F., Bushweller, J.H., & Tamm, L.K.** (2001) Structure of outer membrane protein A transmembrane domain by NMR spectroscopy. *Nat Struct Biol.* 8, 334-338.
- Ayoub, M.A., Couturier, C., Lucas-Meunier, E., Angers, S., Fossier, P., Bouvier, M., & Jockers, R.** (2002) Monitoring of ligand-independent dimerization and ligand-induced conformational changes of melatonin receptors in living cells by bioluminescence resonance energy transfer. *J Biol Chem.* 277, 21522-21528.
- Bockaert, J., & Pin, J.P.** (1999) Molecular tinkering of G protein-coupled receptors: an evolutionary success. *EMBO J.* 18, 1723-1729.
- Ballesteros, J.A., Jensen, A.D., Liapakis, G., Rasmussen, S.G., Shi, L., Gether, U., & Javitch, J.A.** (2001) Activation of the beta 2-adrenergic receptor involves disruption of an ionic lock between the cytoplasmic ends of transmembrane segments 3 and 6. *J Biol Chem.* 276, 29171-29177.
- Brady, A.E., & Limbird, L.E.** (2002) G protein-coupled receptor interacting proteins: emerging roles in localization and signal transduction. *Cell Signal.* 14, 297-309.
- Bouvier, M.** (2001) Oligomerization of G-protein-coupled transmitter receptors. *Nat Rev Neurosci.* 4, 274-286.
- Bax, A.** (1989) Two-dimensional NMR and protein structure. *Annu Rev Biochem.* 58, 223-256.

Blaukat, A. (2003) Structure and signalling pathways of kinin receptors. *Andrologia* 35, 17-23.

Blaukat, A., Pizard, A., Breit, A., Wernstedt, C., Alhenc-Gelas, F., Muller-Esterl, W., & Dikic, I. (2001) Determination of bradykinin B2 receptor in vivo phosphorylation sites and their role in receptor function. *J Biol Chem.* 276, 40431-40440.

Duchene, J., Schanstra, J.P., Pecher, C., Pizard, A., Susini, C., Esteve, J.P., Bascands, J.L., & Girolami, J.P. (2002) A novel protein-protein interaction between a G protein-coupled receptor and the phosphatase SHP-2 is involved in bradykinin-induced inhibition of cell proliferation. *J Biol Chem.* 277, 40375-40383.

Brighton, P.J., Szekeres, P.G., & Willars, G.B. (2004) Neuromedin U and its receptors: structure, function, and physiological roles. *Pharmacol Rev.* 56, 231-248.

Bachvarov, D.R., Houle, S., Bachvarova, M., Bouthillier, J., Adam, A., & Marceau, F. (2001) Bradykinin B(2) receptor endocytosis, recycling, and down-regulation assessed using green fluorescent protein conjugates. *J Pharmacol Exp Ther.* 297, 19-26.

Baenziger, N.L., Jong, Y.J., Yocum, S.A., Dalemar, L.R., Wilhelm, B., Vavrek, R., & Stewart, J.M. (1992) Diversity of B2 bradykinin receptors with nanomolar affinity expressed in passaged IMR90 human lung fibroblasts. *Eur J Cell Biol.* 58, 71-80.

Berger, I., Fitzgerald, D.J., & Richmond, T.J. (2004) Baculovirus expression system for heterologous multiprotein complexes. *Nat Biotechnol.* 12, 1583-1587.

Beukers, M.W., Klaassen, C.H., De Grip, W.J., Verzijl, D., Timmerman, H., & Leurs, R. (1997) Heterologous expression of rat epitope-tagged histamine H2 receptors in insect Sf9 cells. *Br J Pharmacol.* 122, 867-874.

- Binda, C., Newton-Vinson, P., Hubalek, F., Edmondson, D.E., & Mattevi, A.** (2002) Structure of human monoamine oxidase B, a drug target for the treatment of neurological disorders. *Nat Struct Biol.* 9, 22-26.
- Blaukat, A., Herzer, K., Schroeder, C., Bachmann, M., Nash, N., & Muller-Esterl, W.** (1999) Overexpression and functional characterization of kinin receptors reveal subtype-specific phosphorylation. *Biochemistry* 38, 1300-1309.
- Blaukat, A., Micke, P., Kalatskaya, I., Faussner, A., & Muller-Esterl, W.** (2003) Downregulation of bradykinin B2 receptor in human fibroblasts during prolonged agonist exposure. *Am J Physiol Heart Circ Physiol.* 284, 1909-1916.
- Burger, K., Gimpl, G., & Fahrenholz, F.** (2000) Regulation of receptor function by cholesterol. *Cell Mol Life Sci.* 57, 1577-1592.
- Butkerait, P., Zheng, Y., Hallak, H., Graham, T.E., Miller, H.A., Burris, K.D., Molinoff, P.B., & Manning, D.R.** (1995) Expression of the human 5-hydroxytryptamine_{1A} receptor in Sf9 cells. Reconstitution of a coupled phenotype by co-expression of mammalian G protein subunits. *J Biol Chem.* 270, 18691-18699.
- Butz, J.A., Niebauer, R.T., & Robinson, A.S.** (2003) Co-expression of molecular chaperones does not improve the heterologous expression of mammalian G-protein coupled receptor expression in yeast. *Biotechnol Bioeng.* 84, 292-304.
- Cayla, C., Merino, V.F., Cabrini, D.A., Silva, J.A. Jr., Pesquero, J.B., & Bader, M.** (2002) Structure of the mammalian kinin receptor gene locus. *Int Immunopharmacol.* 2, 1721-1727.
- Cereghino, J.L., & Cregg, J.M.** (2000) Heterologous protein expression in the methylotrophic yeast *Pichia pastoris*. *FEMS Microbiol Rev.* 24, 45-66.

- Chalothorn, D., McCune, D.F., Edelman, S.E., Garcia-Cazarin, M.L., Tsujimoto, G., & Piascik, M.T.** (2002) Differences in the cellular localization and agonist-mediated internalization properties of the alpha(1)-adrenoceptor subtypes. *Mol Pharmacol.* 61, 1008-1016.
- Chandrashekar, J., Mueller, K.L., Hoon, M.A., Adler, E., Feng, L., Guo, W., & Zuker, C.S., & Ryba, N.J.** (2000) T2Rs function as bitter taste receptors. *Cell* 100, 703-711.
- Chang, R.S., Lotti, V.J., & Keegan, M.E.** (1982) Inactivation of angiotensin II receptors in bovine adrenal cortex by dithiothreitol: further evidence for the essential nature of disulfide bonds. *Biochem Pharmacol.* 31, 1903-1906.
- Columbus, L., & Hubbell, W.L.** (2002) A new spin on protein dynamics. *Trends Biochem Sci.* 27, 288-95.
- Crawford, K.W., Frey, E.A., & Cote, T.E.** (1992) Angiotensin II receptor recognized by Dup753 regulates two distinct guanine nucleotide-binding protein signaling pathways. *Mol Pharmacol.* 41, 154-162.
- Cregg, J.M., Vedvick, T.S., & Raschke, W.C.** (1993) Recent advances in the expression of foreign genes in *Pichia pastoris*. *Biotechnology (N Y)* 11, 905-910.
- Cregg, J.M., Cereghino, J.L., Shi, J., & Higgins, D.R.** (2000) Recombinant protein expression in *Pichia pastoris*. *Mol Biotechnol.* 16, 23-52.
- Cronan, J.E. Jr.** (1990) Biotination of proteins in vivo. A post-translational modification to label, purify, and study proteins. *J Biol Chem.* 265, 10327-10333.

Cui, T., Nakagami, H., Iwai, M., Takeda, Y., Shiuchi, T., Tamura, K., Daviet, L., & Horiuchi, M. (2000) ATRAP, novel AT1 receptor associated protein, enhances internalization of AT1 receptor and inhibits vascular smooth muscle cell growth. *Biochem Biophys Res Commun.* 279, 938-941.

De Crescenzo, G., Pham, P.L., Durocher, Y., Chao, H., & O'Connor-McCourt, M.D. (2004) Enhancement of the antagonistic potency of transforming growth factor-beta receptor extracellular domains by coiled coil-induced homo- and heterodimerization. *J Biol Chem.* 279, 26013-26018.

de Gasparo, M., Catt, K.J., Inagami, T., Wright, J.W., & Unger, T. (2000) International union of pharmacology. XXIII. The angiotensin II receptors. *Pharmacol Rev.* 52, 415-72.

de Jong, L.A., Grunewald, S., Franke, J.P., Uges, D.R., Bischoff, R. (2004) Purification and characterization of the recombinant human dopamine D2S receptor from *Pichia pastoris*. *Protein Expr Purif.* 33, 176-184.

Demene, H., Granier, S., Muller, D., Guillon, G., Dufour, M.N., Delsuc, M.A., Hibert, M., Pascal, R., & Mendre, C. (2003) Active peptidic mimics of the second intracellular loop of the V(1A) vasopressin receptor are structurally related to the second intracellular rhodopsin loop: a combined 1H NMR and biochemical study. *Biochemistry* 42, 8204-8213.

De Vries, L., Zheng, B., Fischer, T., Elenko, E., & Farquhar, M.G. (2000) The regulator of G protein signaling family. *Annu Rev Pharmacol Toxicol.* 40, 235-71.

Dubel, S.J., Altier, C., Chaumont, S., Lory, P., Bourinet, E., & Nargeot, J. (2004) Plasma membrane expression of T-type calcium channel alpha(1) subunits is modulated by high voltage-activated auxiliary subunits. *J Biol Chem.* 279, 29263-29269.

Duvernay, M.T., Filipeanu, C.M., & Wu. G. (2005) The regulatory mechanisms of export trafficking of G protein-coupled receptors. *Cell Signal.* 17, 1457-1465.

Elling, C.E., Schwartz, T.W. (1996) Connectivity and orientation of the seven helical bundle in the tachykinin NK-1 receptor probed by zinc site engineering. *EMBO J.* 15, 6213-6219.

Estephan, R., Englander, J., Arshava, B., Samples, K.L., Becker, J.M., & Naider, F. (2005) Biosynthesis and NMR analysis of a 73-residue domain of a *Saccharomyces cerevisiae* G protein-coupled receptor. *Biochemistry* 44, 11795-11810.

Feng, W., Cai, J., Pierce, W.M. Jr., & Song, Z.H. (2002) Expression of CB2 cannabinoid receptor in *Pichia pastoris*. *Protein Expr Purif.* 26, 496-505.

Ferguson, S.S. (2001) Evolving concepts in G protein-coupled receptor endocytosis: the role in receptor desensitization and signaling. *Pharmacol Rev.* 53, 1-24.

Gilman, A.G. (1987) G proteins: transducers of receptor-generated signals. *Annu Rev Biochem.* 56, 615-49.

Gimpl, G., Klein, U., Reilander, H., & Fahrenholz, F. (1995) Expression of the human oxytocin receptor in baculovirus-infected insect cells: high-affinity binding is induced by a cholesterol-cyclodextrin complex. *Biochemistry* 34, 13794-13801.

- George, S.R., Fan, T., Xie, Z., Tse, R., Tam, V., Varghese, G., & O'Dowd, B.F.** (2000) Oligomerization of mu- and delta-opioid receptors. Generation of novel functional properties. *J Biol Chem.* 275, 26128-26135.
- George, S.R., O'Dowd, B.F., & Lee, S.P.** (2002) G-protein-coupled receptor oligomerization and its potential for drug discovery. *Nat Rev Drug Discov.* 10, 808-820.
- Girvin, M.E., Rastogi, V.K., Abildgaard, F., Markley, J.L., Fillingame, R.H.** (1998) Solution structure of the transmembrane H⁺-transporting subunit c of the F1F0 ATP synthase. *Biochemistry* 37, 8817-8824.
- Glass, M., & Northup, J.K.** (1999) Agonist selective regulation of G proteins by cannabinoid CB(1) and CB(2) receptors. *Mol Pharmacol.* 56, 1362-1369.
- Grace, C.R., Perrin, M.H., DiGruccio, M.R., Miller, C.L., Rivier, J.E., Vale, W.W., & Riek, R.** (2004) NMR structure and peptide hormone binding site of the first Extracellular domain of a type B1 G protein-coupled receptor. *Proc Natl Acad Sci U S A* 101, 12836-12841.
- Grisshammer, R., Little, J., & Aharony, D.** (1994) Expression of rat NK-2 (neurokinin A) receptor in E. coli. *Receptors Channels* 2, 295-302.
- Grunewald, S., Haase, W., Reilander, H., & Michel, H.** (1996) Glycosylation, palmitoylation, and localization of the human D2S receptor in baculovirus-infected insect cells. *Biochemistry* 35, 15149-15161.
- Grunewald, S., Haase, W., Molsberger, E., Michel, H., & Reilander, H.** (2004) Production of the human D2S receptor in the methylotrophic yeast P. pastoris. *Receptors Channels* 10, 37-50.

- Gu, C., Jan, Y.N., & Jan, L.Y.** (2003) A conserved domain in axonal targeting of Kv1 (Shaker) voltage-gated potassium channels. *Science* 301, 646-649.
- Guo, D.F., Furuta, H., Mizukoshi, M., & Inagami, T.** (1994) The genomic organization of human angiotensin II type 1 receptor. *Biochem Biophys Res Commun.* 200, 313-319.
- Gutierrez, J., Kremer, L., Zaballos, A., Goya, I., Martinez, A. C., & Marquez, G.** (2004) Analysis of post-translational CCR8 modifications and their influence on receptor activity. *J Biol Chem.* 279, 14726-14733.
- Hague, C., Uberti, M.A., Chen, Z., Hall, R.A., & Minneman, K.P.** (2004) Cell surface expression of alpha1D-adrenergic receptors is controlled by heterodimerization with alpha1B-adrenergic receptors. *J Biol Chem.* 279, 15541-15549.
- Hague, C., Uberti, M.A., Chen, Z., Bush, C.F., Jones, S.V., Ressler, K.J., Hall, R.A., & Minneman, K.P.** (2004) Olfactory receptor surface expression is driven by association with the beta2-adrenergic receptor. *Proc Natl Acad Sci U S A* 101, 13672-13676.
- Hampe, W., Voss, R.H., Haase, W., Boege, F., Michel, H., & Reilander, H.** (2000) Engineering of a proteolytically stable human beta 2-adrenergic receptor/maltose-binding protein fusion and production of the chimeric protein in Escherichia coli and baculovirus-infected insect cells. *J Biotechnol.* 77, 219-234.
- Hanahan, D., Jessee, J., & Bloom, F.R.** (1991) Plasmid transformation of Escherichia coli and other bacteria. *Methods Enzymol.* 204, 63-113.
- Hanninen, A.L., Bamford, D.H., & Grisshammer, R.** (1994). Expression in Escherichia coli of rat neurotensin receptor fused to membrane proteins from the membrane-containing bacteriophage PRD1. *Biol Chem Hoppe Seyler.* 375, 833-836.

Hassaine, G., Wagner, R., Kempf, J., Cherouati, N., Hassaine, N., Prual, C., Andre, N., Reinhart, C., Pattus, F., & Lundstrom, K. (2005) Semliki Forest virus vectors for overexpression of 101 G protein-coupled receptors in mammalian host cells. *Protein Expr Purif.* (In Press).

Hepler, J.R. and Gilman, G.A. (1992) G proteins. *Trends Biochem Sci* **17**, 383–387

Herzig, M.C., & Leeb-Lundberg, L.M. (1995) The agonist binding site on the bovine bradykinin B2 receptor is adjacent to a sulfhydryl and is differentiated from the antagonist binding site by chemical cross-linking. *J Biol Chem.* **270**, 20591-20598.

Herzog, H., Munch, G., & Shine, J. (1994) Human neuropeptide Y1 receptor expressed in *Escherichia coli* retains its pharmacological properties. *DNA Cell Biol.*, **12**, 1221-1225.

Higgins, M.K., Demir, M., & Tate, C.G. (2003) Calnexin co-expression and the use of weaker promoters increase the expression of correctly assembled Shaker potassium channel in insect cells. *Biochim Biophys Acta* **17**, 124-32.

Hinni, C., Bottomley, S.P., Duffy, E.J., Hemmings, B.A., & Stone, S.R. (1998) Expression and purification of the human thrombin receptor. *Protein Expr Purif.* **13**, 9-15.

Howard, A.D., Wang, R., Pong, S.S., Mellin, T.N., Strack, A., Guan, X.M., Zeng, Z., Williams, D.L. Jr., Feighner, S.D., Nunes, C.N., Murphy, B., Stair, J.N., Yu, H., Jiang, Q., Clements, M.K., Tan, C.P., McKee, K.K., Hreniuk, D.L., McDonald, T.P., Lynch, K.R., Evans, J.F., Austin, C.P., Caskey, C.T., Van der Ploeg, L.H., & Liu, Q. (2000) Identification of receptors for neuromedin U and its role in feeding. *Nature* **406**, 70-74.

- Hunyady, L., Bor, M., Balla, T., & Catt, K.J.** (1994) Identification of a cytoplasmic Ser-Thr-Leu motif that determines agonist-induced internalization of the AT1 angiotensin receptor. *J Biol Chem.* 269, 31378-31382.
- Hulme, E.C. & Curtis, C.A.** (1998) Purification of recombinant M1 muscarinic acetylcholine receptor. *Biochem Soc Trans.* 26, 361.
- Inagami, T., Iwai, N., Sasaki, K., Yamano, Y., Bardhan, S., Chaki, S., Guo, D.F., & Furuta, H.** (1992) Cloning, expression and regulation of angiotensin II receptors. *J Hypertens.* 10, 713-716.
- Issafras, H., Angers, S., Bulenger, S., Blanpain, C., Parmentier, M., Labbe-Jullie, C., Bouvier, M., & Marullo, S.** (2002) Constitutive agonist-independent CCR5 oligomerization and antibody-mediated clustering occurring at physiological levels of receptors. *J Biol Chem.* 277, 34666-34673.
- Javitch, J.A., Kaback, J., Li, X., & Karlin, A.** (1994) Expression and characterization of human dopamine D2 receptor in baculovirus-infected insect cells. *J Recept Res.* 14, 99-117.
- Jayadev, S., Smith, R.D., Jagadeesh, G., Baukal, A.J., Hunyady, L., & Catt, K.J.** (1999) N-linked glycosylation is required for optimal AT1a angiotensin receptor expression in COS-7 cells. *Endocrinology* 140, 2010-2017.
- Jordan, B.A., & Devi, L.A.** (1999) G-protein-coupled receptor heterodimerization modulates receptor function. *Nature* 397, 697-700.
- Ju, H., Venema, V.J., Marrero, M.B., & Venema, R.C.** (1998) Inhibitory interactions of the bradykinin B2 receptor with endothelial nitric-oxide synthase. *J Biol Chem.* 273, 24025-24029.

- Kang, D.S., Ryberg, K., Morgelin, M., & Leeb-Lundberg, L.M.** (2004) Spontaneous formation of a proteolytic B1 and B2 bradykinin receptor complex with enhanced signaling capacity. *J Biol Chem.* 279, 22102-22107.
- Klein-Seetharaman, J., Reeves, P.J., Loewen, M.C., Getmanova, E.V., Chung, J., Schwalbe, H., Wright, P.E., & Khorana, H.G.** (2002) Solution NMR spectroscopy of [α - ^{15}N]lysine-labeled rhodopsin: The single peak observed in both conventional and TROSY-type HSQC spectra is ascribed to Lys-339 in the carboxyl-terminal peptide sequence. *Proc Natl Acad Sci U S A* 99, 3452-3457.
- Klein-Seetharaman, J., Yanamala, N.V., Javed, F., Reeves, P.J., Getmanova, E.V., Loewen, M.C., Schwalbe, H., & Khorana, H.G.** (2004) Differential dynamics in the G protein-coupled receptor rhodopsin revealed by solution NMR. *Proc Natl Acad Sci U S A* 101, 3409-3413.
- Kule, C.E., Karoor, V., Day, J.N., Thomas, W.G., Baker, K.M., Dinh, D., Acker, K.A., & Booz, G.W.** (2004) Agonist-dependent internalization of the angiotensin II type one receptor (AT1): role of C-terminus phosphorylation in recruitment of beta-arrestins. *Regul Pept.* 120, 141-148.
- Lagane, B., Gaibelet, G., Meilhoc, E., Masson, J.M., Cezanne, L., & Lopez, A.** (2000) Role of sterols in modulating the human mu-opioid receptor function in *Saccharomyces cerevisiae*. *J Biol Chem.* 275, 33197-33200.
- Lanctot, P.M., Leclerc, P.C., Escher, E., Leduc, R., & Guillemette, G.** (1999) Role of N-glycosylation in the expression and functional properties of human AT1 receptor. *Biochemistry* 38, 8621-8627.

- Lawler, O.A., Miggin, S.M., & Kinsella, B.T.** (2001) Protein kinase A-mediated phosphorylation of serine 357 of the mouse prostacyclin receptor regulates its coupling to G(s)-, to G(i)-, and to G(q)-coupled effector signaling. *J Biol Chem.* 276, 33596-33607.
- Leeb-Lundberg, L.M., Marceau, F., Muller-Esterl, W., Pettibone, D.J., & Zuraw, B.L.** (2005) International union of pharmacology. XLV. Classification of the kinin receptor family: from molecular mechanisms to pathophysiological consequences. *Pharmacol Rev.* 57, 27-77.
- Levac, B.A., O'Dowd, B.F., & George, S.R.** (2002) Oligomerization of opioid receptors: generation of novel signaling units. *Curr Opin Pharmacol.* 1, 76-81.
- Liljestrom, P., & Garoff, H.** (1991) A new generation of animal cell expression vectors based on the Semliki Forest virus replicon. *Biotechnology (N Y)* 12, 1356-1361.
- Luca, S., White, J.F., Sohal, A.K., Filippov, D.V., van Boom, J.H., Grisshammer, R., & Baldus, M.** (2003) The conformation of neurotensin bound to its G protein-coupled receptor. *Proc Natl Acad Sci U S A* 100, 10706-10711.
- Luca, S., Heise, H., Lange, A., & Baldus, M.** (2005) Investigation of ligand-receptor systems by high-resolution solid-state NMR: recent progress and perspectives. *Arch Pharm (Weinheim)* 338, 217-228.
- Lundstrom, K., Schweitzer, C., Rotmann, D., Hermann, D., Schneider, E.M., & Ehrengruber, M.U.** (2001) Semliki Forest virus vectors: efficient vehicles for in vitro and in vivo gene delivery. *FEBS Lett.* 504, 99-103.
- Lundstrom, K.** (2003) Semliki Forest virus vectors for rapid and high-level expression of integral membrane proteins. *Biochim Biophys Acta.* 1610, 90-96.
- Lundstrom, K.** (2005) Structural genomics of GPCRs. *Trends Biotechnol.* 23, 103-108.

Regoli, D., Barabe, J., & Park, W.K. (1977) Receptors for bradykinin in rabbit aortae. *Can J Physiol Pharmacol.* 55, 855-867.

Macauley-Patrick, S., Fazenda, M.L., McNeil, B., & Harvey, L.M. (2005) Heterologous protein production using the *Pichia pastoris* expression system. *Yeast* 22, 249-270.

MacKenzie, K.R., Prestegard, J.H., & Engelman, D.M. (1997) A transmembrane helix dimer: structure and implications. *Science* 276, 131-133.

Maeda, Y., Kuroki, R., Haase, W., Michel, H., & Reilander, H. (2004) Comparative analysis of high-affinity ligand binding and G protein coupling of the human CXCR1 chemokine receptor and of a CXCR1-Galpa fusion protein after heterologous production in baculovirus-infected insect cells. *Eur J Biochem.* 271, 1677-1689.

Margeta-Mitrovic, M., Jan, Y.N., & Jan, L.Y. (2000) A trafficking checkpoint controls GABA(B) receptor heterodimerization. *Neuron* 27, 97-106.

Marrero, M.B., Schieffer, B., Paxton, W.G., Heerdt, L., Berk, B.C., Delafontaine, P., & Bernstein, K.E. (1995) Direct stimulation of Jak/STAT pathway by the angiotensin II AT1 receptor. *Nature* 375, 247-250.

Massotte, D., Baroche, L., Simonin, F., Yu, L., Kieffer, B., & Pattus, F. (1997) Characterization of delta, kappa, and mu human opioid receptors overexpressed in baculovirus-infected insect cells. *J Biol Chem.* 272, 19987-19992.

Massotte, D. (2003) G protein-coupled receptor overexpression with the baculovirus-insect cell system: a tool for structural and functional studies. *Biochim Biophys Acta* 1610, 77-89.

- McCune, D.F., Edelmann, S.E., Olges, J.R., Post, G.R., Waldrop, B.A., Waugh, D.J., Perez, D.M., & Piascik, M.T.** (2000) Regulation of the cellular localization and signaling properties of the alpha(1B)- and alpha(1D)-adrenoceptors by agonists and inverse agonists. *Mol Pharmacol.* 57, 659-666.
- Michineau, S., Muller, L., Pizard, A., Alhenc-Gelas, F., & Rajerison, R.M.** (2004) N-linked glycosylation of the human bradykinin B2 receptor is required for optimal cell-surface expression and coupling. *Biol Chem.* 385, 49-57.
- Miggin, S.M., Lawler, O.A., & Kinsella, B.T.** (2002) Palmitoylation of the human prostacyclin receptor. Functional implications of palmitoylation and isoprenylation. *J Biol Chem.* 278, 6947-6958.
- Minamino, N., Kangawa, K., & Matsuo, H.** (1985) Neuromedin U-8 and U-25: novel uterus stimulating and hypertensive peptides identified in porcine spinal cord. *Biochem Biophys Res Commun.* 130, 1078-1085.
- Monastyrskaia, K., Goepfert, F., Hochstrasser, R., Acuna, G., Leighton, J., Pink, J.R., & Lundstrom, K.** (1999) Expression and intracellular localisation of odorant receptors in mammalian cell lines using Semliki Forest virus vectors. *J Recept Signal Transduct Res.* 19, 687-701.
- Mulheron, J.G., Casanas, S.J., Arthur, J.M., Garnovskaya, M.N., Gettys, T.W., & Raymond, J.R.** (1994) Human 5-HT1A receptor expressed in insect cells activates endogenous G(o)-like G protein(s). *J Biol Chem.* 269, 12954-12962.
- Murata, Y., Watanabe, T., Sato, M., Momose, Y., Nakahara, T., Oka, S., & Iwahashi, H.** (2003) Dimethyl sulfoxide exposure facilitates phospholipid biosynthesis and cellular membrane proliferation in yeast cells. *J Biol Chem.* 278, 33185-33193.

- Murphree, L.J., Marshall, M.A., Rieger, J.M., MacDonald, T.L., & Linden J.** (2002) Human A(2A) adenosine receptors: high-affinity agonist binding to receptor-G protein complexes containing Gbeta(4). *Mol Pharmacol.* 61, 455-462.
- Oakley, R.H., Laporte, S.A., Holt, J.A., Barak, L.S., & Caron, M.G.** (2001) Molecular determinants underlying the formation of stable intracellular G protein-coupled receptor-beta-arrestin complexes after receptor endocytosis. *J Biol Chem.* 276, 19452-19460.
- Ochsenbein, R.M., Inaebnit, S.P., Luethy, C.M., Wiesmann, U.N., Oetliker, O.H., & Honegger, U.E.** (1999) Differential regulation of bradykinin receptor density, intracellular Ca²⁺, and prostanoid release in skin and foreskin fibroblasts. Effects of cell density and interleukin-1alpha. *Br J Pharmacol.* 127, 583-589.
- Okada, T., & Palczewski, K.** (2001) Crystal structure of rhodopsin: implications for vision and beyond. *Curr Opin Struct Biol.* 4, 420-426.
- Olson, J.M., Kennedy, S.J., & Cabral, G.A.** (2003) Expression of the murine CB2 cannabinoid receptor using a recombinant Semliki Forest virus. *Biochem Pharmacol.* 65, 1931-1942.
- Nickenig, G., Geisen, G., Vetter, H., & Sachinidis, A.** (1997) Characterization of angiotensin receptors on human skin fibroblasts. *J Mol Med.* 75, 217-222.
- Ng, G.Y., Clark, J., Coulombe, N., Ethier, N., Hebert, T.E., Sullivan, R., Kargman, S., Chateauneuf, A., Tsukamoto, N., McDonald, T., Whiting, P., Mezey, E., Johnson, M.P., Liu, Q., Kolakowski, L.F. Jr., Evans, J.F., Bonner, T.I., & O'Neill, G.P.** (1999) Identification of a GABAB receptor subunit, gb2, required for functional GABAB receptor activity. *J Biol Chem.* 274, 7607-7610.

Palczewski, K., Kumasaka, T., Hori, T., Behnke, C.A., Motoshima, H., Fox, B.A., Le Trong, I., Teller, D.C., Okada, T., Stenkamp, R.E., Yamamoto, M., & Miyano, M. (2000) Crystal structure of rhodopsin: A G protein-coupled receptor. *Science* 289, 739-45.

Parker, E.M., Grisel, D.A., Iben, L.G., Nowak, H.P., Mahle, C.D., Yocca, F.D., & Gaughan, G.T. (1994) Characterization of human 5-HT1 receptors expressed in Sf9 insect cells. *Eur J Pharmacol.* 268, 43-53.

Pierce, K.L., Premont, R.T., & Lefkowitz, R.J. (2002) Seven-transmembrane receptors. *Nat Rev Mol Cell Biol.* 9, 639-50.

Pizard, A., Blaukat, A., Michineau, S., Dikic, I., Muller-Esterl, W., Alhenc-Gelas, F., & Rajerison, R.M. (2001). Palmitoylation of the human bradykinin B2 receptor influences ligand efficacy. *Biochemistry* 40, 15743-15751.

Pucadyil, T.J., Kalipatnapu, S., & Chattopadhyay, A. (2005) The serotonin1A receptor: a representative member of the serotonin receptor family. *Cell Mol Neurobiol.* 25, 553-80.

Raddatz, R., Wilson, A.E., Artymyshyn, R., Bonini, J.A., Borowsky, B., Boteju, L.W., Zhou, S., Kouranova, E.V., Nagorny, R., Guevarra, M.S., Dai, M., Lerman, G.S., Vaysse, P.J., Branchek, T.A., Gerald, C., Forray, C., & Adham, N. (2000) Identification and characterization of two neuromedin U receptors differentially expressed in peripheral tissues and the central nervous system. *J Biol Chem.* 275, 32452-32459.

Ratnala, V.R., Swarts, H.G., VanOostrum, J., Leurs, R., DeGroot, H.J., Bakker, R.A., & DeGrip WJ. (2004) Large-scale overproduction, functional purification and

ligand affinities of the His-tagged human histamine H1 receptor. *Eur J Biochem.* 271, 2636-2646.

Reed, L. J., & Muench, H. (1938) A simple method of estimating fifty percent endpoints. *Am. J. Hygiene.* 27, 493-497.

Rehbock, J., Chondromatidou, A., Miska, K., Buchinger, P., & Hermann, A. (1997) Evidence for bradykinin B2-receptors on cultured human decidua cells. *Immunopharmacology* 36, 135-141.

Reilander, H., Boege, F., Vasudevan, S., Maul, G., Hekman, M., Dees, C., Hampe, W., Helmreich, E.J., & Michel, H. (1991) Purification and functional characterization of the human beta 2-adrenergic receptor produced in baculovirus-infected insect cells. *FEBS Lett.* 282, 441-444.

Rios, C.D., Jordan, B.A., Gomes, I., & Devi, L.A. (2001) G-protein-coupled receptor dimerization: modulation of receptor function. *Pharmacol Ther.* 92, 71-87.

Robeva, A.S., Woodard, R., Luthin, D.R., Taylor, H.E., & Linden, J. (1996) Double tagging recombinant A1- and A2A-adenosine receptors with hexahistidine and the FLAG epitope. Development of an efficient generic protein purification procedure. *Biochem Pharmacol.* 51, 545-555.

Ross, E.M., & Wilkie, T.M. (2000) GTPase-activating proteins for heterotrimeric G proteins: regulators of G protein signaling (RGS) and RGS-like proteins. *Annu Rev Biochem.* 69, 795-827.

Salahpour, A., Angers, S., Mercier, J.F., Lagace, M., Marullo, S., & Bouvier, M. (2004) Homodimerization of the beta2-adrenergic receptor as a prerequisite for cell surface targeting. *J Biol Chem.* 279, 33390-33397.

Sarramegna, V., Demange, P., Milon, A., & Talmont, F. (2002) Optimizing functional versus total expression of the human mu-opioid receptor in *Pichia pastoris*. *Protein Expr Purif.* 24, 212-220.

Sarramegna, V., Talmont, F., Sereede, M., Milon, A., & Demange, P. (2002) Green fluorescent protein as a reporter of human mu-opioid receptor overexpression and localization in the methylotrophic yeast *Pichia pastoris*. *J Biotechnol.* 99, 23-39.

Sarramegna, V., Talmont, F., Demange, P., & Milon, A. (2003) Heterologous expression of G-protein-coupled receptors: comparison of expression systems from the standpoint of large-scale production and purification. *Cell Mol Life Sci.* 60, 1529-1546.

Scheer, A., Bjorklof, K., Cotecchia, S., & Lundstrom, K. (1999) Expression of the alpha 1b-adrenergic receptor and G protein subunits in mammalian cell lines using the Semliki Forest virus expression system. *J Recept Signal Transduct Res.* 19, 369-378.

Schiller, H., Haase, W., Molsberger, E., Janssen, P., Michel, H., & Reilander, H. (2000) The human ET(B) endothelin receptor heterologously produced in the methylotrophic yeast *Pichia pastoris* shows high-affinity binding and induction of stacked membranes. *Receptors Channels* 7, 93-107.

Sen, S., Jaakola, V.P., Heimo, H., Engstrom, M., Larjomaa, P., Scheinin, M., Lundstrom, K., & Goldman, A. (2003) Functional expression and direct visualization of the human alpha 2B -adrenergic receptor and alpha 2B -AR-green fluorescent fusion protein in mammalian cell using Semliki Forest virus vectors. *Protein Expr Purif.* 32, 265-275.

- Sen, S., Jaakola, V.P., Pirila, P., Finel, M., & Goldman, A.** (2005) Functional studies with membrane-bound and detergent-solubilized alpha2-adrenergic receptors expressed in Sf9 cells. *Biochim Biophys Acta.* 1712, 62-70.
- Simaan, M., Bedard-Goulet, S., Fessart, D., Gratton, J.P., & Laporte, S.A.** (2005) Dissociation of beta-arrestin from internalized bradykinin B2 receptor is necessary for receptor recycling and resensitization. *Cell Signal.* 17, 1074-1083.
- Simmen, U., Schweitzer, C., Burkard, W., Schaffner, W., & Lundstrom, K.** Hypericum perforatum inhibits the binding of mu- and kappa-opioid receptor expressed with the Semliki Forest virus system. *Pharm Acta Helv.* 73, 53-56.
- Sitaraman, S.V., Wang, L., Wong, M., Bruewer, M., Hobert, M., Yun, C.H., Merlin, D., & Madara, J.L.** (2002) The adenosine 2b receptor is recruited to the plasma membrane and associates with E3KARP and Ezrin upon agonist stimulation. *J Biol Chem.* 277, 33188-33195.
- Smerdou, C., & Liljestrom, P.** (1999) Two-helper RNA system for production of recombinant Semliki forest virus particles. *J Virol.* 73, 1092-1098.
- Stanasila, L., Massotte, D., Kieffer, B.L., & Pattus, F.** (1999) Expression of delta, kappa and mu human opioid receptors in Escherichia coli and reconstitution of the high-affinity state for agonist with heterotrimeric G proteins. *Eur J Biochem.* 260, 430-438.
- Takeda, S., Kadowaki, S., Haga, T., Takaesu, H., & Mitaku, S.** (2002) Identification of G protein-coupled receptor genes from the human genome sequence. *FEBS Lett.* 520, 97-101.
- Terrillon, S., Durroux, T., Mouillac, B., Breit, A., Ayoub, M.A., Taulan, M., Jockers, R., Barberis, C., & Bouvier, M.** (2003) Oxytocin and vasopressin V1a and V2 receptors

form constitutive homo- and heterodimers during biosynthesis. *Mol Endocrinol.* 17, 677-691.

Terrillon, S., Barberis, C., & Bouvier, M. (2004) Heterodimerization of V1a and V2 vasopressin receptors determines the interaction with beta-arrestin and their trafficking patterns. *Proc Natl Acad Sci U S A* 101, 1548-1553.

Tessier, D.C., Thomas, D.Y., Khouri, H.E., Laliberte, F., & Vernet, T. (1991) Enhanced secretion from insect cells of a foreign protein fused to the honeybee melittin signal peptide. *Gene* 98, 177-183.

Thirstrup, K., Elling, C.E., Hjorth, S.A., & Schwartz, T.W. (1996) Construction of a high affinity zinc switch in the kappa-opioid receptor. *J Biol Chem.* 271, 7875-7878.

Tian, C., Breyer, R.M., Kim, H.J., Karra, M.D., Friedman, D.B., Karpay, A., & Sanders, C.R. (2005) Solution NMR spectroscopy of the human vasopressin V2 receptor, a G protein-coupled receptor. *J Am Chem Soc.* 127, 8010-8011.

Tian, Y., Baukal, A.J., Sandberg, K., Bernstein, K.E., Balla, T., & Catt KJ. (1996) Properties of AT1a and AT1b angiotensin receptors expressed in adrenocortical Y-1 cells. *Am J Physiol.* 270, 831-839.

Tissir, F., Riviere, M., Guo, D.F., Tsuzuki, S., Inagami, T., Levan, G., Szpirer, J., & Szpirer, C. (1995) Localization of the genes encoding the three rat angiotensin II receptors, Agtr1a, Agtr1b, Agtr2, and the human AGTR2 receptor respectively to rat chromosomes 17q12, 2q24 and Xq34, and the human Xq22. *Cytogenet Cell Genet.* 71, 77-80.

Tornqvist, H., & Belfrage, P. (1976) Determination of protein in adipose tissue extracts. *J Lipid Res.* 17, 542-545.

Towbin, H., Staehelin, T., & Gordon, J. (1979) Electrophoretic transfer of proteins from polyacrylamide gels to nitrocellulose sheets: procedure and some applications. *Proc Natl Acad Sci U S A* 76, 4350-4354.

Tucker, J., & Grisshammer, R. (1996) Purification of a rat neurotensin receptor expressed in *Escherichia coli*. *Biochem J.* 317, 891-899.

Vasudevan, S., Reilander, H., Maul, G., Michel, H. (1991) Expression and cell membrane localization of rat M3 muscarinic acetylcholine receptor produced in Sf9 insect cells using the baculovirus system. *FEBS Lett.* 283, 52-56.

von Zastrow, M., Link, R., Daunt, D., Barsh, G., & Kobilka, B. (1993) Subtype-specific differences in the intracellular sorting of G protein-coupled receptors. *J Biol Chem.* 268, 763-766.

Waldhoer, M., Fong, J., Jones, R.M., Lunzer, M.M., Sharma, S.K., Kostenis, E., Portoghese, P.S., & Whistler, J.L. (2005) A heterodimer-selective agonist shows in vivo relevance of G protein-coupled receptor dimers. *Proc Natl Acad Sci U S A* 102, 9050-9055.

Wei, H., Ahn, S., Barnes, W.G., & Lefkowitz, R.J. (2004) Stable interaction between beta-arrestin 2 and angiotensin type 1A receptor is required for beta-arrestin 2-mediated activation of extracellular signal-regulated kinases 1 and 2. *J Biol Chem.* 279, 48255-48261.

Weiss, H.M., Haase, W., Michel, H., & Reilander, H. (1998) Comparative biochemical and pharmacological characterization of the mouse 5HT5A 5-hydroxytryptamine receptor and the human beta2-adrenergic receptor produced in the methylotrophic yeast *Pichia pastoris*. *Biochem J.* 330, 1137-1147.

- Weiss, H.M., & Grisshammer, R.** (2002) Purification and characterization of the human adenosine A(2a) receptor functionally expressed in Escherichia coli. *Eur J Biochem.* 269, 82-92.
- White, J.H., Wise, A., Main, M.J., Green, A., Fraser, N.J., Disney, G.H., Barnes, A.A., Emson, P., Foord, S.M., & Marshall, F.H.** (1998) Heterodimerization is required for the formation of a functional GABA(B) receptor. *Nature* 396, 679-82.
- Wise, A., Gearing, K., & Rees, S.** (2002) Target validation of G-protein coupled receptors. *Drug Discov Today* 15, 235-46.
- Wu, J.J., & Guidotti, G.** (2004) Proreceptor dimerization is required for insulin receptor post-translational processing. *J Biol Chem.* 279, 25765-25773.
- Yu, C.A., & Yu, L.** (1980) Structural role of phospholipids in ubiquinol-cytochrome c reductase. *Biochemistry* 19, 5715-5720.
- Yuan, H., Michelsen, K., & Schwappach, B.** (2003) 14-3-3 dimers probe the assembly status of multimeric membrane proteins. *Curr Biol.* 13, 638-646.

Zusammenfassung

Die G-Protein-gekoppelten Rezeptoren (GPCRs) stellen die größte Familie der Zelloberflächenrezeptoren dar. 1-5% des Wirbeltiergenoms kodiert für diese Rezeptorfamilie. Im Humangenom sind etwa 800-1000 Gene vertreten, die für GPCRs kodieren. Trotz der großen Unterschiede in ihrer Sequenz und Aktivierung haben alle GPCRs zwei Gemeinsamkeiten: (1) Ihre Architektur wird durch sieben Transmembranhelices beschrieben. (2) Ihre Funktion in der Signaltransduktion üben alle durch Aktivierung der heterotrimeren Guanylnukleotid-Bindeproteine (G-Proteine) aus.

Die GPCRs sind an der Regulierung einer Vielzahl von physiologischen Prozessen beteiligt und stellen daher wichtige Ziele für die Medikamentenentwicklung dar. Bisher gibt es kaum Möglichkeiten zur strukturbasierenden Medikamentenentwicklung, da, bis auf das Rinder-Rhodopsin, nur sehr wenige Informationen zur dreidimensionalen Struktur von GPCRs verfügbar sind. Das Rinder-Rhodopsin nimmt allerdings unter den GPCRs eine Sonderstellung ein. Im Gegensatz zu allen übrigen GPCRs bindet es seinen Liganden, 11-cis Retinal, kovalent und liegt dann in der nicht-aktivierten Form vor. Zudem kann Rhodopsin in großen Mengen aus Rinderretina isoliert werden, wohingegen die übrigen GPCRs nur in geringen Mengen in ihren natürlichen Geweben vorkommen.

Die vorliegende Arbeit verfolgt drei Ziele: Erstens sollen GPCRs durch heterologe Expression in hohen Ausbeuten hergestellt und biochemisch charakterisiert werden. Die Etablierung eines Solubilisierungs- und Aufreinigungsprotokolls stellt das zweite Ziel dar. Drittens soll die Interaktion von Ligand und Rezeptor mittels verschiedener Techniken untersucht werden.

Grund für die erste Zielsetzung ist die geringe Verfügbarkeit reinen, homogenen und stabilen Proteins im Milligramm-Maßstab, welches die größte Hürde für strukturelle Untersuchungen von GPCRs darstellt. Hier wurden verschiedene Expressionssysteme zur heterologen Produktion von Membranproteinen etabliert. Die Wahl des Expressionssystems ist hierbei entscheidend, um posttranslationale Modifikationen wie Glykosylierung sowie die korrekte Faltung des Rezeptors zu gewährleisten. Neben *E. coli* haben sich hierbei vor allem eukaryotische Expressionssysteme wie *Pichia pastoris* bewährt.

In der vorliegenden Arbeit wurden drei GPCRs hergestellt und analysiert: der humane Bradykinin Rezeptor Typ 2 (B₂R), der humane Angiotensin II Rezeptor Typ 1 (AT_{1a}R) und der humane Neuromedin U Rezeptor Typ 2 (NmU₂R). Diese drei Rezeptoren wurden in drei Expressionssystemen (*Pichia pastoris*, Insektenzellen und Säugerzellen) heterolog produziert und biochemisch charakterisiert. Für jedes der drei Proteine wurden Solubilisierungs- und Aufreinigungsprotokolle etabliert. Die aufgereinigten Proteine wurden anschließend für Kristallisationsexperimente, für Festkörper NMR Untersuchungen und weitere Experimente eingesetzt.

Der erste untersuchte Rezeptor, B₂R, kann vor allem in Endothelzellen, vaskulären glatten Muskelzellen und Kardiomyozyten nachgewiesen werden. Seine Aktivierung spielt bei der Entstehung von Entzündungen, Schmerz, Gewebsverletzung sowie herzschtützenden Mechanismen eine Rolle. Im Rahmen der Doktorarbeit wurde B₂R in der Hefe *Pichia pastoris* (3,5 pmol/mg), in BHK-Zellen (10 pmol/mg) und in Sf9-Zellen (60 pmol/mg) erfolgreich rekombinant produziert. Zur Charakterisierung wurde die Bindung des Liganden [³H] Bradykinin, die G-Protein-Kopplung, zelluläre Lokalisierung sowie die Glykosylierung des Rezeptors untersucht. Der heterolog produzierte Rezeptor konnte in hoher Reinheit isoliert

werden. Homogenität und Stabilität des aufgereinigten Proteins wurden mittels Gelfiltration analysiert. Aus BHK und Sf9 Zellen konnten Milligramm-Mengen reinen und stabilen Rezeptors isoliert werden, die zu Kristallisationsexperimenten verwendet wurden. Hier zeigten sich kristallartige Strukturen, die zur Zeit weiter charakterisiert werden.

Der zweite untersuchte Rezeptor, AT_{1a}R, kann in glatten Muskelzellen, Leber, Nieren, Herz, Lunge und Hoden nachgewiesen werden. Die Aktivierung dieses Rezeptors spielt eine Rolle bei der Regulation des Blutdrucks und bei kardiovaskulären Erkrankungen. Rekombinanter AT_{1a}R konnte mit hoher Ausbeute (167 pmol/mg) in *Pichia pastoris* hergestellt werden. Die Ausbeute bei Produktion in Insektenzellen (29 pmol/mg) und Säugerzellen (32 pmol/mg) lag im mittleren Bereich. Der rekombinante Rezeptor wurde hinsichtlich der Bindung von [³H] Angiotensin II, der zellulären Lokalisierung und Glykosylierung charakterisiert. Im Anschluss wurde er erfolgreich mittels Affinitätschromatographie gereinigt. Homogenität und Stabilität des gereinigten AT_{1a}R wurden mittels Gelfiltration analysiert. Aus *Pichia pastoris* konnte das Protein im Milligramm-Maßstab isoliert werden, so dass Kristallisationsexperimente möglich waren.

Dem dritten Rezeptor, NmU₂R, konnte erst kürzlich sein Ligand, Neuromedin U, zugeordnet werden. Der Rezeptor ist im zentralen Nervensystem, und hier insbesondere in der *Medulla oblongata*, dem Rückenmark und dem Thalamus lokalisiert. Aufgrund dieser Verteilung wird angenommen, dass er eine Rolle in der Regulation der Weiterleitung sensorischer Nervenimpulse sowie deren Modulation spielt. Während meiner Arbeit konnte ich bei der heterologen Produktion des Rezeptors Ausbeuten von 6 pmol/mg in *Pichia pastoris* und 9 pmol/mg in BHK Zellen erzielen. Der rekombinante Rezeptor wurde mittels Bindung eines

Radioliganden ($[^{125}\text{I}] \text{ NmU}$) charakterisiert. Weiterhin wurde die zelluläre Lokalisierung und Glykosylierung des GPCRs untersucht. Obwohl der rekombinante NmU₂R erfolgreich isoliert werden konnte, sind auf Grund der geringen Produktionsmengen zur Zeit keine Strukturuntersuchungen möglich.

Zur Analyse der pharmakologisch wichtigen Ligand-Rezeptor-Wechselwirkung wurde Festkörper NMR Spektroskopie eingesetzt. Durch die Verwendung von selektiv mit ^{13}C und ^{15}N markierten Peptiden können Konformationsänderung des Peptidliganden beim Binden des Rezeptors untersucht werden. Die Bestimmung der genauen Konformation des gebundenen Liganden ist für die Medikamentenentwicklung von Bedeutung. In der vorliegenden Arbeit wurde mittels der Festkörper NMR Spektroskopie die Konformation des rezeptorgebundenen Liganden, Bradykinin, untersucht. Die ersten Ergebnisse weisen auf signifikante Strukturänderungen Bradykinins hin, sobald es an den B₂R bindet.

Untersuchungen bezüglich Wechselwirkung von GPCRs mit anderen Proteinen sind auch für die Kristallisation relevant. Eine der Herausforderungen in der Kristallisation von GPCRs ist die kleine hydrophile Oberfläche, die zur Bildung von Kristallkontakten im Kristallgitter oft nicht ausreichend ist. Eine Möglichkeit, dieses Problem zu lösen, ist die Bildung eines stabilen Komplexes aus dem Rezeptor und einem interagierenden Protein. Zusätzlich kann der Rezeptor durch die Interaktion in eine weniger flexible Form überführt werden, was die Kristallisation und die spätere Strukturbestimmung erleichtern kann.

Basierend auf diesem Ansatz wurden B₂R und AT_{1a}R, die einen stabilen heterodimeren Komplex bilden, in BHK Zellen ko-exprimiert. Bemerkenswert war hierbei dass B₂R im Komplex mit AT_{1a}R in der Plasmamembran vorzufinden war, während B₂R alleine hauptsächlich in intrazellulären Membranen exprimiert wurde.

Weiterhin führte die Koexpression der beiden Rezeptoren zu einem vierfachen Anstieg der [³H] Bradykinin Bindungsstellen auf der Zelloberfläche. Es konnte ebenfalls nachgewiesen werden, dass nach der Stimulation mit nur einem der beiden rezeptorspezifischen Liganden beide GPCRs zusammen internalisiert wurden. Dieses Phänomen wurde auch in menschlichen Vorhaut- fibroblasten nachgewiesen, in denen beide Rezeptoren vorkommen. Die erhaltenen Ergebnisse deuten darauf hin, dass auch in nativen Geweben die Anwesenheit des AT_{1a}R für die Expression und den Transfer des B₂R zur Plasmamembran nötig ist. Diese Daten unterstützen die Hypothese, dass Heterodimerisierung eine Voraussetzung für die Zelloberflächenlokalisierung bestimmter GPCRs ist.

Der Ko-Komplex aus B₂R und AT_{1a}R konnte mittels dualer Affinitätschromatographie isoliert, wie durch SDS-PAGE Analyse, analytische Gelfiltration und Bindung von Radioliganden gezeigt werden konnte. „Pull-down“ Experimente, die drei Tage nach der Reinigung durchgeführt wurden, wiesen darauf hin, dass der Ko-Komplex nicht stabil war und zerfiel. Bei der Reinigung von Membranproteinen verursacht der Verlust von Lipiden während des Isolationsprozesses oft eine Beeinträchtigung der Stabilität des Proteins. Auch das verwendete Detergenz beeinflusst die Stabilität von Membranproteinen. Experimente zur Verbesserung der Langzeitstabilität des Komplexes durch Zugabe von Lipiden und anderen Detergenzien sind in Vorbereitung.

Die Bildung von Ko-Komplexen wurde zusätzlich mit Beta-Arrestin, einem Inhibitor der Kopplung von G-Proteinen und ihren Rezeptoren untersucht. Beta-Arrestin ist ein zytosolisches Protein, dass an der Desensibilisierung der Agonist-stimulierten GPCRs beteiligt ist. Versuche, eine Ko-Komplexbildung aus gereinigtem B₂R und gereinigtem Beta-Arrestin *in vitro* zu erzielen, schlugen fehl. In „Pull-Down“

Experimenten konnte keine Interaktion nachweisen werden. Wurde anstatt des nativen B₂R eine C-terminale Mutante, bei welcher der C-Terminus des B₂R gegen den des Vasopressinrezeptors ausgetauscht worden war, verwendet, konnte *in vitro* Ko-Komplexbildung mit Beta-Arrestin festgestellt werden. Mit Experimenten zur Bestimmung der Langzeitstabilität des Ko-Komplexes sowie zur Ko-Kristallisations wurde begonnen.

Im Rahmen der vorliegenden Arbeit wurde die Produktion, Charakterisierung und Aufreinigung von drei rekombinanten humanen GPCRs etabliert. Die rekombinanten Rezeptoren wurden im Milligramm-Maßstab produziert. Damit ist die erste, wesentliche Hürde zur Strukturanalyse genommen. Der B₂R-β-Arrestin Komplex kann sich als vorteilhaft für die Kristallisation herausstellen. Zusätzlich konnte zum ersten Mal gezeigt werden, dass der Transfer eines GPCRs an die Zelloberfläche von der Heterodimerisierung mit einem anderen nicht-verwandten GPCR abhängig sein kann.

Abbreviations

AP	alkaline phosphatase
ATP	adenosine-triphosphate
cAMP	cyclic adenosine-monophosphate
cDNA	complementary deoxyribonucleic acid
BHK	baby hamster kidney
BSA	bovine serum albumin
CAP	capsid protein
CHO	chinese hamster ovary
Cpm	counts per minute
DMSO	dimethylsulfoxide
DNA	deoxyribonucleic acid
DTT	dithiothreitol
EDTA	ethylenediaminetetraacetic acid
FCS	fetal calf serum
GDP	guanine diphosphate
GPCR	G protein-coupled receptor
GTP	guanine triphosphate
HEK	human embryonic kidney
HF-15	human foreskin fibroblasts
H5	high five cells
IgG	immunoglobulin G
LB	luria bertani
OD	optical density
PAGE	polyacrylamide gel electrophoresis
PBS	phosphate buffered saline
PEG	polyethylene glycol
PMSF	phenylmethylsulfonylfluoride
RNA	ribonucleic acid
RT	room temperature

SDS	sodium dodecyl sulphate
Sf9	<i>Spodotera frugiperda</i> cells
2-D	two-dimensional
3-D	three-dimensional
TBS	Tris-buffered saline
TCA	trichloroacetic acid
TMH	transmembrane helix

Appendix

Amino-acid sequences of affinity tags used in this work

Flag-tag DYKDDDDK

His10-tag HHHHHHHHHH

Strep II-tag AWSHPQFEK

Bio-tag

GGTGGAPAPAAGGAGAGKAGEGEIPAPLAGTVSKILVKEGDTVKAGQTVLV
LEAMKMETEINAPTDGKVEKVLVKERDAVQGGQGLIKIG

Amino acid sequence of receptors

B₂R

MLNVTLQGPTLNGTFAQSKCPQVEWLGWLNTIQPPFLWVLFVLATLENIFVLSVF
CLHKSSCTVAEIYLGNLAAADLILACGLPFWAITISNFDWLFGETLCRVVNAIIM
NLYSSICFLMLVSDRYLALVKTMSMGRMRGVRWAKLYSLVIWGCTLLSSSPML
VFRMKEYSDEGHNVTACVISYPSLIWEVFTNMLLN VVGFLPLSVITFCTMQIM
QVLRNNEMQKFKEIQTERRATVLLVLLLFHICWLPFQISTFLDLHRLGILSSCQ
DERIIDVITQIASFMAYSNSCLNPLVYVIVGKRFRKKSWEVYQGVQCQKGGCRSEPI
QMENSMGTLRTSISVERQIHKLQDWAGSRQ.

NmU₂R

MSGMEKLQNASWIYQQKLEDPFQKHLNSTEEYLAFLCGPRRSHFFLPVSVVYVPI
FVVGVIGNVLVCLVILQHQAAMKTPTNYLFSLAVSDLLVLLLGMPLEVYEMWR
NYPFLFGPVGCYFKTALFETVCFASILSITTVSVERYVAILHPFRAKLQSTRRRALR
ILGIVWGFSLVFLSPLNTSIHGKIFHYFPNGSLVPGSATFTVIKPMWIYNFIIQVTSFL
FYLLPMTVISVLYYLMALRLKKDKSLEADEGNANIQRPCRKSVNKMLFVLVLFV
AICWAPFHIDRLFFSFVEEWSLAAVFNLVHVVSFVFFYLSSAVNPIIYNLLSRR
FQAAFQNVISSFHKQWHSQHDPQLPPAQRNIFLTECHFVELTEDIGPQFPCQSSMH
NSHLPTALSSEQMSRTNYQSFHFNKT.

AT_{1a}R

MILNSSTEDGIKRIQDDCPKAGRHNHYIFVMIPTLYSIIFVVGIFGNSLVVIVIFYKL
KTVASVFLNLALADLCFLLTLPLWAVYTAMEYRWPFNGNYLCKIASASVSFNLY
ASVFLLTCLSIDRYLAIVHPMKSRLRRTMLVAKVTCIIWLLAGLASLPAPIHRNVF
FIENTNITVCAFHYESQNSTLPIGLGLTKNILGFLFPFLIILTSYTLIWKALKKAYEIQ
KNKPRNDDIFKIIMAIVLFFFSSWIPHQIFTFLDVLQLGIIRDCRIADIVDTAMPITIC
IAYFNNCLNPLFYGFLGKKFKRYFLQLLKYIPPKAKSHSNLSTKMSTLSYRPSDVS
SSTKKPAPCFEVE.

Previously reported K_d values of B₂R, AT_{1a}R in native cells and NmU₂R (COS cells)

GPCR		K _d (nM)	Reference
B ₂ R	Human lung fibroblasts	2.5	Baenziger <i>et al.</i> , 1992
	Human decidual cells	0.85	Rehbock <i>et al.</i> , 1997
AT _{1a} R	Human skin fibroblasts	1.0 +/- 0.7	Nickenig <i>et al.</i> , 1997
NmU ₂ R	COS-7 cells	0.83	Raddatz <i>et al.</i> , 2000

Sequences of peptide ligands

Bradykinin RPPGFSPFR

Angiotensin II DRVYIHPF

Neuromedin U-25 FKVDEEFQGPIVSQNRRYFLFRPRN

Neuromedin U-8 YFLFRPRN

#1	mmb			1	2	3	4	5	6			7	8	9	10	11	12		
				0,5 M								0,5 M							
				Formiate	Citrate	MES	MOPS	Tricine	Borate			Formiate	Citrate	MES	MOPS	Tricine	Borate		
				pH	pH	pH	pH	pH	pH			pH	pH	pH	pH	pH	pH		
				4	5	6	7	8	9			4	5	6	7	8	9		
				0,1 M								0,1 M							
A	50% PEG	400	10%	200			200		600			4M Malonate	0,8 M	200		200		600	A
B			15%	300			200		500				1,6 M	400		200		400	B
C			22%	440			200		360				2,4 M	600		200		200	C
D			33%	660			200		140				3,2 M	800		200		-	D
E	50% PEG	4000	3%	60			200		740			3M K/Na-Pi	0,6 M	200		-		800	E
F			6%	120			200		680			pH 4; 5; 6; 7; 8; 9	1,2 M	400		-		600	F
G			12%	240			200		560				2,1 M	700		-		300	G
H			18%	360			200		440				3 M	1000		-		-	H
									ddH ₂ O										ddH ₂ O

#2	mmb			1	2	3	4	5	6			7	8	9	10	11	12		
				0,5 M								0,5 M							
				Formiate	Citrate	MES	MOPS	Tricine	Borate			Formiate	Citrate	MES	MOPS	Tricine	Borate		
				pH	pH	pH	pH	pH	pH			pH	pH	pH	pH	pH	pH		
				4	5	6	7	8	9			4	5	6	7	8	9		
				0,1 M								0,1 M							
A	50% PEG	2000 MME	6%	120			200		680			4M (NH ₄) ₂ SO ₄	0,8 M	200		200		600	A
B			12%	240			200		560				1,6 M	400		200		400	B
C			18%	360			200		440				2,4 M	600		200		200	C
D			24%	480			200		320				3,2 M	800		200		-	D
E	4M Formiate		0,8 M	200			200		600			2M Citrate	0,4 M	200		200		600	E
F			1,6 M	400			200		400				0,8 M	400		200		400	F
G			2,4 M	600			200		200				1,2 M	600		200		200	G
H			3,2 M	800			200		-				1,6 M	800		200		-	H
									ddH ₂ O										ddH ₂ O

3-D crystallization screening scheme

Acknowledgments

Prof. Hartmut Michel for accepting me as a graduate student in his lab and supervising my PhD work. He allowed me to carry out several different projects in the lab during which I learned to work independently. Despite his busy schedule, he was always available to discuss the progress and further directions of the projects. I consider the last three and half years, which I spent under his guidance, as a golden period of the learning phase in my scientific life.

Prof. Dieter Steinhilber for his academic support and taking the responsibility of external supervision.

Prof. Clemens Glaubitz and Dr. Jakob Lopez (Center for Biomolecular Magnetic Resonance, Frankfurt) for their fruitful collaboration and discussions on the solid-state NMR project.

Karin Heidemann and Prof. Harald Schwalbe (Center for Biomolecular Magnetic Resonance, Frankfurt) for the synthesis and characterization of $^{13}\text{C}/^{15}\text{N}$ labeled peptides.

Dr. Christoph Reinhart for his help during the initial stage of my work and continuous support.

Dr. Helmut Reiländer and Gabi Maul for many useful discussions about the baculovirus expression system and Darui Huo for his help during the initial experiments with the Semliki Forest Virus expression system.

Ingo Focken and Thorsten (at Sanofi-Aventis) for performing large-scale cultures of mammalian cells and insect cells in wave bioreactors, which allowed the isolation of recombinant receptors for crystallization and NMR studies.

Heinz Schewe (Biocentre, Frankfurt) and Ritva Tikannen (Institute of Biochemistry II, Frankfurt) for the help with confocal microscopy.

Prof. Dr. W. Mueller-Esterl (Institute of Biochemistry II, Frankfurt) for providing human foreskin fibroblasts and his valuable comments on the heterodimerization project.

Dr. Winfried Haase and Friederike Joos for performing Immunogold labeling experiments.

All the members of GPCR group for day to day discussions, especially Ankita Srivastava for her help during the initial stage of my stay in Frankfurt and in the lab.

Jan Griesbach, Tina Wenz and Martina Striebeck for translating the summary of my thesis and Dr. Robert Dempski for reading the thesis.

All the members of the department of Molecular Membrane Biology for friendly and jovial working environment.

Many thanks to the library staff for arranging the articles which were not available online.

I am short of words to thank my parents, my elder brother, sisters and other family members for their endless support.

And finally, special thanks to Ankita Roy for her emotional support during last three and half years.

Curriculum Vitae



Arun Kumar Shukla

Nationality Indian
Date & place of Birth 1st November 1981
(Kushinagar, India)

Academic qualifications

1996-1999 Bachelor of Science in Biology
D.D.U. Gorakhpur University, India

2000-2002 Master of Science in Biotechnology
Jawaharlal Nehru University
New Delhi, India

2002-2006 Ph.D.
Max Planck Institute of Biophysics
Frankfurt/M, Germany

Research Experience

M.Sc. dissertation 2001-2002
Centre for Biotechnology, Jawaharlal Nehru University, New Delhi, India
Supervisor: Prof. Dr. Kunal B. Roy

Title: **Transcription Induced, Rec A Independent Homologous Recombination by a Novel Fold Back Quadruplex DNA *in vivo*.**

Ph.D. dissertation 2002-2006
Max Planck Institute of Biophysics, Frankfurt/M, Germany
Supervisor: Prof. Dr. Hartmut Michel

Title: **Heterologous Production, Characterization and Isolation of Selected G Protein-Coupled Receptors for Structural Studies.**

Manuscripts accepted/submitted/under preparation

- 1) **Shukla, A.K.**, & Roy, K.B. (2005) A Palindromic Repeat Sequence Adopts Stable Fold Back Structure Under Supercoiling. *J. Biochem.* (In Press).
- 2) **Shukla, A.K.**, & Roy, K.B. (2005) Rec A Independent Homologous Recombination Induced by A Putative Fold Back Tetraplex DNA. *Biol. Chem.* (In Press).
- 3) **Shukla A.K.**, Reinhart, C., & Michel, H. (2005) Heterodimerization with Angiotensin II subtype 1a Receptor Promotes Surface Localization of Bradykinin subtype 2 Receptor. (Submitted).
- 4) **Shukla A.K.**, Haase, W., Reinhart, C., & Michel, H. (2005) Functional overexpression and characterization of human bradykinin subtype 2 receptor in insect cells using the baculovirus system. (Submitted).
- 5) **Shukla A.K.**, Haase, W., Reinhart, C., & Michel, H. (2006) Biochemical and pharmacological characterization of the human bradykinin subtype 2 receptor produced in mammalian cells using the Semliki Forest virus system. (Submitted).
- 6) **Shukla A.K.**, Haase, W., Reinhart, C., & Michel, H. (2006) Production and characterization of the recombinant human bradykinin subtype 2 receptor in methylotrophic yeast *Pichia Pastoris*. (In preparation).
- 7) **Shukla A.K.**, Haase, W., Reinhart, C., & Michel, H. (2006) Heterologous production and characterization of human neuromedin U receptor subtype 2 in *Pichia pastoris* and Mammalian cells. (In preparation).
- 8) **Shukla A.K.**, Haase, W., Reinhart, C., & Michel, H. (2006) Heterologous overexpression and characterization of human angiotensin II subtype 1 receptor in *Pichia pastoris*, Mammalian cells and Insect cells (In preparation).